UNIVERSITAT DE
BARCELONA

Characterization of polymers and Microencapsulated Phase Change Materials used for Thermal Energy Storage in buildings

Jessica Giró Paloma

ADVERTIMENT. La consulta d’aquesta tesi queda condicionada a l’acceptació de les següents condicions d'ús: La difusió d’aquesta tesi per mitjà del servei TDX (**www.tdx.cat**) i a través del Dipòsit Digital de la UB (**diposit.ub.edu**) ha estat autoritzada pels titulars dels drets de propietat intel·lectual únicament per a usos privats emmarcats en activitats d’investigació i docència. No s’autoritza la seva reproducció amb finalitats de lucre ni la seva difusió i posada a disposició des d’un lloc aliè al servei TDX ni al Dipòsit Digital de la UB. No s’autoritza la presentació del seu contingut en una finestra o marc aliè a TDX o al Dipòsit Digital de la UB (framing). Aquesta reserva de drets afecta tant al resum de presentació de la tesi com als seus continguts. En la utilització o cita de parts de la tesi és obligat indicar el nom de la persona autora.

ADVERTENCIA. La consulta de esta tesis queda condicionada a la aceptación de las siguientes condiciones de uso: La difusión de esta tesis por medio del servicio TDR (**www.tdx.cat**) y a través del Repositorio Digital de la UB (**diposit.ub.edu**) ha sido autorizada por los titulares de los derechos de propiedad intelectual únicamente para usos privados enmarcados en actividades de investigación y docencia. No se autoriza su reproducción con finalidades de lucro ni su difusión y puesta a disposición desde un sitio ajeno al servicio TDR o al Repositorio Digital de la UB. No se autoriza la presentación de su contenido en una ventana o marco ajeno a TDR o al Repositorio Digital de la UB (framing). Esta reserva de derechos afecta tanto al resumen de presentación de la tesis como a sus contenidos. En la utilización o cita de partes de la tesis es obligado indicar el nombre de la persona autora.

WARNING. On having consulted this thesis you’re accepting the following use conditions: Spreading this thesis by the TDX (**www.tdx.cat**) service and by the UB Digital Repository (**diposit.ub.edu**) has been authorized by the titular of the intellectual property rights only for private uses placed in investigation and teaching activities. Reproduction with lucrative aims is not authorized nor its spreading and availability from a site foreign to the TDX service or to the UB Digital Repository. Introducing its content in a window or frame foreign to the TDX service or to the UB Digital Repository is not authorized (framing). Those rights affect to the presentation summary of the thesis as well as to its contents. In the using or citation of parts of the thesis it’s obliged to indicate the name of the author.

Programa de Doctorat: Ciència i Tecnologia dels Materials

Characterization of polymers and Microencapsulated Phase Change Materials used for Thermal Energy Storage in buildings

Memòria per optar al grau de Doctor per la Universitat de Barcelona presentada per:

Jessica Giró Paloma

Directors de Tesi:

Dra. Ana Inés Fernández Renna
Professora Agregada

Dra. Mònica Martínez López
Professora Lectora

Departament de Ciència dels Materials i Enginyeria Metal·lúrgica

FACULTAT DE QUÍMICA

Universitat de Barcelona

Barcelona, Setembre de 2015

Als meus pares i germans. Tots cinc, junts per sempre

"Viu com si anessis a morir demà. Aprèn com si fossis a viure per sempre". *Mahatma Gandhi*

Aquesta Tesi Doctoral té una menció especial en els agraïments a la meva directora, la Dra. Ana Inés Fernández Renna, pel seu suport durant tots aquests anys. Ha sido un camino largo, pero muy bonito. MUCHAS GRACIAS. També vull agrair de manera particular a la meva co-directora de Tesi, la Dra. Mònica Martínez, gràcies pels consells que m'has donat. Així mateix, vull fer referència al Dr. Josep Maria Chimenos, ja que m'ha brindat l'oportunitat de treballar com a tècnic de laboratori de DIOPMA durant aquests darrers anys. Also, I would love to thank Prof. M. Farid for his help and support during my three months stage in Auckland, New Zealand. It was an amazing time in that beautiful country. Hope to see you and your family soon.

M'agradaria tenir un esment singular al Dr. Ferran Espiell, Catedràtic del Departament de Ciència dels Materials i Enginyeria Metal·lúrgica de la Facultat de Quimica de la Universitat de Barcelona. Gràcies per "agafar-me" a l'any 2006 per fer unes pràctiques al Departament durant el mes de juliol com a *bequi* de la Dra. Elena Xuriguera en diferents projectes de recerca. Sense aquella primera oportunitat laboral que em vas brindar, el meu futur laboral i personal hagués sigut ben diferent. I després em vàreu tornar a donar feina, aquest cop de *bequi* de la Dra. Maria Niubó. Vull també nombrar a la Dra. Mercè Segarra per ser una gran Directora, *jefa* i companya del Departament i de DIOPMA durant els anys que porto formant part del grup de recerca.

A l'Esther, una amiga excepcional. La millor secretaria del món, la que et diu totes les solucions a tots els teus problemes, la que sempre et calma quan veu que comença la tempesta, la que ho pregunta tot (Qui? Com? Quan? Perquè?) i ho respon tot (Miss Google). Una amiga que et dona la mà cada dia sense demanar res a canvi. Una amiga de les de veritat. Per sort t'he conegut, i no et deixaré escapar mai!!! Ets simplement GENIAL! També he de donar les gràcies a ese mejicano que me tiene enamorada hasta el infinito y mas allá!!! Gracias Ricardo por esos millones de momentos, de risas y de confidencias que hemos tenido! Sin tí ni sin mis Chimenos Boys and Girls no hubiera sido lo mismo! Per tant, aquí entra en joc el Joan, que gran ets ;) Ets l'ànima de DIOPMA, l'alegria de la huerta! Sense tu res seria igual. I com no, a la Judit! Gracias por haberme enseñado tanto durante este tiempo, y por todas las charlas y risas que hemos tenido. A un ex membre del CBG team és el Titu!! Tinunesquiii! I a tu què t'he de dir? Que al final sí que vaig marxar a Auckland? Increïble però cert, eh? Merci per mil coses. Os lo dice Maria Jessifer Fernanda De Todos Los Santos Spin Pigeon! Ai no, perdón, en este documento oficial debe de ser: J. Giro-Paloma, que queda más fino...!

També vull dedicar-li una frase a la Camila, la meva companya codo con codo del màster, que un cop finalitzat, les altes esferes ens van separar (tu a Lleida i jo a Barcelona), i que un cop et vas convertir en Doctora, ens vam unir, again! També vull nombrar a tots aquells diopmeros com Padiogenes (Jessica va sin acento), Micky (hola rubio!), a la Núria Soria, i l'Alejandro (el otro mejicano) , que han sigut grans companys i dels que he après vàries coses. També m'agradaria agrair als companys de la Universitat de Lleida del GREA (en especial a la Catedràtica Lluïsa Cabeza, com a tots els seus estudiants per totes les col·laboracions impartides, congressos, reunions...). Gracias a todos los co-autores que han participado conjuntamente en los artículos científicos publicados y los que aún se tienen que publicar (Thanks to all the co-authors for your help).

Vull fer referència i agrair a aquells professors i PAS de la planta 7 de la Facultat de Quimica de la Universitat de Barcelona que m'han ajudat a preparar les classes de pràctiques que he impartit durant el curs acadèmic 2013-2014 i 2014-2015. També vull fer esment a tots els tècnics dels Serveis Científico-Tècnics de la Universitat de Barcelona que han col·laborat en aquesta Tesi, en especial al Gerard Oncins, per ensenyar-me tant i tenir tanta paciència amb mi.

Besides, I would like to thank Halime Paksoy for the acceptance on the external correction to qualify the Thesis for the international PhD mention. I would love to have done the three months stage in Adana (Turkey) but, as you well know, it was impossible. Maybe… next time? Also, I would like to acknowledge Dr. Jay M. Khodadadi (University of Alabama) for his external review.

A tots aquells amics que heu estat allà durant aquest temps, aguantant les meves explicacions de feina, les meves queixes. A les més Pesades-Pitjors, a tots i totes els/les de Calella, a les guapes del Pere Vergés... vosaltres ja sabeu qui! També vull agrair de tot cor a mis niñas de la UB. Que grande haberos conocido! Ese máster sin vosotras no hubiera sido lo mismo!!! Y como de costumbre... esto hay que celebrarlo en un Can Pagès!! Víctor tu también, eh?

I per últim, i no per això menys important, he de donar les gràcies a la meva família. Papa, il cappo Giro-Paloma, gràcies per aguantar els meus mals humors a casa, i per tots els teus consells al llarg de la meva vida. Gràcies per obligar-me a estudiar quan tenia 18 anys, perquè sense aquella persistència imposada a casa, ara mateix no estaria escrivint aquesta Tesi Doctoral! I als meus germans, que conjuntament amb les seves parelles i filles, ho són TOT per mi en aquesta vida. Y a tí. Viva la madre que me parió! Us estimo infinit!

De debò, moltes gracies a tothom!

Jess

Index:

Contents, figures, and tables

Thesis structure

This Thesis is divided in two main blocks.

- The first block is dedicated to the characterization of polymers performed by nanoindentation technique, as mechanical measurements in macroscopic samples. The study published in **European Polymer Journal, 2013** was a methodology manuscript where it is compared to different ways on measuring mechanical properties, and it is defined which fits better depending on the viscous character of the polymer. After this publication, it was decided to use the knowledge on the technique and apply it to the characterization on polymers mixed with flame retardants. These results are published in **European Polymer Journal, 2015**. The main idea in this study is to compare the mechanical properties of samples in contact with different PCM, comparing them, at the same time, with samples that had no contact with PCM.

- The second block of this PhD Thesis is focused on microscopic samples. First of all, it is reviewed a paper in **Renewable & Sustainable Energy Reviews** (accepted, 18/09/2015) where it is summarized the types, methods, techniques, and applications for microencapsulated Phase Change Materials (MPCM). After learning the limits and background of other authors in this field, the chemical, physical, thermal, and mechanical characterization of microscopic active and passive MPCM samples are performed. From these studies six papers are published in different journals (**Applied Energy 2013**, **Energy Procedia 2014, Energy 2015, Solar Energy 2015, Renewable & Sustainable Energy Reviews 2015, Renewable Energy 2016**) and one other study is still unpublished, in which it is evaluated the volatile organic compounds of some PCM and passive MCPM. Finally, it is presented a thermogravimetric study for slurries due to some conclusions extracted from previous work and presented to congresses. This investigation is nowadays under investigation.

Summarizing, eight high impact factor manuscripts related to my PhD Thesis are published, one review is accepted, and one more paper will be submitted in the near future. Moreover, two book chapters are published and one book chapter is also accepted in **CRC Press**, all of them related with this PhD Thesis. Other publications non related to my PhD Thesis are published in Chemosphere (2014) and in Journal of Geochemical Exploration (2015). Finally, four more book chapters non related to my PhD Thesis are published.

Resumen y discusión de resultados

El uso de fuentes de calor renovables tiene como resultado una disminución en el consumo de recursos fósiles, siendo su uso discontinuo ya que, habitualmente, no coincide con la demanda. Un correcto diseño del sistema de almacenamiento de energía térmica permitiría eliminar este problema reduciendo el consumo de recursos no renovables y mejorando la eficiencia energética donde se use. En el caso específico de los edificios, el almacenamiento de energía térmica mediante materiales de cambio de fase (PCM) es un instrumento útil para disminuir el consumo de energía, tal y como se pone de manifiesto en muchos trabajos de investigación nacionales e internacionales. Estos sistemas pueden incorporarse tanto en climatización pasiva (en el envolvente) como en activa (en las instalaciones). Así pues, una adecuada selección de los materiales, con estabilidad y comportamiento ante el fuego adecuados para una aplicación concreta, y una caracterización exhaustiva para su posterior uso en almacenamiento de energía térmica, son críticas y necesarias para crear un sistema eficiente, tanto para los de nueva construcción como para los ya construidos, y reducir el impacto ambiental de los sistemas de climatización desde un punto de vista técnico y econónomico.

La presente Tesis Doctoral está centrada en trabajos publicados en revistas científicas de alto factor de impacto, indexadas en el campo de los materiales, la ingeniería y la energía. Ésta se divide en dos bloques, un primer bloque de estudio a nivel macroscópico y un segundo bloque a nivel microscópico. Se recogen un total de 7 artículos publicados y 1 artículo aceptado (18/09/2015) en la presente Tesis Doctoral. Dos de ellos, publicados en la revista European Polymer Journal, forman parte del primer bloque ("*Depth-sensing indentation applied to polymers: A comparison between standard methods of analysis in relation to the nature of the materials, 49 (2013) 4047–4053*", y "*Effect of the filler on the nanomechanical properties of polypropylene in contact with paraffinic phase change material, 63 (2015) 29–36*"*).* El segundo bloque está formado por siete estudios: (5 artículos publicados, 1 artículo aceptado, y 1 artículo finalizado sin enviar) "*Physico-chemical and mechanical properties of microencapsulated phase change material, Applied Energy 109 (2013) 441–448*"*,* "*Physicochemical and thermal study of a MPCM of PMMA shell and paraffin wax as a core, Energy Procedia 48 (2014) 347 – 354*"*, "Preparation and exhaustive characterization of paraffin or palmitic acid microcapsules as novel phase change material, Solar Energy 112 (2015) 300–309",* "*Comparison of phase change slurries: Physicochemical and thermal properties, Energy 87 (2015) 223-227*"*, "Mechanical response evaluation of microcapsules from different slurries, Renewable Energy 85 (2016) 732-739*"; "*Types, methods, techniques, and applications for Microencapsulated Phase Change Materials (MPCM): A review, Renewable & Sustainable Energy Reviews, Accepted*"*,* "*Characterization of Microencapsulated Phase Change Materials* *for use in Building Applications".* Además, derivados de la Tesis doctoral, hay tres capítulos de libro: "*Physico-chemical and mechanical properties of microencapsulated phase change material; Innostock. The 12th international conference on energy storage"* with two different ISBN and *"Microencapsulation of phase change materials from Handbook of Encapsulation & Controlled Release. CRC Press Taylor and Francis Group".*

En este manuscrito de Tesis Doctoral se hace especial émfasis en la caracterización química, física, térmica, mecánica y ambiental tanto de PCM como de MPCM (Microencapsulated Phase Change Materials, materiales de cambio de fase microencapsulados) y PCS (Phase Change Slurries, pulpas con cambio de fase). La motivación para llevar a cabo una caracterización exhaustiva de estos materiales, es que estudios científicos revelan que cuando los PCM son mezclados con materiales de construcción, éstos sufren fugas debido al cambio reiterado de sólido a líquido. Por este motivo era interesante el hecho de minimizar las fugas o proponer alternativas de mejora. Se ha demostrado que el PCM de tipo parafínico con el tiempo tiende a filtrarse por los poros del material de construcción, y acaba migrando hacia la superficie. Por lo tanto, una alternativa para conservar estos PCM dentro de un material de construcción es recubriéndolos con una matriz polimérica, a través de una encapsulación. Como primer estudio, durante el trabajo final del *Màster en Química Avançada* (2009-2011) se estudiaron diversos polímeros como posibles contenedores de PCM. Éste se realizó en la Universitat de Barcelona, dentro del Departamento de Ciència dels Materials i Enginyeria Metal·lúrgica de la Facultad de Química. En él, se concluyó que el polimetilmetacrilato (PMMA) era el mejor candidato de todos los polímeros estudiados para contener PCM. El resto de polímeros que se evaluaron fueron: polietileno de alta densidad (HDPE), polietileno de baja densidad (LDPE), polipropileno (PP), poliestireno (PS), poliamida (PA), policarbonato (PC), polietilentereftalato (PET), policloruro de vinil no plastificado (PVC-U), poliuretano (PUR), polimetilmetacrilato (PMMA), y acronitrilo butadieno estireno (ABS).

Es sabido que los polímeros sufren el mecanismo del *Environmental Stress Cracking* (ESC), que es una interacción física donde hay una plastificación altamente localizada a través de estrés. Ésta no conlleva a degradación molecular ni modificaciones químicas. Así pues, se consideró de gran importancia estudiar la rigidez del sistema MPCM (cáscara + PCM) para comprender cómo evitar este tipo de mecanismos en los MPCM. Dentro de las posibles técnicas de evaluación, se consideró la nanoindentación como técnica innovadora en éste campo, ya que hasta ese preciso momento, no se habían publicado investigaciones donde se realizaran y estudiaran en profundidad este tipo de ensayos con polímeros. Como resultado de esta investigación, se presentó en el año 2011 en el congreso **Multiphase Polymers and Polymer Composites From Nanoscale to Macro Composites (Conference and Training School)** un póster que llevó por título “**Characterization of thermoplastics with Nanoindentation**”. En el año 2012 también se presentó otro póster relacionado con la temática en el **Congreso Nacional de Materiales** titulado “**Estudio comparativo a escala nanométrica de materiales poliméricos mediante el método de Loubet y el de Oliver y Pharr**”.

Se contactó con especialistas en el uso de nanoindentador, exponiendo el estudio a realizar, y se hicieron varios ensayos para determinar los parámetros mecánicos óptimos para ensayar las muestras. Las propiedades mecánicas son un criterio fundamental para la selección de materiales para una aplicación específica, y la técnica de la nanoindentación permite la evaluación de éstas propiedades ya que proporciona, en un corto período de tiempo, una gran cantidad de parámetros mecánicos. Los resultados del estudio titulado “**Depth-sensing indentation applied to polymers: A comparison between standard methods of analysis in relation to the nature of the materials**” han sido publicados en la revista **European Polymer Journal**, en el año 2013, volumen 49, páginas 4047 - 4053 (Factor de impacto: 3.242, Q1).

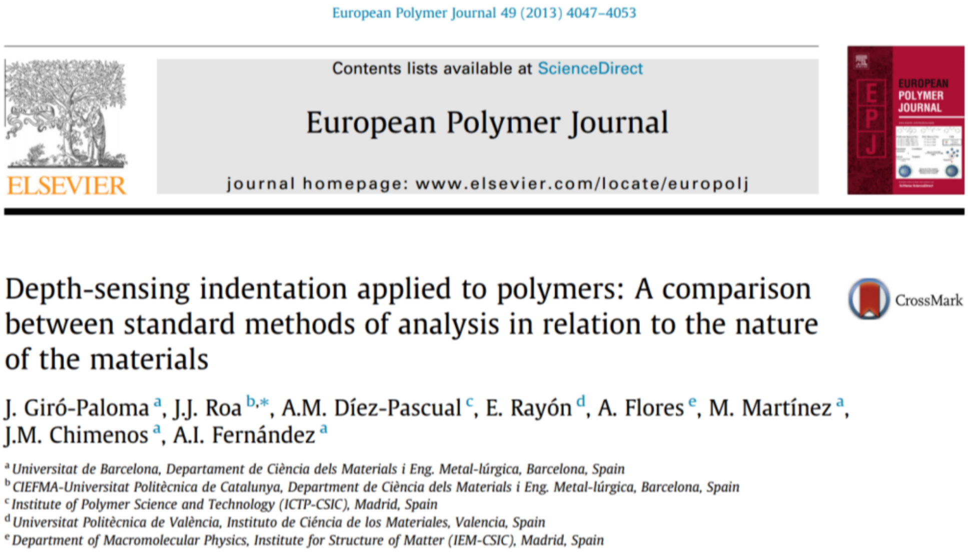

European Polymer Journal 49 (2013) 4047–4053

Contents lists available at ScienceDirect

European Polymer Journal

journal homepage: www.elsevier.com/locate/europolj

Depth-sensing indentation applied to polymers: A comparison between standard methods of analysis in relation to the nature of the materials

J. Giró-Paloma [a], J.J. Roa [b,*], A.M. Díez-Pascual [c], E. Rayón [d], A. Flores [e], M. Martínez [a], J.M. Chimenos [a], A.I. Fernández [a]

[a] Universitat de Barcelona, Departament de Ciència dels Materials i Eng. Metal-lúrgica, Barcelona, Spain
[b] CIEFMA-Universitat Politècnica de Catalunya, Department de Ciència dels Materials i Eng. Metal-lúrgica, Barcelona, Spain
[c] Institute of Polymer Science and Technology (ICTP-CSIC), Madrid, Spain
[d] Universitat Politècnica de València, Instituto de Ciéncia de los Materiales, Valencia, Spain
[e] Department of Macromolecular Physics, Institute for Structure of Matter (IEM-CSIC), Madrid, Spain

Figura R. 1. Primer artículo presentado en la Tesis Doctoral “Depth-sensing indentation applied to polymers: A comparison between standard methods of analysis in relation to the nature of the materials”.

En el artículo, se plantean dos metodologías para el tratamiento de los datos obtenidos, el análisis mediante el método de Oliver y Pharr, y por otro lado el método Loubet. La metodología de los primeros ha sido exitosamente aplicada para el estudio de metales y cerámicos y proporcionan valores fiables de dureza (*H*) y de módulo elástico (*E*). Sin embargo, su aplicación en el estudio de polímeros no está muy desarrollada ya que éstos exigen, además, metodologías donde se proporcione información sobre propiedades viscoelásticas y viscoplásticas. Así pues, con la detección de profundidad con indentación (DSI), se introdujo la posibilidad de aplicar una fuerza oscilante, más comúnmente conocida como la medición contínua de rigidez (CSM) o DSI dinámico. Los primeros en aplicar con éxito el CSM en la caracterización de polímeros fueron Loubet y sus coautores. Para ello, desarrollaron un modelo que introdujo el concepto del defecto de punta "aparente", h_o, lo que representa un cambio en el punto de contacto detectado para materiales poliméricos, que, a su vez, permite obtener datos mecánicos independientes de la profundidad de indentación.

El objetivo principal de este primer estudio de la Tesis Doctoral fue la aplicación de las metodologías de Oliver & Pharr y de Loubet para el análisis de materiales termoplásticos incluyendo cristalinos y semicristalinos, con probetas de tamaño 20 x 11 x 2 mm, como PA6, PMMA, PC, PET, ABS, PP, y PS.

Se hizo una comparación entre ambas metodologías sobre la dureza (H) y el módulo elástico (E). Por otra parte, también se estudiaron las principales ventajas y desventajas de cada metodología. Además, la validez de los dos modelos propuestos se discutió en función de la naturaleza del material polimérico, proporcionando así, algunas premisas para decidir a priori qué método sería más apropiado para un material polimérico específico.

Como conclusiones principales se puede comentar que, para el método de Oliver & Pharr, los valores obtenidos son función del análisis de la curva de descarga; por el contrario, para la metodología seguida por Loubet, éstos valores son función de la profundidad de penetración de la indentación. Además, para éste último, cabe destacar que los materiales poliméricos con rugosidad superficial y alto carácter viscoso (es decir, con temperaturas de transición vítrea por debajo de temperatura ambiente) tienden a tener altos valores de h_0. También, evaluando los valores obtenidos se extrae que mediante el método de Loubet se obtienen valores mecánicos inferiores a los del método de Oliver & Pharr debido a que se usa una aproximación dinámica para extraer la medida de rigidez, y el contacto en profundidad con la muestra es mayor debido a la contribución del efecto punta “aparente”. Así pues, Loubet es un método idóneo para materiales poliméricos con bajo caracter viscoso ($T_g > T_{medida}$).

Una vez se asentaron las bases de la nanoindentación para el estudio de materiales poliméricos, se decidió estudiar con la técnica de la nanoindentación el comportamiento mecánico de un compuesto formado por un polímero como el polipropileno (PP) y con un retardante de llama, como el conocido $Mg(OH)_2$, y el efecto que produce en sus propiedades mecánicas un contacto prolongado con PCM de tipo parafínico. La fabricación de este compuesto con propiedades ignífugas, a escala laboratorio, se realizó en colaboración con el

Centre Català del Plàstic (CCP). Estudios previos han valorado que el PP es un buen contenedor de PCM, aunque Wright demostró que la exposición prolongada de polímeros a sustancias orgánicas puede ser la responsable del fallo mecánico prematuro de dichos contenedores. Es decir, la absorción de PCM plastifica el polímero y reduce su resistencia a la fluencia. Esta reducción se asocia directamente con la concentración de fluido absorbido, así que, para aumentar ciertos parámetros tales como la resistencia mecánica, rigidez, y durabilidad del contenedor polimérico, se decidió evaluar el PP con una carga inorgáncia como el $Mg(OH)_2$ y submergido en PCM parafínico, comparándolo con PP cargado con $Mg(OH)_2$ pero sin estar en contacto con dicho PCM.

En el compuesto formado por 40 % PP y 60 % $Mg(OH)_2$, el uso del $Mg(OH)_2$ aumentó la rigidez, la resistencia mecánica, redujo el efecto de degradación evitando un fallo mecánico prematuro, y mejoró las propiedades contra el fuego. Además, también se estudiaron éstas propiedades cuando el compuesto estuvo submergido 32 días en dos tipos de PCM parafínicos distintos, y a distintas temperaturas. El artículo se publicó en la revista **European Polymer Journal** con el título "**Effect of the filler on the nanomechanical properties of polypropylene in contact with paraffinic phase change material**", en el año 2015, volumen 63, páginas 29 - 36 (Factor de impacto: 3.242, Q1).

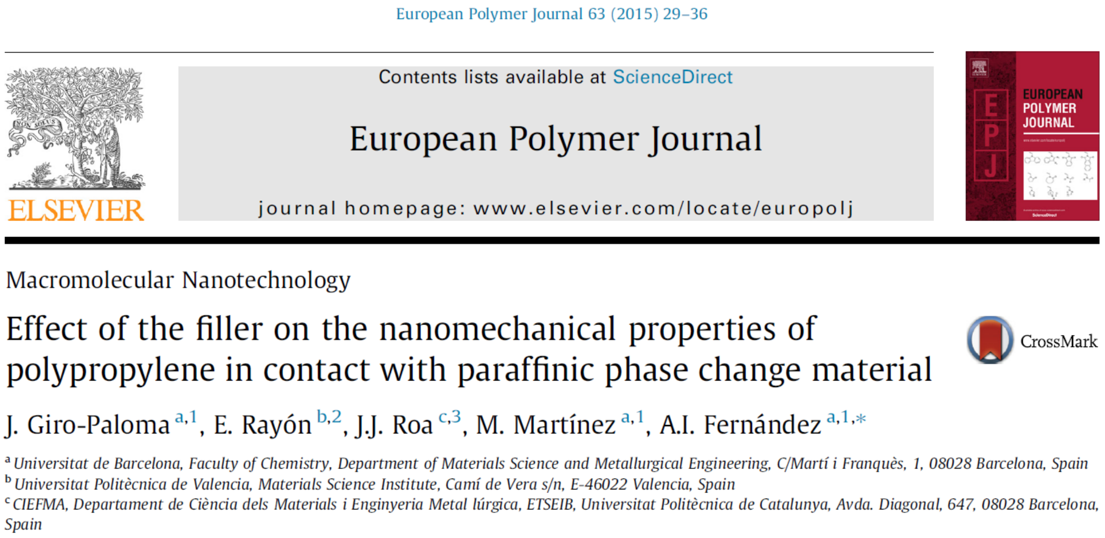
European Polymer Journal 63 (2015) 29–36

Contents lists available at ScienceDirect

European Polymer Journal

journal homepage: www.elsevier.com/locate/europolj

Macromolecular Nanotechnology

Effect of the filler on the nanomechanical properties of polypropylene in contact with paraffinic phase change material

J. Giro-Paloma [a,1], E. Rayón [b,2], J.J. Roa [c,3], M. Martínez [a,1], A.I. Fernández [a,1,*]

[a] Universitat de Barcelona, Faculty of Chemistry, Department of Materials Science and Metallurgical Engineering, C/Martí i Franquès, 1, 08028 Barcelona, Spain
[b] Universitat Politècnica de Valencia, Materials Science Institute, Camí de Vera s/n, E-46022 Valencia, Spain
[c] CIEFMA, Departament de Ciència dels Materials i Enginyeria Metal lúrgica, ETSEIB, Universitat Politècnica de Catalunya, Avda. Diagonal, 647, 08028 Barcelona, Spain

Figura R. 2. Artículo publicado en la revista European Polymer Journal en el año 2015, "Effect of the filler on the nanomechanical properties of polypropylene in contact with paraffinic phase change material".

Las conclusiones principales del estudio fueron que el uso del retardante de llama $Mg(OH)_2$ en el PP provoca cambios significativos el módulo de Young. Así pues, la dureza, el módulo de elasticidad y el módulo de pérdidas aumentan significativamente en comparación con la misma muestra sin $Mg(OH)_2$. Por otra parte, si este material compuesto está en contacto con PCM, las propiedades del material disminuyen de manera severa debido a que el PCM actúa como plastificante, y el polímero se ablanda. Además, también se observó que las propiedades del material empeoraron a medida que se aumentó la temperatura a la que se encontraba el PCM.

Es aquí cuando se procede al segundo bloque de la Tesis Doctoral, estudio a nivel microscópico, que comienza con una revisión de los estudios publicados por otros autores relacionados con los MPCM. Esta revisión está en proceso de aceptación, en la primera revisión. En ella se clasifican los MPCM según el tipo de PCM (orgánico, inorgánico, y eutéctico) y los diferentes tipos de cáscara. En la revisión también se explican detalladamente las distintas maneras de proceder para la fabricación de microcápsulas, según la metodología empleada (química, físico-química, o físico-mecánica). Igualmente, se comentan que los MPCM en contacto con agua son pulpas con materiales con cambio de fase (PCS), comentando estudios actuales con éste tipo de materiales. Al final de dicho manuscrito, se evalúan las maneras posibles de caracterizar MPCM, explicando cada técnica en detalle, con ejemplos de estudios científicos donde se aplican. Finalmente, se hace un apartado del gran abanico de aplicaciones de los MPCM. Esta revisión se titula: “**Types, methods, techniques, and applications for Microencapsulated Phase Change Materials**”, y fue aceptado el día 18/09/2015 en la revista **Renewable & Sustainable Energy Reviews** (Factor de impacto: 5.510, Q1).

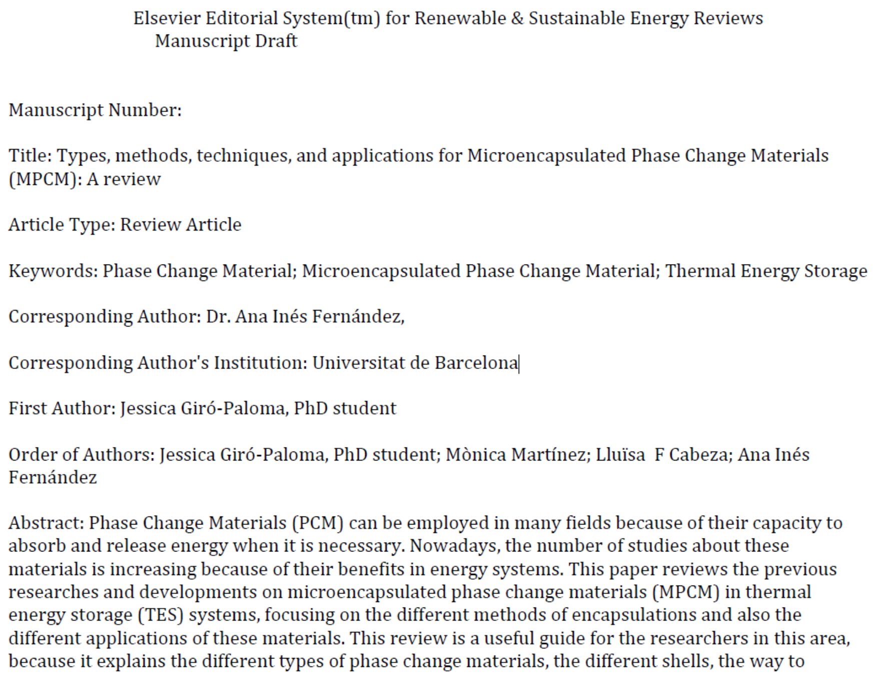

Elsevier Editorial System(tm) for Renewable & Sustainable Energy Reviews
Manuscript Draft

Manuscript Number:

Title: Types, methods, techniques, and applications for Microencapsulated Phase Change Materials (MPCM): A review

Article Type: Review Article

Keywords: Phase Change Material; Microencapsulated Phase Change Material; Thermal Energy Storage

Corresponding Author: Dr. Ana Inés Fernández,

Corresponding Author's Institution: Universitat de Barcelona

First Author: Jessica Giró-Paloma, PhD student

Order of Authors: Jessica Giró-Paloma, PhD student; Mònica Martínez; Lluïsa F Cabeza; Ana Inés Fernández

Abstract: Phase Change Materials (PCM) can be employed in many fields because of their capacity to absorb and release energy when it is necessary. Nowadays, the number of studies about these materials is increasing because of their benefits in energy systems. This paper reviews the previous researches and developments on microencapsulated phase change materials (MPCM) in thermal energy storage (TES) systems, focusing on the different methods of encapsulations and also the different applications of these materials. This review is a useful guide for the researchers in this area, because it explains the different types of phase change materials, the different shells, the way to

Figura R. 3. Estudio de MPCM aceptado en Renewable & Sustainable Energy "Reviews, Types, methods, techniques, and applications for Microencapsulated Phase Change Materials".

Relacionado con la temática de clasificación de PCM, está aceptado el capítulo de libro "**Microencapsulation of phase change materials**".en el libro **Handbook of Encapsulation & Controlled Release. CRC Press Taylor and Francis Group.**

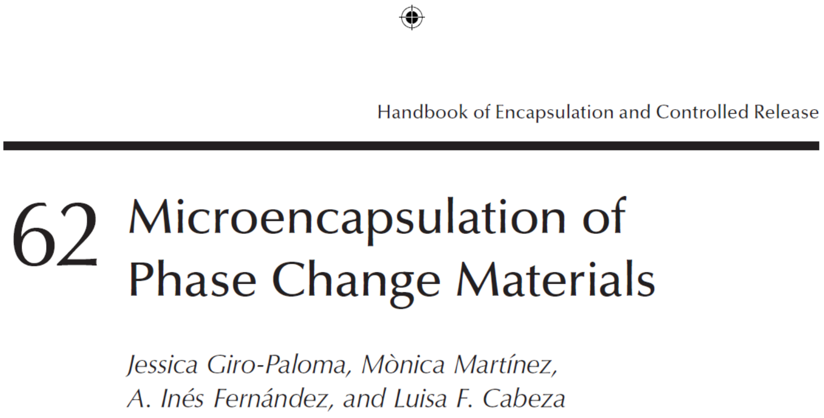

Handbook of Encapsulation and Controlled Release

62 Microencapsulation of Phase Change Materials

Jessica Giro-Paloma, Mònica Martínez, A. Inés Fernández, and Luisa F. Cabeza

Figura R. 4. Capítulo de libro aceptado en el Handbook of Encapsulation & Controlled Release titulado: "Microencapsulation of phase change materials".

También, en el año 2013 se presentó en Irlanda en el congreso **Sustainable Energy Storage in Buildings Conference, the 2nd International Sustainable Energy Storage Conference (IC-SES2)** el póster titulado "**Characterization of PCM conventional and non-conventional technologies**", en el que se incluyeron algunos de los resultados experimentales más relevantes llevados a cabo. Seguidamente se realizó con la caracterización química, física, térmica, mecánica, y ambiental de diferentes muestras de MPCM y PCS. Los primeros resultados de caracterización con AFM se presentaron en un póster en el congreso **BCNano'11** en Barcelona en el año 2011 que se tituló "**Stiffness characterization of Microencapsulated Phase Change Material by Atomic Force Microscopy**". El uso de la técnica de AFM para evaluar las propiedades mecánicas de las muestras se llevó a cabo a distintas temperaturas para simular el estado líquido/sólido del PCM en un sistema real.

Consecutivamente, se caracterizació una muestra comercial de MPCM, Micronal® DS 5001 de la compañía BASF, muy empleada en sistemas de almacenamiento pasivos. Se trata de una muestra sólida, en polvo, con un cambio de fase alrededor a los 26 ºC y es por este motivo que es muy empleada en sistemas constructivos. Se estudió en detalle la muestra usando diferentes técnicas, y los resultados fueron seleccionados como presentación oral en el congreso "**Innostock. The 12th International conference on energy storage**" en Lleida, en el año 2012. Del congreso, además, se publicaron dos capítulos de libro como resultado de la investigación: en el libro de resúmenes **ISBN: 978-84-938793-3-4,** depósito legal: L.638-2012 y también en el libro del congreso **ISBN: 978-84-938793-4-1,** depósito legal: L.742-2012. El artículo presentado en el congreso titulado "**Physico-chemical and mechanical properties of microencapsulated phase change material**", se seleccionó para ser publicado en la revista **Applied Energy** (Índice de impacto: 5.261, Q1), en el volumen 109, páginas 441 - 448. Cabe destacar que, según la bibliografía consultada, fue la primera vez que se usó la Microscopia de Fuerzas Atómicas (AFM) para muestras que contenían PCM.

En el estudio se determinó la composición de la muestra de Micronal® DS 5001, hallándose que las microcápsulas estaban formadas por un 23.5 % de polímero acrílico, un 67 % de PCM orgánico, y 9 % SiO_2. La observación de las MPCM mediante Microscopia Electrónica de Barrido, permitió determinar que la muestra estaba formada por esferas de 150 μm de tamaño compuestas por centenares de otras microcápsulas (las que contienen el PCM) de 6 μm. Además, se evaluaron las propiedades térmicas y también las mecánicas en función del tamaño de las micropartículas y de la temperatura. Para las microcápsulas se obtuvo que el módulo de Young disminuía considerablemente cuando la temperatura del ensayo aumentaba hasta valores próximos a la temperatura de transición vítrea de la cáscara.

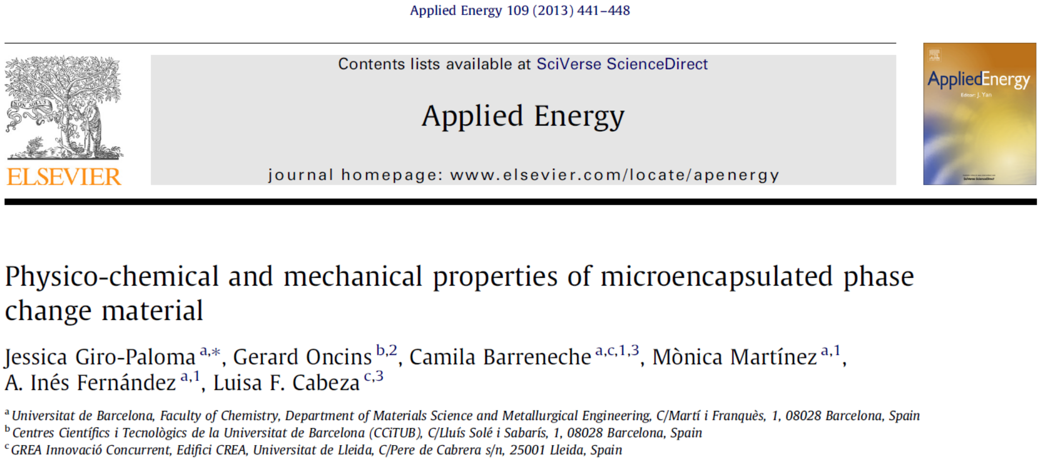

Applied Energy 109 (2013) 441–448

Contents lists available at SciVerse ScienceDirect

Applied Energy

journal homepage: www.elsevier.com/locate/apenergy

Physico-chemical and mechanical properties of microencapsulated phase change material

Jessica Giro-Paloma [a,*], Gerard Oncins [b,2], Camila Barreneche [a,c,1,3], Mònica Martínez [a,1],
A. Inés Fernández [a,1], Luisa F. Cabeza [c,3]

[a] Universitat de Barcelona, Faculty of Chemistry, Department of Materials Science and Metallurgical Engineering, C/Martí i Franquès, 1, 08028 Barcelona, Spain
[b] Centres Científics i Tecnològics de la Universitat de Barcelona (CCiTUB), C/Lluís Solé i Sabarís, 1, 08028 Barcelona, Spain
[c] GREA Innovació Concurrent, Edifici CREA, Universitat de Lleida, C/Pere de Cabrera s/n, 25001 Lleida, Spain

Figura R. 5. Artículo publicado en la revista Applied Energy enel año 2013 titulado “Physico-chemical and mechanical properties of microencapsulated phase change material”.

Aunque en la mayoría de estudios científicos consultados la caracterización de MPCM se hace en muestras comerciales, es importante realizar esta misma caracterización para muestras preparadas en laboratorios a fin de evaluar su competitividad frente a muestras que ya se encuentran en el mercado. Por esto, se evalúan durante la Tesis Doctoral muestras de MPCM obtenidas a escala de laboratorio. El siguiente estudio presentado en esta Tesis Doctoral fue realizado en colaboración con la Nigde University de Turquía y se titula “**Preparation and exhaustive characterization of paraffin or palmitic acid microcapsules as novel phase change material**”. Fue publicado en la revista **Solar Energy** (Índice de impacto: 3.541, Q1) en el año 2015, volumen 112, páginas 300 - 309.

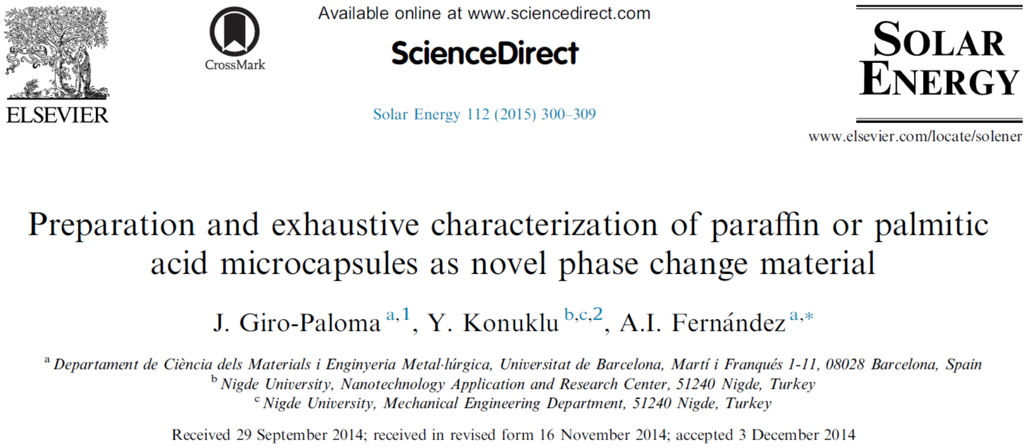

Available online at www.sciencedirect.com

ScienceDirect

Solar Energy 112 (2015) 300–309

SOLAR ENERGY

www.elsevier.com/locate/solener

Preparation and exhaustive characterization of paraffin or palmitic acid microcapsules as novel phase change material

J. Giro-Paloma [a,1], Y. Konuklu [b,c,2], A.I. Fernández [a,*]

[a] Departament de Ciència dels Materials i Enginyeria Metal·lúrgica, Universitat de Barcelona, Martí i Franqués 1-11, 08028 Barcelona, Spain
[b] Nigde University, Nanotechnology Application and Research Center, 51240 Nigde, Turkey
[c] Nigde University, Mechanical Engineering Department, 51240 Nigde, Turkey

Received 29 September 2014; received in revised form 16 November 2014; accepted 3 December 2014

Figura R. 6. Artículo publicado en Solar Energy, “Preparation and exhaustive characterization of paraffin or palmitic acid microcapsules as novel phase change material”.

En este estudio se caracterizaron dos tipos de MPCM donde la cáscara de ambas muestras era poli(estireno-co-acrilato de etilo) (PScEA), y como PCM se usó parafina 42-44 (cápsulas A) y ácido palmítico (cápsulas B). Por lo tanto, se evaluaron dos MPCM con misma cáscara y distinto PCM. La técnica que se empleó para la preparación de las MPCM fue la emulsión de co-polimerización (preparadas en la Universidad de Nidge, Turquía). Para su posterior caracterización se usaron varias técnicas: distribución del tamaño de partícula (PDS), microscopía electrónica de barrido (SEM), espectroscopia de infrarrojo (FT-IR), calorimetría diferencial de barrido (DSC), análisis termogravimétrico (TGA) y microscopía de fuerzas atómicas (AFM). Para éste último ensayo, los experimentos se realizaron a 25 ºC y 70 ºC, y fueron evaluados dos parámetros: el módulo de Young y la fuerza necesaria para romper la cáscara de las dos muestras de MPCM.

En esta investigación, los diámetros medios resultantes para las cápsulas A y B fueron 166 nm y 265 nm, respectivamente. Asimismo, los resultados de TGA indicaron una estabilidad térmica ligeramente superior para la muestra B en la misma las condiciones de trabajo. Los resultados de FT-IR manifestaron que ambos MPCM se encapsularon con éxito, sin pérdidas de PCM. Finalmente, los resultados por AFM confirmaron que no existían diferencias en *E* y que la fuerza aplicada necesaria para romper la microcápsula a diferentes temperaturas (25 ºC y 50 ºC), para la cápsula A es aproximadamente la misma. En cambio, la cápsula B no tiene el mismo comportamiento mecánico a 25 ºC y 70 ºC, debido a que la fuerza necesaria para romper la cáscara a 70 ºC es diez veces inferior, aunque los valores de *E* tuvieron un valor similar para dichas temperaturas.

Después de una evaluación química, física, térmica y mecánica de muestras de MPCM con el mismo tipo de cáscara y distinto PCM, se procedió a evaluar muestras de MPCM con distinta cáscara y mismo PCM. En este caso, se compararon MPCM compuestos por MMA (metil metacrilato) con tetracosano, y PS (poliestireno) con tetracosano de aproximadamente 1 - 2 μm de tamaño para ambas muestras. Se estudiaron en profundidad las propiedades mecánicas de ambos MPCM a dos temperaturas distintas: 23 ºC y 60 ºC. Los resultados obtenidos para las dos muestras denotan un descenso muy importante de las propiedades mecánicas cuando la temperatura aumenta a 60 ºC. A partir de estos resultados, se consideró interesante realizar otra comparativa usando la misma cáscara (PS) y el mismo PCM (tetracosano) a 23 ºC y 60 ºC pero distinta relación de encapsulación, pasando de 1:3 a 1:1 (cáscara:PCM). Se concluyó que la mejor combinación cáscara/PCM/relación de encapsulación para las muestras estudiadas y fabricadas en laboratorios es MMA/tetracosano/1:1.

Se ha comprobado que la caracterización mecánica es efectiva y relativamente rápida para encontrar propiedades muy relevantes de las muestras estudiadas. Es por este motivo, para saber si las muestras preparadas en los laboratorios son suficientemente competitivas, se deben de comparar con muestras comerciales. Esto es lo que se hizo en colaboración con la University of Auckland (New Zealand) durante los 3 meses de estancia realizados en el marco del proyecto Europeo INNOSTORAGE, PIRSES-GA-2013-610692 (Use of innovative Thermal Energy Storage for marked energy savings and significant lowering of CO_2 emissions), en el Department of Chemical & Materials Engineering bajo la supervisión del Prof. Mohammed M. Farid, y que ha dado lugar al artículo "**Characterization of Microencapsulated Phase Change Materials for use in Building Applications**", que se enviará a la revista **Materials**.

Los dos tipos de muestras de MPCM analizadas en el estudio estaban formadas por MMA como cáscara y parafina en el núcleo de la microcápsula. Debido a la temperatura del cambio de fase del PCM de ambas muestras, éstas son adecuadas para aplicaciones en edificios. La muestra comercial estudiada fue Micronal® DS 5008 X (de la compañía BASF) y la muestra que se preparó en el laboratorio de la University of Auckland por uno de los co-autores del artículo (Refat Al-Shannaq), se denominó M-2. Se observó la forma de las MPCM por SEM, y se estudiaron las propiedades térmicas por DSC, las propiedades mecánicas se determinaron mediante nanoindentación (determinando el módulo de Young, E_r, la dureza H, la carga al desplazamiento máximo, P_m, y el desplazamiento a máxima carga, h_m) y las propiedades medioambientales por cromatografía de gases (VOC's). Las conclusiones de este artículo ponen de manifiesto que las muestras preparadas por el equipo del Prof. Mohammed M. Farid presentan mejores propiedades que la muestra comercial. Asimismo, estos resultados fueron incluidos en una presentación oral en la **Training School Nº1. Advanced TES materials for building and Industrial applications** realizada en la Universitat de Barcelona en el año 2014, y que llevó por título "**Mechanical characterization of microencapsulated PCM (AFM, nanoindentation)"**.

Hasta este punto, se han evaluado MPCM para incluirlos en sistemas pasivos. A partir de este punto, se describe la evaluación de microcápsulas para sistemas activos. Cuando una muestra de MPCM se mezcla con un fluido caloportador (por ejemplo el agua), se crea lo que se denomina PCS (Phase Change Slurry o pulpas con material de cambio de fase), y se utilizan en sistemas activos.

En el congreso **Solar Heating and Cooling 2013** celebrado en Freiburg, se presentó una comunicación oral en colaboración con la Universidad de Zaragoza (España) que llevó por título "**Physicochemical and thermal study of a MPCM of PMMA shell and paraffin wax**

as a core”. Los resultados mostrados correspondían al estudio del rendimiento mecánico necesario para ejercer una fuerza en la parte superior de las microcápuslas de un PCS (Micronal® DS 5007 de BASF) utilizando un indentador. De este congreso salió el artículo que lleva por título “**Physicochemical and thermal study of a MPCM of PMMA shell and paraffin wax as a core**” publicado en la revista **Energy Procedia** el año 2014 en el volumen 48 en las páginas 347 -354.

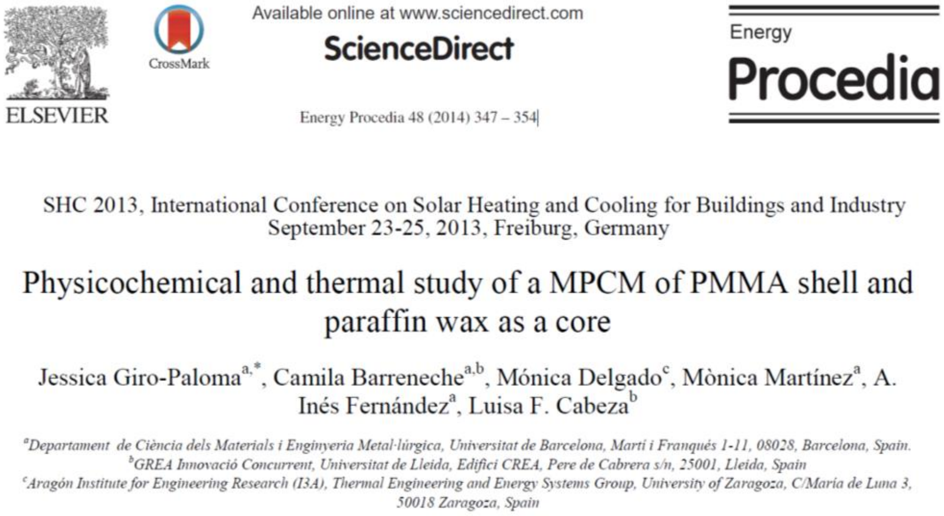

Available online at www.sciencedirect.com

ScienceDirect

Energy Procedia 48 (2014) 347 – 354

Energy Procedia

SHC 2013, International Conference on Solar Heating and Cooling for Buildings and Industry
September 23-25, 2013, Freiburg, Germany

Physicochemical and thermal study of a MPCM of PMMA shell and paraffin wax as a core

Jessica Giro-Paloma[a,*], Camila Barreneche[a,b], Mónica Delgado[c], Mònica Martínez[a], A. Inés Fernández[a], Luisa F. Cabeza[b]

[a]Departament de Ciència dels Materials i Enginyeria Metal·lúrgica, Universitat de Barcelona, Martí i Franqués 1-11, 08028, Barcelona, Spain.
[b]GREA Innovació Concurrent, Universitat de Lleida, Edifici CREA, Pere de Cabrera s/n, 25001, Lleida, Spain
[c]Aragón Institute for Engineering Research (I3A), Thermal Engineering and Energy Systems Group, University of Zaragoza, C/María de Luna 3, 50018 Zaragoza, Spain

Figura R. 7. Portada del artículo “Physicochemical and thermal study of a MPCM of PMMA shell and paraffin wax as a core”, publicado en la revista Energy Procedia, 2014.

Además, en el año 2014, se presentó como presentación oral, el estudio titulado “**Thermal Cycle Feasibility of Phase Change Slurry**”, en el congreso **Eurotherm Seminar #99, Advances in Thermal Energy Storage**, donde se mostraron los resultados obtenidos de la caracterización de muestras cicladas en la planta piloto de la Universidad de Zaragoza, de una muestra de Micronal® DS 5045 X, de la compañía BASF. Las muestras se bombearon 5000 y 7000 ciclos entre 21 y 28 ºC, para la evaluación de su durabilidad y para comparar las propiedades químicas y termofísicas antes y después de bombear la muestra.

Para evaluar la posible degradación de las MPCM durante el ciclado, se estudiaron la cáscara del PCS, la estabilidad de la pulpa, las propiedades químicas, térmicas y mecánicas antes y después del ciclado. Los resultados más destacables se observan en el análisis mediante DSC. En la muestra sin ciclar se obtuvo una única temperatura de fusión a 28 ºC, en cambio, en las muestras de 5000 y 7000 ciclos se observaron dos picos (2 temperaturas). Esto se atribuyó al hecho de que la cadena carbonada de la parafina se rompe después de cierto número de ciclos, obteniendo en el DSC dos puntos de fusión diferentes. Es decir, hay una degradación estructural en la cadena carbonada de la parafina porque no se obtiene un único pico definido. Sin embargo, hay sólo un 10 % de diferencia entre el punto de fusión de 0 y 7000 ciclos, lo que parece indicar que hay una ligera degradación térmica y modificaciones en los valores de entalpía y temperatura de fusión después de los ciclos térmicos, pero considerando que, a pesar de que con 7000 ciclos de las propiedades físicas de la muestra cambiaban, la muestra todavía conservó su comportamiento térmico en el sistema activo. Por este motivo se pudo concluir que las propiedades termo-físicas no cambian significativamente y que el comportamiento térmico para aplicación final acabará siendo prácticamente igual con la muestra ciclada y sin ciclar térmicamente. De la observación por SEM para las muestras 5000 veces cicladas se observó que la forma de las microcápsulas cambiaba con respeto a la no ciclada. Asimismo, no se observaron diferencias en la composición química mediante espectroscopia infrarroja después de los 7000 ciclos.

Después de los resultados obtenidos en el anterior artículo, se decidió profundizar más en las propiedades térmicas de éste mismo PCS. Por ello, se estudió el comportamiento térmico del PCS modificando su estado, de húmedo a seco, y los resultados obtenidos mostraron que cambiaban significativamente. Así pues, se decidió explorar las condiciones óptimas para el análisis del comportamiento térmico de un PCS en estado seco mediante análisis termogravimétrico. Los factores que se tuvieron en cuenta para la muestra PCS fueron la atmósfera de estudio (aire y N_2) y la velocidad de calentamiento (0.5, 1, 5, y 10 $^{\circ}C\ min^{-1}$). Este estudio, pendiente de finalizar para ser publicado, llevará por título "**Thermogravimetric study of a Phase Change Slurry: effect of experimental conditions**". En él la pulpa estudiada es Micronal® DS 5045 X, la cual está formada por microcápsulas con una cáscara acrílica y PCM de parafina. La observación mediante SEM acoplado a un sistema criogénico de N_2 revela que la pulpa está compuesta por cápsulas de 5 μm de diámetro. Los resultados parecen indicar que las mejores condiciones para la determinación de la temperatura del cambio de fase para este material en estado seco, se obtienen realizando el análisis termogravimétrico a una velocidad de calentamiento de 1 $^{\circ}C\ min^{-1}$, en atmósfera de nitrógeno. Por lo tanto, las condiciones experimentales a las que se realiza el ensayo es un punto clave a tener en cuenta.

Además del estudio anterior relacionado con los PCS, se llevó a cabo un análisis comparativo de pulpas entre una muestra comercial (Micronal® DS 5007 X) y una muestra preparada en el laboratorio (PCS28) por el Dr. Boštjan Šumiga coautor del estudio (Iskra Mehanizmi d.o.o., Slovenia). Los dos PCS contenían diferentes materiales para la cáscara y para el núcleo. En dicho estudio se hizo una caracterización química, física, térmica, y mecánica exhaustiva y se publicaronen dos artículos. El primero, "**Comparison of Phase Change**

Slurries. Physicochemical and thermal properties", publicado en el año 2015 en la revista **Energy,** volumen 87 y páginas 223 – 227, incluye los resultados obtenidos mediante DSC, TGA, FT-IR, y TGA/FT-IR. Los resultados confirmaron una cáscara acrílica para la muestra comercial Micronal® DS 5007 X y una cubierta polimérica externa de melamina-formaldehído para la muestra preparada en el laboratorio PCS28. Por otra parte, la muestra comercial tenía un cambio de fase entre 21 ºC y 23 ºC, y una entalpía alrededor de 90 $kJ\cdot kg^{-1}$. En cambio, la suspensión PCS28 tenía una temperatura de fusión de entre 22 ºC y 27 ºC con una entalpía de 50 $kJ\cdot kg^{-1}$. La principal conclusión fue que los PCS estudiados cumplían con los requisitos necesarios para su utilización en el almacenamiento de energía térmica, y pueden ser considerados como candidatos PCM para TES en la creación de aplicaciones activas o pasivas.

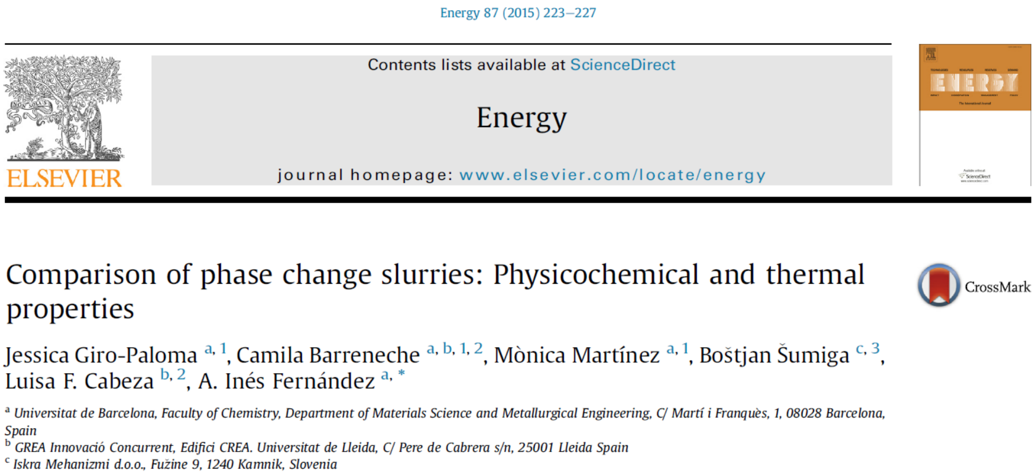
Energy 87 (2015) 223–227

Contents lists available at ScienceDirect

Energy

journal homepage: www.elsevier.com/locate/energy

ELSEVIER

Comparison of phase change slurries: Physicochemical and thermal properties

Jessica Giro-Paloma [a, 1], Camila Barreneche [a, b, 1, 2], Mònica Martínez [a, 1], Boštjan Šumiga [c, 3], Luisa F. Cabeza [b, 2], A. Inés Fernández [a, *]

[a] Universitat de Barcelona, Faculty of Chemistry, Department of Materials Science and Metallurgical Engineering, C/ Martí i Franquès, 1, 08028 Barcelona, Spain
[b] GREA Innovació Concurrent, Edifici CREA. Universitat de Lleida, C/ Pere de Cabrera s/n, 25001 Lleida Spain
[c] Iskra Mehanizmi d.o.o., Fužine 9, 1240 Kamnik, Slovenia

Figura R. 8. Portada del artículo "Comparison of Phase Change Slurries. Physicochemical and thermal properties", publicado en la revista Energy, 2015.

El segundo artículo ha sido publicado en el año 2016 en la revista **Renewable Energy** en el volumen 85 entre las páginas 732-739 y titulado "**Mechanical response evaluation of microcapsules from different slurries**". Este artículo incluye la caracterización de las partículas mediante PSD, SEM y AFM. Como conclusiones principales se observó que la muestra comercial Micronal® DS 5007 X presentaba un tamaño de partícula más grande que la muestra PCS28 preparada en el laboratorio via polimerización in situ, aunque el grosor de la pared de ambas muestras fuese muy similar. Además, la muestra PCS28 mostraba una aglomeración de las partículas tras un tiempo de almacenamiento. Desde el punto de vista mecánico, se corroboró la importancia de la temperatura del ensayo, ya que las propiedades mecánicas de las dos muestras disminuyen bruscamente cuando la temperatura aumenta. En resumen, desde el punto de vista mecánico, cáscaras acrílicas son mejores para sistemas MPCM para sistemas activos que cáscaras de MF.

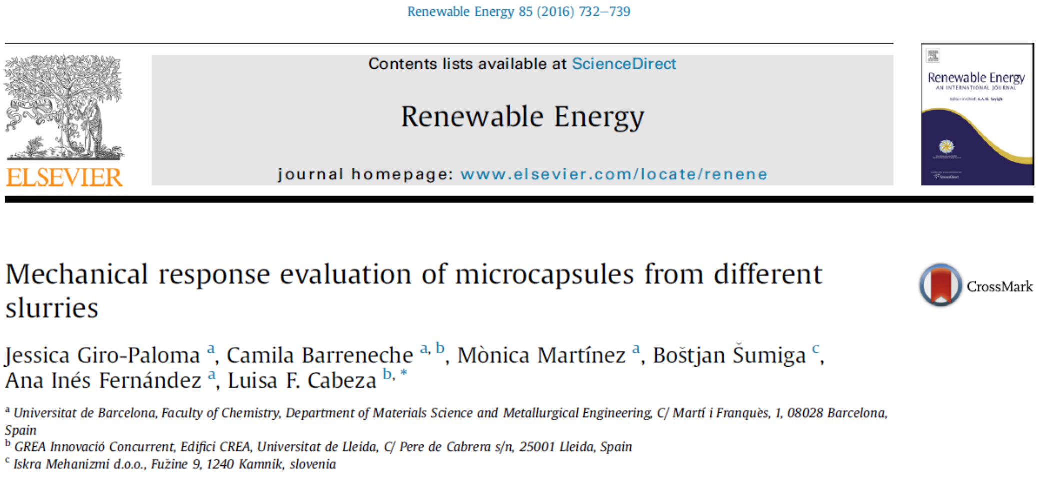

Renewable Energy 85 (2016) 732–739

Contents lists available at ScienceDirect

Renewable Energy

journal homepage: www.elsevier.com/locate/renene

Mechanical response evaluation of microcapsules from different slurries

Jessica Giro-Paloma [a], Camila Barreneche [a, b], Mònica Martínez [a], Boštjan Šumiga [c], Ana Inés Fernández [a], Luisa F. Cabeza [b, *]

[a] Universitat de Barcelona, Faculty of Chemistry, Department of Materials Science and Metallurgical Engineering, C/ Martí i Franquès, 1, 08028 Barcelona, Spain
[b] GREA Innovació Concurrent, Edifici CREA, Universitat de Lleida, C/ Pere de Cabrera s/n, 25001 Lleida, Spain
[c] Iskra Mehanizmi d.o.o., Fužine 9, 1240 Kamnik, slovenia

Figura R. 9. Portada del artículo “Mechanical response evaluation of microcapsules from different slurries”, publicado en la revista Renewable energy, 2015.

Además de todos los estudios publicados y pendientes de publicación que se exponen en la presente Tesis Doctoral, hay otras investigaciones, que incluyen resultados de la presente tesis, como la que lleva por título “**Unconventional technologies used for phase change materials (PCM) characterization. Part 2. Morphological and structural characterization, physico-chemical stability and mechanical properties**.”. Este se ha publicado en el año 2015 en la revista **Renewable & Sustainable Energy Reviews,** volumen 43, entre las páginas 1415 - 1426.

La realización de la Tesis Doctoral ha sido compaginada en los últimos cuatro años con el trabajo de técnico de laboratorio en el grupo de Investigación DIOPMA. Fruto de este trabajo, se han publicado otros trabajos de investigación, los cuales se citan a continuación:

Del Valle-Zermeño R, Chimenos JM, Giro-Paloma J, Formosa J. Use of weathered and fresh bottom ash mix layers as a subbase in road constructions: environmental behavior enhancement by means of a retaining barrier. Chemosphere 2014;117:402–9. doi:10.1016/j.chemosphere.2014.07.095.

Del Valle-Zermeño R, Giro-Paloma J, Formosa J, Chimenos JM. Low-grade magnesium oxide by-products for environmental solutions: Characterization and geochemical performance. Journal of Geochemical Exploration 2015. doi:10.1016/j.gexplo.2015.02.007.

Chapter 1 . Introduction

1.1. The need of storing heat

The quickly growing world energy use has increased the concern over supply difficulties, exhaustion of energy resources, and very important environmental impacts like climate change, global warming, ozone layer depletion, and others. The total contribution from buildings towards energy consumption, taking into account residential and commercial, has progressively raised reaching numbers in between 20 % and 40 % in developed countries [1]. The mode we produce, transfer, and utilize energy is varying a lot in the last few years. Besides, the rise in population, the increasing requirement for building services and comfort levels, and the augment in time in buildings, guarantee the growing tendency in energy demand in the upcoming; consequently, the energy systems and infrastructure have come under an important pressure. Because of this, the energy efficiency in buildings is nowadays a primordial purpose for energy policy at international levels.

Oil is the largest source of energy worldwide and electricity generation from fossil fuel. Thermal plants (combustion of oil) play a crucial role in many countries' electricity system by providing base load, backup, and peak load supply [2]. The demand for crude oil is increasing by approximately 2 % each year and the consumption presently around 28,000 million barrels/year. The continuous rise of oil consumption and the limited resources increase the price of oil year after year.

Among building services, the growth in heating, ventilation, and air-conditioning (HVAC) systems energy use are particularly significant (50% of building consumption) [3]. In an attempt to reduce the dependency on fossil fuels, considerable efforts have been made to find alternative renewable sources of energy or reduce the energy consumption through design and construction of efficient energy systems. One answer to the sporadic generated energy is the technology that can be stored until it is needed.

The Energy Storage (ES) concept differs significantly in how much energy can be stored, for how long, and if it can be achieved through chemical, mechanical, thermal or electromagnetic methods. ES is important to the achievement of any intermittent energy source in meeting demand; for instance, the storage necessity for solar energy applications is severe, especially when the solar availability is lowest, such as in winter. ES systems can contribute notably to meeting society's need for more efficient, environmentally benign energy use in building heating and cooling, aerospace power, and utility applications, among others. The use of ES systems frequently result in noteworthy benefits like reduced energy costs and energy consumption, improvement in the indoor air quality, reduction in the initial and maintenance costs, as well as in the equipment size and pollutant emissions. The energy demand in the commercial, industrial, and utility sectors varies on a daily, weekly, and seasonal basis.

Mechanical and hydraulic ES systems frequently store energy by converting electricity into compression, elevation or rotation energy. Besides, energy can also be stored chemically as reversible chemical reactions. Furthermore, thermal energy in the latent heat of melting materials such as paraffin and salts can be stored. Finally, electric energy in superconducting magnetic systems can also be stored. A large variety of ES techniques are under development, which can be classified as mechanical, thermal, chemical, biological, and magnetic.

Focusing in Thermal Energy Storage (TES), the basic principle is referred to the fact that energy is supplied to a storage system for removal and use at a later time. It is important to emphasize that seasonal storage requires immense storage capacity, where a complete storage process involves three steps: charging, storing, and discharging, as Figure 1.1 shows.

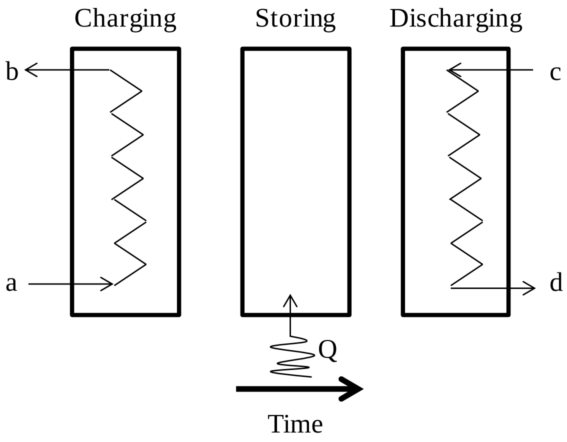

Figure 1.1. The charging, storing, and discharging in the storage process.

The benefits concerning TES field are related to the reduction of the electric bills by using off-peak electricity to produce and store energy for daytime cooling, increase generation capacity, shift energy purchases to low cost periods, and increase system reliability. By this thematic, there are different criteria for TES evaluation:

a) Technical criteria for TES, which is affected by the economics of the resultant systems. Certain criteria are: storage capacity, lifetime, size, cost, efficiency, safety, installation, environmental standards.

b) Environmental criteria for TES: the used materials should not be toxic or dangerous if released, or affect the environment during the manufacture, distribution, installation or operation of the storage system.

c) Economic criteria for TES: the economic justification for storage requires that the annualized capital and operating costs for TES have to be less than those required for primary generating equipment, supplying the same service loads and periods. For this reason, the cost-effectiveness should include hourly thermal loads for the peak day, comparison of the electrical load profile of the base-case system with TES, the size of the storage system and the control methods used, electricity demand charges and time-of-use costs, the costs of the storage, and financial incentives.

d) Energy savings criteria for TES are related to the well-design TES systems, because it can reduce earliest costs on projects due to the reduction of electricity, using the night produced electricity. As a result, significant savings of coal, natural gas, oil or nuclear fuel accrues to electric utilities and reduces pollutant emissions.

e) Sizing criteria for TES: improvement of the undersized and oversized systems.

f) Feasibility criteria for TES: considering the management, financial and economical parameters, the status of the TES system (new or existing), the space availability for the system, and the type of TES system (if open or closed).

g) Integration criteria for TES: information required about the facility occupancy hours and operating requirements, historic energy consumption rates, and financial analysis.

h) Storage durations criteria for TES: evaluate short-term, medium-term, and long-term.

The energy storage (over a number of hours per day) at low cost is a challenge to accomplish. For example, the use of Phase Change Materials (PCM) can increase the quantity of energy stored in a volume compared to hot water cylinders. Therefore, the main objective for scientist in this field is to investigate accurately how and where energy storage can make a more competent energy system over the next years, with the purpose to develop the needed technology for each system that delivers, regulating the regime which makes the concept into a commercial chance for the private sector [4].

Primary energy consumed in European countries comes generally from non-renewable and less sustainable sources, such as oil, gas, coal and nuclear, and the amount of all these primary energy resources have increased substantially in the lasts years. Any kind of extraction of energy products from natural sources to a usable form is called primary production, which takes place when the natural sources are exploited, for example in coal mines, crude oil fields, hydro power plants or fabrication of biofuels. Transformation of energy from one form to another, like electricity or heat generation in thermal power plants or coke production in coke ovens is not primary production. In Figure 1.2 is represented a line graph of primary production of energy in European countries.

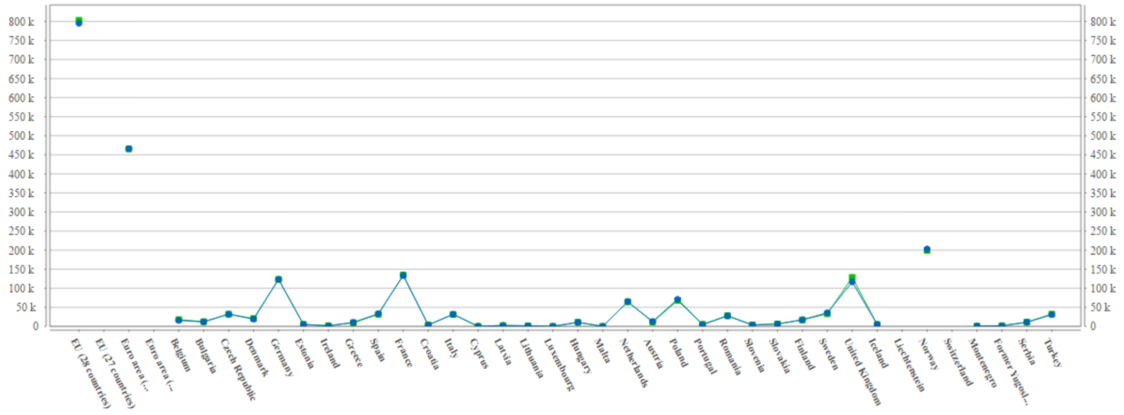

Figure 1.2. Primary production of energy by resource in European countries.

Final energy consumption in most of the European countries has increased as can be seen in Figure 1.3 [5,6]. Therefore, any measure of energy savings in buildings carries on an environmental benefit.

	1990	1992	1994	1996	1998	2000	2002	2004	2006	2008	2010	2012
EU (28 countries)	1,079,968.1	1,061,285.6	1,059,614.8	1,126,239.9	1,123,997.9	1,130,610.9	1,141,229.0	1,185,276.6	1,187,219.3	1,106,838.2	1,104,174.6	1,103,813.3
Belgium	31,621.5	33,287.7	33,883.2	36,668.6	37,386.9	37,766.5	36,406.9	37,994.7	36,306.1	34,137.4	36,069.5	34,802.3
Denmark	13,448.5	14,021.8	14,518.2	15,418.4	15,046.1	14,716.6	14,792.7	15,360.2	15,662.6	14,800.0	14,882.1	14,194.7
Germany	228,924.6	221,019.6	218,323.1	231,080.4	225,750.8	219,989.0	220,098.7	221,532.5	223,423.7	205,845.8	208,821.0	217,251.4
Estonia	5,666.9	3,477.1	2,864.4	2,999.5	2,673.8	2,434.0	2,626.5	2,817.9	2,879.2	2,764.7	2,835.4	2,870.4
Ireland	7,336.6	7,365.1	7,874.5	8,349.2	9,411.2	10,778.9	11,285.7	11,896.0	13,226.1	11,872.1	10,906.5	10,738.9
Greece	14,680.8	15,077.4	15,427.7	16,913.9	18,287.5	18,676.4	19,639.3	20,459.4	21,555.3	20,525.6	18,865.5	15,339.6
Spain	57,143.2	60,566.7	62,725.5	65,608.4	72,161.0	79,897.2	85,180.6	94,709.0	95,473.8	87,768.6	86,670.8	81,137.6
France	136,152.8	145,464.1	141,702.9	150,063.7	153,419.2	155,314.4	156,773.4	161,542.0	158,088.9	150,108.3	144,187.5	152,056.5
Croatia	5,932.6	4,090.9	4,373.2	4,679.4	5,223.0	5,371.3	5,627.4	6,184.2	6,461.2	6,350.7	6,192.8	5,812.5
Italy	107,710.9	110,854.3	109,760.0	115,667.3	120,120.9	124,720.2	125,449.4	132,763.3	132,629.5	120,944.2	122,133.7	118,696.2
Cyprus	1,101.1	1,318.3	1,352.3	1,477.0	1,549.1	1,649.1	1,722.1	1,833.7	1,864.7	1,934.4	1,918.8	1,614.8
Latvia	6,414.2	5,158.5	4,061.0	3,786.6	3,593.5	3,253.8	3,619.5	3,906.7	4,193.5	4,039.8	3,868.9	3,855.1
Lithuania	9,676.4	6,372.9	4,732.7	4,479.3	4,471.5	3,767.2	4,087.0	4,401.5	4,889.2	4,597.0	4,720.7	4,736.4
Luxembourg	3,284.8	3,513.0	3,505.0	3,201.7	3,139.3	3,505.1	3,709.7	4,389.5	4,411.4	4,077.3	4,297.4	4,129.0
Hungary	19,925.9	16,338.6	16,243.6	16,796.6	16,097.1	16,139.8	16,982.1	17,552.7	17,960.4	16,352.5	16,183.8	15,019.0
Malta	334.7	401.9	421.6	391.7	432.7	442.7	364.8	443.3	381.5	445.9	497.8	502.7
Netherlands	41,331.9	44,022.5	45,592.1	51,690.1	49,882.2	50,504.6	51,375.8	52,864.3	51,003.2	50,330.8	50,735.3	51,155.5
Austria	19,315.5	20,241.4	20,314.6	23,032.6	23,297.2	23,673.5	25,291.8	26,990.6	27,881.3	26,725.2	27,470.5	27,950.0
Poland	59,948.5	59,216.2	61,502.4	66,455.1	59,998.5	55,259.7	54,974.9	58,618.5	61,593.4	61,985.6	64,826.0	63,412.7
Portugal	11,896.5	12,801.1	13,512.9	14,647.1	16,262.4	17,918.9	18,639.0	18,932.6	18,781.7	18,188.4	17,310.3	15,846.7
Slovenia	3,738.8	3,401.1	3,865.2	4,481.4	4,377.7	4,457.3	4,586.0	4,819.1	4,946.1	4,737.0	4,963.3	4,798.3
Finland	21,452.0	20,929.6	22,171.3	22,405.1	23,954.1	24,510.3	25,549.4	26,203.4	26,571.1	23,813.3	24,950.6	24,614.7
Sweden	31,160.3	33,239.4	34,279.9	36,008.5	35,614.0	34,972.9	34,235.4	33,960.4	33,219.0	31,436.9	32,398.1	31,593.7
United Kingdom	136,893.5	140,096.9	142,725.2	150,657.2	148,912.0	153,235.9	149,594.4	152,978.1	150,661.0	137,009.4	131,606.8	136,432.4
Norway	16,087.3	15,785.8	16,678.3	17,426.3	18,181.4	18,093.6	18,089.4	18,485.3	18,541.6	18,260.3	18,692.9	18,777.4
Serbia	11,842.4	8,077.1	6,299.2	8,740.1	9,350.7	6,941.2	8,656.8	10,330.3	9,705.8	8,482.2	9,247.4	8,314.5
Turkey	38,648.7	40,065.2	41,040.4	49,106.8	50,334.1	56,162.3	55,274.4	61,111.6	69,063.4	69,827.8	78,680.4	82,921.7

Figure 1.3. Final consumption for sectors in European countries.

In general, the objectives in energy sector are mainly focused on developing a sustainable energy system supplied by renewable resources or widely available on the world market such as clean coal and nuclear energy. The technologies adjusted to achieve energy efficiency improvements and reducing energy consumption are also part of this strategy. Thermal Energy Storage (TES) example should be related on the energy savings in applications such as bioclimatic architecture or free cooling. Other examples are related with the demand curves in renewable energy production and cost reduction for the electrical energy consumption.

1.2. Materials for TES

TES acts as a role in reducing the difference between supply and demand, improving the performance and reliability of the energy systems. TES systems can be divided in two blocks: sensible heat thermal energy storage (SHTES) systems and latent heat thermal energy storage systems (LHTES) [7]. The heat transferred to a storage medium leads to a temperature increase of that medium. The heat stored in a process where the heat transferred to a storage medium increases the temperature of that medium, is known as SHTES. Subsequently, the energy stored by one substance or material as sensible heat is analyzed when it is subjected to temperature changes considering its specific heat. Sensible heat systems involve storing or extracting energy through a solid or liquid without changing phase, increasing and decreasing the temperature of the building envelopes, for example. On the other hand, in LHTES a temperature increment produces a temperature increase on the material evaluated. Then, the temperature remains constant during the phase change occurring but heat stored is increased. LHTES involve the energy released or absorbed during a constant temperature process like a change of state, for example. In Figure 1.4 is shown the difference between SHTES and LHTES.

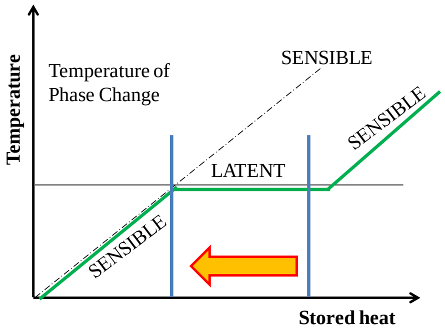

Figure 1.4. Sensible heat vs. Latent heat.

In Figure 1.5 is shown a scheme of the different types of TES, depending on the thermal or chemical energy storage [8]. Thermochemical Energy Storage (TCS) is included as a third category by many authors [9–11].

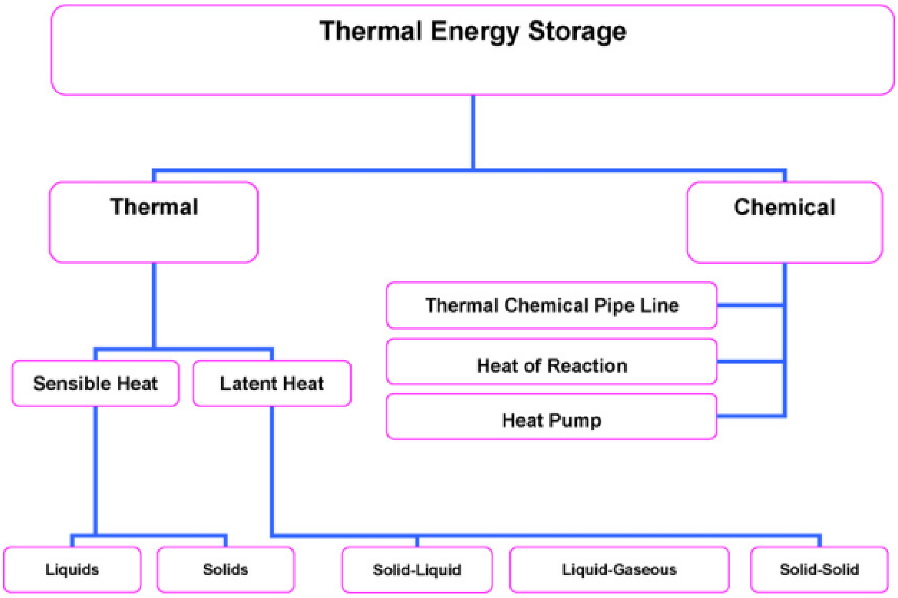

Figure 1.5. Types of thermal energy storage for thermal and chemical energy.

TES technologies, based on the use of phase change of the PCM, has recently caused a enormous interest, due to the high density of energy storage per volume unit in a given temperature range [8,12,13]. The PCM term refers to the material used where the energy absorbing phase change heat when melting and releasing it when solidified, all in a small range of temperatures within the temperature range of comfort, and they do so reproducible with respect to temperature and energy.

Thermal energy can be accumulated either as SHTES, TCS or as LHTES using PCM [14]. In Figure 1.6 is shown a diagram for the process of selection of a TES system.

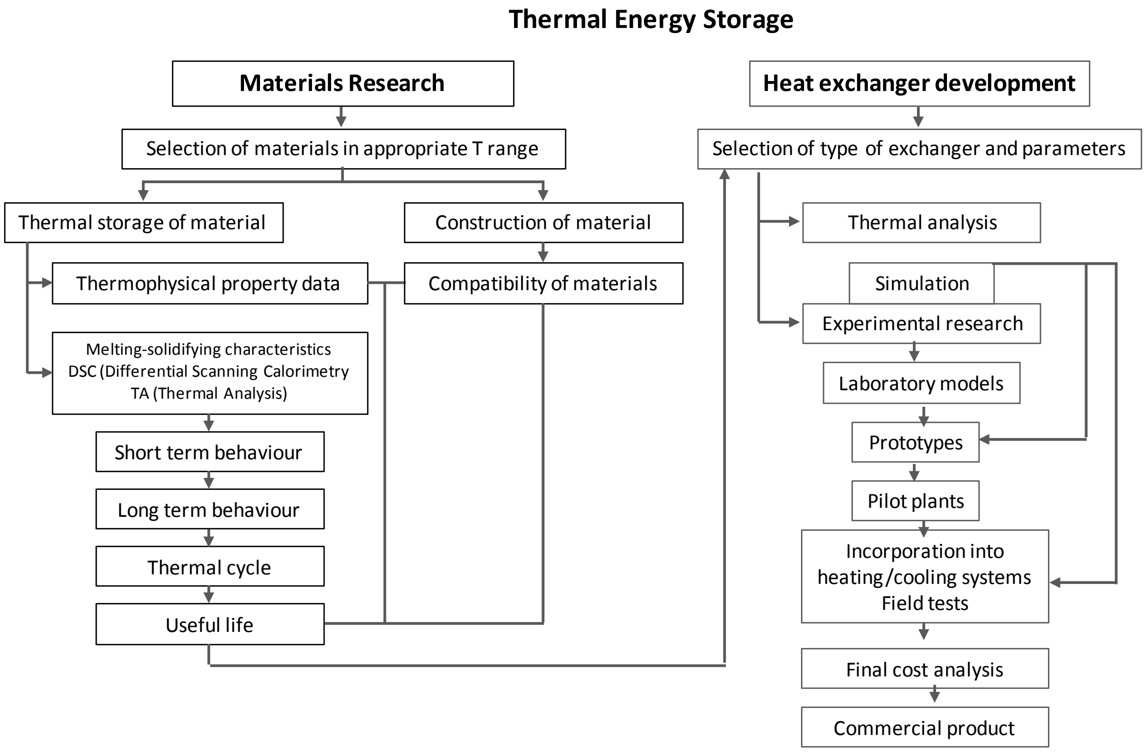

Figure 1.6. Areas of research in thermal storage systems.

TES in general and PCM in particular has been on the forefront of research for many industries for the last 30 years. There are some studies taking into account these materials suitable for TES in so many applications, in particular, in buildings [15,16]. A primordial aspect of solutions is the requisite to store unused energy for later use to diminish energy waste. Besides, the capacity to shift energy consumption and generation into a more controllable procedure gives an enlarged efficiency for power generating facilities [17]. TES can reduce the difference between demand and supply of accessible energy sources, offering security in energy supply, and using thermal protection to the system. The potential for the applications for this TES technology is practically unlimited because of its dense energy storage, the use of renewable sources, and sustainable practices [18]. In Figure 1.7 is represented the typical materials used as PCM as well as the orders of magnitude in terms of phase change temperature and enthalpy of fusion [19]. This figure shows some examples of materials used as PCM, which has been created by CES Selector [105] software, which allows comparing conventional materials with other developed materials in terms of thermal properties, mechanical properties, cost and embodied energy, among others.

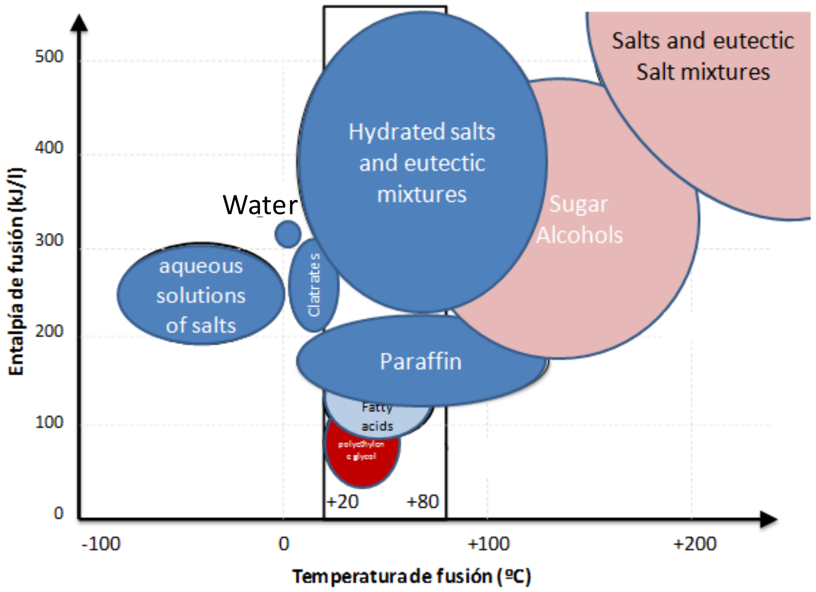

Figure 1.7. Typical materials used as PCM.

Among the different materials that can be used as PCM, a first differentiation is performed according to their nature: organic, inorganic, or eutectic. The main characteristics that will differentiate the behavior of the materials will be their storage capacity, thermal conductivity, phase segregation, undercooling, hysteresis, chemical stability, compatibility with other materials, flammability, and fire behavior.

For TES, the more employed transformations are solid-liquid, but also must be considered the solid-solid ones. The liquid-gas and solid-gas transformations are those involving a larger amount of energy having the disadvantage of requiring large amounts of storage. TES applications by changing solid-liquid phase are undergoing expansion due to the incorporation of new materials with very different properties. In the feasibility analysis of these applications four points are critical:

- to guarantee the stability of the material
- the necessity to know the thermophysical properties of materials as a function of temperature for a proper selection
- usage of numerical models with simulated operations
- price of materials

There are different companies supplying PCM for heat and cold storage such as: BASF (Germany) [20], Rubitherm GmbH (Germany) [21], MPCM Microtek Laboratories Inc. (USA)

[22], Cristopia (France) [23], ClimSel/Climator (Sweden) [24], PCM Thermal Solutions (USA) [25], Latest™ PCM Energy Products Ltd. (India) [26,27], Du Pont™/ Energain® (USA) [28], Aegis (USA) [29], Mitsubishi Chemical (Japan) [30], EPS Ltd (UK) [31], Suntech [32], Merck Kga (Germany) [33], TEAP Energy (Australia), CEPSA (Spain) [34], Condea Vista Company Inc. (USA), Exxon (USA) [35], Repsol YPF (Spain) [36], Shell (Nederland) [37], and Witco (USA) [38].

TES can offer energy efficiency in the economy and environmental impact, the materials used have low thermal conductivity [39] and usually entails loading and unloading of low power levels. In front of the criticism of this limitation, it is important to develop innovative composite materials and high thermal conductivity related to TES units adapted to the expected performances. The use of PCM [8,14,40–43] embedded in passive building elements could reduce the needed for the electricity demand in periods of peak requirement, in the buildings [7,15,44–49], such as cooling systems [50–52], and photovoltaic cells [53].

The main drawbacks of materials in LHTES are related to the low thermal conductivity, density changes, and thermal stability properties for long time utilization, as well as, large undercooling [13,54], and the lack ability to store large amounts of energy considering their volume. In addition, they cannot provide precise temperature control. On the other hand, LHTES systems use the storage capacity of a material’s phase change, releasing or storing a remarkable amount of energy in a small volume, with the inclusion of PCM to increase thermal inertia [55]. The employment of PCM for TES in buildings [56] was one of the firsts studied applications, being the first one described in the literature, by Telkes *et al.* in 1975 [57], considering their use for heating and cooling, and the second one by Lane *et al.* in 1986 [58]. In 1990 Salyer *et al.* [59] described a series of PCM applicable to thermal storage in buildings the reaction of fire to fire-retardant additives (organic halogenous compounds), achieving an improvement on the answer to fire of the material. Two studies by Hadorn [56] in 2005 and Paksoy [60] in 2007, evaluated different TES technologies, being PCM in buildings included [61–63]. Moreover, in 2008 Mehling *et al.* [19] studied deeply the PCM for TES technology. Recently, Zhou *et al*. [49] and Tatsidjodoung *et al*. [64] have reviewed a manuscript where it is summarized the last studies of materials for thermal energy storage in building applications. Although there is a lot of research in this field, unfortunately prior to the large-scale practical application of this technology, it is necessary to resolve numerous problems in the research and development stage because more investigation is needed to find out new more competent and cheap materials giving improved solutions to technical problems, like segregation or leakage, materials compatibility, and subcooling [65].

The application of PCM may be really wide, as any system that requires a small range of temperatures steady for some time, precisely this type of material phase change to take effect. Currently, studying such materials is expanding exponentially around the world. Therefore, it is a subject very innovative in the field of materials science.

Paraffin has been widely used for LHTES applications because of their large latent heat and proper thermal characteristics, which are little or without supercooling, low vapor pressure, good thermal and chemical stability, and self-nucleating behavior. Despite these desirable properties of paraffin, the low thermal conductivity (0.21-0.24 $W\cdot(m\cdot K)^{-1}$) is the major disadvantage of paraffin materials, decreasing the rates of heat stored and released during melting and crystallization processes which, in turn, limits their utility areas [66], [67], and [14]. The thermal conductivity can be increased by adding 5 % of some surfactants [68], such as sodium myristate, sodium palmitate, and sodium stearate. It is well reported that these surfactants are efficient in depressing the liquid/solid phase change temperature, reducing undercooling, and increasing the amount of latent heat of fusion, as well as thermal conductivity of eutectic PCM compared to eutectic PCM without surfactants. Otherwise, melting time test showed that the increasing thermal conductivity of paraffin noticeably decreased its melting time [69].

Another way to overcome the low thermal conductivity problem of paraffin, several studies have been performed with the objective of developing LHTES systems with unfinned and finned configurations [70], [71], [72] and [73], dispersing high conductivity particles in paraffin [74], and inserting a metal matrix into paraffin wax [75]. Nevertheless, uses of such type of heat transfer promoters considerably increase the volume and weight of the LHTES systems. For this reason, carbon fibers and carbon fiber brushes have been lastly used as heat diffusion supporters in paraffin because of their high thermal conductivities and low weight [76] and [77]. The effects of adding various carbon nanofillers on the thermal conductivity and energy storage properties of paraffin based nanocomposite phase change materials (PCMs) for thermal energy storage (including short and long multi-walled carbon nanotubes, carbon nanofibers, and graphene nanoplatelets (GNPs)) were a top topic of research these lasts years. Fan *et al*. [78] stated that the presence of nanofillers decrease the phase change enthalpies and has negligible influence on the phase change temperatures. Moreover, porous graphite matrices also have been used to improve thermal conductivity of paraffin [79] and with PCM [80–82]. One more mode to improve thermal properties in paraffin without any surfactant is by the addition of 20 nm of diameter of TiO_2 nanoparticles [83], concluding that the thermal conductivity increases with the increase of TiO_2 nanoparticles, but decrease with increasing temperature and phase change. Besides, they highlight that the proportion TiO_2/paraffin composites have a lower thermal conductivity in the liquid state than in the solid state. Oxides and nano-additives, such as alumina (Al_2O_3), titania (TiO_2), silica (SiO_2), and zinc oxide (ZnO), are common to improve thermal stability of PCM [38].

A wide variety of PCM with different temperature profiles, hysteresis, and heat storage capacities are available these days for building applications [85]. The ideal thermal characteristics for a PCM takes into account very small hysteresis used for the parametric thermal simulations [86]. The hysteresis phenomenon of the PCM in the enthalpy-temperature curve is a very important point to consider because the thermal performance of the TES unit is seriously affected by this phenomenon [87]. It appears during cooling process of materials, and results in a delay of the phase change. The hysteresis had three main contributions: due to the PCM itself, due to the temperature measurement, and due to the air temperature [88], and the smaller the hysteresis of the PCM, the lower will be the prediction error of the conventional approach [89].

There are some options reported in scientific literature to solve specific particularities such as hysteresis phenomena [87] or sub-cooling [90]. The nucleating agents may incorporate PCM, which have a melting point higher than the selected PCM, or aliphatic derivatives of alkanes, which favor the reduction of hysteresis. Nanosilica, nanoclays, nanotalc, nanoneedles and mineral or organic carbonaceous nanomaterials (fullerenes, nanotubes, and graphenes carbon nanofibers and their derivatives, nanoreinforcements with organic or inorganic modification or without modification), talc, zeolites, and clays can be used to promote the crystallization of the PCM and reduce subcooling and hysteresis of materials [91].

1.3. PCM in buildings

Although water is the mostly used PCM, there is a necessity for improving and developing new applications involving the usage of other materials. There is some international researches who are developing new materials that can be used as PCM at certain temperature for different applications in TES systems [7,47,92–94]. Nevertheless, research is still needed to find new more efficient and cheap materials.

The usage of solar energy for heating and cooling during day/night (storing heat and cold) is an important goal that has to be considered in the application of PCM in buildings. Basically, there are three manners to use PCM in buildings for heating and cooling usage:

- PCM in building walls
    a. PCM Trombe wall [95]
    b. PCM wallboard [96]
    c. PCM shutter [97]
    d. Under-floor heating systems [98]
    e. Ceiling boards [99]
- PCM in other building components
- PCM in heat and cold storage units [19]

PCM in wallboards and wall plasters compensate for temperature peaks, offering comfort owing to their passive building cooling mechanism, and can even allow to distribute with an air-conditioning system overall [100]. As it is shown in Figure 1.8, when the temperature increases, the paraffin wax melts and the PCM absorbs heat. Whereas, when the temperature drops, the paraffin wax solidifies and heat is released. During its phase change, the temperature remains constant. It is because of this that PCM take their name from their action mechanism. Their active temperature compensation mechanism allows construction materials which have been modified to give perfect room comfort.

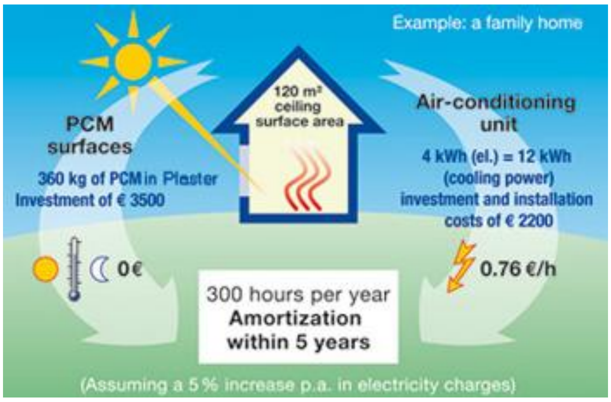

Figure 1.8. Important savings by using PCM in a building [100].

PCM usage in building materials could be aided in two ways:

1) Active solar energy stores which implies less energy consumption [60]. Thus, a temperature fluctuation of surrounding environment should be over and under the PCM melting temperatures during day and night, respectively. During day, PCM absorbs heat and prevents indoor temperature to rise up, while at night, when the temperature drop down, the energy absorbed during the day is released and rising up indoor temperature, in this way no or less cooling and heating required.

2) Electricity peak-load shifting which is related to the economy [101]. The PCM usage in building could be helped in shifts most of the load coming from residential air conditions from peak to off-peak electricity taxes.

When PCM is implemented in gypsum board, plaster, concrete and/or other wall covering materials, thermal storage is part of the building structure, even for light weight buildings [102]. PCM in concrete material has appropriate latent heat storage and thermal performance. Otherwise, PCM have some negative impacts on the properties of concrete. These can be reduced if the proper PCM and a suitable means of incorporation are used during the production of the composite [103].

PCM will be selected depending on their melting temperature, for example materials that melt below 15 ºC will be used for storing coolness in air conditioning applications and materials that melt above 90 ºC will be used for absorption refrigeration [104]. Materials that melt between these two mentioned temperatures can be applied in solar heating and for heat load leveling applications, which represent the class of materials that has been studied the most. Nevertheless, there are some key questions that Pons *et al*. [106] made in their review such as which are most suitable PCM to be used? Also, it is asked if the integration of PCM in buildings with concrete structures can be generalized.

1.4. The PCM leakage

A challenge with PCM undergoing phase change at ambient temperature used in buildings relies in containing them in an appropriate matrix. This is because organic PCM have a tendency to leak to the surface of the matrices in which they are contained, during the phase change process. This leads to the surface becoming oily and stained, and to the thermal storage properties of the PCM gradually diminish.

PCM leakage in the melt phase is an issue that must be controlled for widespread adoption. Most leakage process is made during its solid-liquid phase change [69]. Furthermore, it is known that PCM leakage is influenced by the PCM surface energy and viscosity [107]. Leakage process can be produced in two ways: mixing PCM with constructive materials or in the encapsulation process. Encapsulation of phase change materials in micro scale (MPCM) can be assisted to overcome these leakage problems [102,108–111]. Microencapsulation is an advanced technology to implement PCM avoiding leakage from building materials [112]. In the microencapsulation process it is very important to take into account some parameters such as the mixing temperature, mixing time, PCM content, heating rate, cooling rate, and others [113].

Although the encapsulation and the preparation of form-stable PCM can prevent efficiently leakage in a PCM system, the polymeric shell or the polymeric supporting material leads to reduce thermal conductivity due to their low thermal conductivity coefficient. For this reason, it is really important to deeply study phase change material composites with enhanced heat conductivity, avoiding liquid leakage during its phase change. In most cases, leakage will be avoided if the polymeric shell has an appropriate structural strength [114] and must have adequate robustness to avoid shell rupturing during the mixing process with building materials.

1.5. Why encapsulation is needed?

In order to prevent the liquid leakage during the solid-liquid phase change of PCM, a general solution is to encase PCM in spherical capsules [115,116]. In order to reduce costs, there is a huge interest in looking for different kind of materials to contain PCM. One possibility is the usage of polymers but their main problem is that they soften in contact with organic PCM [117], and eventually can suffer environmental stress cracking (ESC) which is one of the main causes of thermoplastic polymers failure (especially the amorphous ones) [118–121] in secondary fluids.

The ESC mechanism is a physical interaction connecting highly localized plasticization via stress enhanced fluid absorption, which does not carry molecular degradation of the plastic nor chemical variations. The absorption of organic PCM (such as paraffin waxes) plasticizes the polymer and also reduces its yield strength. This reduction is directly associated with the concentration of absorbed fluid [122]. Also, the ESC is the combination of a susceptible material, an specific environment, and an applied force [123–125], as Figure 1.9 shows. In this mechanism there is no breakage of chemical bonds, but secondary polymer joints. For this reason, the ESC can be defined as the physical interaction that involves a high located plasticizing through a tensile given by a fluid absorption, which does not involve a chemical change or plastic molecular degradation.

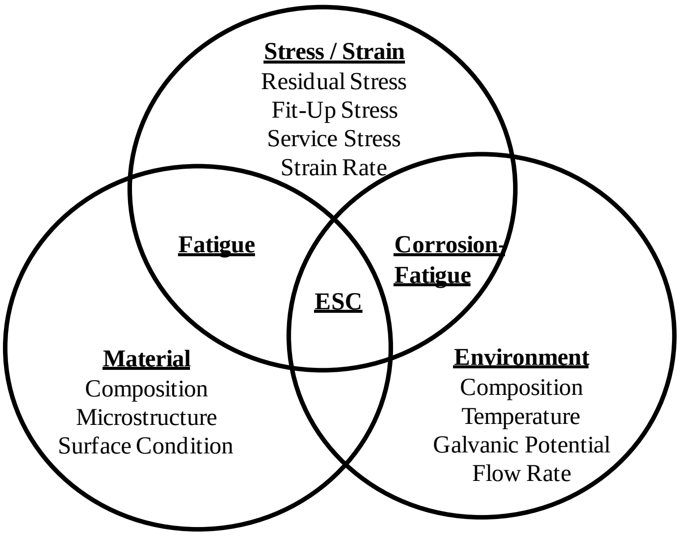

Figure 1.9. ESC mechanism, which involves a material, an environment and an specific stress.

Polymers exposure in a different medium from air will accelerate the ESC mechanism, producing cracks at fewer forces than in air atmosphere. Within the failures, the ESC is estimated to be a 25 % of the general, 15 % due to fatigue, a 14 % static indentation breakage, 8 % for creep, 7 % for chemical attack, 6 % due to UV attack, and 4 % because of thermal degradation, as Figure 1.10 shows [126].

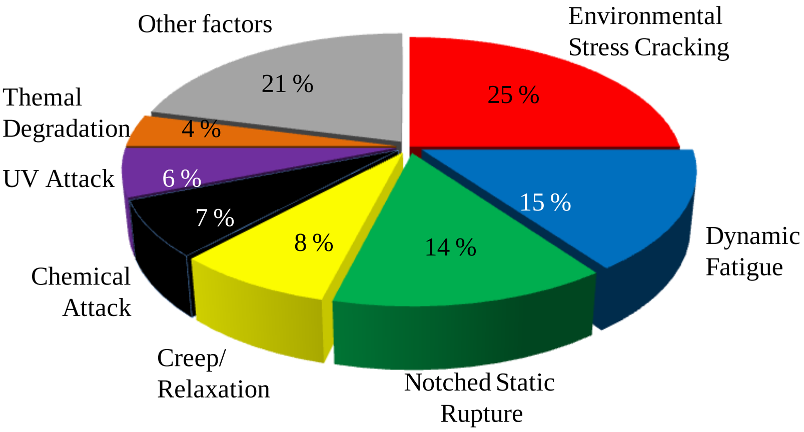

Figure 1.10. Causes of material failure.

As higher density and/or crystallinity of a polymer, higher tensile strength; also, it will lead to higher probability to have ESC in a material over time. Thus, less density means higher ESC resistance (ESCR), as well as, higher molecular weight of a plastic will derive to higher ESCR [127].

Despite all the inconvenient outlined above, energy storage in building envelopes may be improved by encapsulating appropriate PCM within surfaces to capture the solar energy directly [128]. Hence, there exist stable microcapsules as containers made of polymer on the outside, and PCM in it to store energy. For this reason, to study the best polymer acting as encapsulator/container among several polymers, my master degree was about the study of eight polymers in contact prolonged time with paraffin wax as PCM in order to find the best paraffin-polymer compatibility as an alternative for PCM containers. The studied polymers were polyethylene high density (HDPE), polystyrene (PS), acrylonitrile butadiene styrene (ABS), polyamide/Nylon 6 (PA6), polycarbonate (PC), poly(methyl methacrylate) (PMMA), amorphous polyethylene terephthalate (PET), polyvinyl chloride unplasticized (PVCU). It was done several tests for all of these polymers, taking into account the chemical, physical, thermal, and mechanical characterization [129]. Besides, it was studied the behavior of two PCM in contact with these polymers, RT-25 and RT-42. Hence, considering all the studied parameters, it was concluded that:

- Hardness and Young's modulus results were as follows:
  $H_{ABS} < H_{HDPE} < H_{PS} < H_{PA6} < H_{PVCU} < H_{PET} < H_{PC} < H_{PMMA}$,
  being > 3 GPa for the highest and around 2 GPa for the lowest
  $E_{HDPE} < E_{PA6} < E_{PS} < E_{ABS} < E_{PC} < E_{PET} < E_{PVCU} < E_{PMMA}$,
  being >200 MPa for the highest values and < 100 MPa for the lowest one
- Less working temperature means less amount of paraffin absorbed by the polymer
- Paraffin acts as a plasticizer when it is in contact with the studied polymers
- For producing a macrocontenidor or microcontenidor for PCM it has to use a polymer with moderate density, low crystallinity, high Young's modulus and hardness, with low absorption of PCM
- PMMA is the best polymer of the studied ones as a shell due to the mechanical properties. Other polymers with good properties are PVC, PET and PC

Due to the accelerate ESC mechanism that polymers can suffer when they are in contact in a short period of time with a fluid, it was considered the importance of exploring the necessity to characterize these polymers above mentioned to study their stiffness. For this reason, it was evaluated the possibility to make some tests with these polymers to create a working methodology when the mechanical properties were required. In this way, nanoindentation allows to characterize in a fast way some important parameters such as Hardness (H), Young's modulus (E), Loss modulus (E_{loss}), and Loss factor ($\tan \delta$) [130].

1.6. Thesis objectives

After finalizing my Master degree in Advanced Chemistry (specialty in Material Science and Metallurgical Engineering) at Universitat de Barcelona and obtaining some relevant results, it was considered to continue the investigation related with polymers and PCM in my PhD Thesis. As a main result obtained from the Master Degree, poly(methyl methacrylate) is considered the best polymer (taking into account eight studied polymeric samples) as PCM container. Following these investigation paths, it was started the chemical, physical, thermal, and mechanical studies some commercial microencapsulated PCM (MPCM) with acrylic shell. The main objective of this was the evaluation of the durability of these MPCM taking into consideration the stiffness of the shell. For this reason, after the characterization of some commercial MPCM it was studied the same properties into laboratory made microcapsules. Once we obtained good results with samples used for passive systems, we were encouraged to go one step further and evaluate these same samples for active systems (phase change slurries, PCS).

Both active and passive microcapsules were also cycled to study their thermal reliability and it was studied the maximum service life of these materials. Hence, it was needed the physico-chemical and mechanical performance of the durability of MPCM and also PCS samples before and after pumping them through thermal reliability or thermal cycle feasibility.

Because organic PCM are flammable it was decided to study a composite composed by a polymer with a flame retardant such as $Mg(OH)_2$, and compare their mechanical properties when the sample is in contact or not with PCM in liquid state.

As mechanical characterization has an important part in my PhD Thesis, there was the necessity to deepen in this kind of evaluation. Two different techniques were employed: Atomic Force Microscopy (AFM) and nanoindentation technique. The first one is widely employed to characterize materials such as ceramics, metals, and polymers, and nanoindentation technique is a tool extensively used in materials except in polymers. For this reason, it was very innovative the proposed methodology that we defined and it is embodied in this PhD Thesis.

Because of the concern in how PCM volatiles can harm human health, in my PhD stage in Auckland (New Zealand) it was evaluated the main organic compounds that can be spread to the environment.

Chapter 1 References

[1] http://www.iea.org/, 17/02/2015 n.d.

[2] Al Shannaq R. Microencapsulation of Phase Change Materials (PCMs) for Thermal Energy Storage Application. University of Auckland, 2014.

[3] Pérez-Lombard L, Ortiz J, Pout C. A review on buildings energy consumption information. Energy and Buildings 2008;40:394–8. doi:10.1016/j.enbuild.2007.03.007.

[4] Dutil Y, Rousse DR, Salah N Ben, Lassue S, Zalewski L. A review on phase-change materials: Mathematical modeling and simulations. Renewable and Sustainable Energy Reviews 2011;15:112–30. doi:10.1016/j.rser.2010.06.011.

[5] http://www.iea.org/statistics/index.htm, 17/02/2015 n.d.

[6] http://ec.europa.eu/eurostat/tgm/refreshTableAction.do?tab=table&plugin=1&pcode=tsdpc320&language=en, 14/10/2014 n.d.

[7] Cabeza LF, Castell A, Barreneche C, De Gracia A, Fernández AI. Materials used as PCM in thermal energy storage in buildings: A review. Renewable and Sustainable Energy Reviews 2011;15:1675–95.

[8] Sharma A, Tyagi VV, Chen CR, Buddhi D. Review on thermal energy storage with phase change materials and applications. Renewable and Sustainable Energy Reviews 2009;13:318–45. doi:10.1016/j.rser.2007.10.005.

[9] Solé A, Martorell I, Cabeza LF. State of the art on gas–solid thermochemical energy storage systems and reactors for building applications. Renewable and Sustainable Energy Reviews 2015;47:386–98. doi:10.1016/j.rser.2015.03.077.

[10] Solé A, Miró L, Barreneche C, Martorell I, Cabeza LF. Corrosion of metals and salt hydrates used for thermochemical energy storage. Renewable Energy 2015;75:519–23. doi:10.1016/j.renene.2014.09.059.

[11] Mette B, Kerskes H, Drück H, Müller-Steinhagen H. New highly efficient regeneration process for thermochemical energy storage. Applied Energy 2013;109:352–9. doi:10.1016/j.apenergy.2013.01.087.

[12] Dincer I. Thermal Energy Storage: Systems and Applications. 2002.

[13] Khudhair AM, Farid MM. A review on energy conservation in building applications with thermal storage by latent heat using phase change materials. Energy Conversion and Management 2004;45:263–75. doi:10.1016/S0196-8904(03)00131-6.

[14] Zalba B, Marín JM, Cabeza LF, Mehling H. Review on thermal energy storage with phase change: Materials, heat transfer analysis and applications. Applied Thermal Engineering 2003;23:251–83.

[15] Tyagi VV, Buddhi D. PCM thermal storage in buildings: A state of art. Renewable and Sustainable Energy Reviews 2007;11:1146–66. doi:10.1016/j.rser.2005.10.002.

[16] Wang X, Zhang Y, Xiao W, Zeng R, Zhang Q, Di H. Review on thermal performance of phase change energy storage building envelope. Chinese Science Bulletin 2009;54:920–8.

[17] Zalba B, Marín JM, Cabeza LF, Mehling H. Review on thermal energy storage with phase change: materials, heat transfer analysis and applications. Applied Thermal Engineering 2003;23:251–83. doi:10.1016/S1359-4311(02)00192-8.

[18] http://www.puretemp.com/blog1.html n.d.

[19] Mehling H CL. Heat and cold storage with PCM. An up to date introduction into basics and applications. 2008.

[20] http://www.basf.com/group/corporate/es/, 10/03/2014 n.d.

[21] http://www.rubitherm.de/, 10/03/2014 n.d.

[22] http://www.microteklabs.com/index.html, 10/03/2014 n.d.

[23] http://www.cristopia.com/, 10/03/2014 n.d.

[24] http://www.climator.com/en/home/, 10/03/2014 n.d.

[25] http://www.pcm-solutions.com/, 10/03/2014 n.d.

[26] http://www.pcmenergy.com/products/general.htm, 10/03/2014 n.d.

[27] http://www.teappcm.com/, 10/03/2014 n.d.

[28] http://www.dupont.com/, 10/03/2014 n.d.

[29] http://www.aegischemical.com/, 10/03/2014 n.d.

[30] http://www.mitsubishichemical.com/, 10/03/2014 n.d.

[31] http://www.epsltd.co.uk/, 10/03/2014 n.d.

[32] http://www.suntech-power.com/en/, 10/03/2014 n.d.

[33] http://www.merckgroup.com/en/index.html, 10/03/2014 n.d.

[34] http://www.cepsa.com/cepsa/Quienes_somos/La_compania/Historia/, 10/03/2014 n.d.

[35] http://www.exxon.com/usa-english/gfm/, 10/03/2014 n.d.

[36] http://www.repsol.com/es_ca/, 10/03/2014 n.d.

[37] http://www.shell.com/, 10/03/2014 n.d.

[38] http://www.witcoinc.net/, 10/03/2014 n.d.

[39] Calvet N, Py X, Olivès R, Bédécarrats J-P, Dumas J-P, Jay F. Enhanced performances of macro-encapsulated phase change materials (PCMs) by intensification of the internal effective thermal conductivity. Energy 2013;55:956–64. doi:10.1016/j.energy.2013.03.078.

[40] Delgado M, Lázaro A, Mazo J, Zalba B. Review on phase change material emulsions and microencapsulated phase change material slurries: Materials, heat transfer studies and applications. Renewable and Sustainable Energy Reviews 2012;16:253–73. doi:10.1016/j.rser.2011.07.152.

[41] Kuznik F, David D, Johannes K, Roux J-J. A review on phase change materials integrated in building walls. Renewable and Sustainable Energy Reviews 2011;15:379–91. doi:10.1016/j.rser.2010.08.019.

[42] Zhang P, Ma ZW. An overview of fundamental studies and applications of phase change material slurries to secondary loop refrigeration and air conditioning systems. Renewable and Sustainable Energy Reviews 2012;16:5021–58. doi:10.1016/j.rser.2012.03.059.

[43] Pasupathy a., Velraj R, Seeniraj RV. Phase change material-based building architecture for thermal management in residential and commercial establishments. Renewable and Sustainable Energy Reviews 2008;12:39–64. doi:10.1016/j.rser.2006.05.010.

[44] Arce P, Castellón C, Castell A, Cabeza LF. Use of microencapsulated PCM in buildings and the effect of adding awnings. Energy and Buildings 2012;44:88–93.

[45] Cabeza LF, Castellón C, Nogués M, Medrano M, Leppers R, Zubillaga O. Use of microencapsulated PCM in concrete walls for energy savings. Energy and Buildings 2007;39:113–9. doi:10.1016/j.enbuild.2006.03.030.

[46] Castell a., Martorell I, Medrano M, Pérez G, Cabeza LF. Experimental study of using PCM in brick constructive solutions for passive cooling. Energy and Buildings 2010;42:534–40. doi:10.1016/j.enbuild.2009.10.022.

[47] Barreneche C, Fernández AI, Niubó M, Chimenos JM, Espiell F, Segarra M, et al. Development and characterization of new shape-stabilized phase change material (PCM) - Polymer including electrical arc furnace dust (EAFD), for acoustic and thermal comfort in buildings. Energy and Buildings 2013;61:210–4. doi:10.1016/j.enbuild.2013.02.026.

[48] Lazaro A, Dolado P, Marín JM, Zalba B. PCM-air heat exchangers for free-cooling applications in buildings: Experimental results of two real-scale prototypes. Energy Conversion and Management 2009;50:439–43.

[49] Zhou D, Zhao CY, Tian Y. Review on thermal energy storage with phase change materials (PCMs) in building applications. Applied Energy 2012;92:593–605. doi:10.1016/j.apenergy.2011.08.025.

[50] Nogues M, Valles M, Bourouis M, Boer D, Coronas A. Absorption-compression heat pump for space heating and cooling using organic fluids. American Society of Mechanical Engineers, Advanced Energy Systems Division (Publication) AES 2000;40:3–10.

[51] Berhane HG, Gonzalo GG, Laureano J, Dieter B. Design of environmentally conscious absorption cooling systems via multi-objective optimization and life cycle assessment. Applied Energy 2009;86:1712–22.

[52] Gebreslassie BH, Guillén-Gosálbez G, Jiménez L, Boer D. Design of environmentally friendly absorption cooling systems via multi-objective optimization and life cycle assessment. Computer Aided Chemical Engineering 2009;26:1099–103.

[53] Huang MJ, Eames PC, Norton B. Phase change materials for limiting temperature rise in building integrated photovoltaics. Solar Energy 2006;80:1121–30. doi:10.1016/j.solener.2005.10.006.

[54] Calvet N, Olivès R, Bédécarrats JP, Py X, Dumas JP, Jay F. Latent heat storage enhancement by thermal conductivity intensification. EFFSTOCK, the 11th International Conference on Thermal Energy Storage, 2009.

[55] Kenisarin MM, Kenisarina KM. Form-stable phase change materials for thermal energy storage. Renewable and Sustainable Energy Reviews 2012;16:1999–2040. doi:10.1016/j.rser.2012.01.015.

[56] Hadorn JC. Thermal energy storage for solar and low energy buildings. 2005.

[57] Telkes M. Thermal storage for solar heating and cooling. Proceedings of the Workshop on Solar Energy Storage Subsystems for the Heating and Cooling of Buildings, Virginia, USA: 1975.

[58] Lane GA. Solar Heat Storage: Latent Heat Material Vol II. 1986.

[59] Salyer IO, Sircar AK. Phase change materials for heating and cooling of residential buildings and other applications. Proceedings of the 25th Intersociety Energy Conversion Engineering Conference-IECEC 90, 1990.

[60] Paksoy HO. Thermal energy storage for sustainable energy consumption: fundamentals, case studies and design 2007.

[61] Cabeza LF. Storage techniques with phase change materials. 2005.

[62] Mehling H, Cabeza LF. Phase change materials and their basic properties. Thermal energy storage for sustainable energy consumption: fundamentals, case studies and design. 2007.

[63] Mehling H, Cabeza L, Yamaha M. Phase change materials: application fundamentals. Thermal energy storage for sustainable energy consumption: fundamentals, case studies and design. 2007.

[64] Tatsidjodoung P, Le Pierrès N, Luo L. A review of potential materials for thermal energy storage in building applications. Renewable and Sustainable Energy Reviews 2013;18:327–49. doi:10.1016/j.rser.2012.10.025.

[65] Kenisarin M, Mahkamov K. Solar energy storage using phase change materials. Renewable and Sustainable Energy Reviews 2007;11:1913–65. doi:10.1016/j.rser.2006.05.005.

[66] Abhat A. Low temperature latent heat thermal energy storage: heat stoarge materials. Solar Energy 1983;30:313–32.

[67] Sharma SD, Sagara K. Latent Heat Storage Materials and Systems: A Review. International Journal of Green Energy 2005;2:1–56. doi:10.1081/GE-200051299.

[68] Fauzi H, Metselaar HSC, Mahlia TMI, Silakhori M, Nur H. Phase change material: Optimizing the thermal properties and thermal conductivity of myristic acid/palmitic acid eutectic mixture with acid-based surfactants. Applied Thermal Engineering 2013;60:261–5. doi:10.1016/j.applthermaleng.2013.06.050.

[69] Sarı A, Karaipekli A. Thermal conductivity and latent heat thermal energy storage characteristics of paraffin/expanded graphite composite as phase change material. Applied Thermal Engineering 2007;27:1271–7. doi:10.1016/j.applthermaleng.2006.11.004.

[70] Ismail KA., Alves CL., Modesto MS. Numerical and experimental study on the solidification of PCM around a vertical axially finned isothermal cylinder. Applied Thermal Engineering 2001;21:53–77. doi:10.1016/S1359-4311(00)00002-8.

[71] Velraj R, Seeniraj RV, Hafner B, Faber C, Schwarzer K. Heat transfer enhancement in a latent heat storage system. Solar Energy 1999;65:171–80. doi:10.1016/S0038-092X(98)00128-5.

[72] Liu Z, Sun X, Ma C. Experimental investigations on the characteristics of melting processes of stearic acid in an annulus and its thermal conductivity enhancement by fins. Energy Conversion and Management 2005;46:959–69. doi:10.1016/j.enconman.2004.05.012.

[73] Liu Z, Sun X, Ma C. Experimental study of the characteristics of solidification of stearic acid in an annulus and its thermal conductivity enhancement. Energy Conversion and Management 2005;46:971–84. doi:10.1016/j.enconman.2004.05.011.

[74] Siegel R. Solidification of low conductivity material containing dispersed high conductivity particles. International Journal of Heat and Mass Transfer 1977;20:1087–9. doi:10.1016/0017-9310(77)90195-8.

[75] Tonga X, Khana.J.A., RuhulAmin M. Enhancement of heat transfer by inserting a metal matrix into a phase change material. Numerical Heat Transfer, Part A: Applications: An International Journal of Computation and Methodology 1996;30:125–41.

[76] Frusteri F, Leonardi V, Vasta S, Restuccia G. Thermal conductivity measurement of a PCM based storage system containing carbon fibers. Applied Thermal Engineering 2005;25:1623–33. doi:10.1016/j.applthermaleng.2004.10.007.

[77] Fukai J, Kanou M, Kodama Y, Miyatake O. Thermal conductivity enhancement of energy storage media using carbon fibers. Energy Conversion and Management 2000;41:1543–56. doi:10.1016/S0196-8904(99)00166-1.

[78] Fan L-W, Fang X, Wang X, Zeng Y, Xiao Y-Q, Yu Z-T, et al. Effects of various carbon nanofillers on the thermal conductivity and energy storage properties of paraffin-based nanocomposite phase change materials. Applied Energy 2013;110:163–72. doi:10.1016/j.apenergy.2013.04.043.

[79] Py X, Mauran S. Paraffin/porous-graphite-matrix composite as a high and constant power thermal storage material 2001;44:2727–37.

[80] Yu J, Pan DK, Chen Q. Graphite foam encapsulated phase change materials for thermal management of MCM. Frontiers of Energy and Environmental Engineering 2013:136–40.

[81] Pincemin S, Py X, Olives R, Christ M, Oettinger O. Elaboration of Conductive Thermal Storage Composites Made of Phase Change Materials and Graphite for Solar Plant. Journal of Solar Energy Engineering, Transactions of the ASME 2007;130.

[82] Pincemin S, Olives R, Py X, Christ M. Highly conductive composites made of phase change materials and graphite for thermal storage. Solar Energy Materials and Solar Cells 2008;92:603–13. doi:10.1016/j.solmat.2007.11.010.

[83] Wang J, Xie H, Guo Z, Li Y. Improved thermal properties of paraffin wax by the addition of TiO2 nanoparticles. 2nd International Workshop on Heat Transfer Advances for Energy Conservation and Pollution Control, Xina: 2013, p. 1–6.

[84] Teng TP, Yu CC. Characteristics of phase-change materials containing oxide nano-additives for thermal storage. Nanoscale Res Lett 2012;7:611.

[85] Climates SUS, Kosny J, Shukla N, Fallahi A. Cost Analysis of Simple Phase Change Material-Enhanced Building Envelopes in 2013.

[86] Dolado P, Lazaro A, Marin JM, Zalba B. Characterization of melting and solidification in a real scale PCM-air heat exchanger: Numerical model and experimental validation. Energy Conversion and Management 2011;52:1890–907.

[87] Bony J, Citherlet S. Numerical model and experimental validation of heat storage with phase change materials. Energy and Buildings 2007;39:1065–72. doi:10.1016/j.enbuild.2006.10.017.

[88] Dolado P, Lazaro A, Marin JM, Zalba B. Characterization of melting and solidification in a real-scale PCM-air heat exchanger: Experimental results and empirical model. Renewable Energy 2011;36:2906–17.

[89] Gowreesunker BL, Tassou SA, Kolokotroni M. Improved simulation of phase change processes in applications where conduction is the dominant heat transfer mode. Energy and Buildings 2012;47:353–9. doi:10.1016/j.enbuild.2011.12.008.

[90] Günther E, Mehling H, Hiebler S. Modeling of subcooling and solidification of phase change materials. Modelling and Simulation in Materials Science and Engineering 2007;15:879–92. doi:10.1088/0965-0393/15/8/005.

[91] Cabello JM, Masía R, Runbio AA. PCM encapsulation method, 2012.

[92] Barreneche C, Navarro H, Serrano S, Cabeza LF, Fernández AI. New Database on Phase Change Materials for Thermal Energy Storage in Buildings to Help PCM Selection. Energy Procedia 2014;57:2408–15. doi:10.1016/j.egypro.2014.10.249.

[93] Li G, Zhang B, Li X, Zhou Y, Sun Q, Yun Q. The preparation, characterization and modification of a new phase change material: CaCl2·6H2O–MgCl2·6H2O eutectic hydrate salt. Solar Energy Materials and Solar Cells 2014;126:51–5. doi:10.1016/j.solmat.2014.03.031.

[94] Lee T, Chiu YH, Lee Y, Lee HL. Thermal properties and structural characterizations of new types of phase change material: Anhydrous and hydrated palmitic acid/camphene solid dispersions. Thermochimica Acta 2014;575:81–9. doi:10.1016/j.tca.2013.10.008.

[95] Ghoneim AA, Klein SA, Duffie JA. Analysis of collector-storage building walls using phase-change materials. Solar Energy 1991;47:237–42. doi:10.1016/0038-092X(91)90084-A.

[96] Schossig P, Henning H-M, Gschwander S, Haussmann T. Micro-encapsulated phase-change materials integrated into construction materials. Solar Energy Materials and Solar Cells 2005;89:297–306. doi:doi:10.1016/j.solmat.2005.01.017.

[97] Mehling H. Innovative PCM-Technology. Results and future perspectives. 8th expert meeting and workshop, Turkey: 2004.

[98] Nagano K, Mochida T, Iwata K, Hiroyoshi H, Domanski R, Rebow M. Development of new PCM for TES of the cooling system. Terrastock. 8th International Conference on Thermal Energy Storage, 2000.

[99] Gutherz J, Schiler M. A passive solar heating system for the perimeter zone of office buildings. Energy Sources 1991;13:39–54.

[100] http://www.micronal.de/portal/basf/ien/dt.jsp?setCursor=1_290798, 14/10/2014 n.d.

[101] Khudhair AM, Farid MM. Use of phase change materials for thermal comfort and electrical energy peak load shifting: Experimental investigations. ISES Solar World Congress 2007, ISES 2007, vol. 1, 2007, p. 283–8.

[102] Tyagi VV, Kaushik SC, Tyagi SK, Akiyama T. Development of phase change materials based microencapsulated technology for buildings: A review. Renewable and Sustainable Energy Reviews 2011;15:1373–91. doi:10.1016/j.rser.2010.10.006.

[103] Ling T-C, Poon C-S. Use of phase change materials for thermal energy storage in concrete: An overview. Construction and Building Materials 2013;46:55–62. doi:10.1016/j.conbuildmat.2013.04.031.

[104] Farid MM, Khudhair AM, Razack SAK, Al-Hallaj S. A review on phase change energy storage: materials and applications. Energy Conversion and Management 2004;45:1597–615. doi:10.1016/j.enconman.2003.09.015.

[105] Khare S, Dell’Amico M, Knight C, McGarry S. Selection of materials for high temperature latent heat energy storage. Solar Energy Materials and Solar Cells 2012;107:20–7. doi:10.1016/j.solmat.2012.07.020.

[106] Pons O, Aguado A, Fernández AI, Cabeza LF, Chimenos JM. Review of the use of phase change materials (PCMs) in buildings with reinforced concrete structures. Materiales de Construcción 2014;64:315.

[107] Chen F. Leakage control and characterization of form stable phase change materials: Polymer(matrix)/polymer (PCM) binary blends and natural fiber/polymer(matrix)/ polymer (PCM) ternary composites. Washington State University, 2013.

[108] Zhang H, Xu Q, Zhao Z, Zhang J, Sun Y, Sun L, et al. Preparation and thermal performance of gypsum boards incorporated with microencapsulated phase change materials for thermal regulation. Solar Energy Materials and Solar Cells 2012;102:93–102. doi:10.1016/j.solmat.2012.03.020.

[109] Toppi T, Mazzarella L. Gypsum based composite materials with micro-encapsulated PCM: Experimental correlations for thermal properties estimation on the basis of the composition. Energy and Buildings 2013;57:227–36. doi:10.1016/j.enbuild.2012.11.009.

[110] Borreguero AM, Garrido I, Valverde JL, Rodríguez JF, Carmona M. Development of smart gypsum composites by incorporating thermoregulating microcapsules. Energy and Buildings 2014;76:631–9. doi:10.1016/j.enbuild.2014.03.005.

[111] Borreguero AM, Carmona M, Sanchez ML, Valverde JL, Rodriguez JF. Improvement of the thermal behaviour of gypsum blocks by the incorporation of microcapsules containing PCMS obtained by suspension polymerization with an optimal core/coating mass ratio. Applied Thermal Engineering 2010;30:1164–9. doi:10.1016/j.applthermaleng.2010.01.032.

[112] Giro-Paloma J, Barreneche C, Delgado M, Martínez M, Fernández AI, Cabeza LF. Physicochemical and thermal study of a MPCM of PMMA shell and paraffin wax as a core. Energy Procedia, vol. 48, 2014, p. 347–54. doi:10.1016/j.egypro.2014.02.040.

[113] Huan Rui Liu, Yang W Bin, Pu XY, Zhang K. Study on Leakage Rate of HDPE/Paraffin Composite for Phase Change Materials. Advanced Materials Research 2012;549:766–9.

[114] Sari A, Akcay M, Soylak M, Onal A. Polymer-stearic acid blends as form-stable phase change material for thermal energy storage. Journal of Scientific & Industrial Research 2005;64:991–6.

[115] Cho K, Choi SH. Thermal characteristics of paraffin in a spherical capsule during freezing and melting processes. International Journal of Heat and Mass Transfer 2000;43:3183–96. doi:10.1016/S0017-9310(99)00329-4.

[116] Hawlader MNA, Uddin MS, Khin MM. Microencapsulated PCM thermal-energy storage system. Applied Energy 2003;74:195–202. doi:10.1016/S0306-2619(02)00146-0.

[117] Giro-Paloma J, Rayón E, Roa JJ, Martínez M, Fernández AI. Effect of the filler on the nanomechanical properties of polypropylene in contact with paraffinic phase change material. European Polymer Journal 2015;63:29–36. doi:10.1016/j.eurpolymj.2014.11.029.

[118] Henry LF. Prediction and evaluation of the susceptibilities of glassy thermoplastics to environmental stress cracking. Polymer Engineering & Science 1974;14:167–76.

[119] Arnold JC. The influence of liquid uptake on environmental stress cracking of glassy polymers. Materials Science and Engineering: A 1995;197:119–24. doi:10.1016/0921-5093(94)09759-3.

[120] Hansen CM. On predicting environmental stress cracking in polymers. Polymer Degradation and Stability 2002;77:43–53. doi:10.1016/S0141-3910(02)00078-2.

[121] Hough MC, Wright DC. Two new test methods for assessing environmental stress cracking of amorphous thermoplastics. Polymer Testing 1996;15:407–21. doi:10.1016/0142-9418(95)00048-8.

[122] Castellón C, Martorell I, Cabeza LF, Fernández AI, Manich AM. Compatibility of plastic with phase change materials (PCM). International Journal of Energy Research 2011;35:765–71. doi:10.1002/er.1723.

[123] O'Connor C. Material Selection for Plastic Design. n.d.

[124] http://www.rapra.net/consultancy/enviromental-testing-enviromental-stress-cracking.asp, 14/10/2014 n.d.

[125] Bravo J. Estudio del fenómeno de Craqueo por Tensión Ambiental. Universidad de Xile, 2003.

[126] http://www.rapra.net/consultancy/product-design-and-manufacture-plastic-design-and-material-selection.asp, 14/10/2014 n.d.

[127] D.C. W. Environmental Stress Cracking of Plastics. 1996.

[128] Khudhair AM, Farid MM. A review on energy conservation in building applications with thermal storage by latent heat using phase change materials. Energy Conversion and Management 2004;45:263–75. doi:10.1016/S0196-8904(03)00131-6.

[129] Giro-Paloma J. Materials plàstics com a contenidors de PCM. Universitat de Barcelona, 2011.

[130] Herbert EG, Oliver WC, Pharr GM. Nanoindentation and the dynamic characterization of viscoelastic solids. Journal of Physics D: Applied Physics 2008;41:074021. doi:10.1088/0022-3727/41/7/074021.

Block I, Macroscopic samples

Chapter 2: Characterization with nanoindentation

Chapter 2 . Characterization with nanoindentation

2.1 Nanoindentation technique

2.2 Comparison between Loubet and Oliver & Pharr methodologies depending on the nature of the materials

2.3 Study of the effect of $Mg(OH)_2$ as inorganic filler in a PP matrix in contact with different paraffinic PCM

The mechanical properties of a material describe how it will react to external forces. Mechanical properties are inherent to each material and can be determined through a series of standardized mechanical tests [1]. A typical test is the compressive strength, which describes the capacity of a material to resist loads to reduce its size, while hardness is the indentation resistance.

The indentation is a technique that has been broadly applied to measure the mechanical properties of materials with high spatial resolution. The basic concepts used to accurately apply the technique, as well as some of the newest measurement frontiers being explored today, will be presented in this chapter. The process of converting load versus displacement measurements to materials properties through an understanding of the geometry associated with the experiments is the basis for these experiments. The newest techniques that will be mentioned include experiments in electron microscopes, testing at room temperatures and high-speed testing for the mapping of properties. The challenges associated with these frontiers will be briefly discussed. This is applied for assessing fracture toughness due to the simplicity and expediency of experiments, and because it potentially allows the characterization of both local and bulk fracture properties [2].

2.1 Nanoindentation technique

To better characterize materials in nanoscopic scale there are some techniques, such as nanoindentation technique and Atomic Force Microscopy (AFM). According to indentation characterization, there are five main types of indenter tips (Figure 2.1), each one with different geometry depending on the application; hence, it is important to select the correct tip. There are various geometries available for the indenter shape such as three sided pyramids, four sided pyramids, wedges, cones, cylinders or spheres. The tip end of the indenter can be made sharp, flat, or rounded to a cylindrical or spherical shape. Some authors evaluated their differences when tested into the same material [3]. Diamond and sapphire are the primary materials of nanoindenters but other hard materials can also be used such as quartz, silicone, tungsten, steel, tungsten carbide and almost any other hard metal or ceramic. Nanoindenters are mounted on holders which could be the standard design from a manufacturer of nanoindenting equipment, or custom design. The holder material can be steel, titanium, ceramic or other suitable material [4].

a) Vickers indenter is a microhardness test method used for instrumented indentation testing (IIT) to measure mechanical properties on the nanoscale. The Vickers method is based on an optical measurement system. The Vickers indenter tip is a four-sided pyramid shaped diamond. The nominal value of the angle is 68º. There are many applications suitable for the Vickers indenter tips, such as bulk Materials, films and foils, scratch testing, and wear testing.

b) The Cube-Corner indenter tip is a three-sided pyramid with mutually perpendicular faces arranged in geometry like the corner of a cube. The sharpness of the cube corner produces much higher stresses and strains in the area of the contact. This is useful in producing very small, well-defined cracks around hardness impressions in brittle materials. These cracks can be used to estimate fracture toughness at very small scales, allowing plasticity to the material. The Cube-Corner indenter tip is available as a traceable standard. The nominal value of the angle is 35.26º. The main applications are related to thin films, scratch testing, fracture toughness, and wear testing.

c) The conical indenter tip has sharp geometry but the simplicity of its cylindrical symmetry makes it attractive from a modeling standpoint. Conical diamond indenter is not useful in nano-world because the difficulty in letting a sharp edge. This problem does not apply at larger scales. It is commonly used in bi-dimensional numerical simulation studies, as equivalent to the Berkovich and Vickers indenters. There are no recognized standard angles or sizes for conical indenters. Scratch testing and wear testing are the main applications.

d) Stresses are developed different compared to other tips during indentation when using a Spherical indenter tip. Spherical indenter has good transition between elastic deformations to plastic ones; it means, the contact stresses are initially small and produce only elastic deformation. As the spherical indenter is driven into the surface, a transition from elastic to plastic deformation occurs, which can theoretically be used to examine yielding and work hardening, and to recreate the entire uniaxial stress-strain curve from data obtained in a single test. At the microscale, the usage of spherical indenters has been impeded by difficulties in obtaining high-quality spheres made from hard, rigid materials. This is one reason the Berkovich indenter has been the indenter of choice for most small-scale testing, even though it cannot be used to investigate the elastic-plastic transition. The Sphere indenter tip is typically used for Micro-Electro-Mechanical Systems (MEMS) applications.

e) The Berkovich indenter is the most useful in nanoindentation technique to measure mechanical properties on the nanoscale. The Berkovich indenter is designed to have the same area as the Vickers indenter at any given indentation depth. It is a three-sided pyramid that can be ground to a point and thus maintains a self-similar geometry to very small scales. This geometry is often preferred to the Vickers indenter tip which is a four-sided pyramid. The Berkovich indenter tip is ideal for most testing purposes. It is not easily damaged and can be readily manufactured. It induces plasticity at very small loads which produces a meaningful measure of hardness. The Berkovich indenter tip has a large included angle of 142.3º which minimizes the influence of friction. The main applications are referred to bulk materials, thin films, polymers, scratch testing, wear testing, and MEMS applications. This is the tip used for all the experiments and studies in this Thesis related to nanoindentation technique.

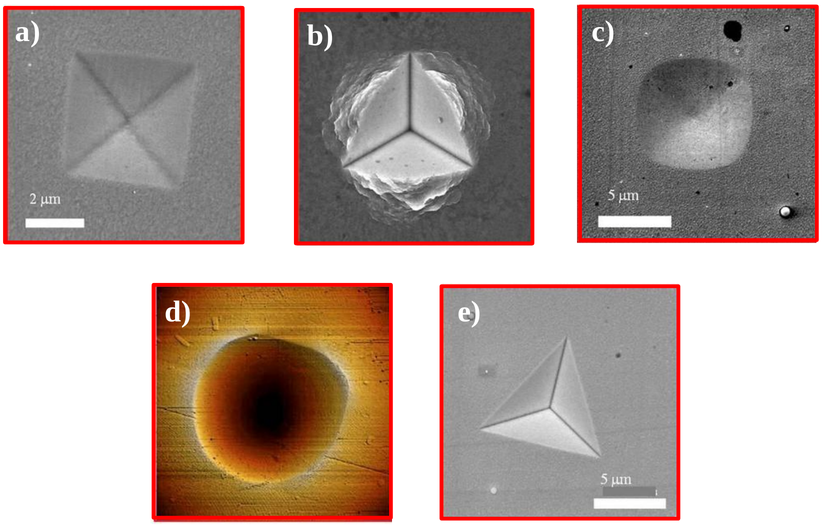

Figure 2.1. Types of indenters a)Vickers, b) Cube corner, c) Conical, d) Spherical, e) Berkovich.

Indentation with spherical tips is more complex than indentation with pyramidal tips, as a consequence of the lack of geometrical similarity [5].

Nanoindentation has become a standard experimental technique for evaluating the mechanical properties of the wide range of materials such as metals [6,7], glass [8,9], ceramics [10–12], and thin films [13,14] in small volumes at nanometric scale, even in polymers [15–29]. The determination of mechanical properties of polymers is more complex than that of many other structural materials, because they display time-dependence in their response to load [28]. Nanoindentation is used to measure static properties.

Because of many polymers are too soft for their indentation responses, the deformation scale can approach the sub-micron or even the nanoscale by using Depth-Sensing Indentation (DSI), which allows recording the applied load as a function of the penetration depth during the loading and unloading cycle, showed in Figure 2.2 DSI is a technique which the mechanical properties of small volumes of material can be determined. As indenter probe is placed in contact with the sample surface and pushed into it. Then, the resistance to indentation and the indent depth are continuously monitored throughout the experiment. For this reason, the indentation depth trace can be obtained. DSI has limited capabilities for studying polymer thin films, polymer composites, and other polymer systems. Nevertheless, DSI procedure proposed by Doerner *et al.* [30], permits to determine Hardness (*H*) and Elastic modulus (*E*) values, applying Sneddon's analysis. The procedure gives stiffness (S) and contact area (A_c) values establishing the possibility of deriving *H* and *E* from depth-sensing data. As it can be observed in Figure 2.2, it takes into account the load (P) in front of the penetration depth (h), obtaining a graph with the loading and unloading curves after an experiment.

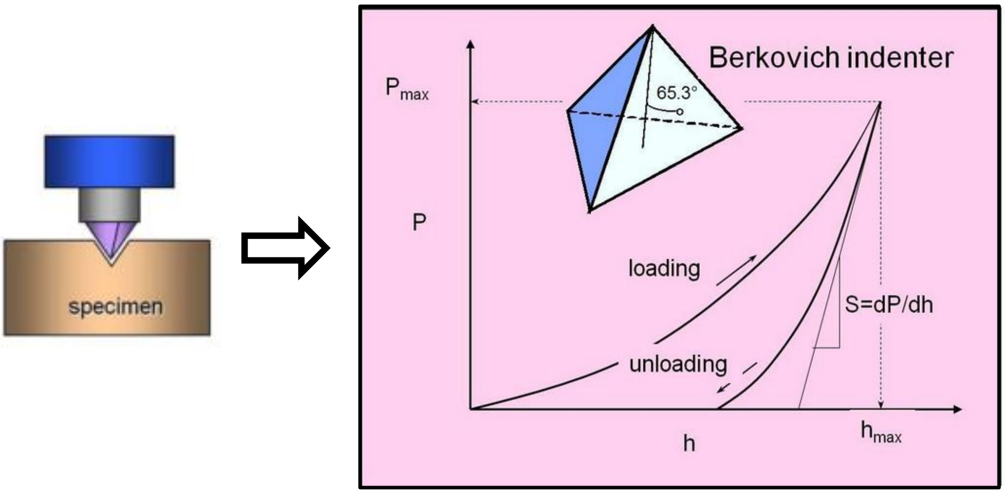

Figure 2.2. Typical loading/unloading curve in indentation technique [31].

Static indents can be analyzed to enable the determination of the viscoelastic response, assuming that different indentation rates will give responses that will vary according to the viscoelasticty of the polymer. Also, these static indents can be modeled taking into account the unloading process considering the time-dependent response as well as time-independent elastic deformation. Nevertheless, numerous parameters have to be taken into account when DSI is applied to polymers:

- Variation on the values of the mechanical properties with the strain-rate and frequency of the modulated load.

- Interaction forces between the indenter and the sample, such as Van der Waals forces and attractive or repulsive forces.

- Optimize parameters to achieve a higher sensitivity for stiffness variations in order to detect the surface efficiently. By this manner, applying an oscillating force will improve the surface detection, but for elastomeric polymers.

When nanoindentation is applied to a polymer, first a plastic deformation occurs. Then, at certain during indentation, pile-up effect of the material occurs next to the contact area between indenter and polymer. An important feature of indentation experiments is that the material around the contact area tends to deform upwards (pile-up) or downwards (sink-in) with respect to the indented surface plane. The occurrence of such pile-up and sink-in patterns is usually interpreted in terms of the strain-hardening behavior of the indented material [32]. Pile-up phenomenon leads to inaccurate determinations of Young's modulus and hardness, regardless of the kind of tip. Besides plastic deformation, other possible parameters evolve in this pile-up which results in small crazes just below the surface of the polymer [33], as it can be observed in Figure 2.3 and Figure 2.4. Pile-up and sink-in are the main limitations of nanointentation technique.

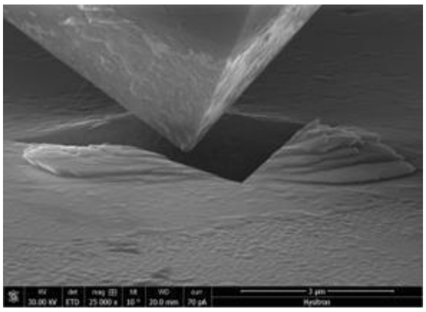

Figure 2.3. Image of pile-up [33].

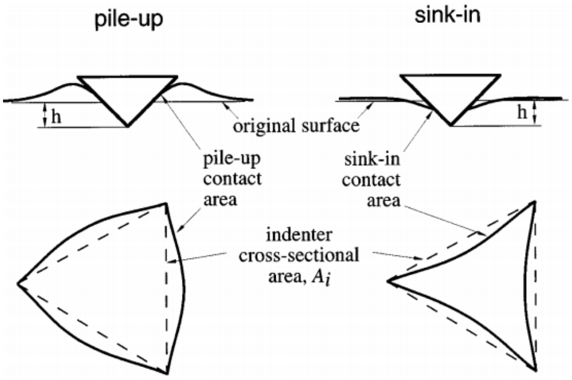

Figure 2.4. A schematic representation of pile-up and sink-in effects during indentation.

After this, Oliver & Pharr [34] projected an analysis procedure to describe non-linear initial unloading. The following equations will describe how to extract some parameters. To evaluate the contact depth (h_c) is necessary to apply Equation 2.1:

$$\boldsymbol{h_c = h_{max} - \varepsilon \frac{P_{max}}{S_{contact}}} \qquad \text{Equation 2.1}$$

being h_{max} the maximum indentation depth, ε is 0.75 for the Berkovich indenter, P_{max} is the maximum indentation load, and $S_{contact}$ is the contact stiffness calculated from the unloading curve, Equation 2.2.

$$\boldsymbol{S_{contact} = \frac{dP_{max}}{dH_{max}}} \qquad \text{Equation 2.2}$$

Besides, the contact area (A_c) will be calculated by using the Equation 2.3:

$$\boldsymbol{A_c = 24.56h_c^2} \qquad \text{Equation 2.3}$$

Hardness (H) will be estimated by using Equation 2.4:

$$\boldsymbol{H = \frac{P_{max}}{A_c}} \qquad \text{Equation 2.4}$$

Moreover, effective elastic modulus (E_{eff}) will be obtained as follows (Equation 2.5):

$$\boldsymbol{E_{eff} = \frac{\sqrt{\pi}}{2} \cdot \frac{S_{contact}}{\sqrt{A_c}}} \qquad \text{Equation 2.5}$$

Then, to obtain the material's effective elastic modulus, Equation 2.6 has to be applied:

$$\boldsymbol{\frac{1}{E_{eff}} = \frac{1-\nu_i^2}{E_i} + \frac{1-\nu^2}{E}} \qquad \text{Equation 2.6}$$

where ν is the Poisson's ratio for the material. The subindex i denotes the parameters for the diamond tip indenter.

On the other hand, in Loubet *et al*'s [35] method, the contact depth (h_c) is obtained using the Equation 2.7:

$$\boldsymbol{h_c = \alpha(h_r' + h_0)} \qquad \text{Equation 2.7}$$

where h_o is the apparent tip defect. The h_o parameter represents an 'apparent' value of the tip defect, that is necessary to ensure a constant stiffness value through the thickness of the material. Loubet *et al*. related h_o parameter to specific phenomena in polymer materials (tip-sample interaction and incorrect detection of the sample surface). The h_c is determined by adding the plastic depth (h_r') to h_o. α parameter is equal to 1.2 when a Berkovich tip indenter is employed. Besides, the contact area (A_c) will be calculated using the following expression (Equation 2.8):

$$\boldsymbol{A_c = \beta\alpha^2(h_r' + h_0)^2} \qquad \text{Equation 2.8}$$

where β is a shape factor, being 24.56 for a Berkovich diamond tip indenter. Furthermore, the indentation hardness (H) value can be defined as in Equation 2.9:

$$\boldsymbol{H = \frac{P_{max}}{\beta\alpha^2(h_r'+h_0)^2}} \qquad \text{Equation 2.9}$$

where P_{max} is defined as the maximum applied load during the nanoindentation test. In Loubet's methodology, the effective elastic modulus (E_{eff}) can be obtained as in Equation 2.10:

$$\boldsymbol{E_{eff} = \frac{1}{\beta}\frac{\sqrt{\pi\beta}}{2\alpha\sqrt{\beta}}} \qquad \text{Equation 2.10}$$

where the β is the same parameter as in Equation 2.7.

In Table 2. 1 is compared Loubet and Oliver & Pharr methods to obtain some relevant parameters in nanoindentation technique.

Table 2. 1. Comparison between Loubet and Oliver & Pharr methodologies.

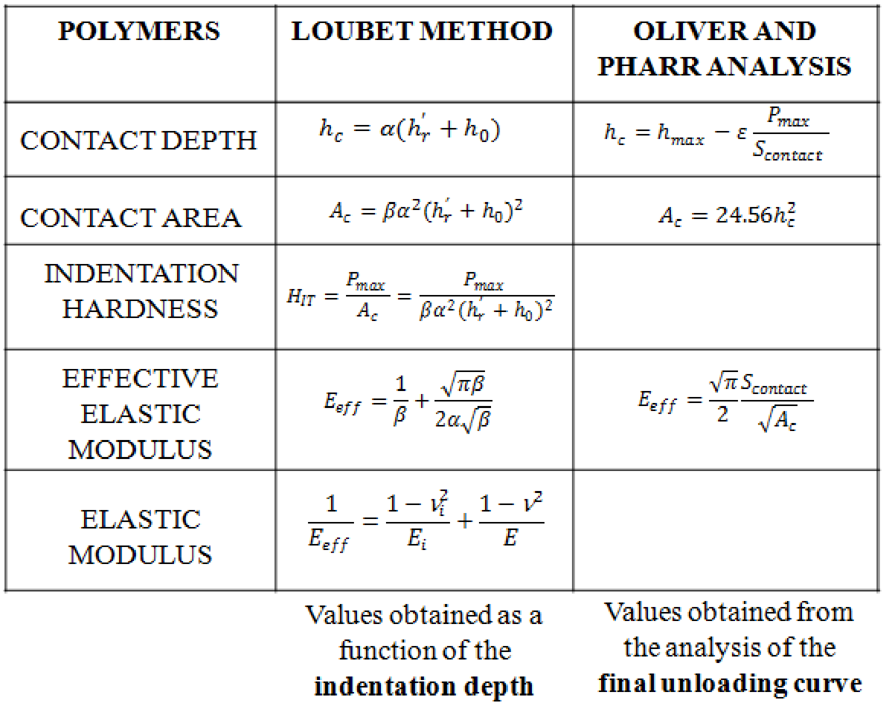

POLYMERS	LOUBET METHOD	OLIVER AND PHARR ANALYSIS
CONTACT DEPTH	$h_c = \alpha(h_r' + h_0)$	$h_c = h_{max} - \varepsilon \frac{P_{max}}{S_{contact}}$
CONTACT AREA	$A_c = \beta\alpha^2(h_r' + h_0)^2$	$A_c = 24.56h_c^2$
INDENTATION HARDNESS	$H_{IT} = \frac{P_{max}}{A_c} = \frac{P_{max}}{\beta\alpha^2(h_r' + h_0)^2}$	
EFFECTIVE ELASTIC MODULUS	$E_{eff} = \frac{1}{\beta} + \frac{\sqrt{\pi\beta}}{2\alpha\sqrt{\beta}}$	$E_{eff} = \frac{\sqrt{\pi}}{2}\frac{S_{contact}}{\sqrt{A_c}}$
ELASTIC MODULUS	$\frac{1}{E_{eff}} = \frac{1-\nu_i^2}{E_i} + \frac{1-\nu^2}{E}$	
	Values obtained as a function of the **indentation depth**	Values obtained from the analysis of the **final unloading curve**

One significant improvement in nanoindentation testing was the continuous stiffness measurement (CSM) technique, which offers a direct measure of dynamic contact stiffness during the loading process of an indentation test. Besides, CSM allows an accurate observation of small volume deformation, being insensitive to thermal drift [36], Figure 2.5.

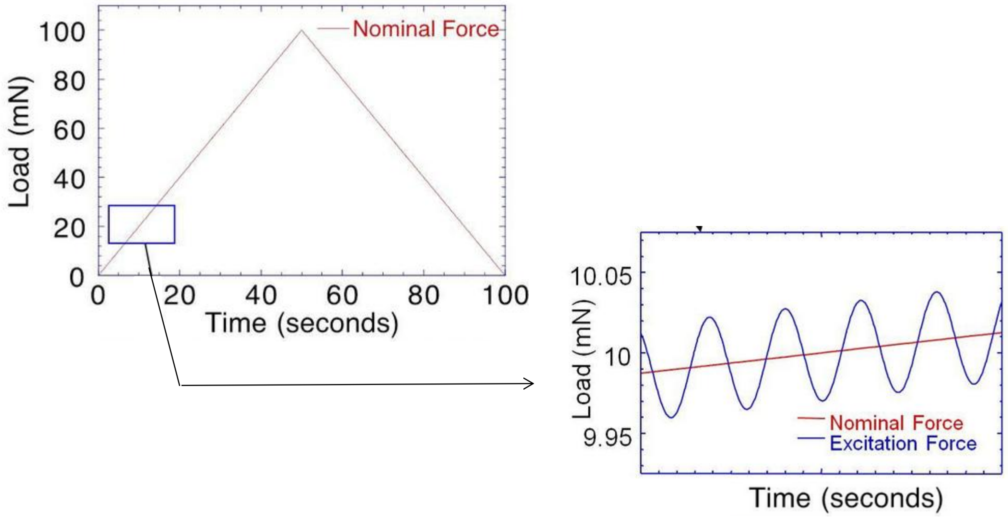

Figure 2.5. Scheme of Continuous Stiffness Measurement (CSM) technique.

2.2 Comparison between Loubet and Oliver & Pharr methodologies depending on the nature of the materials

Due to large errors are introduced in the surface detection of polymers with elastomeric character by using nanoindentation technique, and it may lead to uncertainties in the determination of the mechanical properties, it was considered to study some polymers by means of nanoindentation technique. A paper was published in **European Polymer Journal** in which the main goal was a comparative study between the Loubet's model using continuous stiffness measurement (CSM) and the procedure yielding a single reading from the onset of unloading, obtained from Oliver&Pharr and Loubet's approaches, in relation to the nature of the polymeric material, considering some thermoplastic materials, including glassy and semicrystalline ones. These polymers were polyamide/Nylon 6 (PA6), poly(methyl methacrylate) (PMMA), polycarbonate (PC), amorphous polyethylene terephthalate (PET), acrylonitrile butadiene styrene (ABS), polypropylene (PP), and polystyrene (PS) included in a laboratory set of thermoplastic materials from SIDILAB. The paper titled "**Depth-sensing indentation applied to polymers: A comparison between standard methods of analysis in relation to the nature of the materials**", was published in 2013 in volume 49 between pages 4047 - 4053, Figure 2.6 [37]. It innovates in the examination of nanoindentation analysis and provides valuable information in which method is better to apply, depending on the polymer to study. The impact factor of this journal is 3.242 (2014).

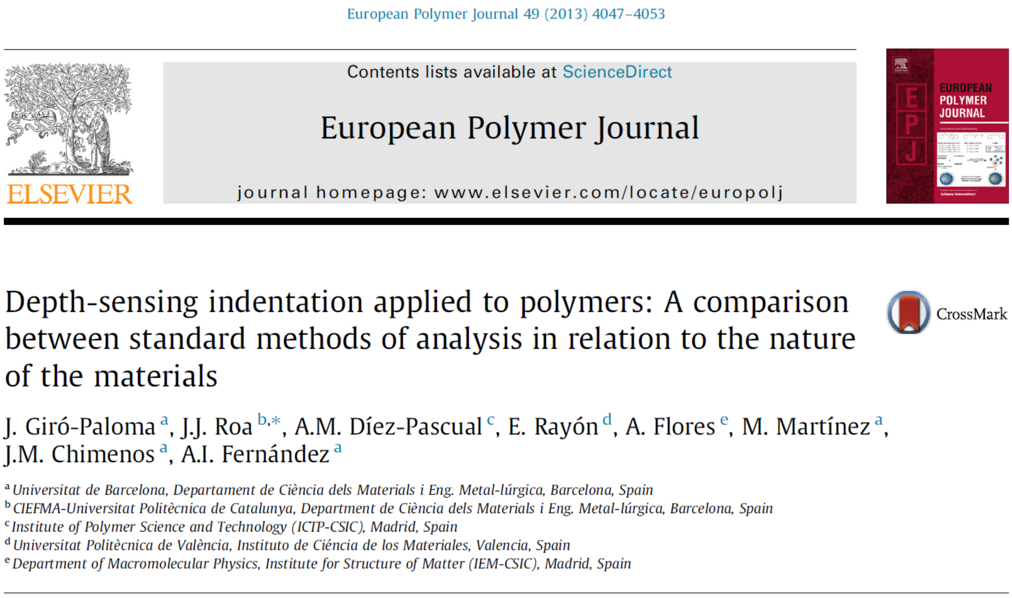

European Polymer Journal 49 (2013) 4047–4053

Contents lists available at ScienceDirect

European Polymer Journal

journal homepage: www.elsevier.com/locate/europolj

Depth-sensing indentation applied to polymers: A comparison between standard methods of analysis in relation to the nature of the materials

J. Giró-Paloma [a], J.J. Roa [b,*], A.M. Díez-Pascual [c], E. Rayón [d], A. Flores [e], M. Martínez [a], J.M. Chimenos [a], A.I. Fernández [a]

[a] Universitat de Barcelona, Departament de Ciència dels Materials i Eng. Metal-lúrgica, Barcelona, Spain
[b] CIEFMA-Universitat Politècnica de Catalunya, Department de Ciència dels Materials i Eng. Metal-lúrgica, Barcelona, Spain
[c] Institute of Polymer Science and Technology (ICTP-CSIC), Madrid, Spain
[d] Universitat Politècnica de València, Instituto de Ciéncia de los Materiales, Valencia, Spain
[e] Department of Macromolecular Physics, Institute for Structure of Matter (IEM-CSIC), Madrid, Spain

Figure 2.6. Article published in European Polymer journal in 2013, titled: "Depth-sensing indentation applied to polymers: A comparison between standard methods of analysis in relation to the nature of the materials".

A comparison between the *H* and *E* values was determined using both methodologies, concluding that Loubet's method will be adequate to polymeric materials measurements with a low viscous character (T_g well above the temperature of measurement), exhibits large values of the apparent tip defect. Besides, *H* and *E* with Loubet's method tend to yield mechanical properties lower values, closer to the modulus data determined by means of DMA. This effect is because of Loubet's model applies a dynamic approach to extract stiffness, *H* and *E* measurements and also due to the contribution of the 'apparent' tip effect.

European Polymer Journal 49 (2013) 4047–4053

Contents lists available at ScienceDirect

European Polymer Journal

journal homepage: www.elsevier.com/locate/europolj

Depth-sensing indentation applied to polymers: A comparison between standard methods of analysis in relation to the nature of the materials

J. Giró-Paloma [a], J.J. Roa [b,*], A.M. Díez-Pascual [c], E. Rayón [d], A. Flores [e], M. Martínez [a], J.M. Chimenos [a], A.I. Fernández [a]

[a] *Universitat de Barcelona, Departament de Ciència dels Materials i Eng. Metal-lúrgica, Barcelona, Spain*
[b] *CIEFMA-Universitat Politècnica de Catalunya, Department de Ciència dels Materials i Eng. Metal-lúrgica, Barcelona, Spain*
[c] *Institute of Polymer Science and Technology (ICTP-CSIC), Madrid, Spain*
[d] *Universitat Politècnica de València, Instituto de Ciéncia de los Materiales, Valencia, Spain*
[e] *Department of Macromolecular Physics, Institute for Structure of Matter (IEM-CSIC), Madrid, Spain*

ARTICLE INFO

Article history:
Received 14 February 2013
Received in revised form 5 September 2013
Accepted 12 September 2013
Available online 25 September 2013

Keywords:
Nanoindentation
CSM
Hardness
Elastic modulus

ABSTRACT

Mechanical data (hardness and elastic modulus) from instrumented indentation testing are often extracted assuming linear elasticity in the initial portion of the unloading. The method is nowadays widely accepted as a convenient tool to interpret depth-sensing data, however it is a matter of controversy when applied to polymer materials due to their time-dependent behavior. More recently, Loubet and co-workers applied continuous stiffness measurements (CSM), consisting of superimposing a small oscillation to the quasi-static component of loading, to the study of the mechanical properties of polymers and proposed a new model to account for the apparent increase in the contact area detected at the first stages of contact. The present work offers a comparative study between the Loubet's model using CSM and the procedure yielding a single reading from the onset of unloading. A wide range of thermoplastic polymer materials including glassy and semicrystalline polymers have been investigated. The most important equations employed for each method are summarized and the advantages and disadvantages of employing one procedure or the other are discussed. The differences found between the results obtained from both approaches are discussed in relation to the nature of the polymer material. A comparison between mechanical data extracted from indentation measurements and from classical dynamic mechanical analysis is offered.

1. Introduction

Mechanical properties are a determinant criterion for the selection of a material for a specific application. Indentation testing represents a convenient way for the characterization of the mechanical properties. On the one hand, the major requirement for sample preparation is a suitable surface finish and this usually allows testing the specimen on its original assembly. On the other hand, the method can provide a wealth of mechanical data in a short period of time. In addition, the indentation technique offers information on the mechanical properties at a local scale and this is the main reason why it has gained increasing interest in the last decades. Coatings, thin films and nanocomposite materials are some examples where indentation testing is extremely useful [1–3]. Using depth-sensing indentation (DSI), the scale of deformation can approach the sub-micron or even the nanoscale. In DSI, the applied load is recorded as a function of penetration depth during

---

* Corresponding author.
E-mail address: joan.josep.roa@upc.edu (J.J. Roa).

0014-3057/$ - see front matter © 2013 Elsevier Ltd. All rights reserved.
http://dx.doi.org/10.1016/j.eurpolymj.2013.09.010

a loading and an unloading cycle. The procedure most widely accepted to analyze the load-depth data from DSI to determine hardness and elastic modulus values was originally proposed by Doerner and Nix [4]. Doerner and Nix applied Sneddon's analysis of the contact between a punch and an elastic solid to the initial portion of the unloading curve. The procedure provided stiffness and contact area values opening up the possibility of deriving hardness and elastic modulus from depth-sensing data. Oliver and Pharr further proposed an analysis procedure to account for nonlinear initial unloadings present when indenters other than flat cylindrical punches are employed [5].

Nanoindentation has been proved to be well suited for the characterization of small volumes of ceramics or metals, such as single grains or phases in a composite [6], dislocation dynamics [7], small structures [8] or thin films and coatings [9]. Oliver and Pharr's analysis has been successfully applied to these materials providing reliable values of hardness and elastic modulus [5]. However, the application of indentation testing to polymers is still behind that of metals and ceramics, especially with respect to depth-sensing devices, although some efforts have been done in the area [10–12]. This is due to the time dependent properties of polymers that question the validity of applying Sneddon's analysis to the onset of unloading [10–12]. In addition, polymer materials demand a method that can provide information on the viscoelastic and viscoplastic properties and not simply the values of hardness and elastic modulus. A step forward was achieved when commercial DSI devices introduced the possibility of applying an oscillating force to the force signal [5,13]. The method is commonly known as continuous stiffness measurement (CSM) or dynamic DSI and opened up the possibility of using DSI devices as sub-micro or nano-scale dynamic mechanical analyzers. Loubet et al. were the first to successfully apply CSM to polymers suggesting a route for the derivation of hardness and elastic modulus in dynamic conditions [14]. In addition, these authors developed a model that introduced the concept on an 'apparent' tip defect, h_o, accounting for a shift in the contact point detected for polymer materials. In the model, the h_o value is added to the plastic depth to estimate the 'apparent' contact area. In turn, such procedure yields mechanical data independent of the indentation depth.

Several effects should be taken into account when applying DSI to 'soft' materials such as polymers: (i) the variation of the mechanical properties with the strain-rate and with the frequency of the modulated load, (ii) the interaction forces between the indenter and the sample (e.g. forces of Van der Waals, repulsive or attractive forces, and others), and (iii) the conditions of testing that should be optimized to achieve a high sensitivity to stiffness variations in order to detect the surface efficiently. Concerning point (iii) above, the application of an oscillating force usually improves the surface detection; however, for polymers with marked elastomeric character large errors are still introduced in the surface detection that lead to uncertainties in the determination of the mechanical properties [15].

The main aim of this study is the application of Loubet's and Oliver and Pharr's analysis to a wide range of thermoplastic materials including glassy and semicrystalline polymers. A comparison between the hardness and elastic modulus values determined using either method will be carried out. Moreover, a discussion on the main advantages/disadvantages of each method will be offered. In addition, the validity of each model is discussed in relation to the nature of the polymer material. Dynamic mechanical analysis (DMA) will be employed to achieve modulus values for comparison with those extracted from the indentation analysis. We intend to provide some bases to decide a priori which indentation method would be most appropriate for a specific polymer material.

2. Experimental procedure

2.1. Samples

A commercial set of polymeric samples supplied by SIDILAB, S.L. was used. The selected polymers are: polyamide/Nylon 6 (PA6), poly(methyl methacrylate) (PMMA), polycarbonate (PC), amorphous polyethylene terephthalate (PET), acrylonitrile butadiene styrene (ABS), polypropylene (PP) and polystyrene (PS). Samples of 75 × 11 × 2 mm were cut transversally obtaining specimens of 20 × 11 × 2 mm size. The different samples were directly glued onto a metallic holder to perform the nanoindentation tests.

2.2. Depth-sensing instrumentation

Nanoindentation tests were performed with a Nanoindenter G200 (Agilent Technologies, Chandler, AZ) provided with Continuous Stiffness Measurement (CSM). A Berkovich diamond tip was employed. Tip shape calibration was performed following the procedure described in detail in [5,13]. Measurements were also corrected for the machine compliance. Experiments were carried out at room temperature (20 °C). The indentation tests were performed using the following sequence: the load was incremented at a constant strain rate of $0.2\ \mathrm{s}^{-1}$ up to a peak load of 500 mN. During this loading cycle, a small oscillating force of 2 nm of amplitude and 45 Hz of frequency was superimposed. This period was followed by a peak hold time of 10 s after which the load was withdrawn up to 90% of the peak load. Finally, a reloading/fully unloading period is carried out.

The Loubet (see Appendix A) and the Oliver and Pharr (see Appendix B) methods were employed to extract the mechanical properties using the Test Works 4 Professional level software. The Loubet method uses the CSM option providing a continuous measure of the indentation stiffness during the loading cycle. In this way, values of the reduced modulus and the indentation hardness are obtained as a function of the indentation depth. In contrast, these mechanical data in the Oliver and Pharr approach are obtained from the analysis of the final unloading curve.

A homogeneous array of 16 indentation imprints was performed on each sample. Each imprint was separated a constant distance (around 25 times the maximum indentation depth) in order to avoid the interaction of the plastic deformation field between indentations. The residual imprints were directly visualized by the optical microscopy coupled to the G200.

2.3. Dynamic mechanical analysis

A dynamic mechanical analyzer (Mettler DMA 861) was used to measure the storage modulus E' and tan δ of the materials. Experiments were carried out in the tensile mode by heating from -100 to 200 °C with a ramping rate of 2 °C/min at a frequency of 1 Hz. A dynamic force of 6 N was used oscillating at fixed frequency and amplitude of 30 μm. Fig. 1 shows the dynamic mechanical spectra for the different samples. The peaks in tan δ curves are related to transitions in polymers. The peak at higher temperature is the α-transition or glass transition, and covers a range of temperatures, of which the so-called glass transition temperature (T_g) is an indicative value determined based on an agreed criterion [16]. In this work, T_g values were determined from the peak maximum of tan δ vs. temperature curves [17]. Lower temperature peaks correspond to secondary transitions (β and γ) that are thought to be related to local small-scale chain motions. In case of the ABS terpolymer, two T_gs are observed: one associated with the poly(butadiene) at -65 °C with very small tan δ magnitude and other at ≈110 °C ascribed to the poly(styrene-co-acrylonitrile) segments. Table 1 collects the E' value for each polymer sample determined at room temperature together with the corresponding T_g value.

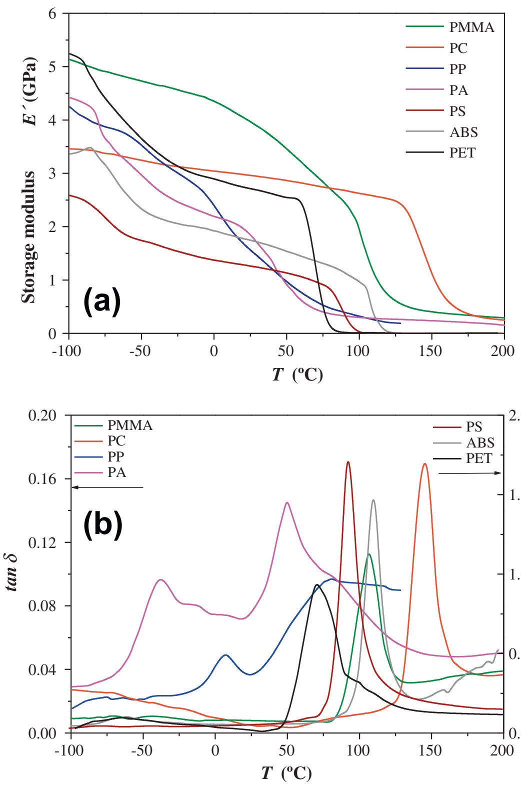

Fig. 1. Evolution of storage modulus E' (a) and tan δ (b) as a function of temperature for the different polymers. The left axis in (b) applies to PMMA, PC, PP and PA while the right axis is for PS, ABS and PET.

Table 1
Storage modulus (E') at 25 °C and glass transition temperature (T_g) values obtained from DMA measurements.

Material	E' (GPa)	T_g (°C)
PS	1.3	92
ABS	1.7	-65, 109[a]
PA	1.8	51
PC	2.9	145
PMMA	4.0	107
PET	2.7	71
PP	1.6	8

[a] The two T_gs correspond to the poly(butadiene) and poly(styrene-co-acrylonitrile) segments, respectively.

3. Results and discussion

3.1. Imprints visualization

The residual area after indentation is different for each sample and, taking into account that experiments were carried out using the same maximum load, yields qualitative information about the hardness of each material. Fig. 2 shows, as an example, the residual imprints performed on the surface of two polymer glasses (PC and PMMA). The scratches and cracks at the sample surfaces, especially evident in the case of PMMA, existed before the indentation measurements and were found not to alter the results at high penetration depths (above 5 μm). A quick inspection of the residual impressions reveals that the hardness of PC is smaller than that of PMMA. Indeed, analysis of the indentation depth data by either method (Oliver and Pharr or Loubet) confirms this finding (see results below).

3.2. Considerations: Loubet method

3.2.1. Tip defect

A typical representation of the Harmonic Contact Stiffness, *HCS*, vs. the plastic deformation depth, h'_r, is shown in Fig. 3. The tip defect (h_o) can be calculated from the x-axis intercept following [13]:

$$HCS = b(h'_r + h_o) \tag{1}$$

where b is the slope of the straight line. The different tip defect (h_o) determined for each sample can be summarized in Table 2. The existence of a linear relationship between these parameters, over a critical plastic depth, is a proof that these polymeric materials meet the constant E assumption.

Table 2 shows significant variations in the h_o values of the different samples with respect to each other. This could be related to a different adhesion of the sample to the tip that in turn, should be a consequence of the material characteristics. One would expect that samples with the highest viscous character, i.e., those with T_g below room temperature and a significant amount of amorphous phase, would exhibit the highest adhesion to the tip (largest h_o values). Indeed, this would explain why PP exhibits one of the highest h_o values (T_g of PP ≈ 10 °C; degree of crystallinity ≈ 0.4–0.7 [10,18]) It would also explain the large

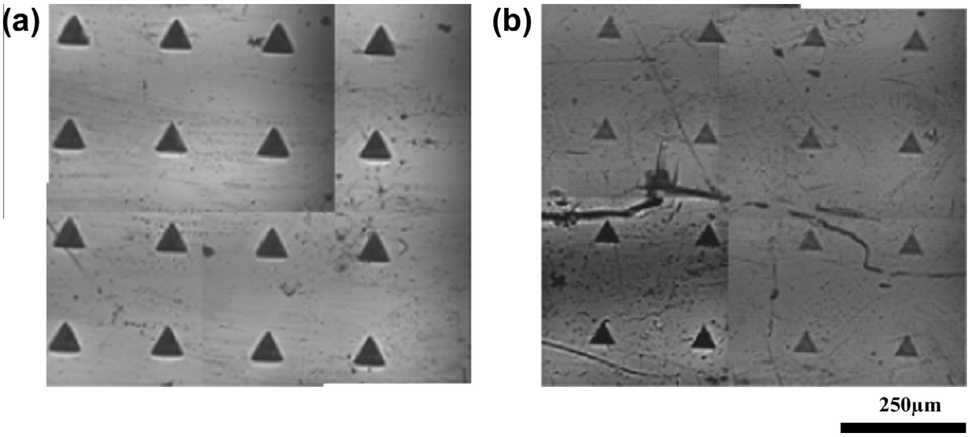

Fig. 2. Optical image of the residual nanoindentation imprints performed on: (a) PC and (b) PMMA.

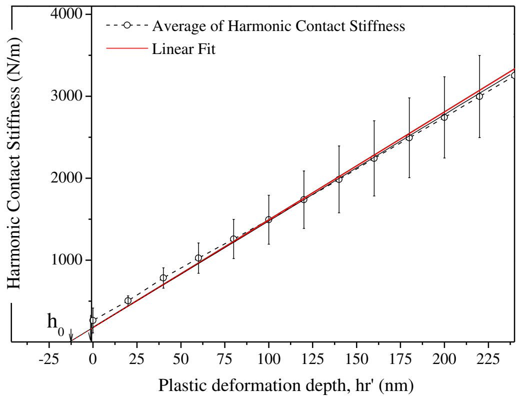

Fig. 3. Representation of the harmonic contact stiffness versus the plastic deformation depth for PS.

Table 2
Tip defect (h_o) at maximum applied load for each polymer studied.

Material	PS	PA	PC	PET	PP	PMMA	ABS
h_o (nm)	76	82	22	11	85	5	86

difference found between the h_o values of PP and that of glassy polymers such as PC, amorphous PET and PMMA, all of them with T_g well above room temperature. In case of the ABS material, the butadiene blocks have already experienced the glass transition at room temperature and hence, this could impart enhanced tip-sample interaction (higher h_o value) with respect to the rest of glassy polymers. However, the data in Table 2 suggest that additional factors other than the viscous character of the polymer material are influencing the apparent tip defect values. Indeed, PS exhibits a significantly higher h_o value that other glassy materials (PC, amorphous PET, PMMA). Moreover, PA6 ($T_g \approx 50$ °C; degree of crystallinity ≈ 0.3–0.4, [19]) displays an h_o value very close to that of PP although the glass transition temperature of the former material is shifted by about 40 °C with respect to that of the latter one. Hence, we must conclude that other factors such as the surface roughness could also play an important role in the tip-sample interaction.

3.2.2. Loading/unloading curve

Using the h_o values of Table 2, corrected P–h curves are obtained and subsequently used to recalculate the indentation hardness (H_{IT}) and elastic modulus (E) following the procedure described in Appendix A. In practice, these corrections are easily introduced using the Test Works 4 software. As an example, Fig. 4 shows a typical loading–unloading–reloading curve after correction of the tip defect. It is noteworthy the overlapping of the unloading–reloading cycles.

3.3. Considerations: Single reading from the unloading

In the Oliver and Pharr analysis, H_{IT} and E are straightforward determined from the initial portion of the final unloading curve. One single reading at the end of the test is extracted instead of a continuous measurement of the mechanical properties as provided by the CSM option. In this case, the P–h curves are only corrected for the point

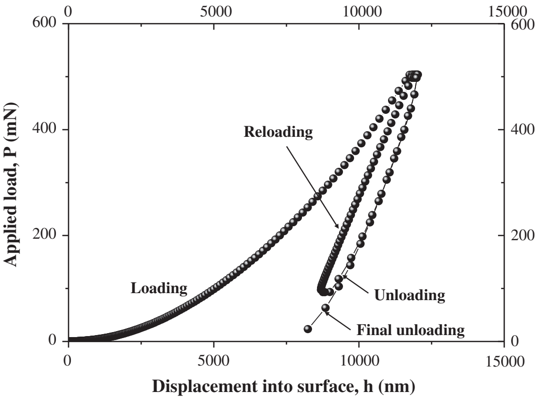

Fig. 4. Loading–partial unloading–reloading-fully unloading cycles for a PS sample after correction for the apparent tip defect following Loubet's method [14].

of initial contact and not for the 'apparent' tip defect. This can be easily done examining the evolution of the contact stiffness with time. The method is less time-consuming but does not take into account the time-dependent properties of polymers.

In the following section we will compare and discuss the mechanical properties obtained using both, Oliver and Pharr and Loubet's methods.

3.4. Mechanical properties

Fig. 5a and b show the evolution of H_{IT} and E, respectively, against the penetration depth for each polymer using the Loubet method. It is found that for all materials, H_{IT} and E reach a plateau at ≈5 μm. The indentation behavior at small penetration depths should be a consequence of superficial defects and surface roughness. However, Fig. 5 shows that, for some of the materials such as PET, PC or PMMA, the mechanical data seem to systematically decrease with increasing penetration depth up to the plateau value. Because the experiments were carried out in constant strain rate conditions and a careful correction for the apparent tip defect has been carried out, we must conclude that this result is due to a surface hardening effect. Preceding indentation work on PC, PS and PMMA, reported enhanced hardness and modulus values at the surface layer with respect to the bulk [20]. The authors explained this result as a modification of the material properties at the surface due to exposure to light and air, or due to the fabrication process itself. Similar ageing, oxidation effects or other morphological gradients across the samples arising from the manufacturing process could take place in our materials.

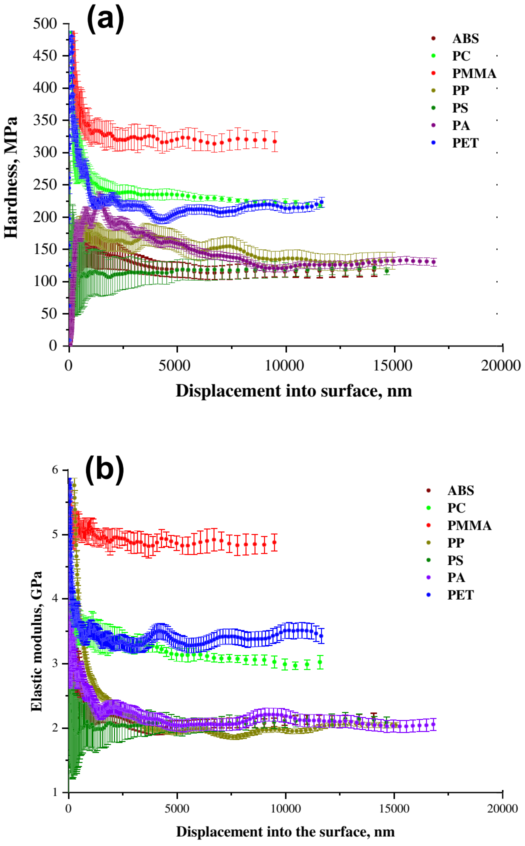

Fig. 5. Mechanical properties obtained using the Loubet method, as a function of displacement into surface: (a) Hardness and (b) elastic modulus.

Let us know focus on the plateau H_{IT} and E 'bulk' values shown in Fig. 5a and b. Two different range of values are observed: (i) high values for: PMMA > PC > PET ($H_{IT} > 200$ MPa, $E > 3$ GPa) and (ii) low values for: PP, PA, ABS and PS ($H_{IT} < 200$ MPa, $E < 3$ GPa). It is noteworthy that the modulus values represented in Fig. 5b are in good agreement with the E' data obtained from DMA tests (see Table 1). In both experiments, PMMA exhibits the highest modulus value, followed by glassy PET and PC, which display values close to each other. Both, indentation and DMA studies reveal significant lower modulus values for the rest of polymer materials (PP, PA, ABS, PS). Comparison between the modulus values obtained by means of indentation and those from DMA reveal differences $\leqslant 20\%$ except for PS where the modulus value obtained using the Loubet method is about 40% higher than E'.

Table 3 summarizes the mechanical properties determined using Loubet and Oliver and Pharr methods. It is clearly seen that the H_{IT} and E values are lower when the Loubet method is used. Two main reasons can explain this result: (i) dynamic testing was used when applying the Loubet method; here, a viscoelastic model is implicit in the derivation of the harmonic stiffness that, in turn, is employed to determine H_{IT} and E and (ii) the contact depth (and hence, the contact area) is larger in case of Loubet's method due to the contribution of an 'apparent' tip effect. Although the elastic modulus values obtained using either method are consistent with the storage modulus values obtained from DMA tests, it seems that Loubet's method tend to yield modulus values closer to those derived from DMA.

Fig. 6 plots the mechanical properties obtained using the Loubet method versus the Oliver and Pharr analysis. A straight line representing the identity function is included on each plot. It is clearly seen that Loubet's method tends to yield smaller values of H_{IT} and E than Oliver and Pharr, as argued above. However, most interesting is the fact that some materials deviate to a larger extent than

Table 3
Summary of the mechanical properties for each polymer studied determined using the Loubet and Oliver&Pharr methods at maximum indentation depth.

Material	Loubet method		Oliver&Pharr method	
	H (MPa)	E (GPa)	H (MPa)	E (GPa)
ABS	118 ± 9	2.1 ± 0.1	135.2 ± 0.4	2.7 ± 0.4
PC	218 ± 3	3.0 ± 0.1	236.1 ± 0.3	3.6 ± 0.3
PMMA	317 ± 16	4.9 ± 0.1	344.3 ± 0.7	4.5 ± 0.2
PP	132 ± 13	2.0 ± 0.04	131.5 ± 0.3	3.3 ± 0.5
PS	116 ± 6	2.1 ± 0.1	156.2 ± 0.4	1.9 ± 0.3
PA	130 ± 6	2 ± 0.1	171.6 ± 0.9	2.6 ± 0.1
PET	223 ± 8	3.4 ± 0.1	251.2 ± 0.2	3.6 ± 0.2

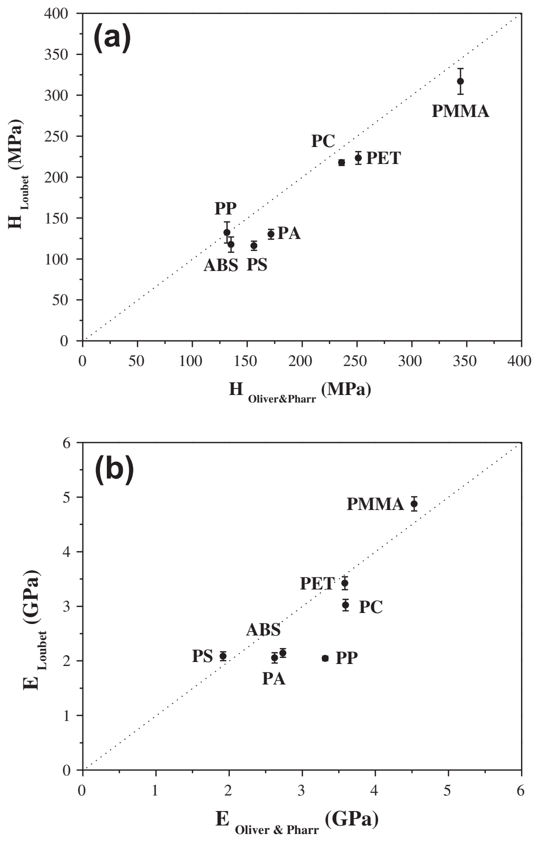

Fig. 6. Comparison of mechanical properties obtained by Loubet and Oliver&Pharr analysis: (a) Hardness and (b) elastic modulus.

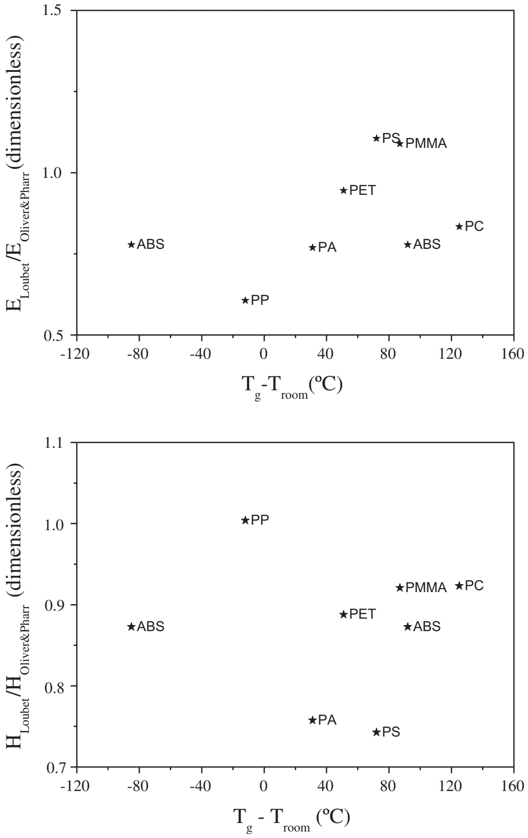

Fig. 7. $E_{Loubet}/E_{Oliver\&Pharr}$ and $H_{Loubet}/H_{Oliver\&Pharr}$ as a function of the difference between the glass transition of each material obtained from DMA tests (see Table 1) and the measurement temperature.

others. This prompted us to correlate such deviations with the corresponding glass transition temperatures obtained from DMA (see Table 1). Fig. 7a and b shows the plot of $H_{\text{Loubet}}/H_{\text{Oliver\&Pharr}}$ and $E_{\text{Loubet}}/E_{\text{Oliver\&Pharr}}$, respectively, as a function of the difference between the glass transition of each material and the temperature of measurement (T_g – 20 °C). In case of the ABS terpolymer, we have adopted the highest T_g value (≈110 °C) because the integrated area of the corresponding tan δ transition is substantially larger than that of the low-T_g α-transition (see Fig. 1b). It is seen that the elastic modulus ratio tend to increase with increasing glass transition values. This observation is most interesting because it suggests that the validity of the Oliver and Pharr approach is restricted to polymers with a low viscous character, i.e. with T_g well above the temperature of measurement. Hence, for room temperature indentation measurements, Loubet's method should be preferentially applied if the polymer material exhibits a T_g below or on the vicinity of room temperature. On the other hand, Fig. 7b shows that a clear trend with T_g is not observed for the hardness ratio. The viscous character of a polymer material clearly influences the material's behavior upon unloading that in turn determines the stiffness values calculated at peak load using Oliver and Pharr analysis (S_{contact} in Eq. (B1)). Because the E values are directly related to S_{contact}, the selection of a method that adequately contemplates viscoelasticity such as Loubet's is of great importance in the case of polymers with a marked viscous character. However, in the case of H_{IT}, no clear recommendation to use one method or the other is inferred from our results because this magnitude is not directly related to the stiffness. Hence, in this case, either method seems to be equally valid for the derivation of hardness values.

4. Conclusions

The most common methods employed for analysis of the mechanical properties of polymers, Oliver and Pharr's analysis and Loubet's, have been critically examined.

In case of application of Loubet's method, polymer materials with a marked viscous character (glass transition values below room temperature) exhibit large values of the apparent tip defect. In addition, this parameter is also envisaged to be influenced by surface roughness.

Comparison of the hardness and elastic modulus values derived from both approaches suggests that Loubet's method tend to yield lower values of the mechanical properties, closer to the modulus data determined by means of DMA. This effect is attributed to two main factors: (i) Loubet's model uses a dynamic approach to extract stiffness measurements that, in turn, are employed to derive H_{IT}

and E and (ii) the contact depth is larger in case of Loubet's method due to the contribution of the 'apparent' tip effect.

Results obtained from the analysis of the onset of unloading suggest that this method should be limited to polymer materials with a low viscous character, i.e., with T_g well above the temperature of measurement.

Acknowledgements

The authors would like to thank C. Ferrer and M.D. Salvador of the Universidad Politécnica de Valencia, the European Union (COST Action TU0802), and the Catalan Government for the quality accreditation given to research group DIOPMA (2009 SGR 645). One of us (AF) thanks the MICINN (Ministerio de Ciencia e Innovación), Spain, for financial support under the grant FIS2010-18069. We would like to thank the Linguistic Services at the Universitat de Barcelona for linguistic and stylistic advice.

Appendix A. Loubet method [14]

In this method, the contact depth is obtained using the following equation:

$$h_c = \alpha(h'_r + h_0) \tag{A1}$$

where h_o represents the apparent tip defect, i.e., the apparent missing portion of the diamond from the height of a perfect Berkovich pyramid. The h_o parameter does not represent a "real" tip defect but is introduced in Loubet's model as an "apparent" value that is necessary to ensure a constant stiffness value through the thickness of the material. Loubet et al. related the h_o parameter to specific phenomena in polymer materials (tip-sample interaction, incorrect detection of the sample surface, etc.). The contact depth in Loubet's model, h_c, is determined by adding the plastic depth, h'_r, to the apparent tip defect. The α parameter is a coefficient, which is equal to 1.2 when a Berkovich tip indenter is employed.

The contact area (A_c) can be calculated using the following expression:

$$A_c = \beta\alpha^2(h'_r + h_0)^2 \tag{A2}$$

where β is a shape factor, which for a Berkovich diamond tip indenter is equal to 24.56. The indentation hardness (H_{IT}) value can be defined as:

$$H_{IT} = \frac{P_{\max}}{A_c} = \frac{P_{\max}}{\beta\alpha^2(h'_r + h_0)^2} \tag{A3}$$

where $P_{\max}$ is the maximum applied load during the nanoindentation test. The effective elastic modulus (E_{eff}) can be obtained as:

$$E_{eff} = \frac{1}{\beta}\frac{\sqrt{\pi\beta}}{2\alpha\sqrt{\beta}} \tag{A4}$$

where the b parameter is defined in Eq. (1). The elastic modulus can be extracted using:

$$\frac{1}{E_{\text{eff}}} = \frac{1 - v_i^2}{E_i} + \frac{1 - v^2}{E} \tag{A5}$$

where v is Poisson's ratio for the material. The subindex i denotes the parameters for the diamond tip indenter (0.07 and 1141 GPa, respectively [5]).

Appendix B. Oliver and Pharr analysis [4,5]

The contact depth using this method can be obtained following:

$$h_c = h_{\max} - \varepsilon\frac{P_{\max}}{S_{\text{contact}}} \tag{B1}$$

where $h_{\max}$ is the maximum indentation depth, ε is a constant (0.75 for a Berkovich indenter), $P_{\max}$ is the maximum indentation load and S_{contact} is the contact stiffness calculated from the unloading curve.

The contact area (A_c) is calculated using the following expression:

$$A_c = 24.56h_c^2 \tag{B2}$$

H_{IT} can be estimated using Pmax/Ac, and E_{eff} can be obtained as follows:

$$E_{\text{eff}} = \frac{\sqrt{\pi}}{2}\frac{S_{\text{contact}}}{\sqrt{A_c}} \tag{B3}$$

Finally, Eq. (A5) can be used to derive the elastic modulus of the material.

References

[1] Bull SJ. J Phys D: Appl Phys 2005;38:R393–413.
[2] Hay J, Crawford B. J Mater Res 2011;26(6):727–38.
[3] Liu TX, Phang IY, Shen L, Chow SY, Zhang WD. Macromolecules 2004;37:7214–22.
[4] Doerner MF, Nix WD. J Mater Res 1986;1(4):601–9.
[5] Oliver WC, Pharr GM. J Mater Res 1992;7:1564.
[6] Roa JJ, Capdevila XG, Martínez M, Espiell F, Segarra M. Nanotechnology 2007;18:1–6.
[7] Gaillard Y, Tromas C, Woirgard J. Acta Mater 2006;54:1409–17.
[8] Choi Y, Suresh S. Scripta Mater 2003;48:249–54.
[9] Roa JJ, Gilioli E, Bissoli F, Patini F, Rampino S, Capdevila XG, et al. Thin Solid Films 2009;518:227–32.
[10] Flores A, Ania F, Balta-Calleja FJ. Polymer 2009;50:729–46.
[11] VanLandingham MR, Villarrubia JS, Guthrie WF, Meyers GF. Macromol Symp 2001;167:15–43.
[12] Kranenburg JM, Tweedie CA, Van Vliet KJ, Schubert US. Adv Mater 2009;21:3551–61.
[13] Oliver WC, Pharr GM. J Mater Res 2004;19:3–20.
[14] Hochstetter G, Jimenez A, Loubet JL. J Macromol Sci Phys B 1999;38(5–6):681–92.
[15] Deuschle J, Enders S, Arzt E. J Mater Res 2007;22:3107–19.
[16] Kalogeras IM, Hagg Lobland HE. J Mater Educ 2012;34:69–94.
[17] Menard KP. Thermal transitions and their measurement. In: Brostow Witold, editor. Performance of plastics. München: Carl Hanser Verlag; 2001. p. 163–71.
[18] Meille SV, Brückner S. X-ray scattering. In: Karger Kocsis J, editor. Polypropylene. An A–Z reference. Dordrecht: Kluwer Academic Publishers; 1999. p. 891–6.
[19] Brucato V, Piccarolo S, Titomanlio G. Macromol Chem Macromol Symp 1993;68:245–55.
[20] Briscoe BJ, Fiori L, Pelillo E. J Phys D: Appl Phys 1998;31:2395–405.

2.3 Study of the effect of $Mg(OH)_2$ as inorganic filler in a PP matrix in contact with different paraffinic PCM

Because of variations on the mechanical properties with depth of indentation offer important information suitable for design purpose, nanoindentation is a proper technique for nanomechanical parameters in polymers [38]. For this reason, it was considered to continue the study related to nanoindentation technique in polymers. In this case, it was compared the H, E, and E_{loss} of four different polypropylene (PP) samples. Polyolefins like polyethylene (PE) or polypropylene (PP) are commonly used as containers of inorganic salts and organic fluids. In particular, containers for PCM made of PP may be used for TES in passive systems or heating and cooling usages. Besides, inorganic fillers increase the mechanical resistance and stiffness of thermoplastics, as well as can reduce the degradation effect avoiding the premature mechanical failure and improve properties against fire, which is relevant in studies related with paraffin used as PCM, because these materials are flammable. The inflammability of these products has been severely restricted in wide applications, especially in building fields. A filler commonly used for polymers in general is $Mg(OH)_2$ [39] because of its flame retardant property [40,41], which also improves the mechanical responses [42–44]. Other fillers are graphite, ammonium polyphosphate, zinc borate [45,46], among others.

As in the previous study, PMMA was considered to exhibit the highest hardness and Young’s modulus value, and as it is known as a good container for PCM, it was decided to study another polymer to contain PCM as a possible substitute of PMMA. In this case, PP was the selected polymer due to it has the highest value of the low values in the previous study. The samples under study were PP, filled polypropylene with 60 % $Mg(OH)_2$ (PP-60Mg), PP-60Mg in contact with PCM (RT-25), and PP-60Mg in contact with PCM (RT-45). The analysis was performed at different temperatures (30 ºC, 45 ºC and 60 ºC for PCM RT-25 and 45 ºC for PCM RT-42), and the contact of the polyolefin with the PCM was done for 32 days. It was performed the nanoindentation characterization following the main conclusions of the previous paper. The most important conclusions were related with the increase on the mechanical properties for PP-60Mg compared with PP ones. However, the mechanical parameters considered decreased considerably when PP and PP-60Mg were in contact with the organic fluid. The main reason was that PCM acts as a plasticizer, deteriorating the polymer. Another important conclusion was that for higher temperatures in service for a PCM and the higher PCM's melting point of its PCM, the lower mechanical properties were observed.

The paper accepted in **European Polymer Journal** is titled "**Effect of the filler on the nanomechanical properties of polypropylene in contact with paraffinic phase change material**" [47]. It was published in 2015 in the volume number 63 between pages 29 - 36, as Figure 2.7 shows.

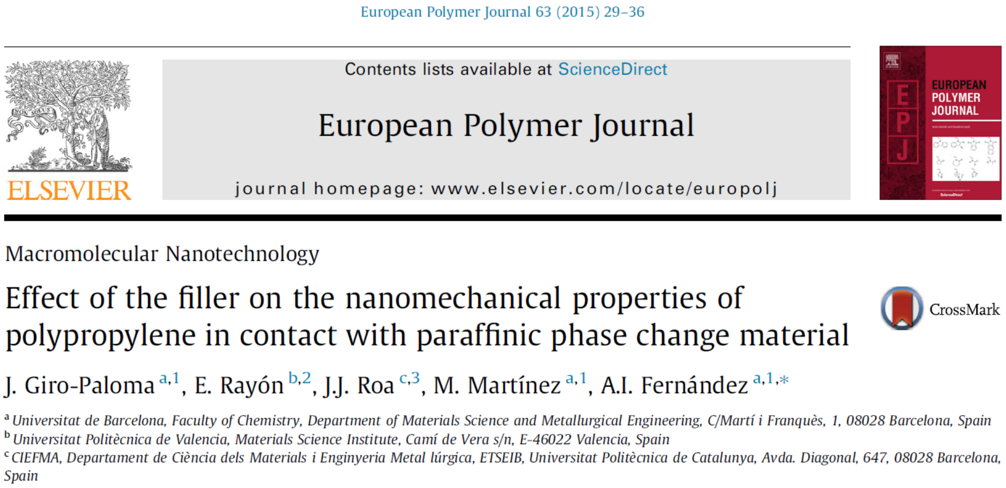

European Polymer Journal 63 (2015) 29–36

Contents lists available at ScienceDirect

European Polymer Journal

journal homepage: www.elsevier.com/locate/europolj

Macromolecular Nanotechnology

Effect of the filler on the nanomechanical properties of polypropylene in contact with paraffinic phase change material

J. Giro-Paloma [a,1], E. Rayón [b,2], J.J. Roa [c,3], M. Martínez [a,1], A.I. Fernández [a,1,*]

[a] Universitat de Barcelona, Faculty of Chemistry, Department of Materials Science and Metallurgical Engineering, C/Martí i Franquès, 1, 08028 Barcelona, Spain
[b] Universitat Politècnica de Valencia, Materials Science Institute, Camí de Vera s/n, E-46022 Valencia, Spain
[c] CIEFMA, Departament de Ciència dels Materials i Enginyeria Metal lúrgica, ETSEIB, Universitat Politècnica de Catalunya, Avda. Diagonal, 647, 08028 Barcelona, Spain

Figure 2.7. Article published in European Polymer journal in 2015, titled "Effect of the filler on the nanomechanical properties of polypropylene in contact with paraffinic phase change material".

European Polymer Journal 63 (2015) 29–36

Contents lists available at ScienceDirect

European Polymer Journal

journal homepage: www.elsevier.com/locate/europolj

Macromolecular Nanotechnology

Effect of the filler on the nanomechanical properties of polypropylene in contact with paraffinic phase change material

J. Giro-Paloma [a,1], E. Rayón [b,2], J.J. Roa [c,3], M. Martínez [a,1], A.I. Fernández [a,1,*]

[a] *Universitat de Barcelona, Faculty of Chemistry, Department of Materials Science and Metallurgical Engineering, C/Martí i Franquès, 1, 08028 Barcelona, Spain*
[b] *Universitat Politècnica de Valencia, Materials Science Institute, Camí de Vera s/n, E-46022 Valencia, Spain*
[c] *CIEFMA, Departament de Ciència dels Materials i Enginyeria Metal lúrgica, ETSEIB, Universitat Politècnica de Catalunya, Avda. Diagonal, 647, 08028 Barcelona, Spain*

ARTICLE INFO

Article history:
Received 23 September 2014
Received in revised form 19 November 2014
Accepted 22 November 2014
Available online 3 December 2014

Keywords:
Polypropylene
Nanoindentation
Phase change material
Mechanical properties

ABSTRACT

As the changes on the mechanical properties with depth of indentation provide valuable information that may be suitable for design purposes, nanoindentation is an adequate technique for investigating the nanomechanical changes in the surface and in the inner polymers. This research focuses on the study of the nanomechanical properties of two grades of polypropylene (PP) after the long term exposure to an organic fluid, such as paraffin wax used as a phase change materials (PCM). PCM are used for thermal energy storage (TES) in buildings applications for passive systems or heating and cooling usages. In any of these uses PCM must be encapsulated and PP is a possibility within the container materials used. Four different samples of the polypropylene were evaluated: PP, filled polypropylene with 60% $Mg(OH)_2$ (PP-60Mg), PP-60Mg with PCM (RT-25), and PP-60Mg with PCM (RT-42). It was studied the thermal stability by Thermogravimetrical analysis of these samples, and also it was evaluated the Hardness (H), Elastic modulus (E) and Loss modulus (E_{loss}) for the unfilled PP and PP-60Mg in contact with two different PCM at different temperatures (30 °C, 45 °C and 60 °C for RT-25 and 45 °C for RT-42) for 32 days. Results show that the mechanical properties H, E, and E_{loss} are higher for PP-60Mg than for PP. Nevertheless, these properties decrease significantly when the PP and the PP-60Mg are in contact with PCM, because it acts as a plasticizer, softening the polymer. Besides, the higher PCM's melting point, the lowest mechanical properties were observed.

1. Introduction

Phase change materials (PCM) have the principal advantage of high capacity energy storage in form of latent heat [1–4]. When a solid PCM is heated up and reaches its melting point, it goes through a phase change, from solid to liquid absorbing heat, known as melting enthalpy while the temperature remains constant. Equally, when the phase change process is reversed, that is from liquid to solid, the stored latent heat is released, again at a nearly constant temperature [5]. Materials studied for this application are salt hydrates, paraffin waxes, fatty acids, and eutectics of organic and non-organic compounds [6]. Paraffin waxes are one of the organic PCM most employed [7,8] due to their latent heat, thermal energy storage (TES) capacity, abundance, low cost, large number of applications, and because their stability after several charging/discharging cycles [9]. Paraffin waxes with a melting point between 30 °C and 90 °C have chains with the number of

---

* Corresponding author. Tel.: +34 934021298; fax: +34 934035438.
E-mail addresses: jessicagiro@ub.edu (J. Giro-Paloma), emraen@upvnet.upv.es (E. Rayón), joan.josep.roa@upc.edu (J.J. Roa), monicamartinez@ub.edu (M. Martínez), ana_inesfernandez@ub.edu (A.I. Fernández).
[1] Tel.: +34 934021298; fax: +34 934035438.
[2] Tel.: +34 963879625.
[3] Tel.: +34 93 401 07 12.

http://dx.doi.org/10.1016/j.eurpolymj.2014.11.029
0014-3057/© 2014 Elsevier Ltd. All rights reserved.

carbons atoms in the range between 18 and 50. The longer the chain of the paraffin waxes, the higher the melting point [10]. Depending on the service temperature, it will be chosen one PCM or another, so the temperature of the system is really important when the PCM has to be selected [11].

PCM can be used in passive systems such as floors [12] and walls, or in active systems like in domestic applications as heating [13] and hot water [14,15]. Otherwise, they must be encapsulated or contained to avoid leakage when phase change occurs. This encapsulation may be in the microscale [16], leading to microencapsulated PCM (MPCM), or in the macroscale where the use of common thermoplastics as container materials for PCM macroencapsulation is used in commercial applications [17], being the polypropylene (PP) suitable for active systems in domestic hot water applications (DHW). It has been also tested as good container for PCM in microscale, as a PCM shell [18]. Krupa et al. [19] reported the use of PP as matrix to create a shape stabilize PCM, a polymer blend obtained by mixing isotactic PP and paraffin. They report a plasticizer effect of the paraffin on the viscoelastic properties of the PP. Besides, long exposure to organic substances may be responsible of the premature mechanical failure of containers made of polypropylene [20]. ESC mechanism is a physical interaction connecting highly localised plasticisation via stress enhanced fluid absorption, which does not carry molecular degradation of the plastic nor chemical variations. The absorption of organic PCM (such as paraffin waxes) plasticises the polymer and also reduces its yield strength. This reduction is directly associated with the concentration of absorbed fluid [1]. For this reason, it was decided to evaluate filled PP as it is well known that inorganic fillers increase the mechanical resistance and stiffness of thermoplastics. Moreover, fillers may reduce the degradation effect avoiding the premature mechanical failure, and improve properties against fire, which is relevant in this study because the paraffin used as PCM are flammable materials. A filler that is commonly used for PP is $Mg(OH)_2$ [21,22] because of its flame retardant property [23], which also improves the mechanical response [24–26]. Therefore, the filler used in this work has been $Mg(OH)_2$, and the nanomechanical properties of filled PP compared with PP unfilled.

The nanoindentation technique was used to measure the nanomechanical properties of selected materials containing PCM. Nanoindentation technique is perhaps the most commonly applied means of testing the mechanical properties of materials at micrometric and nanometric scale. The ability to measure the microscopic regions responses is a key to understand the mechanical behavior of technological material systems [27].

The probe in nanoindentation technique is forced into the surface at a programmed rate and to a selected maximum force or depth. By means of special transducers the load and penetration depth are registered during the experiment. The area of contact between indenter and sample is then estimated using the known geometry of the indenter. For a Berkovich indenter, which is used in this work, the relationship between the projected area A of indentation and the indentation depth h beneath the contact is $A = 24.5h^2$. Consequently, Hardness (H) and Elastic modulus (E) can be calculated by the stiffness obtained by the known equations reported elsewhere [27] without the necessity to observe the indentation marks. This procedure has the advantage that very low loads can be used avoiding the material damage and makes possible to analyze thin films and small volume of material.

There are a great number of studies using the nanoindentation technique in polymers showing that is a simple but effective mechanical testing method. Nanoindentation has been successfully used to study the hardness and elastic properties of several polymers and nanocomposites. To give some examples of these studies on several polymers under different experimental strategies, Lee et al. [28], studied the H and E of a single cellulose fiber and PP matrix in a cellulose fiber-reinforced PP composite using the continuous stiffness measurement technique. Besides, Fang and Chang [29] studied the nanomechanical characteristics of polycarbonate polymer films under different applied loads, hold times, and loading rates. Moreover, Hu et al. [30] used it to investigate mechanical properties of Nylon 11 (PA11) and its nanocomposites with different clay loading.

Nanoindentation has been successfully compared with other techniques normally used to study the mechanical properties of polymers such as the Atomic Force Microscopy (AFM) and the Dynamic Mechanical Analysis (DMA) instruments; Griepentrog et al. [31] compared the nanoindentation technique and the Atomic Force Microscopy (AFM) methodology for the determination of mechanical properties of poly(methyl methacrylate) (PMMA) and polycarbonate (PC) polymers. Besides, Jee and Lee [32] studied AFM through both the force–indentation and area–depth curves for different polymers, concluding that the two methods give almost identical results with self-consistency. In a previous work, Giro-Paloma et al. [27] published a comparison study between mechanical data extracted from nanoindentation measurements and from classical dynamic mechanical analysis of several amorphous and crystalline polymers. In that study, we demonstrated that the elastic modulus obtained by nanoindentation can be well correlated with that obtained by DMA.

In this study were used two different types of paraffin waxes provided by Rubitherm® with different melting temperatures (T_m): RT-25 (T_m = 25 °C) and RT-42 (T_m = 41 °C).

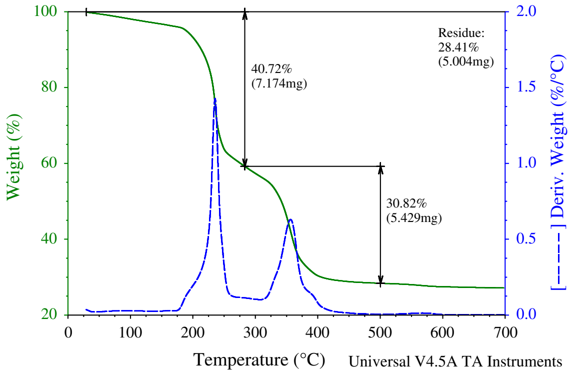

Fig. 1. Thermogravimetrical analysis of PP-60Mg.

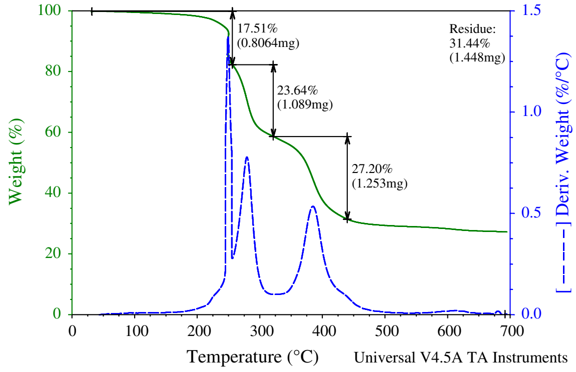

Fig. 2. Thermogravimetrical analysis of PP-60Mg with PCM.

These paraffin waxes were melted in separate vessels and two different polymeric materials were submerged in each paraffin sample for 32 days. Polypropylene (PP) was chosen as case study as it has been evaluated as container material of PCM [1] and a filled PP sample with a filler content of 60% $Mg(OH)_2$ (PP-60Mg) was also evaluated to compare the effect of the filler in the decrease of mechanical properties after long exposure to an organic fluid.

2. Experimental procedure

2.1. Materials

Polymeric samples were prepared at the Centre Català del Plastic (CCP). Two kinds of polypropylene samples were used, PP homopolymer and PP filled with 60% $Mg(OH)_2$) named PP and PP-60Mg, respectively. They were obtained by melt compounding with a co-rotating twin screw extruder. PP (Sabic PP 513A) was used and the PP-60Mg sample prepared by mixing PP with 60% magnesium hydroxide powder (Magnifin H-5 kV from Martinswerk). The obtained pellets were compressed moulded with a hot press plate, and different specimens were machined from the discs.

Paraffin waxes used were commercial products from Rubitherm (RT-25 and RT-42), having melting temperatures around 25 °C and 41 °C for RT-25 and RT-42, respectively.

2.2. Procedure

Polymeric specimens of 1 cm × 1 cm × 0.4 cm were submerged during 32 days in two different melted PCM and the temperature was kept constant. The temperatures tested were 30 °C, 45 °C and 60 °C for the RT-25 and 45 °C for the RT-42.

2.3. Characterization

2.3.1. Thermogravimetrical analysis (TGA)

Thermogravimetrical analysis (TGA) was used to study the thermal stability of the materials [33]. Thermal stability of the samples under study was evaluated with a TA Instruments, Simultaneous SDT Q600 under 100 ml min^{-1} N_2 atmosphere. The procedure of the TGA analysis was a scanning rate of 10 °C min^{-1} in the temperature range between 30 °C and 700 °C.

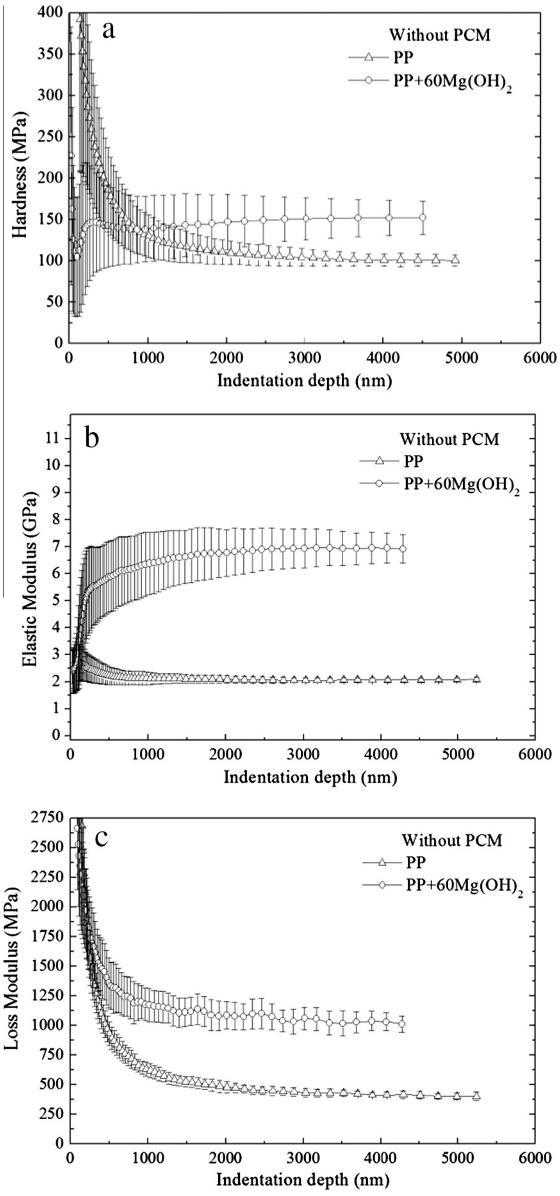

Fig. 3. Comparison of filled and unfilled PP without PCM. (a) Hardness, *H*; (b) Elastic modulus, *E*; and (c) Loss modulus, E_{loss}.

2.3.2. Nanoindentation technique

It was performed nanoindentation assays to evaluate the mechanical response in an indentation analysis with the purpose to calculate Hardness (*H*), Elastic modulus (*E*), and Loss modulus (E_{loss}) on the microscopic length scale and to estimate the changes produced by the contact with the organic fluid. Nanoindentation measurements were performed on samples PP and PP-60Mg at room temperature before and after being immersed during 32 days in two different types of PCM (RT-25 and RT-42) at the experimented temperatures.

A Nanoindenter G-200 (Agilent Technologies) was employed using a diamond three-sided Berkovich indenter geometry. This was calibrated with a silica standard specimen with a known Young's modulus. The stiffness

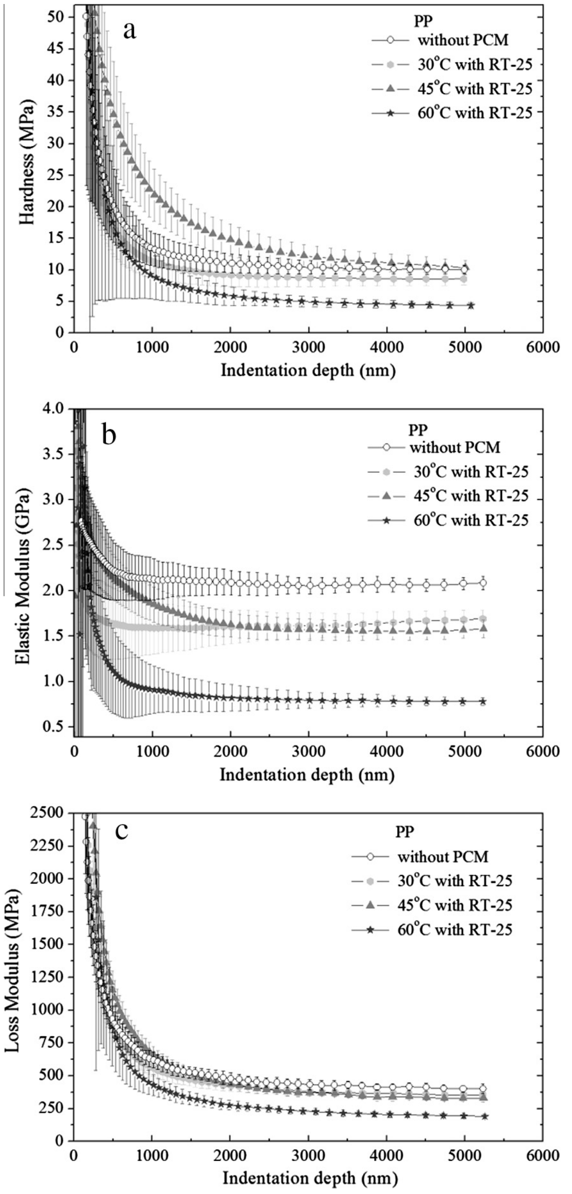

Fig. 4. Comparison of PP: without PCM, and in contact with RT-25 at 30 °C, 45 °C and 60 °C of (a) Hardness, H; (b) Elastic modulus, E; and (c) Loss modulus, E_{loss}.

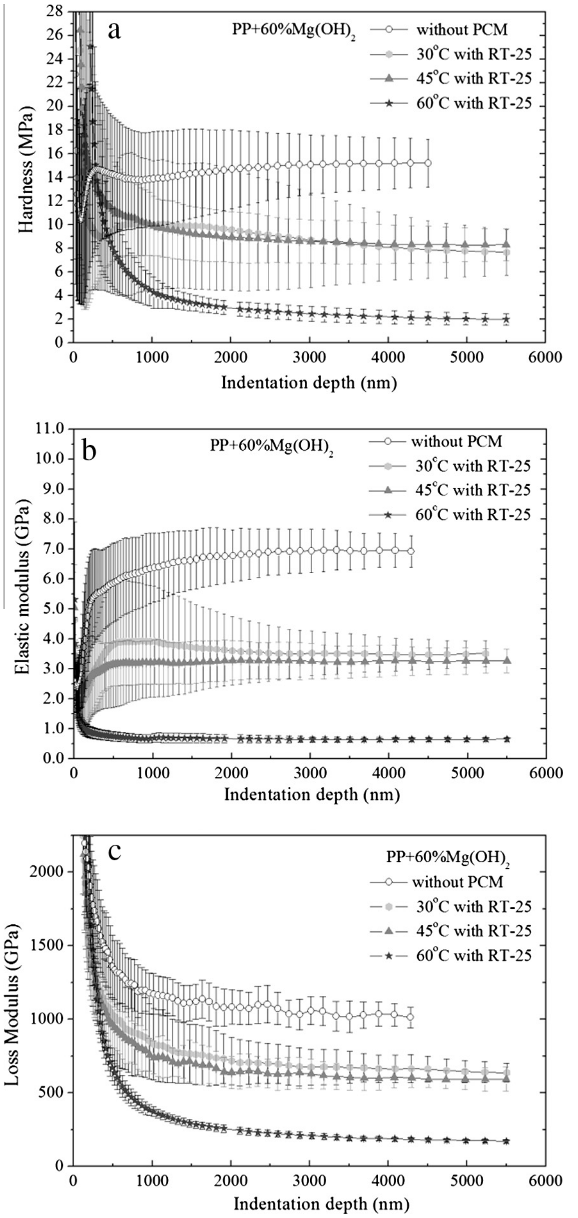

Fig. 5. Comparison of (a) Hardness, H; (b) Elastic modulus, E; and (c) Loss modulus, E_{loss} of PP and filled PP that was in contact with PCM RT-25, at different temperatures.

was acquired under the continuous stiffness measurement (CSM) at an oscillating frequency of 75 Hz and at 10 nm harmonic amplitude.

An array of 100 nanoindentation imprints was performed at 600 mN maximum load and each nanoindentation imprint was separated a constant distance of 500 µm. Several considerations were carefully observed. Due to the viscoelastic characteristic behavior of these materials, the typical hold segments in the unload curve were avoided by setting the hold time segment to cero. In order to calculate the thermal drift without constant load segments, a double P–h curve was executed for each test. Thermal drift is then considered well corrected by overlapping both unloading curves. Besides, a strain rate of 0.2 s^{-1} was chosen to assure that this parameter is not sensitive to the mechanical properties, following the study of Giro-Paloma et al. [27].

3. Results and discussion

3.1. Thermogravimetrical analysis

The thermal oxidative degradation of PP-60Mg was complete at temperatures up to 450 °C, with 28% of residue remaining, as it is shown in Fig. 1, revealing two decomposition steps. The first step corresponds to $Mg(OH)_2$ decomposition around 250 °C and the second step is attributed to

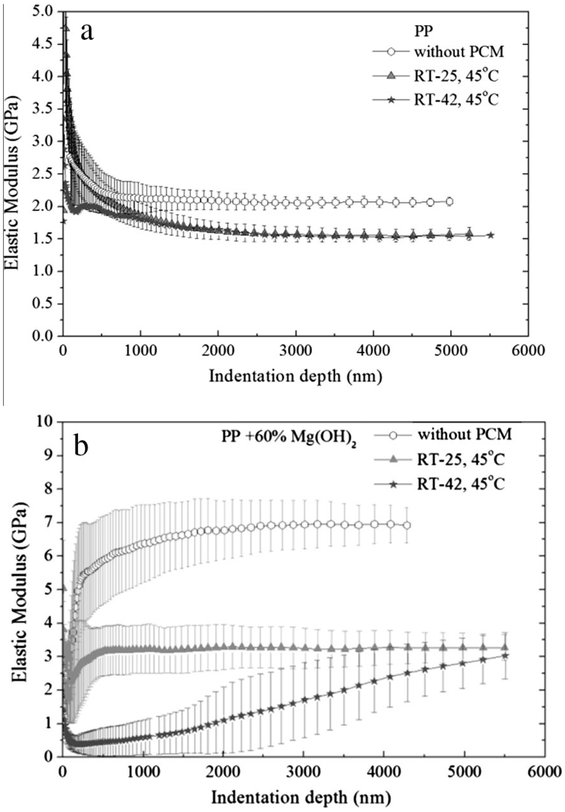

Fig. 6. Elastic modulus comparison at 45 °C for RT-25 and RT-42 (a) unfilled PP, and (b) filled PP.

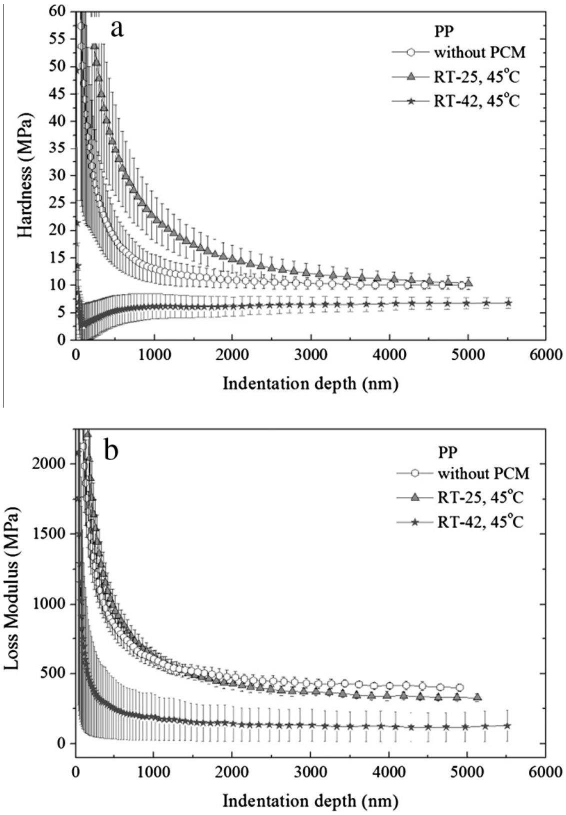

Fig. 7. Comparison of PP: without PCM, and in contact with RT-25 and RT-42 at 45 °C of (a) Hardness, H; and (b) Loss modulus, E_{loss}.

the thermo oxidative decomposition of polypropylene matrix which is in accordance with literature [34].

The thermal degradation curve of the PP-60Mg, after being submerged in PCM RT-25 during 32 days, shows three decomposition steps, as it is shown in Fig. 2. Thermal analysis of polymer immersed in organic PCM, such as paraffin wax, show a PCM absorption by the plastic in agreement to the observations made by Castellón et al. [1].

The first degradation is because of $Mg(OH)_2$ decomposition being around 17%. Then, the degradation of the PCM, around 24% of the sample takes place between 250 °C and 325 °C. Finally, the third step PP degradation finishes around 450 °C [35]. The 31% of residue corresponds to the MgO.

3.2. Nanoindentation technique

3.2.1. Mechanical properties of filled PP and unfilled PP

The filler effect on mechanical properties can be observed in Fig. 3. As expected, the sample of PP-60Mg presents higher H, E, and E_{loss} than PP ones, due to the reinforcement effect of filler.

3.2.2. Filled PP and unfilled PP in contact with an organic fluid (PCM)

A prolonged contact of PP with PCM softens the material. The results for PP samples in contact with RT-25 during 32 days at different temperatures (30 °C, 45 °C and 60 °C) are shown in Fig. 4. It is seen that the plasticizer effect of the paraffin increases with the temperature of exposition to the organic fluid. Also, it is observed a strong correlation between the temperature and the drop of mechanical properties when the temperature increases.

For this reason, after 32 days at 60 °C, the E, H and E_{loss} decrease significantly, whereas the mechanical properties after these 32 days in contact with the paraffin at 35 °C and 45 °C do not differ significantly between them and are slightly lower than those for the reference sample.

Notably, when it is used the same paraffin (RT-25) in contact with the filled PP, it is observed that the studied mechanical properties decrease in the same way as the temperature increase after 32 days of exposure as it can be observed in Fig. 5.

If the properties of Figs. 4 and 5 are compared, it can be observed the effect of the filler on the mechanical properties. As expected, E and E_{loss} values for the PP-60Mg are higher than the unfilled PP as the filler contributes making the composite stiffer and reducing the viscoelastic behavior. The presence of the filler counteracts the softening effect produced by continuous contact with PCM, except for those samples exposed to PCM at 60 °C, temperature in which the softening effect caused by the diffusion of paraffin in the polymer is highly favored. This effect is not so relevant in H values, which do not differ significantly of

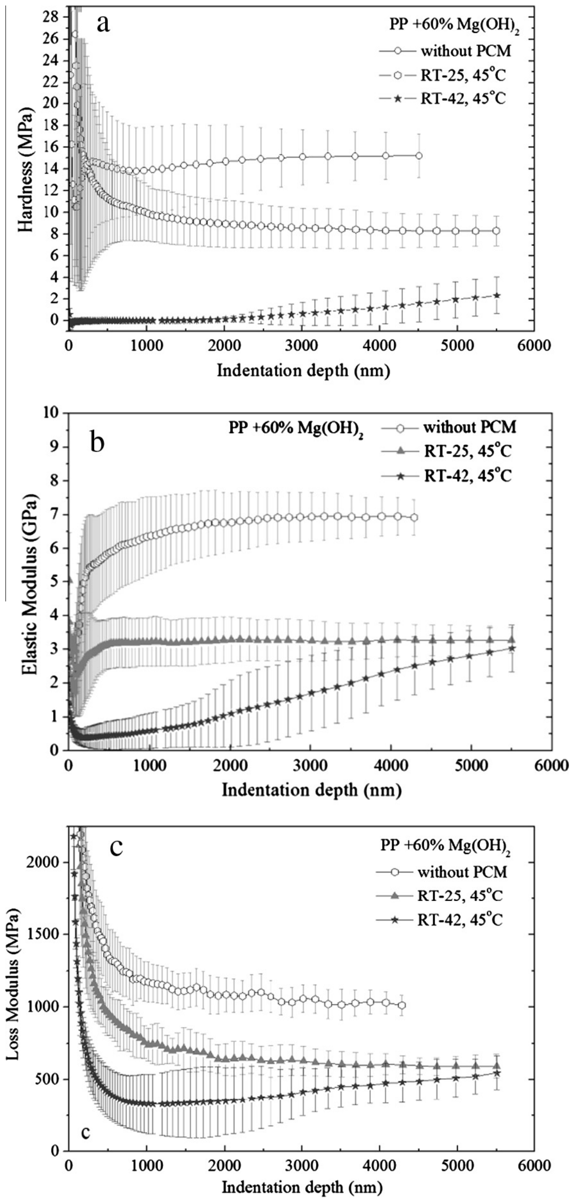

Fig. 8. Comparison of filled PP: without PCM, and in contact with RT-25 at 45 °C and RT-42 at 45 °C of (a) Hardness, *H*; (b) Elastic modulus, *E*; and (c) Loss modulus, E_{loss}.

the unfilled PP. Both samples follow the same tendency after being in contact with PCM, showing lower *H* values, even lower for the samples subjected to higher temperatures, as PCM has a tendency to infiltrate and soften some plastics [36].

When a paraffin of a higher melting point as RT-42 is used as organic fluid, no significant differences were observed in the measured elastic modulus of unfilled PP respect to the sample submerged in RT-25, showing both samples a modulus reduction around 35% over the measured modulus for reference PP sample, as is shown in Fig. 6a. For the PP-60Mg sample the reduction of this parameter is almost the 60% of the initial value (Fig. 6b).

Another effect observed between samples immersed in different paraffin waxes is the low value of elastic modulus at penetrations lower than 2000 nm, which is attributed to the presence of a residual paraffin coating that diminishes while the tip penetrates in the sample.

Otherwise, there are some differences in the *H* and E_{loss} between PP unfilled samples in contact with RT-25 and RT-42 PCM at 45 °C, as Fig. 7 shows. As mentioned before, curves obtained for PP sample tested with RT-42, show anomalous behavior at indentation depths lower than 2000 nm, which are attributed to a residual paraffin coating on the sample. There is a stabilization of the curve after this indentation depth and for *H* and E_{loss} it is seen that the softening effect and the viscoelastic behavior are higher when RT-42 was used as organic fluid. Thus, this softening effect needs to be considered when choosing unfilled PP as a polymeric container of paraffinic PCM. The container wall will soften during thermal cycles, and the effect will be more noticeable for paraffin with higher melting points.

However, when a filled PP is considered, the results are quite different. In Fig. 8 can be observed that the presence of inorganic filler in the PP-60Mg partially counteracts the softening effect, as the PCM cannot be soaked up in this sample as much as in unfilled PP. For the sample that was submerged in RT-25, even though there is a reduction in mechanical properties compared with the reference PP-60Mg, the results show that PP-60Mg is a better option than unfilled PP (especially at indentation depths higher than 3000 nm). Nevertheless, for the sample that was submerged in RT-42 there is a severe reduction in mechanical properties that is not counteracted by the filler content.

Table 1 summarizes the results of *E*, *H* and E_{loss} for a maximum penetration depth of 5000 nm.

Table 1
Comparison of the nanoindentation results for the filled and unfilled studied samples.

Sample	PCM	Working temperature of PCM (°C)	*H* (MPa)	*E* (GPa)	E_{loss} (MPa)
PP	Without	–	105.0 ± 10.0	2.0 ± 0.1	437 ± 10
	RT-25	30	8.7 ± 0.9	1.7 ± 0.1	365 ± 0.0
		45	10.4 ± 1.0	1.2 ± 0.1	345 ± 0.0
		60	5.0 ± 0.7	0.8 ± 0.0	205 ± 0.0
	RT-42	45	6.2 ± 1.1	1.5 ± 0.1	126 ± 60
PP-60Mg	Without	–	150 ± 20	6.8 ± 0.3	1095 ± 90
	RT-25	30	8.5 ± 1.9	3.5 ± 0.2	675 ± 80
		45	8.5 ± 3.5	3.2 ± 0.1	620 ± 85
		60	2.3 ± 0.4	0.6 ± 0.0	205 ± 15
	RT-42	45	1.2 ± 1.2	2.5 ± 1.0	350 ± 110

4. Conclusions

Nanoindentation technique is an adequate tool to evaluate nanomechanical properties for polymers. The usage of the fire retardant inorganic filler $Mg(OH)_2$, in a polypropylene (PP) matrix, improves significantly the Hardness (H), Elastic modulus (E) and Loss modulus (E_{loss}). PP is used as material container for paraffinic PCM in TES systems, and in this study it is demonstrated that there is a severe reduction in the mechanical properties after thermal cycles and a long exposure to paraffin. Moreover, for a given PCM as contact fluid, the lowest mechanical properties were observed for the higher temperature tested. Even though the softening effect of the paraffin is counteracted using the filled PP sample with paraffin RT-25, this improvement was not observed testing the paraffin RT-42, with a higher melting point. The main conclusion is that is better to use a filled PP instead of unfilled PP as a container material for paraffin in TES systems. In the case of paraffin with melting point above 25 °C, the decrease of mechanical properties because of softening effect must be considered in the design of the containers as it can compromise their mechanical performance.

Acknowledgments

The authors would like to thank the CCP for their kindly supply of the polymeric samples. The work is partially funded by the Spanish government (ENE2011-28269-C03-02). The authors would like to thank the Catalan Government for the quality accreditation given to their research group DIOPMA (2014 SGR 1543). The research leading to these results has received funding from the European Union's Seventh Framework Programme (FP7/2007-2013) under grant agreement no PIRSES-GA-2013-610692 (INNOSTORAGE).

References

[1] Castellón C, Martorell I, Cabeza LF, Fernández AI, Manich AM. Compatibility of plastic with Phase Change Materials (PCM). Int J Energy Res 2010;35:765–71.
[2] Bayés-García L, Ventolà L, Cordobilla R. Phase Change Materials (PCM) microcapsules with different shell compositions: preparation, characterization and thermal stability. Sol Energy Mater Sol C 2010;94:12535–40.
[3] García Almiñana D, Castell A, Cabeza LF. Estudio sobre el sistema de almacenamiento de agua caliente sanitaria en un sistema solar térmico. Espacio de reflexión y comunicación en Desarrollo Sostenible; 2006.
[4] Mehling H, Cabeza LF. Heat and cold storage with PCM. An up to date introduction into basics and applications. Berlin (Germany): Springer Berlin Heidelberg; 2008. ISBN: 978-3-540-68556-2.
[5] Farid MM, Khudhair AM, Razack SAK, Al-Hallaj S. A review on phase change energy storage: materials and applications. Energy Convers Manage 2004;45:1597–615.
[6] Tyagi VV, Kaushik SC, Tyagi SK, Akiyama T. Development of phase change materials based microencapsulated technology for buildings: a review. Renew Sust Energy Rev 2011;15:1373–91.
[7] Wang Y, Shi H, Xia TD, Zhang T, Feng HX. Fabrication and performances of microencapsulated paraffin composites with polymethylmethacrylate shell based on ultraviolet irradiation-initiated. Mater Chem Phys 2012;135:181–7.
[8] Sánchez P, Sánchez-Fernández MV, Romero A, Rodríguez JF, Sánchez-Silva L. Development of thermo-regulating textiles using paraffin wax microcapsules. Thermochim Acta 2010;498:16–21.
[9] Sharma SD, Buddhi D, Sawhney RL. Accelerated thermal cycle test of latent heat-storage materials. Sol Energy 1999;66:483–90.
[10] Bader M. Microencapsulated paraffin in polyethylene for thermal energy storage. Department of Chemical & Material Engineering, School of Engineering. University of Auckland: New Zeland, 2002.
[11] Giro-Paloma J, Oncins G, Barreneche C, Martínez M, Fernández AI, Cabeza LF. Physico-chemical and mechanical properties of microencapsulated phase change material. Appl Energy 2013;109:441–8.
[12] Lin CC, Yu KP, Zhao P, Lee GWM. Evaluation of impact factors on VOC emissions and concentrations from wooden flooring based on chamber tests. Build Environ 2009;44:525–33.
[13] Kabbaraa MJ, Abdallaha N Ben. Experimental investigation on phase change material based thermal energy storage unit. Proc Comp Sci 2013;19:694–701.
[14] Cabeza LF, Ibáñez M, Solé C, Roca J, Nogués M. Experimentation with a water tank including a PCM module. Sol Energy Mater Sol C 2006;90:1273–82.
[15] Mehling H, Cabeza LF, Hippeli S, Hiebler S. PCM-module to improve hot water heat stores with stratification. Renew Energy 2003;28:699–711.
[16] Jamekhorshid A, Sadrameli SM, Farid MM. A review of microencapsulation methods of phase change materials (PCMs) as a thermal energy storage (TES) medium. Renew Sust Energy Rev 2014;31:531–42.
[17] Rubitherm GmbH. Hamburg: Germany; 2002.
[18] Mokgaotsa Jonas Mochane. Polymer encapsulated paraffin wax to be used as phase change material for energy storage. Master of Science in the Department of Chemistry. Faculty of Natural and Agricultural Sciences at the University of the Free State; 2011.
[19] Krupa I, Miková G, Luyt AS. Polypropylene as a potential matrix for the creation of shape stabilized phase change materials. Eur Polym J 2007;43:895–907.
[20] Wright DC. Environmental stress cracking of plastics. Rapra Technology Ltd.; 2001. ISBN: 978-1-85957-064-7.
[21] Velasco JI, Morhain C, Arencón D, Maspoch ML. Polypropylene filled with flame retardant fillers: mechanical and fracture properties. Macromol Symp 2001;169(1):165–70.
[22] Velasco JI, Morhain C, Martínez AB, Rodríguez-Pérez MA, de Saja JA. The effect of filler type, morphology and coating on the anisotropy and microstructure heterogeneity of injection-moulded discs of polypropylene filled with aluminium and magnesium hydroxides. Part 2. Thermal and dynamic mechanical properties. Polymer 2002;43:6813–9.
[23] Antunes M, Velasco JI, Haurie L. Characterization of highly filled magnesium hydroxide–polypropylene composite foams. J Cell Plast 2011;47(1):17–30.
[24] Yanga J, Lianga JZ, Tang CY. Studies on melt flow properties during capillary extrusion of PP/$Al(OH)_3$/$Mg(OH)_2$ flame retardant composites. Polym Test 2009;28:907–11.
[25] Liang JZ, Yang J, Tang CY. Melt shear viscosity of PP/$Al(OH)_3$/$Mg(OH)_2$ flame retardant composites at high extrusion rates. J Appl Polym Sci 2011;119:1835–41.
[26] Chen D, Zhang H, Zheng Q, Liu F, Xu K, Chen M. Polypropylene composites filled by magnesium hydroxide coprecipitated with foreign ions. Polym Adv Technol 2008;19:1353–60.
[27] Giro-Paloma J, Roa JJ, Diez-Pascual AM, Rayón E, Flores A, Martínez M, et al. Depth-sensing indentation applied to polymers: a comparison between standard methods of analysis in relation to the nature of the materials. Eur Polym J 2013;49(12):4047–53.
[28] Lee SH, Wang S, Pharr GM, Xu H. Evaluation of interphase properties in a cellulose fiber-reinforced polypropylene composite by nanoindentation and finite element analysis. Compos Part A – Appl Sci 2007;38:1517–24.
[29] Fang TH, Chang WJ. Nanoindentation characteristics on polycarbonate polymer film. Microelectr J 2004;35:595–9.
[30] Hu Y, Shen L, Yang H, Wang M, Liu T, Liang T, et al. Nanoindentation studies on Nylon 11/clay nanocomposites. Polym Test 2006;25:492–7.
[31] Griepentrog M, Krämer G, Cappella B. Comparison of nanoindentation and AFM methods for the determination of mechanical properties of polymers. Polym Testing 2013;32:455–60.
[32] Jee AY, Lee M. Comparative analysis on the nanoindentation of polymers using atomic force microscopy. Polym Test 2010;29:95–9.

[33] Chen X, Yu J, Guo S. Thermal oxidative degradation kinetics of PP and PP/$Mg(OH)_2$ flame-retardant composites. J Appl Polym Sci 2006;103(3):1978–84.

[34] Ardanuy M, Velasco JI. Mg–Al Layered double hydroxide nanoparticles evaluation of the thermal stability in polypropylene matrix. Appl Clay Sci 2011;51:341–7.

[35] del Valle-Zermeño R, Chimenos JM, Formosa J, Fernández AI. Hydration of a low-grade magnesium oxide. Lab-scale study. J Chem Technol Biotechnol 2012;87:1702–8.

[36] Lane G. Latent heat materials, vol. 1. Boca Raton (FL): CRC Press; 1983.

Chapter 2 References

[1] Shim S, Bei H, Miller MK, Pharr GM, George EP. Effects of focused ion beam milling on the compressive behavior of directionally solidified micropillars and the nanoindentation response of an electropolished surface. Acta Materialia 2009;57:503–10. doi:10.1016/j.actamat.2008.09.033.

[2] Kruzic JJ, Kim DK, Koester KJ, Ritchie RO. Indentation techniques for evaluating the fracture toughness of biomaterials and hard tissues. Journal of the Mechanical Behavior of Biomedical Materials 2009;2:384–95. doi:10.1016/j.jmbbm.2008.10.008.

[3] Sakharova NA, Fernandes JV, Antunes JM, Oliveira MC. Comparison between Berkovich, Vickers and conical indentation tests: A three-dimensional numerical simulation study. International Journal of Solids and Structures 2009;46:1095–104. doi:10.1016/j.ijsolstr.2008.10.032.

[4] www.microstartech.com, 14/10/2014 n.d.

[5] Maneiro MAG, Rodríguez J. Pile-up effect on nanoindentation tests with spherical–conical tips. Scripta Materialia 2005;52:593–8. doi:10.1016/j.scriptamat.2004.11.029.

[6] Sun PL, Chu JP, Lin TY, Shen YL, Chawla N. Characterization of nanoindentation damage in metal/ceramic multilayered films by transmission electron microscopy (TEM). Materials Science and Engineering: A 2010;527:2985–92. doi:10.1016/j.msea.2010.01.040.

[7] Kartheek SSM, Vamsi KV, Ravisankar B, Sivaprasad K, Karthikeyan S. Microstructural and Nanoindentation Studies Across Diffusion-bonded Interfaces in Al/Cu Metal Intermetallic Laminates. Procedia Materials Science 2014;6:709–15. doi:10.1016/j.mspro.2014.07.087.

[8] Nevarez-Rascon A, Orrantia-Borunda E, González-Hernández J, Flores-Gallardo S, Hurtado-Macías A. Mechanical characterization of optical glass fiber coated with a thin film of silver nanoparticles by nanoindentation. Materials Letters 2014;136:63–6. doi:10.1016/j.matlet.2014.08.005.

[9] Smith CM, Jiang D, Gong J, Yin L. Determination of the mechanical behavior of lithium disilicate glass ceramics by nanoindentation & scanning probe microscopy. Materials Chemistry and Physics 2014;148:1036–44. doi:10.1016/j.matchemphys.2014.09.015.

[10] Woirgard J, Tromas C, Girard JC, Audurier V. Study of the mechanical properties of ceramic materials by the nanoindentation technique. Journal of the European Ceramic Society 1998;18:2297–305. doi:10.1016/S0955-2219(98)00083-1.

[11] Zhang Y, Allahkarami M, Hanan JC. Measuring residual stress in ceramic zirconia-porcelain dental crowns by nanoindentation. Journal of the Mechanical Behavior of Biomedical Materials 2012;6:120–7. doi:10.1016/j.jmbbm.2011.11.006.

[12] Guicciardi S, Balbo A, Sciti D, Melandri C, Pezzotti G. Nanoindentation characterization of SiC-based ceramics. Journal of the European Ceramic Society 2007;27:1399–404. doi:10.1016/j.jeurceramsoc.2006.05.057.

[13] Cabibbo M, Spigarelli S. A Calibration Round-Robin Protocol for Nanoindentation Measurements of Thin Film Coatings. Physics Procedia 2013;40:1–8. doi:10.1016/j.phpro.2012.12.001.

[14] Ozmetin AE, Sahin O, Ongun E, Kuru M. Mechanical characterization of MgB2 thin films using nanoindentation technique. Journal of Alloys and Compounds 2015;619:262–6. doi:10.1016/j.jallcom.2014.09.015.

[15] Díez-Pascual AM, Gómez-Fatou MA, Ania F, Flores A. Nanoindentation in polymer nanocomposites. Progress in Materials Science 2015;67:1–94. doi:10.1016/j.pmatsci.2014.06.002.

[16] Fang T-H, Chang W-J, Tsai S-L. Nanomechanical characterization of polymer using atomic force microscopy and nanoindentation. Microelectronics Journal 2005;36:55–9. doi:10.1016/j.mejo.2004.10.003.

[17] Gibson RF. A review of recent research on nanoindentation of polymer composites and their constituents. Composites Science and Technology 2014;105:51–65. doi:10.1016/j.compscitech.2014.09.016.

[18] Wornyo E, Gall K, Yang F, King W. Nanoindentation of shape memory polymer networks. Polymer 2007;48:3213–25. doi:10.1016/j.polymer.2007.03.029.

[19] Fang T-H, Chang W-J. Nanoindentation characteristics on polycarbonate polymer film. Microelectronics Journal 2004;35:595–9. doi:10.1016/j.mejo.2004.02.004.

[20] Vanlandingham MR, Villarrubia JS, Guthrie WF, Meyers GF, Dow T, Company C, et al. Nanoindentation of Polymers : An Overview. Macromolecular Symposia 2001;167:15–43.

[21] Hayes S a., Goruppa A a., Jones FR. Dynamic nanoindentation as a tool for the examination of polymeric materials. Journal of Materials Research 2004;19:3298–306. doi:10.1557/JMR.2004.0437.

[22] Loubet JL, Oliver WC, Lucas BN. Measurement of the loss tangent of low-density polyethylene with a nanoindentation technique. Journal of Materials Research 2000;15:1195–8.

[23] Odegard GM, Bandorawalla T, Herring HM, Gates TS. Characterization of Viscoelastic Properties of Polymeric Materials Through Nanoindentation. Experimental Mechanics 2005;45:130–6. doi:10.1177/0014485105052320.

[24] Larsson P-L, Carlsson S. On microindentation of viscoelastic polymers. Polymer Testing 1998;17:49–75. doi:10.1016/S0142-9418(97)00038-X.

[25] Lu H, Wang B, Ma J, Huang G, Viswanathan H. Measurement of Creep Compliance of Solid Polymers by Nanoindentation. Mechanics of Time-Dependent Materials 2003;7:189–207. doi:10.1023/B:MTDM.0000007217.07156.9b.

[26] Bucaille JL, Felder E, International E, Maur S. Identification of the viscoplastic behavior of a polycarbonate based on experiments and numerical modeling of the nano-indentation test. Journal of Materials Science 2002;37:3999–4011.

[27] Van Melick HG., Bressers OFJ., den Toonder JM., Govaert L., Meijer HE. A micro-indentation method for probing the craze-initiation stress in glassy polymers. Polymer 2003;44:2481–91. doi:10.1016/S0032-3861(03)00110-1.

[28] Van Melick H, Van Dijken A, Den Toonder J, Govaert L, Meijer H. Near-surface mechanical properties of amorphous polymers. Philosophical Magazine 2002;82:2093–102.

[29] Kermouche G, Loubet JL, Bergheau JM. Extraction of stress–strain curves of elastic–viscoplastic solids using conical/pyramidal indentation testing with application to polymers. Mechanics of Materials 2008;40:271–83. doi:10.1016/j.mechmat.2007.08.003.

[30] Doerner MF, Nix WD. A method for interpreting the data from depth-sensing indentation instrurnents. Journal of Materials Research 1986;1:601–9.

[31] MRS. Materials Research Society. Advancing Improving the quality of life. Nanoindentation: Fundamentals and frontiers n.d.

[32] Wang Y, Raabe D, Klüber C, Roters F. Orientation dependence of nanoindentation pile-up patterns and of nanoindentation microtextures in copper single crystals. Acta Materialia 2004;52:2229–38. doi:10.1016/j.actamat.2004.01.016.

[33] http://www.blue-scientific.com/picoindenter/, 14/10/2014 n.d.

[34] Oliver WC, Pharr GM. An improved technique for determining hardness and elastic modulus using load and displacement sensing indentation experiments. J Mater Res 1992;7(6):1564–80.

[35] Hochstetter G, Jimenez a., Loubet JL. Strain-rate effects on hardness of glassy polymers in the nanoscale range. Comparison between quasi-static and continuous stiffness measurements. Journal of Macromolecular Science, Part B 2006;38:681–92. doi:10.1080/00222349908248131.

[36] Li X, Bhushan B. A review of nanoindentation continuous stiffness measurement technique and its applications. Materials Characterization 2002;48:11–36. doi:10.1016/S1044-5803(02)00192-4.

[37] Giro-Paloma J, Roa JJ, Díez-Pascual AM, Rayón E, Flores A, Martínez M, et al. Depth-sensing indentation applied to polymers: A comparison between standard methods of analysis in relation to the nature of the materials. European Polymer Journal 2013;49:4047–53. doi:10.1016/j.eurpolymj.2013.09.010.

[38] Griepentrog M, Krämer G, Cappella B. Comparison of nanoindentation and AFM methods for the determination of mechanical properties of polymers. Polymer Testing 2013;32:455–60. doi:10.1016/j.polymertesting.2013.01.011.

[39] Velasco J., Morhain C, Martínez A., Rodríguez-Pérez M., de Saja J. The effect of filler type, morphology and coating on the anisotropy and microstructure heterogeneity of injection-moulded discs of polypropylene filled with aluminium and magnesium hydroxides. Part 2. Thermal and dynamic mechanical properties. Polymer 2002;43:6813–9. doi:10.1016/S0032-3861(02)00669-9.

[40] Velasco J, Morhain C, Arencón D, Maspoch M. Polypropylene filled with flame retardant fillers: mechanical and fracture properties. Macromolecular Symposia 2001;169:165–70.

[41] Antunes M, Velasco J, L H. Characterization of highly filled magnesium hydroxide–polypropylene composite foams. Journal of Cellular Plastics 2011;47:17–30.

[42] Yang J, Liang JZ, Tang CY. Studies on melt flow properties during capillary extrusion of PP/Al(OH)3/Mg(OH)2 flame retardant composites. Polymer Testing 2009;28:907–11. doi:10.1016/j.polymertesting.2009.08.005.

[43] Liang JZ, Yang J, Tang CY. Melt Shear Viscosity of PP / Al (OH) 3 / Mg (OH) 2 Flame Retardant Composites at High Extrusion Rates 2010:1–7. doi:10.1002/app.

[44] Chen D, Zhang H, Zheng Q, Liu F, Xu K, Chen M. Polypropylene composites filled by magnesium hydroxide coprecipitated with foreign ions 2008;4:1353–60. doi:10.1002/pat.

[45] Cai Y, Wei Q, Huang F, Lin S, Chen F, Gao W. Thermal stability, latent heat and flame retardant properties of the thermal energy storage phase change materials based on paraffin/high density polyethylene composites. Renewable Energy 2009;34:2117–23. doi:10.1016/j.renene.2009.01.017.

[46] Cai Y, Wei Q, Huang F, Gao W. Preparation and properties studies of halogen-free flame retardant form-stable phase change materials based on paraffin/high density polyethylene composites. Applied Energy 2008;85:765–75. doi:10.1016/j.apenergy.2007.10.017.

[47] Giro-Paloma J, Rayón E, Roa JJ, Martínez M, Fernández AI. Effect of the filler on the nanomechanical properties of polypropylene in contact with paraffinic phase change material. European Polymer Journal 2015;63:29–36. doi:10.1016/j.eurpolymj.2014.11.029.

Block II, Microscopic samples

Chapter 3: Methods of PCM microencapsulation and characterization of MPCM

Chapter 4: Characterization of MPCM

Chapter 5: Phase Change Slurries

Chapter 6: Characterization of Micronal® DS 5045 X

Chapter 3 . Methods of PCM microencapsulation and characterization of MPCM

The necessity of using special latent heat devices and/or heat exchange surfaces using PCM causes the effect of the increment of the system cost. The idea of improving the thermal comfort of lightweight buildings by integrating PCM into the building structure has been investigated in various research projects over several decades [1]. PCM are regarded as one possible solution for reducing buildings energy consumption [2] by storing and releasing heat within a certain temperature range (comfortable temperature), raising buildings inertia and stabilizing indoor climates. For this reason, it was investigated the necessity of encapsulate PCM in a container as a supporting material keeping the shape when the transitions from solid to liquid and from liquid to solid occurs. The main advantages of the PCM encapsulation are providing large heat transfer area, reduction of the PCM reactivity towards the outside environment, and controlling the variations in volume of the storage materials as phase change occurs [3].

3.1 Microencapsulation methodology

Microencapsulation of Phase Change Materials (MPCM) is an effective way of preventing possible interaction with the surrounding and leakage during the melting process at microscale [4]. It is important to notice that the microencapsulation methodology is widely employed in many fields, such as cosmetics, perfumes, flavors, food, adhesives, carbonless copy paper, oils, textiles, pharmaceuticals, and Phase Change Materials (PCM). This chapter will be focused in the microencapsulation of PCM.

All three states of material (solids, liquids, and gases) can be microencapsulated. This allows liquid and gas phase materials to be handled more easily as solids, and can also provide a physical barrier between the core material and the shell material. Depending on the core’s physico-chemical properties, the wall composition, the core material, the deposition process of the shell, and the used microencapsulation techniques, different types of particles can be obtained, as Figure 3.1 shows: particle containing an irregular shape core (Figure 3.1a); simple sphere surrounded by a coating of uniform thickness (Figure 3.1b); multi-walled microcapsules (Figure 3.1c); several core particles embedded in a continuous matrix of wall material (Figure 3.1d); and several distinct cores within the same capsule (Figure 3.1e). Among them, simple sphere particle is the most common one being fabricated and utilized.

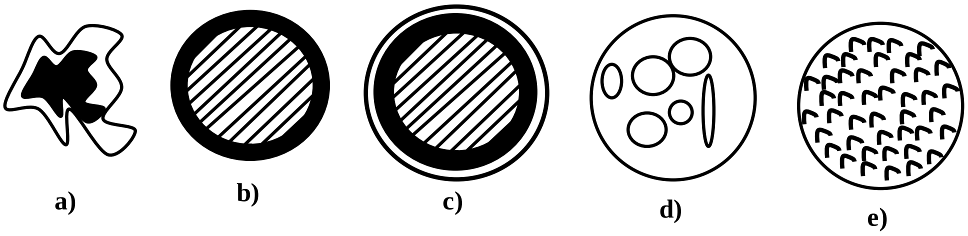

Figure 3.1. Possible shapes of microcapsules: a) Irregular shape; b) Simple; c) Multi-wall; d) Multi-core; e) Matrix particle.

The most common methods described in the literature for the production of MPCM are interfacial polymerization, suspension polymerization, coacervation, emulsion polymerization, and spray drying. All these polymerization techniques are explained in the review included in this chapter, section 3.3, (**Types, methods, techniques, and applications for Microencapsulated Phase Change Materials (MPCM): A review)**. At the moment, this document is accepted but it is not published yet.

3.1.1. Interfacial polymerization

Interfacial polymerization is a sort of step growth polymerization of two reactants occurring on the interface between two liquid phases (each liquid phase contains one of the reactants). Polyamide is the most common polymer used for this methodology, where diamine and diacid chloride react to form polyamide and hydrogen chloride. A base is needed to neutralize the acid formed during the reaction [5,6]. The aqueous phase contains the diamine, and the organic phase contains the HCl, having both reactants very low solubility in the other liquid phase. This ensures a controlled introduction of aqueous reactant into an excess of reactant in the organic phase. The reaction rate of this reaction is high, allowing the reactants to diffuse to the interface and to be combined almost stoichiometrically, forming a high molecular weight polymer. Being the reaction rate elevated, it is not possible that the diamine penetrates through the polymer to start new polymer chains in the organic phase. When obtaining the MPCM, the obtained walls are flexible and are formed rapidly at the interface. A solute of the pesticide and the diacid chloride are emulsified in water and an aqueous solution is added. The main advantage of this polymerization is that it is done at room temperature, because there are some polymers that do not allow high temperatures due to their glass transition temperature. Otherwise, the main disadvantage is related to the large amount of solvent that is needed, which can be costly in energy and money.

3.1.2. Suspension polymerization

Suspension polymerization is a radical heterogeneous polymerization process that uses mechanical agitation to mix a monomer (or mixture of monomers) in a liquid phase whilst the monomers polymerize. This process is governed by multiple simultaneous mechanisms such as particle coalescence and break-up, secondary nucleation, and the diffusion of monomer to the interface [7,8]. The collective effect of these mechanisms confers the size, the structure and the surface properties to the microcapsules [9,10]. This polymerization is applied to produce shell microcapsules of resins, polyvinyl chloride (PVC), polystyrene (PS), poly(styrene-acrylonitrile) and poly(methyl methacrylate) (PMMA), for example.

3.1.3. Coacervation

Coacervation consists of forming a liquid rich in polymer phase in equilibrium with another liquid phase. It is governed by three different steps under continuous agitation. The first one where it is needed the formation of immiscible chemical phases such as the liquid manufacturing vehicle phase, the core material, and finally the coating material phase (shell). The second step is related with the deposition of the coating; the core material is needed to be dispersed in the coating polymer solution. Besides, the deposition of the coating around core by polymer adsorbed at the interface formed between core material and vehicle phase will be achieved. Finally, the third step consist of the rigidization of the coating, doing it by thermal, cross-linking, or dissolvation techniques [11]. This type of polymerization is applied to produce shell microcapsules of Urea Formaldehyde (UF), Melamine Formaldehyde (MF), Poly-vinyl Alcohol (PVA), among others.

3.1.4. Emulsion polymerization

Emulsion polymerization is a radical polymerization that starts with an emulsion incorporating water, monomer, and surfactant. It consists of mixing a polymer in an oiled system in which droplets of the oiled monomer are emulsified with surfactants in a continuous phase of water. Subsequent to this, an emulsification is needed to create a water/oil emulsion and to generate a crosslinked system (chemically, thermally, or in an enzymatic way). The final step is to wash the emulsion to remove the oil and to create the isolated microcapsules [12]. This polymerization creates high molecular weight polymers. The main advantage of this process is the fast polymerization rates without loss of temperature control due to the continuous water phase is an excellent conductor of heat. The major drawback is the water removal costs, which it is an energy-intensive process. This type of polymerization is mostly used to produce synthetic rubber.

3.1.5. Spray drying

Spray drying is a technique to produce dry powder from a liquid by rapidly drying using a hot gas, being air the heated drying medium, ethanol when the liquid is a flammable solvent, or nitrogen when the product is oxygen-sensitive. This is the preferred method of drying of many thermally-sensitive materials. It has the ability to handle labile materials due to the small contact time in the dryer. In addition, the operation is economic [13–15].

3.2 Characterization of MPCM

The most employed techniques to characterize microcapsules reported in bibliography, particularly for MPCM, are optical microscopy, particle size distribution, scanning electron microscopy, transmission electron microscopy, infrared spectroscopy, differential scanning calorimetry, thermal reliability, thermogravimetrical analysis, thermogravimetrical analysis coupled with infrared spectroscopy, dynamic mechanical analysis, nanoindentation technique, atomic force microscopy, and gas chromatography/mass spectrometry.

In this Thesis an exhaustive characterization of MPCM is carried out using some of these techniques and thus, the equipments used are briefly described in this section.

3.2.1. Optical Microscope (OM)

A microscope is an optical instrument equipped with one or more lenses that increases the image size of an object and makes it visible or observable in detail. The optical microscope is a type of microscope which uses visible light, and it can be reflected or transmitted to the sample. In the reflection microscope, the light comes from the side of the objective by a mirror that surrounds it, or by an internal source and a mirror that require passing through the light into the objective, which also acts as a condenser.

The optical part consists of an ocular lens, which increases the real image by magnifying it, giving a virtual image. The objective is a lens located near to the object with short focal length and it creates a real and increased image between the eyepiece and the focus. There is a third lens, which the condenser collects the light provided by the lighting and it is located uniformly in the area of the object. The objectives are on a rotating drum which allows exchanging them easily. To focus the images, a screw position (macrometric) and an adjustment screw (micrometer) are needed.

The resolving power (D) is the minimum distance between two points on the object that are able to distinguish with clarity. It is a measure of the quality of the amplification and is determined by Equation 3.1:

$$D = \frac{\lambda}{2n \sin i} \qquad \text{Equation 3.1}$$

where λ is the wavelength of the incident light (visible 400 µm), n is the refractive index of the medium (air, water, oil), and i is half the opening angle.

The function to create a magnified image of a specimen consists of three basic functions such as obtaining a clear and sharp image, changing the magnification, and bringing the sample magnified into focus [16].

As examples of the usage of this technique, Sánchez *et al*. [17] developed thermo-regulating textiles using MPCM with paraffin in the core, and evaluated their morphology, fixation and durability, using a transmitted light and reflection mode. Bayés-García *et al*. [18] used a thermo-optical microscope at different temperatures to characterize gelatine/arabic gum (G/AG) MPCM. The optical microscope used in this Thesis was an OLIMPUS, AXIOVERT 405M.

3.2.2. Scanning Electron Microscopy (SEM)

SEM technique is based on the interaction of a primary beam of electrons (10-20 nm) on the surface that is going to be to analyze, it means, there is an interaction between the electron beam and the atoms of the sample. SEM uses an electron beam to impact the sample, thus obtaining high-resolution images of the topography surface of the sample. The wavelength (λ) of electrons used in electron microscopes is 0.5 Å, whereas the λ in shorter visible light is 4000 Å. Therefore, having less λ in an electron microscope will reveal the smallest details regarding its structure. From the interaction above mentioned, arise simultaneously various signals that are detected by different detectors. These signals are:

- The secondary electrons (SE): emitted by the sample as a result of ionizations from the electrons inelastic interactions in the primary beam with the sample.

- The backscattered electrons (BSE): scattered by the sample itself and they retain high energy. They allow obtaining compositional information of the sample.

- Energy Dispersive X-Ray Analysis (EDX): they are obtained due to the electronic relaxation between internal orbitals of the atoms in the sample. It gives information of the composition of the sample.

The basic elements of an electron microscope are tungsten filament, electron gun that collide with the surface of the sample, electromagnetic lenses that generate magnetic fields that modulate the speed and trajectory of the electron beam, and a vacuum system that removes air molecules that can deflect the electron beam. The SEM uses a focused beam of high-energy electrons to generate a variety of signals at the surface of solid specimens. The signals that derive from electron-sample interactions expose information about the sample including the texture, chemical composition, crystalline structures, and orientation of materials.

The samples have to be conductive, and if they are not, it is necessary to spread a thin film of conductive particles on the surface of the sample. The sample preparation is very simple and fast. The sample has to be stuck on the sample holder using a double-sided tape and then the sample morphology can be observed. Data is collected over a selected area of the surface of the sample, and a 2-D image is generated that displays spatial variations in these properties.

The SEM instruments used in this Thesis were ESEM, Quanta 200 FEI, XTE 325/D8395, obtaining images by SE, and a Jeol JSM-6510 device when the sample was needed to be cryonized prior observation, using a Cryo Unit GATAN accessory (Alto 1000 model).

3.2.3. Transmission Electron Microscopy (TEM)

The morphology and the structure of samples can also be observed by TEM, when their size is below micrometers. The studied specimen has to have low density, allowing the electrons to travel through the sample. There are different ways to prepare the material: it can be cut in very thin slices either by fixing it in plastic or working with it as frozen material [19,20]. Although TEM is a useful technique to characterize MPCM, it was not used in this Thesis.

3.2.4. Particle Size Distribution (PSD)

Particle size influences many properties of particulate materials and it is a valuable indicator of quality and performance. In PSD the interaction between light and the ensemble of all illuminated particles is analyzed [21]. Interpreting results of a particle size measurement requires an understanding of the calculations. There is an importance in PSD of the model applied to calculate the particle size of the sample. It can be analyzed using the mathematical models Fraunhofer or Mie [22,23]. The use of one or the other depends on the particle size and the opacity of the material. The Fraunhofer model is used for opaque particles bigger than 30 μm, whereas the Mie model fits better for homogenous and spherical particles, opaque or transparent and with diameters below 30 μm [22]. Rather than use a single point in the distribution as a specification, it is suggested to include other size parameters in order to describe the width of the distribution. The d_{90} parameter describes the diameter where ninety percent of the distribution has a smaller particle size and ten percent has a larger particle size. The d_{10} diameter has ten percent smaller and ninety percent larger. For this reason, a three point specification featuring, the d_{10}, d_{50}, and d_{90} will be considered complete and appropriate for describing most particulate materials.

PSD can be calculated based on some models, but the most often are related to number or volume/mass distribution. Figure 3.2 is represented a graphical example to better understand this difference. In the number distribution each particle size accounts for one third of the total, in volume distribution 75 % of the total volume comes from the 3 μm particles and less than 3 % comes from the 1 μm particles.

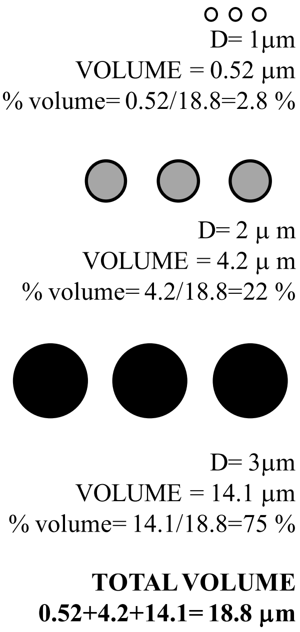

Figure 3.2.- Example to explain number and volume in PSD.

Figure 3.3 shows a comparative graph where it can be seen the difference between both models.

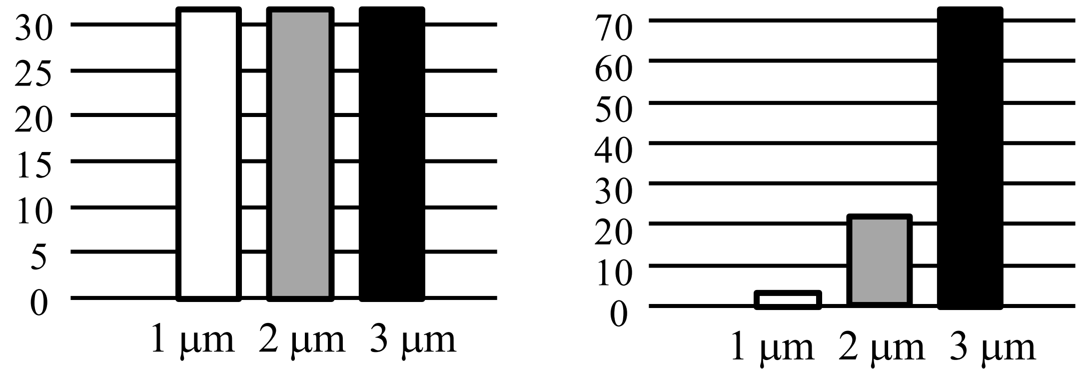

Figure 3.3.- Number vs. volume distribution [24].

Yu *et al.* [12] used PSD technique in number distribution to evaluate the diameter distribution of microcapsules containing PCM prepared with different mass ratios of emulsifier.

When a microencapsulated sample suffers agglomeration, it can be avoided by treating it in an ultrasonic bath during 60 seconds in water with a dispersing agent, to promote deagglomeration of particles. In this case, the samples were mixed with water and with a non-ionic surfactant (the dispersing agent), 0.01 % of Tween 80 (Polysorbate 80). Samples analyzed in this Thesis by PSD technique were performed by using a Beckman Coulter® LSTM 13 320 with Universal Liquid Module device.

3.2.5. Fourier Transformed Infrared spectroscopy (FT-IR)

Infrared technique allows identifying, studying, and evaluating compounds in a solid liquid or gas state. The infrared segment of the electromagnetic spectrum is separated in three regions; the near (14000 - 4000 cm^{-1}), the mid (4000 - 400 cm^{-1}) and the far infrared (400 - 10 cm^{-1}). It can be analyzed by Attenuated Total Reflectance (ATR) or by Transmission (with a KBr pellets) [25–27]. In Figure 3.4 is represented the difference between ATR and transmission [28], and in Table 3.1 different parameters between transmittance and reflectance techniques [28] are compared. The comparison between ATR and reflectance data is not straightforward as a correction is needed. In transmission, the optical path is the material thickness, whereas in ATR, the depth of the penetration (d_p) (which is the analogue of the optical path) is directly proportional to the wavelength (λ), as described in Equation 3.2. The consequence of this fact is that in ATR spectrum, when the wavenumber decreases, the band intensity is also increased accordingly, due to a deeper penetration (d_p) of the radiation into the sample.

$$d_p = \frac{\lambda}{2\Pi n_1 (\sin^2 \Theta_{ef} - n_{21}^2)^{1/2}} \qquad \text{Equation 3.2}$$

where d_p is the penetration depth of the radiation, λ the wavelength in μm, n_1 the refraction index of the ATR crystal, n_{21} the ratio between the refraction indexes of the sample and of the crystal and Θ_{ef} the effective incident angle in degrees.

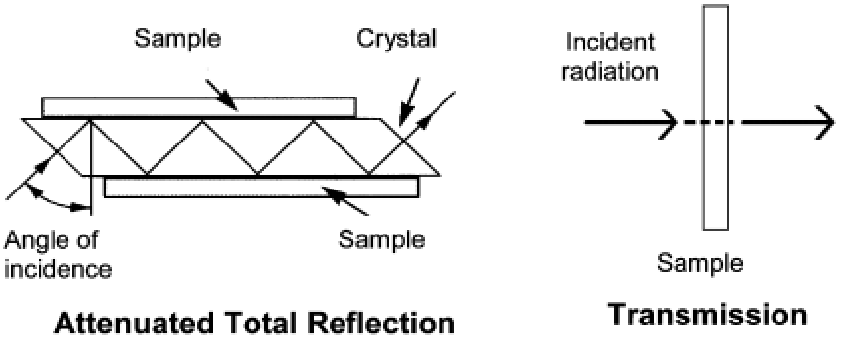

Figure 3.4. Schematic representation of the infrared radiation path and contact type for the different techniques.

Table 3.1. Transmittance and reflectance characteristics for a polymer analysis by FT-IR.

Technique		**Use**	**Sample preparation**	**Remarks**
Transmittance	Film	Polymer identification general purpose	Heating and pressing	Heating could alter the material. Very thin films show fringes in the spectra
	Disk	Very seldom used in thermoplastics	Pressing of the pure material with KBr	A fine powder is often difficult to obtain
Reflectance	ATR	Soft polymers surface analysis	None. Different accessories may be needed	The spectra from those obtained by transmittance. A good constant crystal/sample is needed

ATR is a very sensitive technique and especially suitable for surface analysis. This technique gives well-resolved even though less intense bands. The advantage of ATR is the possibility of obtaining the spectra directly from the sample, without any further sample preparation. Besides, the obtained spectrum peaks can be quantifiable.

One example related with the MPCM field using FT-IR device is the one performed by Zou *et al*.[27], who verified that polyurea microcapsules containing *n*-hexadecane as PCM have been successfully synthesized.

There were two FT-IR devices used in this Thesis:

- Spectrum Two™ from Perking Elmer supported by Dynascan™ interferometer and OpticsGuard™ technology was used to perform the analyses. This equipment can measure substances at liquid and solid state, and it was optimized by a wavelength range between 4000 cm^{-1} and 350 cm^{-1} (mid IR segment) and its standard spectral resolution is 0.5 cm^{-1}.
- FT-IR Bomem ABB FTLA using a working ranges from 350 to 4000 cm^{-1}.

3.2.6. Differential Scanning Calorimetry (DSC)

Differential Scanning Calorimetry (DSC) is the thermal analysis technique most used for studying the thermal behavior and thermal properties of materials [29,30]. DSC measures the difference in temperature (heat flow, $mW = mJ\cdot s^{-1}$) between a sample and an inert reference (for instance, empty pan) as a function of time and temperature. This technique gives information of the melting temperature (T_m) and solidification temperature (T_s) of a sample and the enthalpy value for each process (melting and solidification, H_m and H_s, respectively), which is equivalent to the area under the curve. DSC can detect glass transition (T_g, which is reversible, it is due to the amorphous part of the polymer and it is detected in a DSC instrument as a change in the C_p), fusion, crystallization, and C_p [31], as Figure 3.5 shows. It determines endothermic and/or exothermic transitions as function of temperature [32].

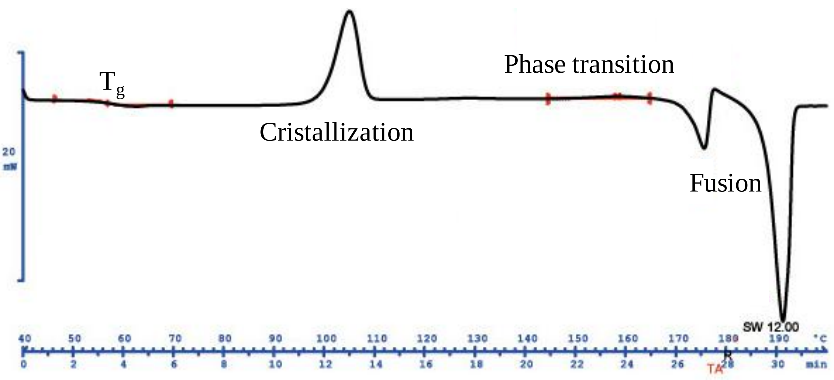

Figure 3.5. Transitions in DSC technique.

The main applications in DSC experiments are related to those which can determine transition temperatures, including: melting, glass transition, thermal stability, oxidation onset, cure onset, crystallization, polymorphic transition, polymorphic transition, liquid crystal, protein denaturation, solid-solid transition. Besides, heat flow, thermal story, kinetics, photocuring, degree of cure, and pharmaceutical polymorph analysis are other applications concerning DSC technique [33].

The sample in DSC device is located inside a pan. DSC pan materials are available in aluminum, alodine-coated aluminum, gold, platinum, graphite, and stainless steel versions. They can be used under a variety of temperature and pressure conditions. Samples can be run in open pans, pressed pans or hermetically sealed pans. The pan selection will depend on the temperature and pressure assay conditions. In Table 3.2 is listed some examples for standard and hermetic pans.

Table 3.2. Standard and hermetic pans for DSC technique.

Standard	Temperature (ºC)	Pressure
Aluminum	from -180 to 600	100 kPa
Platinum	from -180 to 725	100 kPa
Gold	from -180 to 725	100 kPa
Graphite	from -180 to 725	100 kPa

Hermetic	Temperature (ºC)	Pressure
Aluminum	from -180 to 600	300 kPa
Alodined Aluminum	from -180 to 200	300 kPa
Gold	from -180 to 725	600 kPa
High Volume	from -100 to 250	3.7 MPa
Stainless Steel	ambient to 250	10 MPa

DSC heat flow signal is commonly used to measure and quantify a wide variety of transitions and events, often occurring in the same material as a function of temperature. Moreover, DSC is an excellent tool for determining the thermal history of a polymeric sample. In this case, the sample is subjected to a “heat-cool-reheat” cycle and a comparison is made between the two heating cycles. The heat of fusion of 100 % crystalline polymer is required to obtain percent crystallinity by DSC.

Regarding to the MPCM field, Zheng *et al*. [29] used this calorimetric technique to characterize two PCM suitable for applications in concentrating solar power systems.

The thermal properties such as melting/solidification temperature and melting/solidification enthalpy during this PhD were evaluated with the help of the Research Group Grea at the University of Lleida, using a DSC 822-e from Mettler Toledo. Aluminum crucibles of 40 μl under N_2 atmosphere flow of 80 mL·min^{-1} were used. The regular heating rate used was 0.5 ºC·min^{-1} [34].

3.2.7. Thermal reliability

The thermal cycling test exposes the thermal reliability and chemical stability of samples. It consist on the estimation of the samples quality to guarantee no alteration on its geometrical shape or breakage after numerous thermal cycles [36,18]. The thermal reliability can be evaluated in a DSC device or in a specific cycle instrument as a thermocyclator [37,38].

As an example regarding of MPCM thermal cycling, Alkan *et al*. [35] studied the thermal reliability as well as thermal properties of MPCM with *n*-eicosane in the core and polymethylmethacrylate (PMMA) as shell.

When a sample in this Thesis was cycled, the experimental installation located in Zaragoza (Spain) was used [39], Figure 3.6. It is a flow loop designed to study flow and heat transfer characteristics of Phase Change Slurries, PCS. To obtain local convective heat transfer coefficients and pressure loss measurements, this setup allowed to subject to the sample to solidification and melting cycles, at the same time that the sample is being pumped. This installation consisted on a thermostatic bath with a centrifugal pump, a Coriolis flow meter, a heat transfer section and control valves.

The PCS has to be pumped from the thermostatic bath, where the PCM of the microcapsules in suspension are in solid phase. It flows through the loop, passing through the heat transfer section (a 10 mm of diameter copper tube with 1.82 m length), where heating wires provide uniformly-distributed heat flux, melting these PCM microcapsules. Then, the PCS returns to the thermostatic bath by cooling down, and solidifying the PCM in the microcapsules. The mass flow was measured by a Coriolis flow meter and adjusted by control valves. The heat flux supplied on the heat transfer section was controlled by a phase angle regulator, so that the fluid temperature at the outlet of this section increased up, and to guarantee that the PCM microcapsules in suspension have melted. This temperature has been measured by a 4-wire Pt100 datalogger. From the velocity of the PCS and from the volume of the installation (that is from the volume of the pumped PCS), the needed time for a melting/solidification cycle can be calculated. Thus, the total number of cycles can be obtained.

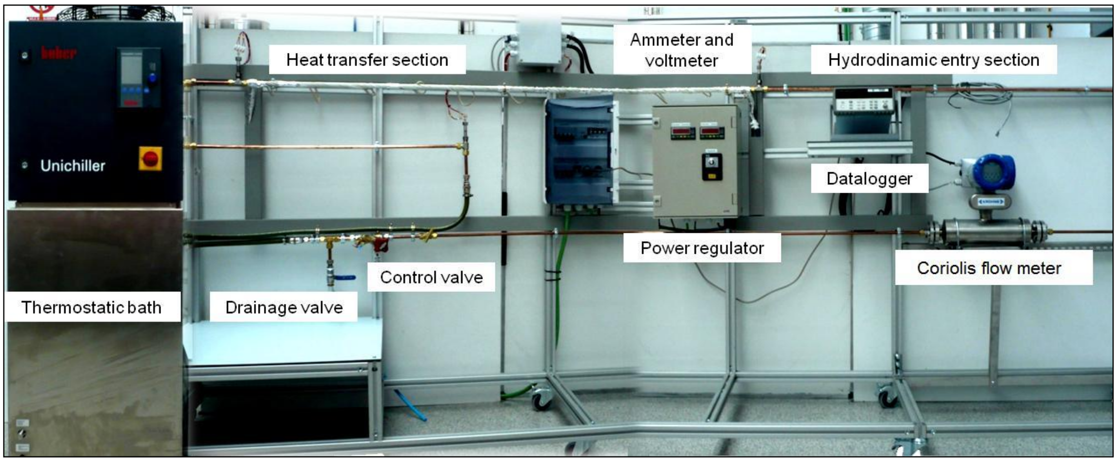

Figure 3.6.- Installation used to pump and cycle samples in this PhD Thesis.

3.2.8. Thermogravimetrical Analysis (TGA)

Thermogravimetric Analysis (TGA) measures the amount and rate of change in weight of a material as a function of temperature or time in a controlled atmosphere [40]. Measurements are used primarily to determine the composition of materials and to predict their thermal stability at temperatures up to 1000 ºC. The technique allows characterizing materials that exhibit weight loss or gain due to the decomposition, oxidation, or dehydration [25].

This technique is widely employed in MPCM field, particularly for characterizing PCM and MPCM. As an example, Zhang *et al.*[40] evaluated the step thermal degradation and the thermal reliability of a MPCM composed by silica as shell and *n*-octadecane in its core.

The TGA instrument used in this Thesis was a Q600 from TA instruments, which provides simultaneous measurement of weight change (TGA) and true differential heat flow (DSC) on the same sample as a function of temperature (from ambient temperature to 1500 ºC) or time in a controlled atmosphere. The complimentary information obtained allows differentiation between endothermic and exothermic events which have no associated weight loss (e.g. melting and crystallization) and those which involve a weight loss or gain (e.g. degradation). It features a field-proven horizontal dual beam design with automatic beam growth compensation, and the ability to analyze two TGA samples simultaneously. DSC heat flow data is dynamically normalized using the instantaneous sample weight at any given temperature. Although ceramic pans of 40 µl were used to operate between room temperature to 1500 ºC, the temperature range in this PhD Thesis was between room temperature and 600 ºC.

3.2.9. Evolved gas analysis: TGA/FT-IR

The main reason on using the evolved gas analysis coupling the TGA to FT-IR is to separate, identify, and quantify individual degradation products (off-gases) when it is not possible to recognize products by using only TGA technique. The main advantages of this coupling are on-line measurement. The main drawbacks implies that there is no detection of inert gases (no dipole moment, µ=0) and for this reason only vibrations causing change in dipole moments are detected. Besides, the detection of inorganic gases is very limited. It is important to highlight that there are not bibliographic references concerning the evolved gas analysis by TGA and FT-IR in MPCM characterization, being very innovative. Figure 3.7 shows the coupling TGA to FT-IR.

Figure 3.7.- TGA instrument coupled to FT-IR device.

3.2.10. Dynamic Mechanical Analysis (DMA)

Dynamic Mechanical Analysis (DMA) is a technique used to measure the mechanical properties of a wide range of materials as function of time, temperature, frequency, stress, atmosphere or a combination of these parameters [42]. It measures the properties of materials as they are deformed under periodic stress. Specifically, a variable sinusoidal stress is applied and the resultant sinusoidal strain is measured. By this manner, it measures the viscoelastic properties using either transient or dynamic oscillatory tests. The most common test is the dynamic oscillatory test. Besides, DMA records the temperature-dependent viscoelastic properties and determines the modulus of elasticity and the damping values by applying an oscillating force to the sample. Some of the properties that can be measured by DMA include storage and loss modulus, tan δ, complex and dynamic viscosity, storage and loss compliance, transition temperatures, creep, and stress relaxation, as well as rate and degree of cure, sound absorption and impact resistance, and morphology.

Many materials behave both like in elastic solid and viscous fluid, thus the term viscoelastic. DMA differs from other mechanical testing devices in two important ways. First, typical tensile test devices focus only on the elastic component. In many applications, the inelastic, or viscous component, is critical. It is the viscous component that determines properties such as impact resistance. Second, tensile test devices work primarily outside the linear range. DMA works primarily in the linear viscoelastic range and it is therefore more sensitive to structure.

Although DMA is a useful technique to characterize polymers, it was not used in this PhD Thesis because it is not possible to use this technique with MPCM, but bulk samples.

3.2.11. Nanoindentation technique

Nanoindentation technique allows measuring mechanical properties at small scales and it is an adequate technique for investigating the nanomechanical changes in the surface and in the inner polymers [43,44]. Besides it can perform experimental studies of fundamental materials physics. High-resolution load-displacement data, discrete events including dislocation source activation, shear instability initiation, and phase transformations can be detected during a nanoindentation test [45]. To extract the mechanical characterization of materials this technique seems to be adequate [46,47].

Nanoindentation technique is perhaps the most commonly applied means of testing the mechanical properties of materials at micrometric and nanometric scale. The ability to measure the microscopic regions responses is a key to understand the mechanical behavior of technological material systems [48]. The most common use of nanoindentation is for the measurement of hardness and elastic modulus, and there has been considerable progress in the measurement of other mechanical parameters as well, including hardening exponents, creep parameters, and residual stresses.

The principal components in a nanoindenter device are the test material, the sensors and actuators used to apply and measure the mechanical load and indenter displacement, and the indenter tip. The latter component is conventionally made of diamond, formed into a sharp, symmetric shape such as the three-sided Berkovich pyramid geometry.

During a typical nanoindentation test, force and displacement are recorded as the indenter tip is pressed into the test material's surface with a prescribed loading and unloading profile. The response of interest is the load-displacement curve (often called the P-h curve). The global shape of the P-h curve differs from one material to the next, and these variations usually reflect different mechanical properties. This technique was widely explained in Chapter 2 of this Thesis.

Some studies related with MPCM are those presented by Su *et al.* [49], where the evaluation of the size and shell thickness of microcapsules was performed using nanoindentation technique. Moreover, Lee *et al.* [50] employed nanoindentation technique to evaluate the mechanical behavior of polymeric microcapsules.

The two employed devices (Scientific and Technological Centers (CCiTUB) of Universitat de Barcelona and University of Auckland) in this Thesis were equal instruments, a Nano Indenter® XP System (Agilent Technologies) equipped with Nanosuite 6.1 software, provided with Continuous Stiffness Measurement (CSM). It was used Berkovich tips in both devices.

3.2.12. Atomic Force Microscopy (AFM)

Atomic Force Microscopy (AFM) is a surface technique that can obtain topographic images at nanometric resolution and it can be used as a nanomanipulator in order to test the surface of the samples. AFM allows obtaining atomic surface resolution while analyzed samples remain in their native environment. Besides, AFM is the only instrument that gives a clear view of the nano-scale structure with profound implications for the advancement of nanotechnology in material science. The accessible force range is shifted to small values (pN to μN) accompanied with high resolution. Consequently, it is a suitable tool for capsule systems to study shell mechanical properties in the small deformation regime, on the order of the shell thickness [53]. It can work in different atmospheres (air, nitrogen, argon) and in different states of the material (liquid and solid). The system can work between room temperature and 250 ºC, thus being able to study samples at variable temperature to detect changes in the mechanical properties. The scanning of the sample is done mechanically. The sample goes and comes back by the same way, and the final image obtained is the retrace one. It is very important to consider that what it is moving in x, y and z axis at sub-nanometric scale is the piezoelectric, not the tip indenter. Moreover, if the sample is scanned too fast deformed images will be obtained, and the final image will have a lot of background noise.

AFM is a powerful characterization tool for polymers and is capable of revealing surface structures with high spatial resolution [13,54–56]. AFM has rapidly increased in applications in polymer characterization and has distinguished itself as a primary technique for such characterization. AFM required simple or no sample preparation and preserves sample structure. The surface uses a physical probe, as well as creates images by mechanically moving the probe in a raster scans. In Figure 3.8 is shown a pattern of the AFM device, which consists on a piezo scanner, cantilever, laser, and a photodiode.

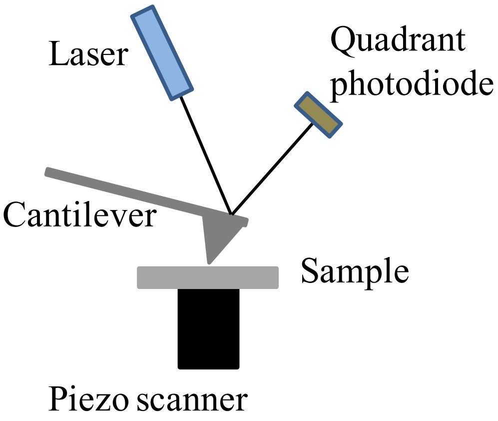

Figure 3.8. Scheme of the AFM instrument.

There are different AFM modes. The *feedback* is very important due to it controls one parameter constant (this parameter can be the beam deflection or the vibration). The modes that are used in this PhD thesis are the contact mode and the tapping mode. The possible modes in AFM are as follows:

- Contact mode: the sharp tip at the end of the microfabricated AFM cantilever is in contact with the sample surface. In this mode, the cantilever deflection (constant magnitude) is the key point of the system (the set point), so the cantilever deflection is constant during all the data collected. The most correct way to perform the experiments is to choose a value close to zero because the image has to be as real as possible. The touching between sample and tip is very soft, and it does not provide mechanical information. The deflection image on a soft sample often reveals subsurface structure more clearly than the topography image. If it is applied the same force in the entire sample, the images are comparable. No sample preparation is needed and good resolution is obtained. Figure 3.9 shows a sketch of contact mode. The first image shows the different parts of the device and the sample (semicircumference). When the tip finds the sample, the cantilever and the tip reacts moving up and down. By this way, the laser that collides against the detector moves some degrees, causing the final sample AFM image.

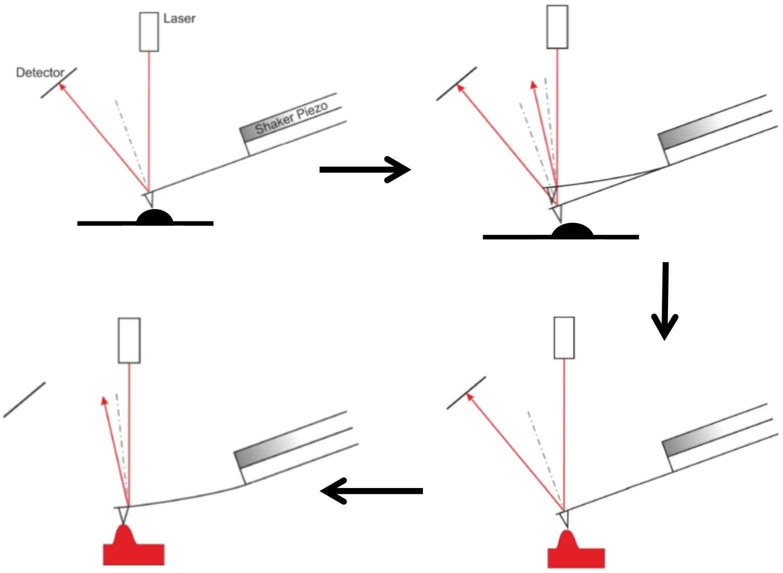

Figure 3.9. Scheme of the contact mode.

- Force Spectroscopy mode: it is used to measure and control the polarity and strength of the interation between the AFM tip and the sample.
- Tapping mode: in Intermittent Contact Mode AFM, the oscillation amplitude of the cantilever is compared with a set point value. The difference between the two is called error signal, and is the input into the feedback system, the output of which drives the Z-actuator. This output signal is the quantity that is most often plotted for each X, Y coordinate to synthesize the 3D image, usually called the topographic image. The methodology allows more control in the way of measuring, and it is more usual than contact mode. In this mode the constant parameter is the vibration amplitude. The tapping mode takes information of the resonance frequency of the cantilever. The amplitude on the laser belongs to the tip vibration.
- Phase imaging mode: phase imaging is a derivative mode of Dynamic Mode AFM (both lateral and vertical), where the phase of the cantilever oscillations φ, measured relative to the drive signal oscillations, has turned out to be a powerful signal for studying the properties of the sample surface, especially heterogeneous surfaces.
- Polarization Microscopy (SPFM) mode: it is a non-contact technique where the tip scans the surface at a height of a few hundred angstroms, which is sufficient to minimize perturbation of the liquid film. The resolution is few hundred angstroms horizontally and one angstrom vertically. The information of SPFM includes topography, contact potential and dielectric mapping.
- Conducting AFM (C-AFM) mode: in this mode, the tip is coated with a conductor. For this reason, the tip can turn into an electrical probe by applying a voltage.

- Tunneling AFM mode: a voltage between the AFM tip and the sample induces a current between the two, which is measured and mapped simultaneously with the topography image.
- Magnetically activated Dynamic AFM mode: in this mode, the AFM cantilever is partially coated with a magnetic thin film. The drive force is applied directly to the cantilever, close to the cantilever free end. The images are in black and white color, and they provide information about the different magnetic structures.
- Lateral Force Microscopy (LFM) mode: the tip is constantly in contact with the sample surface. In LFM, the last direction of the raster scanning is perpendicular to the long axis of the cantilever, which twists laterally as the raster scanning proceeds. The detector can collect a sizeable lateral deflection signal from the cantilever's twisting motion.

Besides, depending on the desired information about the sample, the measure and the methodology used will be different, as Table 3.3 shows.

Table 3.3. Information obtained in AFM technique depending on the performed measurement.

Interaction	**Measure**	**Information**
Force	Displacement	Topography
Tunneling current	Current	Topography
Magnetic force	Phase	Magnetic structure
Electric force	Phase	Charge distribution

The AFM technique can be used in several fields and applications, such as chemical processes on surfaces (corrosion, catalysis, etc.), coatings (finishing, functionalization, etc.), life Science (cells, hair, virus, etc.), material science (polishing, shapes, hardening, etc.), microstructures (lenses, CD/DVD/Blue Ray, etc.), and semiconductors (chip fabrication, solar cells, hard disk, etc.).

In Table 3.4 different types of tips are shown. Depending on the hardness of the material, it will be used one tip or another. Typical tip indentors are SiO_2 (0.35 $N\cdot m^{-1}$), Si_3N_2, Pt, Au, diamond (300 - 400 $N\cdot m^{-1}$), considering high hardness being 40 $N\cdot m^{-1}$ and low hardness being 1 $N\cdot m^{-1}$.

Table 3.4. Types of tip indenters.

Tip	Information/Possibilities
Standard Si tip	Topography
Soft cantilever	Soft samples (biological samples)
Hard cantilever	Nanoindentation
Conducting tips	Conductivity measurements
Magnetic tips	Magnetic measurements
Heatable tips	Thermal properties
Hollow tips	Whole new range of possibilities - Pick and place - Adhesion measurements - Spotting - Injection - Etc.

Ghorbanzadeh *et al.* [57] employed AFM technique to evaluate the micromechanical properties of microcapsules. Besides, included in this PhD Thesis, there are some studies related to the AFM performance and the microcapsules containing PCM. The first study performed by DIOPMA research group using AFM technique with MPCM was applied to microcapsules named Micronal® DS 5001 [58]. After having success in its characterization, AFM has been employed in other type of MPCM. The last project was the characterization and comparison performed into Poly(styrene-coethylacrylate) (PScEA) microcapsules containing paraffin wax and PScEA MPCM with palmitic acid in the core by using several methods, including AFM [59].

The instrument used at the Scientific and Technological Centers (CCiTUB) of Universitat de Barcelona was a Peak Force Quantitative NanoMechanics mode (QNM) with a system Multimode 8, Nanoscope V electronics, from Bruker. The AFM probe was different depending on the experiment. It was tested a diamond MDNISP one, with a nominal spring constant: 388 $nN \cdot nm^{-1}$, and also a diamond probe from Bruker with the same value for the spring constant. The sensitivity was 68.2 nm·V^{-1} with a set point (maximum vertical force) between 400 and 550 nN. Moreover, the working conditions for the peak force amplitude were between 150 nm and 300 nm, the DMT Modulus limit 1 TPa, and finally the peak force frequency was 0.5 kHz.

3.2.13. Volatile Organic Compounds (VOC’s)

A validated method for air-quality by multi-sorbent adsorption and gas chromatography/mass spectrometry (GC/MS) thermal desorption system (TD) [60] can be measured. The thermal desorption is a high versatile sample preparation technique (TD technologies) for the measurement of volatile and semi-volatile organic compounds in air and materials [61]. GC/MS is a selective instrumental technique, allowing good chromatographic separation, and at the same time VOC’s identification through mass spectra. Moreover, it is useful for measuring VOC's in new buildings because it is easy to get results directly in the field. It will be very important to take into account different variables, such as the time of the exposure, the relative humidity, the temperature, the material studied and the VOC’s to be analyzed.

A GC-17A Gas chromatograph Shimadzu coupled to a GCMS-QP5000 Gas chromatograph/Mass Spectrometer Shimadzu was used in Auckland (New Zealand) to characterize the VOC’s emissions of some samples.

3.3 Review on Microencapsulated Phase Change Materials

After the explanation of some relevant techniques widely employed to characterize samples, it was considered to summarize studies related to TES, particularly in MPCM field, and write a paper in review format. By this manner, a review titled: “**Types, methods, techniques, and applications for Microencapsulated Phase Change Materials (MPCM): A review**” was accepted in **Renewable & Sustainable Energy Reviews** journal in 2015 (18/09/2015).

Elsevier Editorial System(tm) for Renewable & Sustainable Energy Reviews
Manuscript Draft

Manuscript Number: RSER-D-14-01331R1

Title: Types, methods, techniques, and applications for Microencapsulated Phase Change Materials (MPCM): A review

Article Type: Review Article

Section/Category: Solar

Keywords: Phase Change Material; Microencapsulated Phase Change Material; Thermal Energy Storage

Corresponding Author: Dr. Ana Inés Fernández, Ph.D

Corresponding Author's Institution: Universitat de Barcelona

First Author: Jessica Giró-Paloma, PhD student

Order of Authors: Jessica Giró-Paloma, PhD student; Mònica Martínez; Lluïsa F Cabeza; Ana Inés Fernández

Abstract: Phase Change Materials (PCM) can be employed in many fields because of their capacity to absorb and release energy when it is necessary. Nowadays, the number of studies about these materials is increasing because of their benefits in energy systems. This paper reviews the previous researches and developments on microencapsulated phase change materials (MPCM) in thermal energy storage (TES) systems, focusing on the different methods of encapsulations and also the different applications of these materials. This review aims to be a useful guide for the researchers in this area, because it explains the different types of phase change core materials, the different shells, the methods to microencapsulate these PCM, the most used techniques to characterize these microencapsulated phase change materials, and a revision of the main applications

Response to Reviewers: Title: Types, methods, techniques, and applications for Microencapsulated Phase Change Materials (MPCM): A review

Authors: Jessica Giro-Paloma, Mònica Martínez, Luisa F. Cabeza, A. Inés Fernández
Ref Number: RSER-D-14-01331
Journal: Renewable & Sustainable Energy Reviews

Types, methods, techniques, and applications for Microencapsulated Phase Change Materials (MPCM): A review

Jessica Giro-Paloma[1,a]; Mònica Martínez[2,a]; Luisa F. Cabeza[3,b]; A. Inés Fernández[4,a,*]

[a]Departament de Ciència dels Materials i Enginyeria Metal·lúrgica, Universitat de Barcelona, Martí i Franqués 1-11, 08028, Barcelona, Spain, Phone: 34-934021316, Fax: 34-93.4035438
[b]GREA Innovació Concurrent. Edifici CREA. Universitat de Lleida. C/ Pere de Cabrera s/n, 25001-Lleida (Spain), Phone: 34-973003576, Fax: 34-973003575

[1]*jessicagiro@ub.edu*; [2]*monicamartinez@ub.edu*; [3]*lcabeza@diei.udl.cat*; [4]*ana_inesfernandez@ub.edu*
**Corresponding author*

Abstract

Phase Change Materials (PCM) can be employed in many fields because of their capacity to absorb and release energy when it is necessary. Nowadays, the number of studies about these materials is increasing because of their benefits in energy systems. This paper reviews the previous researches and developments on microencapsulated phase change materials (MPCM) in thermal energy storage (TES) systems, focusing on the different methods of encapsulations and also the different applications of these materials. This review aims to be a useful guide for the researchers in this area, because it explains the different types of phase change core materials, the different shells, the methods to microencapsulate these PCM, the most used techniques to characterize these microencapsulated phase change materials, and a revision of the main applications.

Keywords: Phase Change Material; Microencapsulated Phase Change Material; Thermal Energy Storage

1. Introduction

Phase Change Materials (PCM) are well known in Thermal Energy Storage (TES) applications [1–3]. PCMs are used to store energy when it is available, absorbing it and releasing it when needed. The most important requirements to be a good PCM may be divided in physical, chemical or economical requirements:

- Physical requirements: Suitable phase change temperature, complete reversible freeze/melt cycle, large change in enthalpy (ΔH), large specific heat capacity (C_p), large thermal conductivity (k), and little subcooling.
- Chemical requirements: Small volume pressure, low vapor pressure, good compatibility with other materials, chemical stability, physical stability, and non-toxicity.
- Economical requirements: Low price, recyclable and abundant.

PCM are used in several applications, due to the research done last forty years in this field. It had been published a total of 10,892 documents in TES field for the last 10 years (January 2005 - April 2015) [4]. Taking into account TES subject, if it is emphasized in PCM field, 2,319 documents can be counted. Following the same bibliographic search, but deepening and specializing the topic, the representation for the search in microencapsulated phase change material (MPCM) in TES field, is shown in

Figure 1, with 449 documents for the last ten years (January 2005 - April 2015).

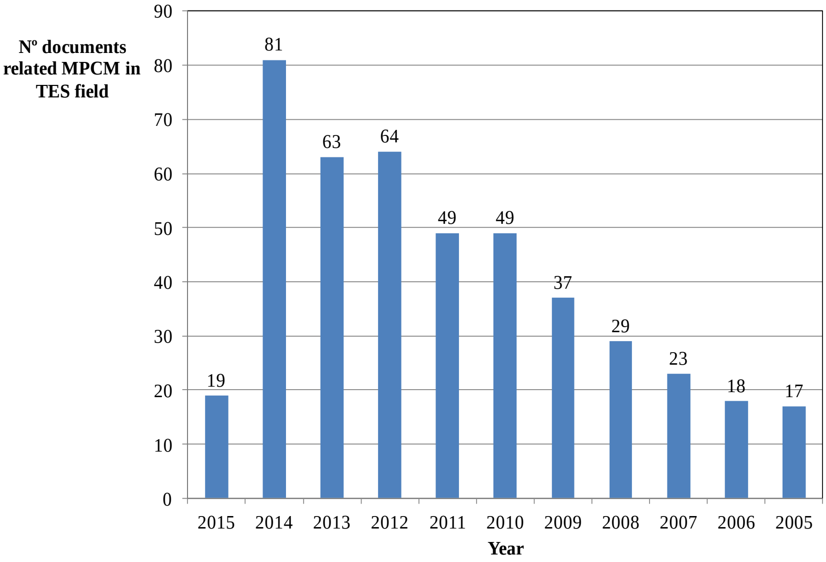

Figure 1. Representation of the publications total number related to MPCM in TES field between 2005 and 2015.

These 449 documents related to MPCM were published in different subjects inside TES area. The most part were from Engineering (46.1 %), Materials Science (30.1 %), and Energy (28.1%) journals, as Figure 2a illustrates. The studies connected with this thematic were produced in different kind of publications, such as articles (70.2 %), conference papers (24.3

%), and reviews (2.9 %), as examples showed in Figure 2b. Up to date, there are no reviews on MPCM.

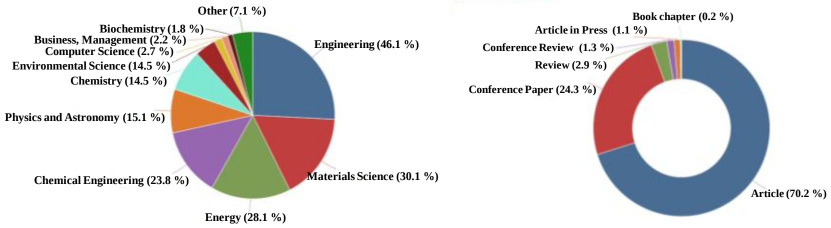

a) b)

Figure 2. a) Documents by subjects for MPCM in TES field; b) Documents by type for MPCM materials in TES field.

From these figures the study of PCM and MPCM is a topic that generates more interest every year. These materials can be applied in textiles [5,6], buildings [7–9], packaging, food, medical therapies, etc. PCM have been considered for TES in buildings since 1980, and only the PCM with a phase transition close to the human comfort can be used, which is around 20 ºC. One of these applications for PCM is climatization [10], which has different uses, for example in solar cooling, as the study of Gil *et al.* [11] shows. Besides, inside the refrigeration area, food conservation [12,13] can be included. Oró *et al.* [14] studied the effect of the PCM introduction outer a freezer, improving the quality in the ice cream. The container drinks can also incorporate these type of materials to store energy, and release it when the systems needed, for example, the chilly bins studied by Oró *et al.* [15] to enhance the thermal performance. Also, it is possible to use phase change materials in cold storage needs, as Oró *et al.* [16] evaluate, studying the compatibility of PCM with metallic materials, but a common problem in PCM cooling applications is the subcooling, which happens when a material is cooled and the crystallization does not start below the freezing temperature [17].

Another very significant application of PCM is the one in the building sector [18], in passive applications like floors [19], walls [20–23] (for example conventional and alveolar brick [24]), and ceiling studies. There is another case, which is in active systems in domestic applications as heating [25] and hot water [26–29].

Since PCM undergo the solid-liquid states, they need to be encapsulated for their inclusion in the final system. Due to the leakage in the liquid state when mixing the PCM with other materials, such as building construction materials [30], and because of the corrosion and the thermal reliability, the possibility to make a polymeric container for PCM, in small vessels, using the encapsulation technology and producing capsules calling them encapsulated Phase Change Material for energy storage [31] has been investigated. Encapsulation techniques vary from macroencapsulation in slabs, panels, etc. to microencapsulation [32,33]. When the sizes of these capsules are micrometers, these are called Microencapsulated Phase Change Material (MPCM), which consisted on a polymeric shell and a core made of the storage material. The microencapsulation is a process of enclosing micron-sized particles of solids or droplets of liquids or gases in an inert shell, which in turn isolates and protects them from the external environment. The captivity of waxes into the microcapsules allows to increase the heat transfer [3] and to control de volume changes when the phase change is happening. Microencapsulation methodology for PCM still needs to be improved because the microcapsules can break easily when they collide with other microcapsules when they are used in active systems. Moreover, the shell has to be strong enough to sustain the stresses that are generated due to the volumetric changes during the phase change process of the PCM.

There are three requirements for the microencapsulation process: the formation of the shell around the desired PCM, guaranteeing that there is not leakage and ensuring that no impurities are included in the system core/shell MPCM. Besides, the thickness of the coating material has to assess the effectiveness of the encapsulated PCM. For this reason, the MPCM have to be highly resistant to mechanical and thermal stresses.

Two studies by Jamekhorshid *et al.* [34] and Sukhorukov *et al*. [35] explain that the size of the MPCM is very significant, because MPCM are more stable in the nanosize than in the microsize. They observed less mechanical deformation in 10 nm MPCM in size than in 10 μm. To avoid the breakage of the microcapsules, it is important to take into account the whole system we are using (shell/core). Moreover, the compatibility of plastics with PCM is a key point as Castellón *et al*. [36] evaluated, concluding that LDPE and PP show worst behavior compared with HDPE to encapsulate PCM. Hardness and Young’s Modulus of different polymers were evaluated by Giro-Paloma *et al*. [37], because in passive systems case [38], the main problem of the leakage is the compression of this microcapsules inside the wall in a building [39].

As Kuznik *et al*. [23] studied, there are three relevant characteristics to evaluate for the quality of the MPCM: the mean diameter, the thickness of the shell, and the mass percentage of PCM compared to the total mass of the capsule. Once the PCM which will be used in a system as a good material to store energy is chosen, it is very important modeling the system with the finality to know how it will perform [40].

Microencapsulation has been studied widely by many researchers, but the literature is scattered. Therefore, this paper presents a review, which includes the different types of PCM that can be microencapsulated, the different shell materials used, the way to microencapsulate these PCM, and finally the most used techniques to characterize these MPCM with the idea to organize such literature and help researchers to use it as a guide in their future work. At the end of the review, the most important applications where MPCM are used are summarized. The future directions of research and development on Microencapsulated Phase Change Materials will focus on the improvement of characterization methodology for such complex materials, and deeply studying other relevant properties as the volatile organic compounds spread by MPCM, as well as their fire behavior.

2. Types of Phase Change Materials (PCM)

In microencapsulation, the core material is defined as the specific material to be coated and can be in liquid or solid state depending on the temperature. The composition of the solid core can be a single solid substance or a mixture of active constituents, stabilizers, diluents, excipients and release-rate retardants or accelerators [41,42]. There are three type of PCM: organic, inorganic and eutectic PCM. The most important property to take into account in a material to be used as a PCM is that it must have high thermal energy storage capacity, and in general, inorganic have it higher than organics, but there are some other subjects to take into account for choosing these materials. Cabeza *et al*. [43] listed in their review many PCM specifying their type, melting temperature, heat of fusion, thermal conductivity, density, and their source.

- **Organic PCM**: This type of PCM is further described as paraffinic and non-paraffinic. The principal advantages are their chemical and thermal stability, they are non-corrosive, recyclable and they have no subcooling. On the other hand, the disadvantages of using organic PCM are their flammability, their low thermal conductivity and a phase change enthalpy lower than other type of PCM. The most used ones are paraffin and fatty acids:

    - Paraffin: This chemical is produced as a by-product of petroleum refinery. It consists of carbon and hydrogen atoms joined with single bonds with the general formula: C_nH_{2n+2}, where n is the number of carbons (C). When *n* is between 1 and 4 C atoms the material is gaseous; between 5 and 17 C is liquid, and for more than 17 C is solid. It is considered a paraffin wax when the C is in the range of 20 - 40.

    - Fatty acids: It is a carboxylic acid with a long hydrocarbon chain of carbon (from 10 to 30) and hydrogen atoms with a general formula $CH_3(CH_2)_{2n}COOH$. It has the carboxyl group (COOH) at the end of the chain and due to the protection of this group, fatty acids based PCMs are non-toxic, with low corrosion activity, and chemically and thermally stable. Moreover, they can be found in natural products, not being a fossil fuel derivative. The fatty acids can be saturated or unsaturated, with one or more double bounds. Unsaturated fatty acids have lower melting points due to the molecular structure that allows closer molecular interactions. Moreover, unsaturated fatty acids can exist in the *cis* and *trans* configuration having the intermolecular interactions weaker than in saturated ones. Besides, different fatty acids can be mixed to design PCMs with different melting temperatures. There is a study of Suppes *et al*. [44] where the possibility to use natural fatty acid mixtures as high performance PCM is demonstrated.

- **Inorganic PCM**: They are classified as salt hydrates, salts, and metals. This type of materials has fewer advantages than organics. The pro is that they have higher phase change enthalpy, but the corrosion, subcooling, phase segregation, lack of thermal stability, and phase separation are the most important cons.

  - Salt hydrates: It is defined as the inorganic salts that have water molecules combined in a definite ratio as part of the crystal, as $X_nY_m{\cdot}aH_2O$ formula, where *X* is a cation, *Y* is an anion, and *a* is the number of water molecules. They are solid at room temperature, and when the melting point is reached, the salt starts to dissolve in their own water crystal.

  - Salts: They are inorganic salts with a formula as X_nY_m, where *X* is a cation and *Y* is an anion. These salts are used for higher temperature ranges but they have lower enthalpy than salt hydrates. An example of a high temperature energy storage use is in a concentrated solar power (CSP) plant, which uses salt to store energy for later use.

  - Metals: This subcategory of inorganic PCM includes the low melting metals and metal eutectics. They are good candidates to take into account for elevate temperature of phase change, when the volume is a consideration in the system, because of their high heat of fusion per unit volume. This type of PCM has high thermal conductivity, low specific heat, and low vapor pressure.

- **Eutectics**: The eutectics are a combination of chemical compounds or elements that has a single chemical composition and solidifies at a lower temperature than any other composition obtained from the same components. The combinations can be organic-

organic, inorganic-inorganic, or inorganic-organic [45]. There are numerous eutectic mixtures suitable to be used as PCM, and they are preferred in cooling applications.

3. Types of shell

There are over fifty different polymers known that can be used as wall materials in microencapsulation; both natural and synthetic polymers controlling release under specific conditions. The shell coating materials have to have some properties or requirements. The polymer should be capable of forming a thin film that it must be cohesive with the core material, being tasteless, pliable, and stable. It should be chemically compatible and non-reactive with the core material, and also soluble in an aqueous media or solvent. Moreover, it should provide the desired coating properties such as strength, flexible, impermeable, optical properties, and stability. The film thickness can be varied considerably depending on the surface area of the material to be coated, and other physical characteristics of the system. Besides, the shell coating material has to be non-hygroscopic, with medium/low viscosity, and low cost.

4. Types of Microencapsulated Phase Change Materials (MPCM)

There are several studies about MPCM, where choosing the combination shell/core is the most important point. The proportion of core material in the capsule is usually between 20 and 95 % by mass [46]. The microcapsules may consist on a single particle or clusters of particles.

Paraffin wax is one of the most employed PCM in MPCM systems. Among paraffin, *n*-octadecane is the PCM most used microencapsulated in building applications [47–51].

There are a lot of studies about the shell. One possibility is the transparent and thermoplastic acrylic polymer for the shell [42,52–55], such as poly(methyl methacrylate) (PMMA) [56–60]. It has good mechanical properties and good protection against the environment. For these reasons, PMMA is an adaptable material and it is a good polymer as shell material in the preparation of MPCM for thermal energy storage applications. Moreover, as example of commercial MPCM, BASF® has a variety of products with PMMA as shell material. As examples of studies with BASF® materials, Tzevetkov *et al.* [61] studied one of the products, Micronal®, using scanning transmission X-ray spectromicroscopy. This PMMA has good compatibility with a wide variety of PCM, for example with fatty acids, such as stearic acid, palmitic acid, myristic acid and, lauric acid as studied by Alkan *et al.* [62]. Besides, Giro-

Paloma *et al.* [63] evaluated in detail the physical, chemical and mechanical properties of Micronal® DS 5001.

Another polymeric shell very employed is the melamine-formaldehyde (MF). Su *et al.* [64] studied the influence of the temperature in the deformation, concluding that the yield point of MPCM decreased with the increasing of temperature. Also, Palanikkumaran *et al.* [65] used the MF shell to contain *n*-octadecane as PCM using the in-situ polymerization technique.

In Table 1 a list of some manufacturers' trademark name, the PCM they use, the shell material, and the particle size distribution (PSD), and its application is shown.

Table 1. Manufacturers of MPCM.

Trademark name	PCM	Shell material	PSD	Application
Cristopia	Eutectic salts	Polyolefin	77 mm	Industrial refrigeration, building, conditioning
ClimSel/climator	Sodium acetate, sodium sulphate	-	-	Medicine transportation, clothing, air-conditioning, electronic cooling, fire protection
Rubitherm	Paraffin, salt hydrate in granulate, powder and compounds forms	Plastic	-	Storage and transport food, medical equipments, storage materials for textile
Latest™/TEAP Energy	Glauber's salt, soda ash, sodium acetate, and paraffin wax	Polyethylene	25.4 mm	Hot pads and solar heating telecom enclosure, back-up air-conditioning, cold storage
PCM Products Ltd.	Eutectics, salt hydrates, organic materials, and high temperature salts	Rubber, HDPE plastic	40 mm	Space International space station, automotive passive cooling, solar heating and heat recovery
MPCM Microtek Laboratories Inc.	Paraffin	Polymer	17-20 μm	Active wear clothing, woven and non-woven textiles, building materials, packaging, and electronics
Micronal®/ BASF®	Paraffin wax	Polymer	5 μm	Building conditioning, surface cooling
Aegis	Inorganic salts	High Density Polyethylene	75 mm	Cold storage, boilers, solar water heaters, transport of blood, frozen food, fruits and vegetables

5. Methods to encapsulate PCM

The system core/shell is a key point in the fabrication of microcapsules, being the shell function to protect the core, and the core function to contain the active material, in this case the

PCM. The MPCM's morphology can be diverse as Figure 3 shows, but the most common are the spherical and the irregular ones.

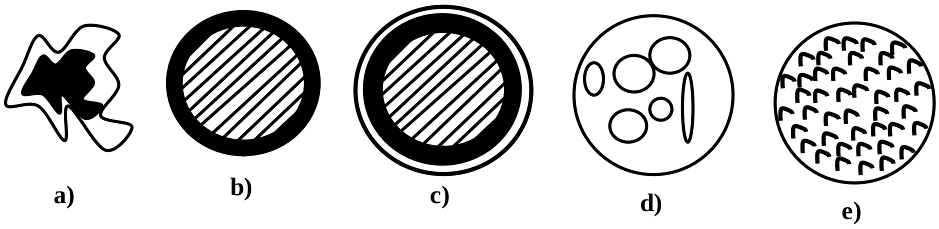

Figure 3. Possible morphologies of microcapsules a) Irregular shape; b) Simple; c) Multi-wall; d) Multi-core; e) Matrix particle.

The microcapsule description and their morphology depend on the core material and the deposition process of the shell. There are four types, as Figure 4 shows:

a) Mononuclear (core/shell): a single core wrapped with a continuous shell material
b) Polynuclear: many cores coated with a continuous shell material
c) Matrix encapsulation: in which the core material is distributed homogeneously into the shell material
d) Multi-film: a continuous core coated with multilayer continuous shell material

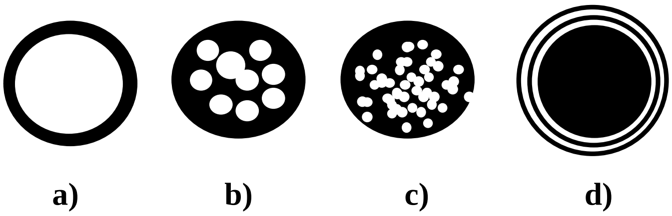

Figure 4. Scheme of the types of MPCM, adapted from [66] a) Mononuclear; b) Polynuclear; c) Matrix encapsulation; d) Multi-film.

There are three different methodologies to microencapsulate PCM based on the mechanisms of microparticle formation: chemical, physical and chemical, or physical and mechanical mode.

- **Chemical methodology**: Suspension, dispersion, emulsion, in situ and interfacial polymerization, or polycondensation are different procedures widely employed for the fabrication of PCM microcapsules (MPCM). Table 2 enumerates the advantages and the drawbacks of each procedure.

- Suspension polymerization: Sánchez-Silva *et al.* [67] exposed that the suspension polymerization process is governed by multiple simultaneous mechanisms such as particle coalescence and break-up, secondary nucleation, and the diffusion of monomer to the interface. The collective effect of these mechanisms confers the size, the structure and the surface properties to the microcapsules. Figure 5 shows a scheme of the suspension polymerization methodology. Sánchez *et al.* [68] developed a method based on a suspension free radical polymerization process to fabricate microencapsulated non-polar PCM. The same authors [69] investigated the influence of the reaction temperature, the stirring rate and the mass ratio of paraffin to styrene on the thermal properties of MPCM. Borreguero *et al.* [70] considered the microencapsulation by suspension polymerization with gypsum in two steps: a continuous one formed by deionizated water and the stabilizer (Polyvinyl-pyrrolidone, PVP), and a discontinuous one containing the styrene monomer, the paraffin wax and the benzoyl peroxide. As main result they achieve an improvement of the thermal insulation capacity of the gypsum by the addition of the prepared MPCM.

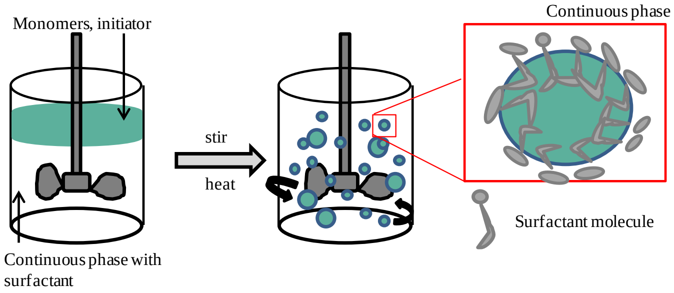

Figure 5. Scheme of the suspension polymerization microencapsulation process.

- Dispersion polymerization: Dispersion polymerization is a very attractive method due to its inherent simplicity of the single-step process. Typical examples of this method are the dispersion polymerization of styrene in hydrocarbons, alcohols, alcohol-ether and alcohol-water mixtures. In this methodology it is important to control the parameters such as initiator, monomer, stabilizer concentration, and the reaction time on the characteristics of the final particles with this methodology. One way to do it is by UV photo-initiated dispersion polymerization of stearic acid in PMMA shell as described by Wang *et al.* [71], which has high efficiency as they exposed in their study. Kim *et al.* [72] show that monodisperse poly(methyl methacrylate) microspheres were successfully synthesized by the dispersion polymerization using hydrophilic polyvinylalcohol (PVA) in a methanol/water mixture media. Figure 6 presents a graphic description of the dispersion before and after the polymerization process.

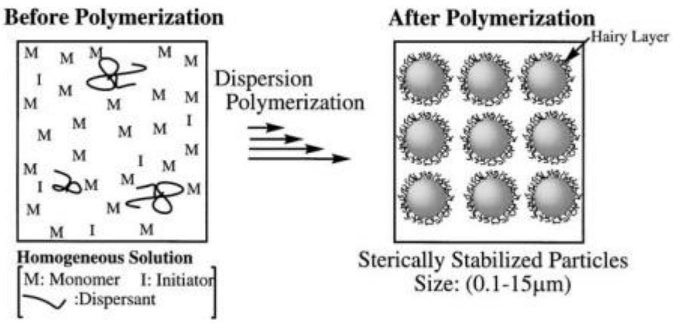

Figure 6. Schematic description of dispersion polymerization [73].

- Emulsion polymerization: This method consists on mixing the polymer in an oiled system, adding an emulsifier. After this, an emulsification is needed, to create a water/oil emulsion and to generate a crosslinked system (chemically, thermally, or in an enzymatic way). The final step is washing the emulsion, to remove the oil and to create the isolated microcapsules. In Figure 7 a scheme of this methodology can be observed. Sarı *et al.* [74] used this technique to prepare and characterize the MPCM for TES of PMMA as shell and *n*-heptadecane as PCM.

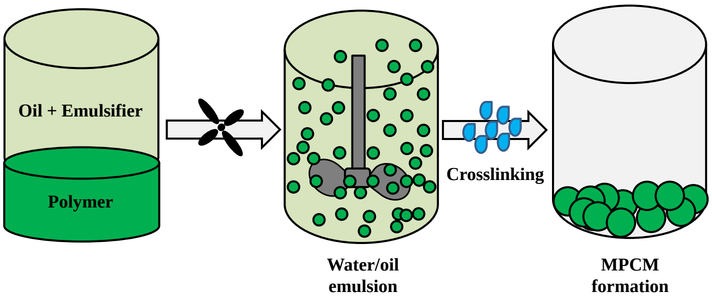

Figure 7. Scheme of the emulsion polymerization microencapsulation method. Adapted from [75].

- In situ polymerization: In this methodology the capsule shell formation occurs because of the polymerization of monomers added to the reactor. In this process no reactive agents are added to the core material and polymerization occurs exclusively in the continuous phase. This method to microencapsulate PCM has to have all the materials for the microcapsule wall originate from continuous phase of the emulsion system, and have to be water soluble [76]. Initially a low molecular weight pre-polymer will be formed, as time goes on the pre-polymer grows in size, it deposits on the surface of the dispersed core material thereby generating solid capsule shell [77]. First, a PCM emulsion is prepared and then the synthesis of the pre-polymer solution is carried out through the mixture of two polymers, which will form the cover, and water. This pre-polymer is added to the emulsion in the form of droplets, while the emulsion is agitated during a specific time. The emulsion is cooled and filtered, obtaining the microcapsules, which have to be dried. To enhance the mechanical properties, it is suggested to add modifying agents [78]. Boh *et al*. [79] have used a modified in situ polymerization method with melamine-formaldehyde pre-polymers as wall materials and styrene-maleic acid anhydride copolymers as modifying/emulsifying agents. Furthermore, Boh *et al.* [80] define this technique as the procedure where monomers or pre-condensates are added only to the aqueous phase of emulsion. Moreover, Yang *et al.* [81] studied the best shell to encapsulate tetradecane as PCM with polystyrene (PS), PMMA, poly(ethyl methacrylate) (PEMA) and polyvinyl acetate (PVAc) as Phase Change Slurries (PCS) using this technique, and the study concludes that PMMA and PEMA are the best shells. After this study, Yang *et al*. [82] had used the same PCM contained in different shell materials, Acrylonitrile-styrene copolymer (AS), acrylonitrile-styrene-butadiene copolymer (ABS), polycarbonate (PC), concluding that all the three shell materials could be used to microencapsulate *n*-tetradecane. Using this same PCM, Fang *et al*. [83] encapsulated it with urea and formaldehyde, concluding that the *n*-tetradecane encapsulation is efficient with good thermal stability and attractive for thermal energy storage and heat transfer applications. Besides, Chen *et al*. [84] synthesize and characterize MPCMs made of paraffin/SiO_2 obtained by this process, being a good MPCM because the SiO_2 protect the paraffin from reacting with the outside environment. Finally, there is a study of Song *et al.* [85] where MPCM with hexadecane as core material were prepared by this methodology by using urea-formaldehyde resin and urea-formaldehyde resin modified with melamine as shell materials respectively, concluding that the addition of melamine into the urea-formaldehyde resin reduced the microcapsule size and the microencapsulation efficiency. Moreover, the effects of the system concentration, the agitation speed and mass ratio of the wall are key factors to take into account, as it is referred in the last references.

- Interfacial polymerization: In this technique the shell capsule is formed at or on the surface of the droplet or on the particle by polymerization of the reactive monomers, and involves dispersing an organic phase (containing poly-functional monomers and/or oligomers) into an aqueous phase (containing a mixture of emulsifiers and protective colloid stabilizers) along with the material to be encapsulated. The presence of crosslinks affects the morphology of the external microcapsule surface [86]. The substances used as a shell are multifunctional monomers. The multifunctional monomer is dissolved in liquid core material and it will be dispersed in aqueous phase containing a dispersing agent. Generally, used shell forming material includes co-reactant multifunctional reagent like diamines, isocyanates and diacid chlorides. These results in rapid polymerization at the interface and the generation of the capsule shell takes place [77]. The main advantages of this technique are the high reaction speed, mild reaction course, and also that its products have low penetrability. Liang *et al*. [87] [46] succeed with the interfacial polymerization to prepare MPCM of butyl stearate as a PCM in a polyurea system. Li *et al*. [88] fabricated nanoparticles of SiO_2/paraffin using this process of polymerization and concluded that the methodology can be extended to fabricate other organic and inorganic PCM with different core/shell compositions. Figure 8 shows a scheme of interfacial polymerization where it is highlighted that high pressure is needed to obtain MPCM.

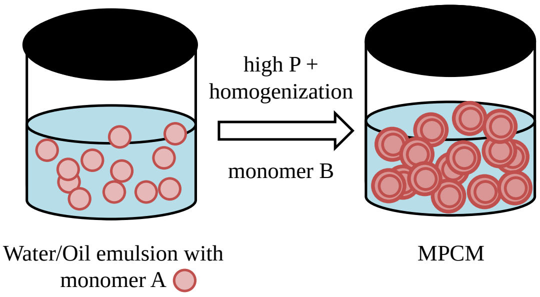

Figure 8. Scheme of the Interfacial polymerization microencapsulation method. Adapted from [89].

Table 2 shows the advantages and disadvantages of the different techniques for chemical methodology described.

Table 2. Techniques for chemical methodology in microencapsulation process.

Technique	Advantages	Disadvantages
Suspension polymerization	Good heat control of the reaction	Few monomers are water soluble. Size around 2 - 4000 μm [107]
	Cost effective	
Dispersion polymerization	Micron-size Monodisperse polymer particles in a single batch process	Not reported
Emulsion polymerization	High MW polymer fast	Purify polymer from the surfactant
In situ polymerization	Uniform coating.	Size between 1- 2000 μm
Interfacial polymerization	Versatile, good properties in size, degradability, mechanical resistance	Size MPCM 2 - 2000 μm

- **Physico-chemical methodology**: It includes coacervation, layer-by-layer assembly, sol-gel encapsulation and supercritical CO_2-assisted methods. Table 3 lists the advantages and disadvantages of each technique in the physico-chemical methodology.

- Coacervation: There are described two methods for coacervation process, the simple one and the complex one. The microcapsule formation mechanism for both processes is the same, with the exception on the way in which the phase separation is carried out. For simple coacervation, a desolvation agent is added for phase separation. By contrast, a complex coacervation involves complexation between two oppositely charged polymers. Figure 9 shows a scheme of this procedure.

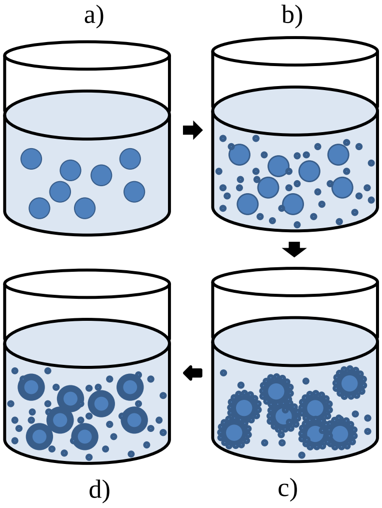

Figure 9. Scheme of simple coacervation technique, where (a) the core material is dispersed in a shell polymer solution; (b) the separation of the coacervate from the solution; (c) coating of core material by coacervate droplets; (d) coalescence of coacervate to form continuous shell around core particles. Adapted from [90].

Besides, there are three steps in complex coacervation. The first step is the formation of three immiscible phases, the liquid manufacturing vehicle, the core material, and the coating material. The core material is dispersed in a solution of the coating polymer. It is needed a changing temperature of polymer solution and a addition of salt, nonsolvent, and of an incompatible polymer to the polymer solution. The second step is the deposition of the coating, and the third step is the coating rigidization. The prepared microcapsules are stabilized by crosslinking, desolvation or thermal treatment. Figure 10 shows the steps involved in the complex coacervation technique.

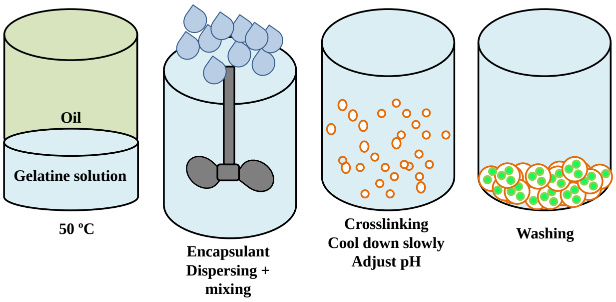

Figure 10. General processing scheme for microcapsule preparation by complex coacervation using gelatin and Arabic gum.

In the complex process, the polymeric solute is separated in the form of small liquid droplets, forming the coacervate. Then, it is deposited around the insoluble particles dispersed into a liquid. These droplets slowly unite and form a continuous cover around the core. In order to obtain a longer lifetime of microcapsules, this technique can be completed in two steps, adding the polymer twice. Through this mechanism, a smaller thickness of the microencapsulate shell can be obtained. Compactability and impermeability are improved (a lower speed of polymer deposition increases impermeability), giving greater stability to the microcapsules, conserving size and spherical form. The texture is smoother and the spherical form is more regular, compared to one-step coacervation, where microcapsules with many protrusions, rougher, coarser and more porous are obtained. Hence, it is a phenomenon which takes place in colloid systems, where macromolecular colloid rich coacervate droplets surround dispersed microcapsule cores, and form a viscous microcapsule wall, which is solidified with cross-linking agents. Özonur *et al*. [91] used this technique concluding that gelatin + Arabic gum mixture was the best wall material for microencapsulating coco fatty acid mixtures compared with urea-formaldehyde resin, melamine-formaldehyde resin, and β-naphtol-formaldehyde.

- <u>Sol-gel encapsulation</u>: This methodology is described as the formation of an oxide association through polycondensation reactions of a molecular predecessor in a liquid. A sol is a stable dispersion of polymers or colloidal particles in a solvent, where the particles can be crystalline or amorphous. On the other hand, a gel consists on a three dimensional continuous network, which includes a liquid phase, building an agglomeration of colloidal particles. Besides, in a polymer gel the particles have a polymeric substructure composed by aggregates of subcolloidal particles. In general, the sol particles interact by Van der Waals forces or hydrogen bonds, but can also be formed from linking polymer chains. Fang *et al*. [92] used the sol-gel methodology to prepare form stable lauric acid/silicon dioxide composite PCM. This material can be used for TES in waste heat recovery as well as solar heating systems. Li *et al*.

[93], using the sol-gel methodology, prepared a shape-stabilized paraffin/silicon dioxide composite PCM. Also, Tang *et al*. [94] enhanced the thermal conductivity of PEG/SiO_2 via in situ chemical reduction of $CuSO_4$ through ultrasound-assisted sol-gel process, concluding that the Cu/PEG/SiO_2 hybrid material have excellent thermal stability and a good-stable performance. Figure 11 shows a scheme of the sol-gel process.

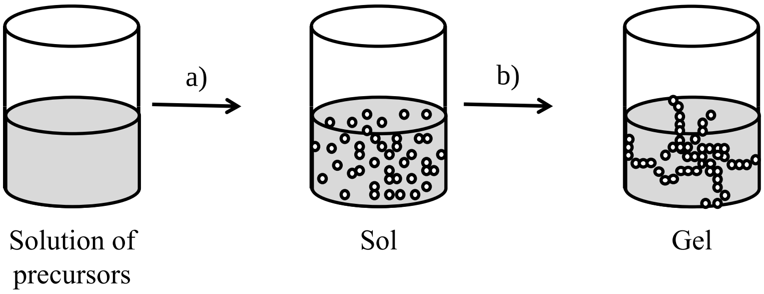

Figure 11. Sol-gel process microencapsulation method, where a) is the condensation, and b) is the gelation. Adapted from [95].

- Supercritical CO_2-assisted: Supercritical carbon dioxide has attracted a great deal of attention as an alternative to the conventional processing because it is an effective and green synthetic method. Supercritical CO_2-assisted have gained a strong interest in the synthesis of polymeric composites because it has low critical temperature value, is non-toxic and has non-flammable properties. Moreover, it is readily available, highly pure and cost-effective. Wu *et al.* [96] used this technique studying the effects of some factors on the particle size of PMMA particles prepared via a supercritical assisted-atomization (SAA) process using acetone as a solvent and supercritical carbon dioxide as a spraying medium. These factors included the concentration of polymer solution, temperature in saturator and volumetric flow rate ratio of carbon dioxide to polymer solution. More recently, Haldorai *et al*. [97] has summarized on the synthesis of polymer-inorganic filler nanocomposites in supercritical CO_2 and conclude that although there are three methods for the preparation of nanocomposites (blending, sol-gel and in situ polymerization), the super-critical CO_2 has been demonstrated to be a viable alternative to the conventional solvents.

Table 3. Encapsulation techniques for physical and chemical methodology.

Technique	Advantages	Disadvantages
Coacervation	Two methods	Agglomeration
	Versatile	
	Good control of the particle size and thickness	Difficult to scale-up
Sol-gel encapsulation	Inorganic shell with high thermal conductivity	Still under research
Supercritical CO_2-assisted	Effective and green method	Not very used
	Cost effective	

- **Physico-mechanical methodologies** include spray-drying, electrostatic encapsulation, and one-step method. These techniques are inherently not capable of producing microcapsules smaller than 100 μm [66]. In Table 4 the benefits and disadvantages of each technique in the physical and mechanical methodology is listed**.**

- Spray-drying: it is a low-cost commercial process which consists on the preparation of an emulsion, dispersing the material of the PCM in a concentrated solution of the material forming the capsule, until the desired size of the microcapsule is achieved. Then, this emulsion is pulverized into droplets. Afterwards, it will be dried, evaporating the water, which let the active material to be trapped inside a film of encapsulating material. This technique involves the atomization of a homogeneous liquid stream in a drying chamber where the solvent is evaporated and solid particles are obtained. It is suitable for heat-sensitive materials. This technique was studied by Borreguero *et al.* [98] mixing LDPE and EVA to create the polymeric shell. They chose these two polymers due to their similarity of the chemical structure, besides the low density, their versatility, and the inexpensive cost. Moreover, Hawlader *et al.* [99] and Fei *et al*. [100] used also this technique to produce other types of microcapsules, using different shells (formaldehyde and titania, respectively), and cores (Gum Arabic, paraffin wax, and n-octadecane, respectively).

- Electrostatic encapsulation: This technique is effective for production of particles, around 100 μm. It might be used to prepare spherical microbeads with a hydrophobic core and a hydrophilic or hydrophobic shell [101].

- One-step method: The benefits of using this method include easy scale-up and no need for a stabilizing agent due to self-stabilization. It allows tuning of the size and polydispersity of the capsules, and the use of different core materials. Jin *et al*. [102] uses this methodology without surfactants or dispersants nor acids/bases for stabilizing the capsules via oil/water emulsion, and the obtained results shows that the method allows tuning of the size and polydispersity of the capsules, and the use of different core materials.

Table 4. Scheme for physical and mechanical methodology in microencapsulation process.

Technique	Advantages	Disadvantages
Spray-drying	Easy to scale-up	High temperature
	Versatile	Agglomeration of particles
	Low cost	Remaining uncoated particles
Electrostatic encapsulation	Spherical microbeads	Only for < 50μm
One-step method	Easy to scale-up	-
	Self-stabilization	-

6. Phase Change Slurries

Phase Change Slurries (PCS) [103] is another important part of MPCM [104,105]. When the MPCM is fabricated in a dried state [106,107] it can be mixed with a carrier fluid, mainly water [108] or with other substances such as glycol [109,110] or glycerol [111,112], creating a PCS. These are widely employed in several fields, such as pumping active systems [113,114], using them for refrigeration [103,115], in air conditioning [116,117], in heat exchangers [118], heating [119], ventilation and air-conditioning (HVAC) [120–122], in solar energy [123], in cold storage [124], and heat exchangers [118] applications. As Salunkhe *et al.* review [125], the PCS not only acts as an energy storage device but also as a heat transport system. The way of pumping the slurries in an active system is very important [113,126], because it is know that microcapsules can broke when they collide ones to each other. Moreover, Zeng *et al.* [127] studied numerically the influences of microparticles and phase change in fluid-pure water, PCS and MPCM. Besides, Huang *et al*. [128] and Günter *et al.* [129] studied the subcooling in PCM emulsion, remarking that in PCS applications, the changed nucleation and solidification behavior is critical.

7. Characterization of MPCM

7.1. Experimental characterization techniques reported in the study of MPCM

7.1.1. Particle Size Distribution (PSD)

For the evaluation of the microspheres' size and the percentage in number or in volume of each size, is used laser diffraction spectrometry. The results must be evaluated taking into account the size as well as the transparency of the MPCM, so there are two mathematical models to do so: Mie and Fraunhofer [130]. Mie model fits better for homogenous and spherical particles, opaque or transparent and with diameters below 30 μm. Also, to calculate the size of the microcapsule it is needed the refractive index and the absorption of the substance. For using the Fraunhofer model is needed opaque particles bigger than 30 μm. Most of the MPCM evaluation studies included this technique. Yu *et al.* [131] used this technique to study the diameter distribution of MPCM prepared with different mass ratios of emulsifier to PCM.

7.1.2. **Optical Microscopy (OM)**

This technique provides images of microspheres with a good resolution, allowing the evaluation of their morphology, fixation, durability, and without a complex sample preparation. Sánchez *et al.* [5] used in their study transmitted light and reflection mode to develop thermo-regulating textiles using MPCM of paraffin in the core. Besides, Bayés-García *et al.* [132] characterize MPCM with Gelatine/Arabic Gum (G/AG) by using a thermo-optical microscope at different temperatures.

7.1.3. **Scanning Electron Microscopy (SEM)**

This technique is essential to evaluate the shape and size of the MPCM. Besides it is useful to study the surface of the microcapsules, as well as if there is PCM spread. It is a fast technique and it is widely employed. Bajare *et al*. [133] studied the shell thickness of BASF® Micronal® DS 5001x by using this technique.

7.1.4. **Transmission Electron Microscopy (TEM)**

The morphology and the structure of the microcapsules can be observed also by TEM, when their size is below micrometers, as Pan *et al.* [134] evaluated for nanostructures prepared through in-situ interfacial polycondensation, resulting colloidal sphere microcapsules with diameter around 200 nm.

7.1.5. **X-Ray Diffraction (XRD)**

This technique is used to analyze the crystalloid phase of the microencapsulated paraffin, like Fang *et al*. [135] show in their study, synthesizing and characterizing MPCM paraffin composites with SiO_2 shell. Moreover, this technique is used to assure the encapsulation of the PCM, as Fang *et al*. [136] used XRD patterns of *n*-octadecane, styrene and the nanoencapsulated PCM, suggesting that *n*-octadecane was successfully encapsulated by the shell of polystyrene. So, this technique plays an important role on studying the prevention of leakage of PCM.

7.1.6. **Wide Angle X-ray Scattering (WAXS) and Low Angle Laser Light Scattering (LLALS)**

The crystalline structure of polymers and PCM can be examined by this technique. It is convenient to evaluate the crystallographic forms of the encapsulated PCM. Zhang *et al*. [137] analyzed the WAXS patterns of the MPCM with different weight ratios of core/shell (*n*-octadecane/resorcinol-modified melamine-formaldehyde) materials. Moreover, Sánchez-Silva *et al.* [67] had used LLALS technique to better characterize the MPCM styrene-methyl methacrylate copolymer shell.

7.1.7. **Fourier Transformed Infrared Spectroscopy (FT-IR**)

This technique is used to evaluate the microcapsule shell material, as well as to study the possible degradation of the external part of the microsphere. It can be analyzed by Attenuated Total Reflectance (ATR) or with a KBr pellets [138]. An example of this use is the study of Zhang *et al.* [139] whom characterize the polycarbonate shell before and after 1000 thermal cycles to evaluate the matrix thermal distortion temperature.

7.1.8. Differential Scanning Calorimeter (DSC)

This is one of the most popular thermal analysis techniques. It measures endothermic and exothermic transitions in function of the temperature. It also can detect glass transitions, fusion, crystallization, and oxidation. It can measure specific heat capacities [140]. For these reasons, this technique is widely employed to characterize the thermophysical properties of MPCM. It provides the melting and solidifying temperature, as well as, the melting and solidifying enthalpy of a sample, revealing if the material has a good capacity to store energy. Ostrý *et al.* [141] confirmed by DSC technique the suitability of some PCM for their integration in building structures. Table 5 summarizes the main thermal properties (latent heat and phase change peak temperature) of the MPCM analyzed in this review, describing the composition of the core and shell material.

Table 5. Thermal properties.

Ref	**MPCM**	**PCM content (%)**	**latent heat [J·g^{-1}]**		**Phase change (°C) peak temperature**		**diameter (μm)**
5	PS + paraffin wax	-	104.7		40	45	5.5
48	PMMA + *n*-octadecane	-	198.5	197.1	29.2	33.6	0.05 to 0.3
	PEMA + *n*-octadecane	-	208.7	205.9	31.1	32.3	0.06 to 0.36
52	PMMA + docosane	-	54.6	-48.7	41	40.6	0.16
54	Acrylate/butyl stearate + paraffin	48-68	85		-		10 to 30
57	PMMA + eicosane		35.2	34.9	54.2	87.5	0.7
58	PMMA+ *n*-hexadecane	29.04-61.4	68.89 and 145.61		-		0.22 to 1.050
59	PMMA + paraffin		106.9	112.3	55.8	50.1	0.21
60	MMA + *n*-pentadecane	-	107	97	10	9.5	650 to 760
62	PMMA + SA	80	187	190	67	66	-
	PMMA + PA	80	173	175	60	59	-
	PMMA + MA	80	166	168	51	50.7	-
	PMMA + LA	80	149	151	41	41.5	-
67	Melamine-formaldehyde + paraffin	-	87.5		45		380

81	PMMA + PCM	-	66.26	60.62	2.95	5.97	5 to 30
	PEMA + PCM	-	80.62	65.35	3.19	5.68	6 to 30
82	Acrylonitrile-styrene copolymer + *n*-tetradecane	-	142.3		10		<1
	ABS + *n*-tetradecane	-	107.1		10		<1
	PC + *n*-tetradecane	-	49.5		10		<1
83	Urea/formaldehyde + *n*-tetradecane	60	134.16		-		0.1
84	SiO_2 + paraffin	-	156.86	144.09	57.96	55.78	40 to 60
87	Polyurea + butyl stearate	-	80		29		20 to 35
88	paraffin + SiO_2	-	45.5	43.8	56.5	45.5	0.2 to 0.5
92	SiO_2 + polyethylene glycol	-	117.21	90	44.78	40.33	-
93	SiO_2 + paraffin	-	35.8	32.51	57.8	56.85	-
102	Silica + nonadecane-	-	124.7		-		27
100	LDPE/EVA + RT27	49.32	98.14		25.42	31.15	3.5
	Polystyrene + RT27	48.61	96.14		26.12	30.28	360
123	BASF slurries	-	-		up to 70ºC		2 to 8
128	RT-20 emulsion		21.2	-	0.2-12.5		-
131	MF + *n*-dodecanol	-	187.5		21.5		30.6
132	Gelatine/Arabic Gum + RT-27	-	-		-		9
	Sterilized Gelatine/Arabic Gum + RT-27	-	79		25.15	28.15	12
	Agar-Agar/Arabic Gum + RT-27	-	78		26.35	29.35	4.3
136	Polystyrene + *n*-octadecane	-	124.4		-		0.100 to 0.123
137	MF + *n*-octadecane	-	122.5	132.2	26.75	20.33	12.45
139	Polycarbonate + Stearic Acid	-	91.4	96.8	60.2	51.2	0.5

168	HDPE + paraffin		96.79	37 55	300
174	Polysiloxane + *n*-eicosane	-	139	37.4 30	22.9
188	Micronal (BASF)		100	26	5

7.1.9. **Thermogravimetrical Analysis (TGA)**

This technique measures the amount and rate of change in the weight of a material as a function of temperature or time in a controlled atmosphere. Measurements are used primarily to determine the composition of materials and to predict their thermal stability. The technique characterize materials that exhibit weight loss or gain due to decomposition, oxidation or dehydration and also their thermal stability. There are a lot of studies using it. Zhang *et al.* [142] evaluate the step thermal degradation of a silica/*n*-octadecane MPCM, as well as the thermal reliability by using this technique.

7.1.10. **Atomic Force Microscopy (AFM)**

It is a surface technique which has the ability to obtain topographic images of surfaces with nanometric resolution. It can be used as a nanomanipulator in order to move and test the surface of the samples in a variety of ways, such as electrically, magnetically and mechanically. The microcapsules' mechanical properties can be evaluated by using this technique. The microcapsule maximum force and the total deformation of an individual microcapsule [98] have to be measured increasing the applied force until obtaining the typical force displacement curves. It is necessary to repeat this procedure several times (at least 3 times). Furthermore, it can be extracted the deformation histogram and the Young's modulus histogram taking into account a small area on the top of the microcapsule. Giro-Paloma *et al*. [143] evaluated the maximum force that a dried PCS can support on the top of the microsphere using Atomic Force Microscopy (AFM) technique. Besides, Giro-Paloma *et al*. [63] also evaluated the maximum force that the MPCM Micronal® DS 5001 can support before their breakage at three different temperatures: 25 ºC, 45 ºC and 80 ºC by using this technique. They conclude that the required applied load in order to break the sample depends on the working temperature. Hence, the temperature is a key point to take into account when a PCM have to be chosen for a specific application.

7.1.11. Emission of Volatile Organic Compounds

The volatile organic compounds (VOC's) evaluation at different temperatures is an important issue to better characterizing PCM and MPCM. Materials for indoor environments should not emit hazardous gases in the form of volatile organic compounds. There are studies over the past decade of measuring the air quality (indoor environment) in building materials through volatile organic compounds (VOC's) because they play a major role in construction [144–155]. Therefore, the VOC's emission from building materials can be studied experimentally and theoretically (using mathematical models) to predict the quality of indoor air. There are some others studies about the outdoor environment [156,157]. Also, it is studied that multi-layer materials have much longer VOC's emission time and a slower VOC's decay rate compared with single-layer materials [158]. Moreover, it has to take into account that the adsorption/desorption phenomena of relatively high vapor pressure compounds are negligible in building [159]. Besides, the percentage of approximately 40 % of the indoor air quality levels originated from building materials [160] are VOC's associated with the perception of bad odors. In buildings which are renovated or new (considering *new* buildings that are less than 10 years old) the levels of indoor air pollutants are higher than the VOC's levels in aged buildings [161].

Implementing MPCM in gypsum board, concrete, plaster or other wallboard material, thermal storage can be a part of construction technology for light weight buildings, and the MPCM could be used for high density thermal energy storage [162,163], so the final product would achieve energy savings in buildings. The fact of using gypsum, cement and heavyweight sheet with PCM could produce some VOC's in the indoor air in a cubicle [164,165]. Consequently, it is important to preserve the air quality of a room. Hence, it is used MPCM to reduce the toxic effects that could be expelled in a system [166]. Although using MPCM mixed with other constructive materials, there is a main concern on the use of organic PCM because of the possible emission of volatile compounds [157,167]. Due to most commercial PCM microcapsules have not been well characterized for volatile emission, a proposition for future studies could be to characterize and measure the volatile organic compounds for PCM, MPCM and constructive materials containing these kind of materials."

7.2. Properties to analyze

7.2.1. Flammability

Due to the lower thermal stability and inflammability properties of MPCM, their usage has been severely restricted especially in building applications [50]. For this reason, the studies of determining the flammability properties of MPCM are of importance in many applications. The Cone calorimeter is one of the most effective bench scale methods for investigating the combustion properties of polymer materials. Cai *et al*. [168] evaluate this property on form-stable PCM based on paraffin/ high density polyethylene (HDPE) composites with expanded graphite (EG) and ammonium polyphosphate (APP) flame retardant system.

7.2.2. **Viscosity measurement, density, and conductivity**

The viscosity of melted PCM or PCS is very important in flowage and is important to measure it at different temperatures with a rotation viscosimeter. High viscosity will increase the pump energy consumption.

Another important property to take into account in a PCS system is the density (ρ_{PCS}) which is given by Equation 1, where X_i is the weight fraction and ρ_i is the density of each component:

$$\boldsymbol{\rho_{PCS}} = \mathbf{1} \Big/ \sum_{\mathrm{i}} \frac{\mathrm{x_i}}{\mathrm{\rho_i}} \qquad \text{Equation 1}$$

Density can be obtained by using a specific gravitymetre or a pycnometer by determining the volume.

Another property used to characterize MPCM and PCS is the thermal conductivity (k), which can be calculated in different ways, as Youssef *et al.* [94] report in their review. One way to calculate the thermal conductivity of a MPCM is by Maxwell's *et al*. [169] relation:

$$\boldsymbol{K_{MPCM}} = \mathbf{K_{cont}} \frac{2 + {}^{\mathbf{K_{MPCM}}}\!/\!_{\mathbf{K_{cont}}} + 2\mathbf{C_{MPCM}}\left({}^{\mathbf{K_{MPCM}}}\!/\!_{\mathbf{K_{cont}}} - \mathbf{1}\right)}{2 + {}^{\mathbf{K_{MPCM}}}\!/\!_{\mathbf{K_{cont}}} - \mathbf{C_{MPCM}}({}^{\mathbf{K_{MPCM}}}\!/\!_{\mathbf{K_{cont}}} - \mathbf{1}} \qquad \text{Equation 2}$$

Furthermore, Wang *et al*. [170] evaluated these three properties in a microencapsulated phase change material (MPCM) slurry flow in a circular horizontal tube. The viscosity was evaluated as well as the density of the slurry, which was calculated by weighted fraction of the densities of PCM, the coating material, and the water, based on the mass and energy balance. The thermal conductivity of the microcapsule was calculated based on a composite sphere approach.

7.2.3. **Cycling**

The thermal cycling test reveals the thermal reliability and chemical stability of a microcapsule [171]. For this reason, it is an essential test to evaluate the quality of the microcapsules to assure the no alteration on its geometrical profile after several cycles [172,173]. The thermal reliability can be evaluated in a DSC device, as Fortuniak *et al.* [174] used to withstand 50 fusion-crystallization cycles tests, or in a thermocyclator. There is another study by Sarı *et al.* [56] where it was tested the thermal cycling test with 5000 cycles of a PMMA shell and *n*-octacosane PCM.

8. MPCM applications

In between the applications of MPCM, the use of MPCS for cooling in Narita Airport (Tokyo, Japan) can be found [115]. Here MPCS was used to compensate the decrease of energy capacity caused when the refrigerant was substituted due to environmental reasons. The slurry used is the mixture of water and 2 μm microcapsules, and the melting temperature and the corresponding latent heat of which are 8 ºC and 75.9 $kJ\cdot kg^{-1}$, respectively. The storage tank is 24.7 m in height and 7.4 m in diameter. Cold energy is stored during night time and released during day time.

Another interesting application of MPCM is in buildings. Here active and passive systems can be considered. In active systems, MPCS are involved, since the MPCM needs to be movable. Griffiths *et al*. [175] investigated the use of MPCS in a ceiling panel. MPCS with a melting temperature of 18 ºC and 2 - 8 μm microcapsules produced by BASF (40 % concentration) was used as heat transfer medium in a test chamber (with working temperature of 16 - 18 ºC).

As for passive systems, MPCM have been combined with different building materials, such as gypsum, concrete [140,176–181], and insulating materials, and tested in different set-ups. In 2005, Schossig *et al.* [182] presented the results of adding PCM in plaster and testing the new product in real offices. Since comparison was quite difficult due to the influence of users, two new full-size test rooms with a lightweight construction at the facade testing facility and coated the interior walls with PCM plaster and reference plaster were built. The measured data showed the potential for PCM products to reduce the cooling demand and increase the comfort in lightweight buildings. Later, MPCM incorporated in gypsum boards has been investigated by many researchers [70,183–185].

The performance of PCM in building structures are usually investigated via a dynamic building performance simulation. In order to avoid the need of measuring the thermal properties each time the composition changes, Toppi *et al.* derived experimental correlations to calculate the composite material properties as function of its composition [186]. Such correlations may also be used, when choosing the material composition, in order to obtain the required properties. The correlations are based on experimental results obtained from gypsum based composite material containing BASF MPCM.

Cabeza *et al*. [162] and Castellón *et al*. [187] developed a new innovative concrete with microencapsulated phase change materials (MPCM) without losing any of the initial concrete characteristics and achieving high energy savings in cooling. The experimental setup used consisted of two identically shaped cubicles of concrete, one with conventional concrete, and the other one with the modified concrete which included MPCM. The MPCM used was a commercial microencapsulated PCM called Micronal® PCM (from BASF) with a melting point of 26 ºC, and a phase change enthalpy of 110 $kJ \cdot kg^{-1}$. The developed concrete reached a compressive strength over 25 MPa and a tensile splitting strength over 6 MPa (after 28 days). Moreover, concrete panels were produced in a way close to common concrete production methods. The results of this study showed improved thermal inertia as well as lower inner temperatures, demonstrating a real opportunity in energy savings for buildings.

One of the main drawbacks found in this experimentation was the severe influence of high outdoor temperature peaks and solar radiation over the PCM during the summer, which prevented its solidification during night and thus diminished its achievable potential benefits. Therefore, Arce *et al.* [9] tried to overcome such a problem and to increase the operation time of the PCM and the thermal comfort achieved. For such a purpose, in 2008 - 2009 similar experiments have been performed with awnings added to the set-up, providing them with solar protection. Results showed that peak temperatures were reduced about 6 %. Moreover, PCM remained active for at least 4 % more hours, and the comfort time was increased at least 10 % in cubicles with awnings.

MPCM was also added to sandwich panels [188] to increase their thermal inertia and to reduce the energy demand of the final buildings [186]. To manufacture the sandwich panel with microencapsulated PCM three different methods were tested. In case 1, the PCM was added mixing the microencapsulated PCM with one of the components of the polyurethane. In the other two cases, the PCM was added either a step before (case 2) or a step after (case 3) to the addition of the polyurethane to the metal sheets. The results show that in case 1 the effect of PCM was overlapped by a possible increase in thermal conductivity, but an increase of thermal inertia was found in case 3. In case 2, different results were obtained due to the poor distribution of the PCM. Some samples showed the effect of the PCM (higher thermal inertia), and other samples results were similar to the conventional sandwich panel. In both cases (2 and 3), it is required to industrialize the process to improve the results. In these experiments, 8 % in weight of MPCM with respect to the weight of the PUR was added. Here also Micronal® PCM (from BASF) with a melting point of 26 ºC was used.

Similarly, Borreguero *et al*. developed new rigid polyurethane foam containing microencapsulated Rubitherm RT27 [189]. 21 wt% content of MPCM could be incorporated in RPU foams, improving the TES capacity of these materials but depressing their mechanical properties. Results indicated that the foaming process was affected by the microcapsules content decreasing the foam rising rate and its final size. Later on, they used catalyst Tegoamin 33 in the process, being able to include 18 wt% MPCM in the foam maintaining the mechanical properties of the neat foam, and catalyst Tegoamin BDE, being to include 21 wt% MPCM with higher mechanical resistance than the previous foams [190]. Finally, rigid polyurethane (RPU) foams were synthesized incorporating up to 18 wt % of two different kinds of thermo-regulating microcapsules having a different shell material consisting of polystyrene or poly(methyl methacrylate), named as mSP-(PS-RT27) and Micronal® DS 5001x, respectively [191]. The type of microcapsules and their content affected the final foam height, which decreased with the content and particle size. However, the foam rising curve shape was not dependent on the microcapsules type or content and was successfully predicted by means of a model of reaction curve of four tanks in series. Thermal energy storage (TES) capacity of PU foams was improved by incorporating both, mSP-(PS-RT27) or Micronal® DS 5001x, with the values close to those reported in the literature (16 $J \cdot g^{-1}$) for the highest content. Nevertheless, the highest particle size of the microcapsules from PS and the agglomeration of the microcapsules from poly(methyl methacrylate), promoted by their additive SiO_2, led to the strut rupture, damaging the final mechanical properties.

One of the first applications where MPCM was used is in textiles to enhance thermal comfort in clothes [5,192–195] and, more recently, footwear [196]. In this last application, for example, a nonwoven fabric, three foams and leather, commonly used as fabrics for shoe manufacturing, were doped with microcapsules containing phase change materials (PCMs) and also with carbon nanofibers (CNFs) in order to improve the thermal comfort provided by the shoes. The maximum microcapsule content that can be incorporated and the influence on the weight, thickness and the thermal properties and behavior of the fabrics were evaluated. The resulting materials showed a thermal energy storage (TES) capacity up to 13.74 $J \cdot g^{-1}$ and a maximum thickness increase of the composite fabric of 0.6 mm. The PCMs addition promoted a slight modification of the steady-state temperatures of the fabrics subjected to heating or cooling processes and the stored and released heats confirmed that PCMs work in a reversible way. On the other hand, the addition of CNFs compensated for the insulating effect of the PCMs. Finally, it was found that footwear containing these materials could hold the foot temperature for a longer time than parent fabrics.

9. Conclusions

In this paper, classification of the research carried out in microencapsulation of PCM is presented with the aim of rationalize the scattered material on the topic available in the literature. The different types of PCM, the different shell materials used, the methods of encapsulation, the most used techniques for their characterization, and the main applications are the different sections presented.

PCM can be organic and inorganic; up to now, mainly organic PCM have been encapsulated, with a big focus in paraffin and fatty acids. Only recently, microencapsulation of salts and salt hydrates is presented by some researchers. Only a few manufacturers of MPCM have been identified. When MPCM are used as heat transfer fluid they are presented as phase change slurries (PCS).

Both natural and synthetic polymers can be used as shell material; this review shows that many different polymers have been used, depending on the requirements of the PCM and the application considered. The combination core/shell is one of the most important parameters in microencapsulation.

The morphology of the microcapsules in MPCM can be very diverse (irregular shape, simple, multi-wall, multi-core, or matrix particle), and there are four types of MPCM (mononuclear, polynuclear, matrix encapsulation, and multi-film).

There are three different methodologies to microencapsulate PCM, based on the mechanism of microparticle formation, and each one is divided in different modes: chemical methodology (suspension polymerization, dispersion polymerization, emulsion polymerization, in situ polymerization, and interfacial polymerization), physico-chemical methodology (coacervation, layer-by-layer assembly, sol-gel encapsulation and supercritical CO_2-assisted methods), and physico-mechanical methodology (spray-drying, electrostatic encapsulation, and one-step method).

Characterization of MPCM has attracted a lot of attention between researchers and a lot of methods have been used depending on the aim of the analysis and the application considered. This review describes shortly the main techniques used for MPCM characterization at lab scale, including particle size distribution, optical microscopy, SEM, TEM, X-Ray diffraction, wide angle X-ray scattering and low angle laser light scattering, FT-IR, DSC, TGA, and AFM, and some properties analyzed such as flammability, viscosity, density and conductivity measurement, and cycling.

Finally, some applications of MPCM are shortly described. These are cooling systems, active and passive systems in buildings, and textiles and footware.

Acknowledgments

The work is partially funded by the Spanish government (ENE2011-28269-C03-02 and ENE2011-22722). The authors would like to thank the Catalan Government for the quality accreditation given to their research group GREA (2014 SGR 123) and research group DIOPMA (2014 SGR 1543). The research leading to these results has received funding from the European Union's Seventh Framework Programme (FP7/2007-2013) under grant agreement nº PIRSES-GA-2013-610692 (INNOSTORAGE).

References

[1] Zalba B, Marín JM, Cabeza LF, Mehling H. Review on thermal energy storage with phase change: materials, heat transfer analysis and applications. Appl Therm Eng 2003;23:251–83. doi:10.1016/S1359-4311(02)00192-8.

[2] Pomianowski M, Heiselberg P, Zhang Y. Review of thermal energy storage technologies based on PCM application in buildings. Energy Build 2013;67:56–69. doi:10.1016/j.enbuild.2013.08.006.

[3] Kumar R, Misra M, Kumar R, Gupta D, Khatri P, Tak B, et al. Phase Change Materials: Technology Status and Potential Defence Applications. Def Sci J 2011;61:576–82. doi:10.14429/dsj.61.363.

[4] http://www.scopus.com/ n.d.

[5] Sánchez P, Sánchez-Fernandez MV, Romero A, Rodríguez JF, Sánchez-Silva L. Development of thermo-regulating textiles using paraffin wax microcapsules. Thermochim Acta 2010;498:16–21. doi:10.1016/j.tca.2009.09.005.

[6] Keyan K, Ramachandran T, Shamugasundaram OL, Balasubramaniam M, RagavendraT. Microencapsulation of PCMs in Textiles: A Review. J Text Apparel, Technol Manag 2012;7:1–10.

[7] Baetens R, Jelle BP, Gustavsen A. Phase change materials for building applications: A state-of-the-art review. Energy Build 2010;42:1361–8. doi:10.1016/j.enbuild.2010.03.026.

[8] Tyagi VV, Buddhi D. PCM thermal storage in buildings: A state of art. Renew Sustain Energy Rev 2007;11:1146–66. doi:10.1016/j.rser.2005.10.002.

[9] Arce P, Castellón C, Castell A, Cabeza LF. Use of microencapsulated PCM in buildings and the effect of adding awnings. Energy Build 2012;44:88–93. doi:10.1016/j.enbuild.2011.10.028.

[10] Oró E, Gil A, Miró L, Peiró G, Álvarez S, Cabeza LF. Thermal Energy Storage Implementation Using Phase Change Materials for Solar Cooling and Refrigeration Applications. Energy Procedia 2012;30:947–56. doi:10.1016/j.egypro.2012.11.107.

[11] Gil A, Oró E, Miró L, Peiró G, Ruiz Á, Salmerón JM, et al. Experimental analysis of hydroquinone used as phase change material (PCM) to be applied in solar cooling refrigeration. Int J Refrig 2014;39:95–103. doi:10.1016/j.ijrefrig.2013.05.013.

[12] Lu W, Tassou S a. Characterization and experimental investigation of phase change materials for chilled food refrigerated cabinet applications. Appl Energy 2013;112:1376–82. doi:10.1016/j.apenergy.2013.01.071.

[13] Oró E, Miró L, Farid MM, Cabeza LF. Thermal analysis of a low temperature storage unit using phase change materials without refrigeration system. Int J Refrig 2012;35:1709–14. doi:doi:10.1016/j.ijrefrig.2012.05.004.

[14] Oró E, De Gracia A, Cabeza LF. Active phase change material package for thermal protection of ice cream containers. Int J Refrig 2013;36:102–9. doi:doi:10.1016/j.ijrefrig.2012.09.011.

[15] Oró E, Cabeza LF, Farid MM. Experimental and numerical analysis of a chilly bin incorporating phase change material. Appl Therm Eng 2013;58:61–7. doi:doi:10.1016/j.applthermaleng.2013.04.014.

[16] Oró E, Miró L, Barreneche C, Martorell I, Farid MM, Cabeza LF. Corrosion of metal and polymer containers for use in PCM cold storage. Appl Energy 2013;109:449–53. doi:doi:10.1016/j.apenergy.2012.10.049.

[17] Günther E, Schmid T, Mehling H, Hiebler S, Huang L. Subcooling in hexadecane emulsions. Int J Refrig 2010;33:1605–11. doi:10.1016/j.ijrefrig.2010.07.022.

[18] Dutil Y, Rousse D, Lassue S, Zalewski L, Joulin A VJ. Modeling phase change materials behaviour in building applications: selected comments. World Renew. Energy Congr., Sweden: 2011.

[19] Lin C-C, Yu K-P, Zhao P, Whei-May Lee G. Evaluation of impact factors on VOC emissions and concentrations from wooden flooring based on chamber tests. Build Environ 2009;44:525–33. doi:10.1016/j.buildenv.2008.04.015.

[20] Rozanna D, Salmiah A, Chuah TG, Medyan R, Thomas Choong SY SM. A study on thermal characteristics of phase change material (PCM) in gypsum board for building application. J Oil Palm Res 2005;17:41–6.

[21] Kuznik F, Virgone J, Roux J-J. Energetic efficiency of room wall containing PCM wallboard: A full-scale experimental investigation. Energy Build 2008;40:148–56. doi:10.1016/j.enbuild.2007.01.022.

[22] Feldman D, Banu D, Hawes D, Ghanbari E. Obtaining an energy storing building material by direct incorporation of an organic phase change material in gypsum wallboard. Sol Energy Mater 1991;22:231–42. doi:10.1016/0165-1633(91)90021-C.

[23] Kuznik F, David D, Johannes K, Roux J-J. A review on phase change materials integrated in building walls. Renew Sustain Energy Rev 2011;15:379–91. doi:10.1016/j.rser.2010.08.019.

[24] Castell A, Martorell I, Medrano M, Pérez G, Cabeza LF. Experimental study of using PCM in brick constructive solutions for passive cooling. Energy Build 2010;42:534–40.

[25] Kabbara MJ, Abdallah NB. Experimental Investigation on Phase Change Material based Thermal Energy Storage Unit. Procedia Comput Sci 2013;19:694–701. doi:10.1016/j.procs.2013.06.092.

[26] Cabeza LF, Ibáñez M, Solé C, Roca J, Nogués M. Experimentation with a water tank including a PCM module. Sol Energy Mater Sol Cells 2006;90:1273–82. doi:doi:10.1016/j.solmat.2005.08.002.

[27] Jordan U VK. Realistic domestic hot-water profiles in different time scales. IEA SHC. Task 26Solar combisystems, 2001.

[28] Mehling H, Cabeza LF, Hippeli S, Hiebler S. PCM-module to improve hot water heat stores with stratification. Renew Energy 2003;28:699–711.

[29] Haillot D, Nepveu F, Goetz V, Py X, Benabdelkarim M. High performance storage composite for the enhancement of solar domestic hot water systems. Sol Energy 2012;86:64–77. doi:10.1016/j.solener.2011.09.006.

[30] Pasupathy a., Velraj R, Seeniraj RV. Phase change material-based building architecture for thermal management in residential and commercial establishments. Renew Sustain Energy Rev 2008;12:39–64. doi:10.1016/j.rser.2006.05.010.

[31] Zheng Y, Zhao W, Sabol JC, Tuzla K, Neti S, Oztekin A, et al. Encapsulated phase change materials for energy storage – Characterization by calorimetry. Sol Energy 2013;87:117–26. doi:10.1016/j.solener.2012.10.003.

[32] Pendyala S. Macroencapsulation of Phase Change Materials for Thermal Energy Storage. Univ South Florida Sch Commons 2012.

[33] S B. Microencapsulation: methods and industrial applications. CRC Press, 2006.

[34] Jamekhorshid A, Sadrameli SM, Farid M. A review of microencapsulation methods of phase change materials (PCMs) as a thermal energy storage (TES) medium. Renew Sustain Energy Rev 2014;31:531–42. doi:10.1016/j.rser.2013.12.033.

[35] Sukhorukov G, Fery a., Möhwald H. Intelligent micro- and nanocapsules. Prog Polym Sci 2005;30:885–97. doi:10.1016/j.progpolymsci.2005.06.008.

[36] Castellón C, Martorell I, Cabeza LF, Fernández AI, Manich AM. Compatibility of plastic with phase change materials (PCM). Int J Energy Res 2011;35:765–71. doi:10.1002/er.1723.

[37] Giro-Paloma J, Roa JJ, Díez-Pascual AM, Rayón E, Flores A, Martínez M, et al. Depth-sensing indentation applied to polymers: A comparison between standard methods of analysis in relation to the nature of the materials. Eur Polym J 2013;49:4047–53. doi:10.1016/j.eurpolymj.2013.09.010.

[38] Soares N, Costa JJ, Gaspar a. R, Santos P. Review of passive PCM latent heat thermal energy storage systems towards buildings' energy efficiency. Energy Build 2013;59:82–103. doi:10.1016/j.enbuild.2012.12.042.

[39] Tyagi VV, Kaushik SC, Tyagi SK, Akiyama T. Development of phase change materials based microencapsulated technology for buildings: A review. Renew Sustain Energy Rev 2011;15:1373–91. doi:10.1016/j.rser.2010.10.006.

[40] Dutil Y, Rousse D, Lassue S, Zalewski L, Joulin A, Virgone J, et al. Modeling phase change materials behavior in building applications: Comments on material characterization and model validation. Renew Energy 2014;61:132–5. doi:10.1016/j.renene.2012.10.027.

[41] Wang H, Wang JP, Wang X, Li W, Zhang X. Preparation and Properties of Microencapsulated Phase Change Materials Containing Two-Phase Core Materials. Ind Eng Chem Res 2013;52:14706–12. doi:10.1021/ie401055r.

[42] Ma Y, Sun S, Li J, Tang G. Preparation and thermal reliabilities of microencapsulated phase change materials with binary cores and acrylate-based polymer shells. Thermochim Acta 2014;588:38–46. doi:10.1016/j.tca.2014.04.023.

[43] Cabeza LF, Castell a., Barreneche C, de Gracia a., Fernández a. I. Materials used as PCM in thermal energy storage in buildings: A review. Renew Sustain Energy Rev 2011;15:1675–95. doi:10.1016/j.rser.2010.11.018.

[44] Suppes GJ, Goff MJ, Lopes S. Latent heat characteristics of fatty acid derivatives pursuant phase change material applications. Chem Eng Sci 2003;58:1751–63. doi:10.1016/S0009-2509(03)00006-X.

[45] Sharma A, Tyagi VV, Chen CR, Buddhi D. Review on thermal energy storage with phase change materials and applications. Renew Sustain Energy Rev 2009;13:318–45. doi:10.1016/j.rser.2007.10.005.

[46] Das A. Study of Microencapsulation in Dyeing n.d. http://es.slideshare.net/Arkatextile/microencapsulation-in-dyeing.

[47] Tan FL, Hosseinizadeh SF, Khodadadi JM, Fan L. Experimental and computational study of constrained melting of phase change materials (PCM) inside a spherical capsule. Int J Heat Mass Transf 2009;52:3464–72. doi:10.1016/j.ijheatmasstransfer.2009.02.043.

[48] Zhang GH, Bon SAF, Zhao CY. Synthesis, characterization and thermal properties of novel nanoencapsulated phase change materials for thermal energy storage. Sol Energy 2012;86:1149–54. doi:10.1016/j.solener.2012.01.003.

[49] Wang X, Zhang X, Tao X, Yick K. Structure and thermal stability of microencapsulated phase-change materials. Colloid Polym Sci 2004;282:330–6. doi:10.1007/s00396-003-0925-y.

[50] Khudhair AM, Farid MM. A review on energy conservation in building applications with thermal storage by latent heat using phase change materials. Energy Convers Manag 2004;45:263–75. doi:10.1016/S0196-8904(03)00131-6.

[51] Qiu X, Lu L, Wang J, Tang G, Song G. Preparation and characterization of microencapsulated n-octadecane as phase change material with different n-butyl methacrylate-based copolymer shells. Sol Energy Mater Sol Cells 2014;128:102–11. doi:10.1016/j.solmat.2014.05.020.

[52] Alkan C, Sarı A, Karaipekli A, Uzun O. Preparation, characterization, and thermal properties of microencapsulated phase change material for thermal energy storage. Sol Energy Mater Sol Cells 2009;93:143–7. doi:10.1016/j.solmat.2008.09.009.

[53] Qiu X, Li W, Song G, Chu X, Tang G. Microencapsulated n-octadecane with different methylmethacrylate-based copolymer shells as phase change materials for thermal energy storage. Energy 2012;46:188–99. doi:10.1016/j.energy.2012.08.037.

[54] Ma Y, Chu X, Tang G, Yao Y. Synthesis and thermal properties of acrylate-based polymer shell microcapsules with binary core as phase change materials. Mater Lett 2013;91:133–5. doi:10.1016/j.matlet.2012.09.084.

[55] Qiu X, Song G, Chu X, Li X, Tang G. Microencapsulated n-alkane with p(n-butyl methacrylate-co-methacrylic acid) shell as phase change materials for thermal energy storage. Sol Energy 2013;91:212–20. doi:10.1016/j.solener.2013.01.022.

[56] Sarı A, Alkan C, Karaipekli A, Uzun O. Microencapsulated n-octacosane as phase change material for thermal energy storage. Sol Energy 2009;83:1757–63. doi:10.1016/j.solener.2009.05.008.

[57] Alkan C, Sarı A, Karaipekli A. Preparation, thermal properties and thermal reliability of microencapsulated n-eicosane as novel phase change material for thermal energy storage. Energy Convers Manag 2011;52:687–92. doi:10.1016/j.enconman.2010.07.047.

[58] Alay S, Alkan C, Göde F. Synthesis and characterization of poly(methyl methacrylate)/n-hexadecane microcapsules using different cross-linkers and their application to some fabrics. Thermochim Acta 2011;518:1–8. doi:10.1016/j.tca.2011.01.014.

[59] Wang Y, Shi H, Xia TD, Zhang T, Feng HX. Fabrication and performances of microencapsulated paraffin composites with polymethylmethacrylate shell based on ultraviolet irradiation-initiated. Mater Chem Phys 2012;135:181–7. doi:10.1016/j.matchemphys.2012.04.050.

[60] Taguchi Y, Yokoyama H, Kado H, Tanaka M. Preparation of PCM microcapsules by using oil absorbable polymer particles. Colloids Surfaces A Physicochem Eng Asp 2007;301:41–7. doi:10.1016/j.colsurfa.2006.12.019.

[61] Tzvetkov G, Graf B, Wiegner R, Raabe J, Quitmann C, Fink R. Soft X-ray spectromicroscopy of phase-change microcapsules. Micron 2008;39:275–9. doi:10.1016/j.micron.2007.04.002.

[62] Alkan C, Sari A. Fatty acid/poly(methyl methacrylate) (PMMA) blends as form-stable phase change materials for latent heat thermal energy storage. Sol Energy 2008;82:118–24. doi:10.1016/j.solener.2007.07.001.

[63] Giro-Paloma J, Oncins G, Barreneche C, Martínez M, Fernández AI, Cabeza LF. Physico-chemical and mechanical properties of microencapsulated phase change material. Appl Energy 2013;109:441–8. doi:10.1016/j.apenergy.2012.11.007.

[64] Su J-F, Wang X-Y, Dong H. Influence of temperature on the deformation behaviors of melamine–formaldehyde microcapsules containing phase change material. Mater Lett 2012;84:158–61. doi:10.1016/j.matlet.2012.06.074.

[65] Palanikkumaran M, Gupta KK, Agrawal AK, Jassal M. Effect of emulsion preparation method on microencapsulation of n -octadecane using melamine-formaldehyde pre-polymers. Indian J Fibre Text Res 2010;35:101–6.

[66] Zhao CY, Zhang GH. Review on microencapsulated phase change materials (MEPCMs): Fabrication, characterization and applications. Renew Sustain Energy Rev 2011;15:3813–32. doi:10.1016/j.rser.2011.07.019.

[67] Sánchez-Silva L, Rodríguez JF, Romero A, Borreguero AM, Carmona M, Sánchez P. Microencapsulation of PCMs with a styrene-methyl methacrylate copolymer shell by suspension-like polymerisation. Chem Eng J 2010;157:216–22. doi:10.1016/j.cej.2009.12.013.

[68] Sánchez L, Sánchez P, de Lucas A, Carmona M, Rodríguez JF. Microencapsulation of PCMs with a polystyrene shell. Colloid Polym Sci 2007;285:1377–85. doi:10.1007/s00396-007-1696-7.

[69] Sánchez L, Sánchez P, Carmona M, de Lucas A, Rodríguez JF. Influence of operation conditions on the microencapsulation of PCMs by means of suspension-like polymerization. Colloid Polym Sci 2008;286:1019–27. doi:10.1007/s00396-008-1864-4.

[70] Borreguero AM, Carmona M, Sanchez ML, Valverde JL, Rodriguez JF. Improvement of the thermal behaviour of gypsum blocks by the incorporation of microcapsules containing PCMS obtained by suspension polymerization with an optimal core/coating mass ratio. Appl Therm Eng 2010;30:1164–9. doi:10.1016/j.applthermaleng.2010.01.032.

[71] Wang Y, Xia TD, Feng HX, Zhang H. Stearic acid/polymethylmethacrylate composite as form-stable phase change materials for latent heat thermal energy storage. Renew Energy 2011;36:1814–20. doi:10.1016/j.renene.2010.12.022.

[72] Kim OH, Lee K, Kim K, Lee BH, Choe S. Effect of PVA in dispersion polymerization of MMA. Polymer (Guildf) 2006;47:1953–9. doi:10.1016/j.polymer.2006.01.025.

[73] Kawaguchi S. Dispersion Polymerization 2005:299–328. doi:10.1007/b100118.

[74] Sarı A, Alkan C, Karaipekli A. Preparation, characterization and thermal properties of PMMA/n-heptadecane microcapsules as novel solid–liquid microPCM for thermal energy storage. Appl Energy 2010;87:1529–34. doi:10.1016/j.apenergy.2009.10.011.

[75] Mollidain S. M.Pharmacy (pharmaceutical technology). SHIFT- II n.d. http://www.slideshare.net/mollidain/microencapsulation-by-sandeep.

[76] Choi Y, Lee JG, Kim JH, Yang H. Preparation of microcapsules containing phase change materials as heat transfer media by in-situ polymerization. J Ind Eng Chem 2001.

[77] Jyothi NVN, Prasanna PM, Sakarkar SN, Prabha KS, Ramaiah PS, Srawan GY. Microencapsulation techniques, factors influencing encapsulation efficiency. J Microencapsul 2010;27:187–97. doi:10.3109/02652040903131301.

[78] Sumiga B, Knez E, Vrtačnik M, Ferk-Savec V, Starešinič M, Boh B. Production of Melamine-Formaldehyde PCM Microcapsules with Ammonia Scavenger used for Residual Formaldehyde Reduction. Acta Chim Slov 2011;58:14–25.

[79] Boh B, Knez E, Staresinic M. Microencapsulation of higher hydrocarbon phase change materials by in situ polymerization. J Microencapsul 2005;22:715–35. doi:10.1080/02652040500162139.

[80] Boh B, Šumiga B. Microencapsulation technology and its applications in building construction materials. RMZ- Mater Geoenvironment 2008;55:329–44.

[81] Yang R, Xu H, Zhang Y. Preparation, physical property and thermal physical property of phase change microcapsule slurry and phase change emulsion. Sol Energy Mater Sol Cells 2003;80:405–16. doi:10.1016/j.solmat.2003.08.005.

[82] Yang R, Zhang Y, Wang X, Zhang Y, Zhang Q. Preparation of n-tetradecane-containing microcapsules with different shell materials by phase separation method. Sol Energy Mater Sol Cells 2009;93:1817–22. doi:10.1016/j.solmat.2009.06.019.

[83] Fang G, Li H, Yang F, Liu X, Wu S. Preparation and characterization of nano-encapsulated n-tetradecane as phase change material for thermal energy storage. Chem Eng J 2009;153:217–21. doi:10.1016/j.cej.2009.06.019.

[84] Chen Z, Cao L, Fang G, Shan F. Synthesis and Characterization of Microencapsulated Paraffin Microcapsules as Shape-Stabilized Thermal Energy Storage Materials. Nanoscale Microscale Thermophys Eng 2013;17:112–23. doi:10.1080/15567265.2012.761305.

[85] Song XQ, Li YX, Wang JW. Preparation and Characterization of Hexadecane Microcapsule Phase Change Materials by *In Situ* Polymerization. Adv Mater Res 2013;815:367–70. doi:10.4028/www.scientific.net/AMR.815.367.

[86] Pascu O, Garcia Valls R, Giamberini M. Interfacial polymerization of an epoxy resin and carboxylic acids for the synthesis of microcapsules. Polym Int 2008;57:995–1006. doi:10.1002/pi.2438.

[87] Liang C, Lingling X, Hongbo S, Zhibin Z. Microencapsulation of butyl stearate as a phase change material by interfacial polycondensation in a polyurea system. Energy Convers Manag 2009;50:723–9. doi:10.1016/j.enconman.2008.09.044.

[88] Li B, Liu T, Hu L, Wang Y, Gao L. Fabrication and Properties of Microencapsulated Paraffin@SiO 2 Phase Change Composite for Thermal Energy Storage. ACS Sustain Chem Eng 2013;1:374–80. doi:10.1021/sc300082m.

[89] Nagavarma BVN, Yadav HKS, Ayaz a., Vasudha LS, Shivakumar HG. Different techniques for preparation of polymeric nanoparticles- A review. Asian J Pharm Clin Res 2012;5:16–23.

[90] Shivakumar. Microencapsulation. B. pharmacy. kottam institute of pharmacy, A.P n.d.

[91] Özonur Y, Mazman M, Paksoy HÖ, Evliya H. Microencapsulation of coco fatty acid mixture for thermal energy storage with phase change material. Int J Energy Res 2006;30:741–9. doi:10.1002/er.1177.

[92] Fang G, Li H, Liu X. Preparation and properties of lauric acid/silicon dioxide composites as form-stable phase change materials for thermal energy storage. Mater Chem Phys 2010;122:533–6. doi:10.1016/j.matchemphys.2010.03.042.

[93] Li H, Fang G, Liu X. Synthesis of shape-stabilized paraffin/silicon dioxide composites as phase change material for thermal energy storage. J Mater Sci 2009;45:1672–6. doi:10.1007/s10853-009-4146-8.

[94] Tang B, Qiu M, Zhang S. Thermal conductivity enhancement of PEG/SiO2 composite PCM by in situ Cu doping. Sol Energy Mater Sol Cells 2012;105:242–8. doi:10.1016/j.solmat.2012.06.012.

[95] Ghosh SK. Functional Coatings and Microencapsulation: A General Perspective. Funct Coat 2006.

[96] Wu H-T, Yang M-W. Precipitation kinetics of PMMA sub-micrometric particles with a supercritical assisted-atomization process. J Supercrit Fluids 2011;59:98–107. doi:10.1016/j.supflu.2011.08.001.

[97] Haldorai Y, Shim J-J, Lim KT. Synthesis of polymer–inorganic filler nanocomposites in supercritical CO2. J Supercrit Fluids 2012;71:45–63. doi:10.1016/j.supflu.2012.07.007.

[98] Borreguero a. M, Valverde JL, Rodríguez JF, Barber a. H, Cubillo JJ, Carmona M. Synthesis and characterization of microcapsules containing Rubitherm®RT27 obtained by spray drying. Chem Eng J 2011;166:384–90. doi:10.1016/j.cej.2010.10.055.

[99] Hawlader MNA, Uddin MS, Khin MM. Microencapsulated PCM thermal-energy storage system. Appl Energy 2003;74:195–202. doi:10.1016/S0306-2619(02)00146-0.

[100] Fei B, Lu H, Qi K, Shi H, Liu T, Li X, et al. Multi-functional microcapsules produced by aerosol reaction. J Aerosol Sci 2008;39:1089–98. doi:10.1016/j.jaerosci.2008.07.007.

[101] De Windt L, Dabo D, Lidelöw S, Badreddine R, Lagerkvist A. MSWI bottom ash used as basement at two pilot-scale roads: comparison of leachate chemistry and reactive transport modeling. Waste Manag 2011;31:267–80. doi:10.1016/j.wasman.2010.06.002.

[102] Jin Y, Lee W, Musina Z, Ding Y. A one-step method for producing microencapsulated phase change materials. Particuology 2010;8:588–90. doi:10.1016/j.partic.2010.07.009.

[103] Youssef Z, Delahaye A, Huang L, Trinquet F, Fournaison L, Pollerberg C, et al. State of the art on phase change material slurries. Energy Convers Manag 2013;65:120–32. doi:10.1016/j.enconman.2012.07.004.

[104] Zhang P, Qiu ZZ, He M. Review on Microencapsulated Phase Change Materials (MPCM) Slurries: Materials, Rheological Behavior and Applications. Adv. Mater. Res., vol. 953-954, 2014, p. 1109–12. doi:10.4028/www.scientific.net/AMR.953-954.1109.

[105] Zhang GH, Zhao C-Y. Thermal and rheological properties of microencapsulated phase change materials. Renew Energy 2011;36:2959–66. doi:doi:10.1016/j.renene.2011.04.002.

[106] Dry powder mixes comprising Phase change Materials. Patent US 5370814, n.d.

[107] Chen Z, Fang G. Preparation and heat transfer characteristics of microencapsulated phase change material slurry: A review. Renew Sustain Energy Rev 2011;15:4624–32. doi:10.1016/j.rser.2011.07.090.

[108] Baronetto S, G S, F G, M P. Numerical Model of a Slurry PCM-Based Solar Thermal Collector. Proc. 8th Int. Symp. Heating, Vent. Air Cond. Lect. Notes Electr. Eng., 2014, p. 13–20. doi:10.1007/978-3-642-39578-9_2.

[109] Knodel BD, France DM, Choi US, Wambsganss MW. Heat transfer and pressure drop in ice-water slurries. Appl Therm Eng 2000;20:671–85. doi:10.1016/S1359-4311(99)00046-0.

[110] Stamatiou E, Kawaji M. Thermal and flow behavior of ice slurries in a vertical rectangular channel. Part I: Local distribution measurements in adiabatic flow. Int J Heat Mass Transf 2005;48:3527–43. doi:10.1016/j.ijheatmasstransfer.2005.03.020.

[111] Inaba H, Zhang Y, Horibe A, Haruki N. Numerical simulation of natural convection of latent heat phase-change-material microcapsulate slurry packed in a horizontal rectangular enclosure heated from below and cooled from above. Heat Mass Transf 2007;43:459–70. doi:10.1007/s00231-006-0121-y.

[112] Sarı A, Biçer A, Karaipekli A, Alkan C, Karadag A. Synthesis, thermal energy storage properties and thermal reliability of some fatty acid esters with glycerol as novel solid–liquid phase change materials. Sol Energy Mater Sol Cells 2010;94:1711–5. doi:10.1016/j.solmat.2010.05.033.

[113] Lu W, Tassou SA. Experimental study of the thermal characteristics of phase change slurries for active cooling. Appl Energy 2012;91:366–74. doi:10.1016/j.apenergy.2011.10.004.

[114] Chen L, Wang T, Zhao Y, Zhang X-R. Characterization of thermal and hydrodynamic properties for microencapsulated phase change slurry (MPCS). Energy Convers Manag 2014;79:317–33. doi:10.1016/j.enconman.2013.12.026.

[115] Zhang P, Ma ZW. An overview of fundamental studies and applications of phase change material slurries to secondary loop refrigeration and air conditioning systems. Renew Sustain Energy Rev 2012;16:5021–58. doi:10.1016/j.rser.2012.03.059.

[116] Al-Abidi A a., Bin Mat S, Sopian K, Sulaiman MY, Lim CH, Th A. Review of thermal energy storage for air conditioning systems. Renew Sustain Energy Rev 2012;16:5802–19. doi:10.1016/j.rser.2012.05.030.

[117] Domínguez M, García C. Aprovechamiento de los Materiales de Cambio de Fase (PCM) en la Climatización. Inf Tecnológic 2009;20:107–15.

[118] Delgado M, Lázaro A, Mazo J, Zalba B. Review on phase change material emulsions and microencapsulated phase change material slurries: Materials, heat transfer studies

and applications. Renew Sustain Energy Rev 2012;16:253–73. doi:10.1016/j.rser.2011.07.152.

[119] Alvarado JL, Marsh C, Sohn C, Phetteplace G, Newell T. Thermal performance of microencapsulated phase change material slurry in turbulent flow under constant heat flux. Int J Heat Mass Transf 2007;50:1938–52. doi:10.1016/j.ijheatmasstransfer.2006.09.026.

[120] Huang L, Doetsch C, Pollerberg C. Low temperature paraffin phase change emulsions. Int J Refrig 2010;33:1583–9. doi:10.1016/j.ijrefrig.2010.05.016.

[121] Zhang P, Ma ZW, Wang RZ. An overview of phase change material slurries: MPCS and CHS. Renew Sustain Energy Rev 2010;14:598–614. doi:10.1016/j.rser.2009.08.015.

[122] Al-Abidi AA, Bin Mat S, Sopian K, Sulaiman MY, Lim CH, Th A. Review of thermal energy storage for air conditioning systems. Renew Sustain Energy Rev 2012;16:5802–19. doi:10.1016/j.rser.2012.05.030.

[123] Huang MJ, Eames PC, McCormack S, Griffiths P, Hewitt NJ. Microencapsulated phase change slurries for thermal energy storage in a residential solar energy system. Renew Energy 2011;36:2932–9. doi:10.1016/j.renene.2011.04.004.

[124] Augood PC, Newborough M, Highgate DJ. Thermal behaviour of phase-change slurries incorporating hydrated hydrophilic polymeric particles. Exp Therm Fluid Sci 2001;25:457–68. doi:10.1016/S0894-1777(01)00099-1.

[125] Salunkhe PB, Shembekar PS. A review on effect of phase change material encapsulation on the thermal performance of a system. Renew Sustain Energy Rev 2012;16:5603–16. doi:10.1016/j.rser.2012.05.037.

[126] Zhang S, Niu J. Experimental investigation of effects of supercooling on microencapsulated phase-change material (MPCM) slurry thermal storage capacities. Sol Energy Mater Sol Cells 2010;94:1038–48. doi:10.1016/j.solmat.2010.02.022.

[127] Zeng R, Wang X, Chen B, Zhang Y, Niu J, Wang X, et al. Heat transfer characteristics of microencapsulated phase change material slurry in laminar flow under constant heat flux. Appl Energy 2009;86:2661–70. doi:10.1016/j.apenergy.2009.04.025.

[128] Huang L, Günther E, Doetsch C, Mehling H. Subcooling in PCM emulsions—Part 1: Experimental. Thermochim Acta 2010;509:93–9. doi:10.1016/j.tca.2010.06.006.

[129] Günther E, Huang L, Mehling H, Dötsch C. Subcooling in PCM emulsions – Part 2: Interpretation in terms of nucleation theory. Thermochim Acta 2011;522:199–204. doi:10.1016/j.tca.2011.04.027.

[130] De Boer GBJ, de Weerd C, Thoenes D, Goossens HWJ. Laser Diffraction Spectrometry: Fraunhofer Diffraction Versus Mie Scattering. Part Part Syst Charact 1987;4:14–9. doi:10.1002/ppsc.19870040104.

[131] Yu F, Chen Z-H, Zeng X-R. Preparation, characterization, and thermal properties of microPCMs containing n-dodecanol by using different types of styrene-maleic anhydride as emulsifier. Colloid Polym Sci 2009;287:549–60. doi:10.1007/s00396-009-2001-8.

[132] Bayés-García L, Ventolà L, Cordobilla R, Benages R, Calvet T, Cuevas-Diarte M a. Phase Change Materials (PCM) microcapsules with different shell compositions: Preparation, characterization and thermal stability. Sol Energy Mater Sol Cells 2010;94:1235–40. doi:10.1016/j.solmat.2010.03.014.

[133] Bajāre D, Kazjonovs J, Korjakins A, Merijs-Meri R. Development of Cement and Lime Based Plaster with Microencapsulated Phase Change Materials (PCM). 12th Int. Conf. Energy Storage, 2012, p. 1–7.

[134] Pan L, Tao Q, Zhang S, Wang S, Zhang J, Wang S, et al. Preparation, characterization and thermal properties of micro-encapsulated phase change materials. Sol Energy Mater Sol Cells 2012;98:66–70. doi:10.1016/j.solmat.2011.09.020.

[135] Fang G, Chen Z, Li H. Synthesis and properties of microencapsulated paraffin composites with SiO2 shell as thermal energy storage materials. Chem Eng J 2010;163:154–9. doi:10.1016/j.cej.2010.07.054.

[136] Fang Y, Kuang S, Gao X, Zhang Z. Preparation and characterization of novel nanoencapsulated phase change materials. Energy Convers Manag 2008;49:3704–7. doi:10.1016/j.enconman.2008.06.027.

[137] Zhang H, Wang X. Fabrication and performances of microencapsulated phase change materials based on n-octadecane core and resorcinol-modified melamine–formaldehyde shell. Colloids Surfaces A Physicochem Eng Asp 2009;332:129–38. doi:10.1016/j.colsurfa.2008.09.013.

[138] Alkan C. Enthalpy of melting and solidification of sulfonated paraffins as phase change materials for thermal energy storage. Thermochim Acta 2006;451:126–30. doi:10.1016/j.tca.2006.09.010.

[139] Zhang T, Wang Y, Shi H, Yang W. Fabrication and performances of new kind microencapsulated phase change material based on stearic acid core and polycarbonate shell. Energy Convers Manag 2012;64:1–7. doi:10.1016/j.enconman.2012.04.011.

[140] Pomianowski M, Heiselberg P, Jensen RL, Cheng R, Zhang Y. A new experimental method to determine specific heat capacity of inhomogeneous concrete material with incorporated microencapsulated-PCM. Cem Concr Res 2014;55:22–34. doi:10.1016/j.cemconres.2013.09.012.

[141] Ostrý M, Pøikryl R, Charvát P, Mlcoch T, Bakajová B. Laboratory assessment of micro-encapsulated phase-change materials. Mater Technol 2012;46:531–4.

[142] Zhang H, Sun S, Wang X, Wu D. Fabrication of microencapsulated phase change materials based on n-octadecane core and silica shell through interfacial polycondensation. Colloids Surfaces A Physicochem Eng Asp 2011;389:104–17. doi:10.1016/j.colsurfa.2011.08.043.

[143] Giro-Paloma J, Barreneche C, Delgado M, Martínez M, Fernández AI, Cabeza LF. Physicochemical and thermal study of a MPCM of PMMA shell and paraffin wax as a core. Energy Procedia, vol. 48, 2014, p. 347–54. doi:10.1016/j.egypro.2014.02.040.

[144] Huang H, Haghighat F. Building materials VOC emissions—a systematic parametric study. Build Environ 2003;38:995–1005. doi:10.1016/S0360-1323(03)00062-3.

[145] Kim S, Choi Y-K, Park K-W, Kim JT. Test methods and reduction of organic pollutant compound emissions from wood-based building and furniture materials. Bioresour Technol 2010;101:6562–8. doi:10.1016/j.biortech.2010.03.059.

[146] Jia C, Batterman S, Godwin C. VOCs in industrial, urban and suburban neighborhoods, Part 1: Indoor and outdoor concentrations, variation, and risk drivers. Atmos Environ 2008;42:2083–100. doi:10.1016/j.atmosenv.2007.11.055.

[147] Jia C, Batterman S, Godwin C, Charles S, Chin J-Y. Sources and migration of volatile organic compounds in mixed-use buildings. Indoor Air 2010;20:357–69. doi:10.1111/j.1600-0668.2010.00643.x.

[148] Schlink U, Rehwagen M, Damm M, Richter M, Borte M, Herbarth O. Seasonal cycle of indoor-VOCs: comparison of apartments and cities. Atmos Environ 2004;38:1181–90. doi:10.1016/j.atmosenv.2003.11.003.

[149] Zhang Y, Xu Y. Characteristics and correlations of VOC emissions from building materials. Int J Heat Mass Transf 2003;46:4877–83. doi:10.1016/S0017-9310(03)00352-1.

[150] Lee C-S, Haghighat F, Ghaly WS. A study on VOC source and sink behavior in porous building materials - analytical model development and assessment. Indoor Air 2005;15:183–96. doi:10.1111/j.1600-0668.2005.00335.x.

[151] Lee C-S, Haghighat F, Ghaly W. Conjugate Mass Transfer Modeling for VOC Source and Sink Behavior of Porous Building Materials: When to Apply It? J Build Phys 2006;30:91–111. doi:10.1177/1744259106067683.

[152] Ayoko GA. Volatile Organic Compounds in Indoor Environments. 2004.

[153] Magee RJ, Bodalal A, Biesenthal TA, Lusztyk E, Brouzes M, Shaw CY. Prediction of VOC concentration profiles in a newly constructed house using samll chamber data and an IAQ simulation program. 9th Int. Conf. IAQ Clim., 2002, p. 298–303.

[154] Berrios IT, Zhang J, Guo B, Smith J, Zhang Z. Volatile organic compounds (VOCS) emissions from sources in a partitioned office environment and their impact on IAQ. 10th Int. Conf. indoor air Qual. Clim. (indoor air), 2005.

[155] Molhave L, Clausen G, Berglund B, Ceaurriz JDE, Kettrup A, Lindvall T. Total Volatile Organic Compounds (TVOC) in Indoor Air Quality Investigations ". Indoor Air 1997;7:225–40.

[156] Filella I, Peñuelas J. Daily, weekly, and seasonal time courses of VOC concentrations in a semi-urban area near Barcelona. Atmos Environ 2006;40:7752–69. doi:10.1016/j.atmosenv.2006.08.002.

[157] Jia C, Batterman SA, Relyea GE. Variability of indoor and outdoor VOC measurements: an analysis using variance components. Environ Pollut 2012;169:152–9. doi:10.1016/j.envpol.2011.09.024.

[158] Haghighat F, Huang H. Integrated IAQ model for prediction of VOC emissions from building material. Build Environ 2003;38:1007–17. doi:10.1016/S0360-1323(03)00064-7.

[159] Huang H, Haghighat F, Blondeau P. Volatile organic compound (VOC) adsorption on material: influence of gas phase concentration, relative humidity and VOC type. Indoor Air 2006;16:236–47. doi:10.1111/j.1600-0668.2005.00421.x.

[160] Missia DA, Demetriou E, Michael N, Tolis EI, Bartzis JG. Indoor exposure from building materials: A field study. Atmos Environ 2010;44:4388–95. doi:10.1016/j.atmosenv.2010.07.049.

[161] Jalaludin J, Nordiyana MS., Suhaimi NF. Exposure to indoor air pollutants (formaldehyde, VOCs, ultrafine particles) and respiratory health symptoms among office workers in old and new buildings in Universiti Putra Malaysia. Int J Appl Nat Sci 2014;3:69–80.

[162] Cabeza LF, Castellón C, Nogués M, Medrano M, Leppers R, Zubillaga O. Use of microencapsulated PCM in concrete walls for energy savings. Energy Build 2007;39:113–9. doi:10.1016/j.enbuild.2006.03.030.

[163] Lee SH, Yoon SJ, Kim YG, Choi YC, Kim JH, Lee JG. Development of building materials by using micro-encapsulated phase change material. Korean J Chem Eng 2007;24:332–5. doi:10.1007/s11814-007-5054-8.

[164] Zhou G, Zhang Y, Wang X, Lin K, Xiao W. An assessment of mixed type PCM-gypsum and shape-stabilized PCM plates in a building for passive solar heating. Sol Energy 2007;81:1351–60. doi:10.1016/j.solener.2007.01.014.

[165] Safari V, Barreneche C, Castell A, Basatni A, Navarro L, Cabeza L, et al. Volatile organic emission from PCM building materials. Innostock 2012 - 12th Int. Conf. Energy Storage, 2012.

[166] Hunger M, Entrop AG, Mandilaras I, Brouwers HJH, Founti M. The behavior of self-compacting concrete containing micro-encapsulated Phase Change Materials. Cem Concr Compos 2009;31:731–43. doi:10.1016/j.cemconcomp.2009.08.002.

[167] Shin SH, Jo WK. Volatile organic compound concentrations, emission rates, and source apportionment in newly-built apartments at pre-occupancy stage. Chemosphere 2012;89:569–78. doi:10.1016/j.chemosphere.2012.05.054.

[168] Cai Y, Wei Q, Huang F, Lin S, Chen F, Gao W. Thermal stability, latent heat and flame retardant properties of the thermal energy storage phase change materials based on paraffin/high density polyethylene composites. Renew Energy 2009;34:2117–23. doi:10.1016/j.renene.2009.01.017.

[169] JC M. A treatise on electricity and magnetism. New York: 1954.

[170] Wang X, Niu J. Heat Transfer of Microencapsulated PCM Slurry Flow in a Circular Tube 2008;54. doi:10.1002/aic.

[171] Silakhori M, Naghavi M, Metselaar H, Mahlia T, Fauzi H, Mehrali M. Accelerated Thermal Cycling Test of Microencapsulated Paraffin Wax/Polyaniline Made by Simple Preparation Method for Solar Thermal Energy Storage. Materials (Basel) 2013;6:1608–20. doi:10.3390/ma6051608.

[172] Hawlader MN a., Uddin MS, Zhu HJ. Encapsulated phase change materials for thermal energy storage: Experiments and simulation. Int J Energy Res 2002;26:159–71. doi:10.1002/er.773.

[173] Sharma SD, Buddhi D, Sawhney RL. Accelerated thermal cycle test of latent heat-storage materials. Sol Energy 1999;66:483–90. doi:10.1016/S0038-092X(99)00045-6.

[174] Fortuniak W, Slomkowski S, Chojnowski J, Kurjata J, Tracz A, Mizerska U. Synthesis of a paraffin phase change material microencapsulated in a siloxane polymer. Colloid Polym Sci 2013;291:725–33. doi:10.1007/s00396-012-2782-z.

[175] Griffiths PW, Eames PC. Performance of chilled ceiling panels using phase change material slurries as the heat transport medium. Appl Therm Eng 2007;27:1756–60. doi:10.1016/j.applthermaleng.2006.07.009.

[176] Pons O, Aguado A, Fernández AI, Cabeza LF, Chimenos JM. Review of the use of phase change materials (PCMs) in buildings with reinforced concrete structures. Mater Construcción 2014;64:e031. doi:10.3989/mc.2014.05613.

[177] Norvell C, Sailor DJ, Dusicka P. The Effect of Microencapsulated Phase-Change Material on the Compressive Strength of Structural Concrete. J Green Build 2013;8:116–24. doi:http://dx.doi.org/10.3992/jgb.8.3.116.

[178] Hunger M, Entrop a. G, Mandilaras I, Brouwers HJH, Founti M. The behavior of self-compacting concrete containing micro-encapsulated Phase Change Materials. Cem Concr Compos 2009;31:731–43. doi:10.1016/j.cemconcomp.2009.08.002.

[179] Ling T-C, Poon C-S. Use of phase change materials for thermal energy storage in concrete: An overview. Constr Build Mater 2013;46:55–62. doi:10.1016/j.conbuildmat.2013.04.031.

[180] Thiele AM, Sant G, Pilon L. Diurnal thermal analysis of microencapsulated PCM-concrete composite walls. Energy Convers Manag 2015;93:215–27. doi:10.1016/j.enconman.2014.12.078.

[181] Cheng R, Pomianowski M, Wang X, Heiselberg P, Zhang Y. A new method to determine thermophysical properties of PCM-concrete brick. Appl Energy 2013;112:988–98. doi:10.1016/j.apenergy.2013.01.046.

[182] Schossig P, Henning H-M, Gschwander S, Haussmann T. Micro-encapsulated phase-change materials integrated into construction materials. Sol Energy Mater Sol Cells 2005;89:297–306. doi:doi:10.1016/j.solmat.2005.01.017.

[183] Borreguero AM, Luz Sánchez M, Valverde JL, Carmona M, Rodríguez JF. Thermal testing and numerical simulation of gypsum wallboards incorporated with different PCMs content. Appl Energy 2011;88:930–7. doi:10.1016/j.apenergy.2010.08.014.

[184] Barreneche C, de Gracia A, Serrano S, Elena Navarro M, Borreguero AM, Inés Fernández a., et al. Comparison of three different devices available in Spain to test thermal properties of building materials including phase change materials. Appl Energy 2013;109:421–7. doi:10.1016/j.apenergy.2013.02.061.

[185] Borreguero AM, Garrido I, Valverde JL, Rodríguez JF, Carmona M. Development of smart gypsum composites by incorporating thermoregulating microcapsules. Energy Build 2014;76:631–9. doi:10.1016/j.enbuild.2014.03.005.

[186] Toppi T, Mazzarella L. Gypsum based composite materials with micro-encapsulated PCM: Experimental correlations for thermal properties estimation on the basis of the composition. Energy Build 2013;57:227–36. doi:10.1016/j.enbuild.2012.11.009.

[187] Castellón C, Castell A, Medrano M, Martorell I, Cabeza LF. Experimental study of PCM inclusion in different building envelopes. J Sol Energy Eng 2009;131:410061–6. doi:10.1115/1.3197843.

[188] Castellón C, Medrano M, Roca J, Cabeza LF, Navarro ME, Fernández AI, et al. Effect of microencapsulated phase change material in sandwich panels. Renew Energy 2010;35:2370–4. doi:10.1016/j.renene.2010.03.030.

[189] Borreguero AM, Valverde JL, Peijs T, Rodríguez JF, Carmona M. Characterization of rigid polyurethane foams containing microencapsulated Rubitherm® RT27. Part I. J Mater Sci 2010;45:4462–9. doi:10.1007/s10853-010-4529-x.

[190] Borreguero AM, Rodríguez JF, Valverde JL, Arevalo R, Peijs T, Carmona M. Characterization of rigid polyurethane foams containing microencapsulated Rubitherm® RT27: catalyst effect. Part II. J Mater Sci 2010;46:347–56. doi:10.1007/s10853-010-4824-6.

[191] Borreguero AM, Rodríguez JF, Valverde JL, Peijs T, Carmona M. Characterization of rigid polyurethane foams containing microencapsulted phase change materials: Microcapsules type effect. J Appl Polym Sci 2013;128:582–90. doi:10.1002/app.38226.

[192] Shim H, McCullough EA, Jones BW. Using Phase Change Materials in Clothing. Text Res J 2001;71:495–502. doi:10.1177/004051750107100605.

[193] Ying B, Kwok Y, Li Y, Zhu Q, Yeung C. Assessing the performance of textiles incorporating phase change materials. Polym Test 2004;23:541–9. doi:10.1016/j.polymertesting.2003.11.002.

[194] Shin Y, Yoo D-I, Son K. Development of thermoregulating textile materials with microencapsulated phase change materials (PCM). II. Preparation and application of PCM microcapsules. J Appl Polym Sci 2005;96:2005–10. doi:10.1002/app.21438.

[195] Sun YC, Cheng ZH. Heat Buffering Property of Phase Change Materials in Textiles. Key Eng. Mater., vol. 474-476, 2011, p. 1024–8. doi:10.4028/www.scientific.net/KEM.474-476.1024.

[196] Borreguero AM, Talavera B, Rodriguez JF, Valverde JL, Gonzalez JL, Carmona M. Enhancing the thermal comfort of fabrics for the footwear industry. Text Res J 2013;83:1754–63. doi:10.1177/0040517513481872.

Chapter 3 References

[1] Schossig P, Henning H-M, Gschwander S, Haussmann T. Micro-encapsulated phase-change materials integrated into construction materials. Sol Energy Mater Sol Cells 2005;89:297–306.

[2] Baetens R, Jelle BP, Gustavsen A. Phase change materials for building applications: A state-of-the-art review. Energy Build 2010;42:1361–8. doi:10.1016/j.enbuild.2010.03.026.

[3] Farid MM, Khudhair AM, Razack SAK, Al-Hallaj S. A review on phase change energy storage: Materials and applications. Energy Convers Manag 2004;45:1597–615.

[4] Jamekhorshid A, Sadrameli SM, Farid M. A review of microencapsulation methods of phase change materials (PCMs) as a thermal energy storage (TES) medium. Renew Sustain Energy Rev 2014;31:531–42.

[5] Pascu O, Garcia Valls R, Giamberini M. Interfacial polymerization of an epoxy resin and carboxylic acids for the synthesis of microcapsules. Polym Int 2008;57:995–1006.

[6] Liang C, Lingling X, Hongbo S, Zhibin Z. Microencapsulation of butyl stearate as a phase change material by interfacial polycondensation in a polyurea system. Energy Convers Manag 2009;50:723–9. doi:10.1016/j.enconman.2008.09.044.

[7] Sánchez-Silva L, Rodríguez JF, Romero A, Borreguero AM, Carmona M, Sánchez P. Microencapsulation of PCMs with a styrene-methyl methacrylate copolymer shell by suspension-like polymerisation. Chem Eng J 2010;157:216–22. doi:10.1016/j.cej.2009.12.013.

[8] Sánchez L, Sánchez P, de Lucas A, Carmona M, Rodríguez JF. Microencapsulation of PCMs with a polystyrene shell. Colloid Polym Sci 2007;285:1377–85. doi:10.1007/s00396-007-1696-7.

[9] Borreguero AM, Carmona M, Sanchez ML, Valverde JL, Rodriguez JF. Improvement of the thermal behaviour of gypsum blocks by the incorporation of microcapsules containing PCMS obtained by suspension polymerization with an optimal core/coating mass ratio. Appl Therm Eng 2010;30:1164–9. doi:10.1016/j.applthermaleng.2010.01.032.

[10] Sánchez L, Sánchez P, Carmona M, de Lucas A, Rodríguez JF. Influence of operation conditions on the microencapsulation of PCMs by means of suspension-like polymerization. Colloid Polym Sci 2008;286:1019–27. doi:10.1007/s00396-008-1864-4.

[11] Özonur Y, Mazman M, Paksoy HÖ, Evliya H. Microencapsulation of coco fatty acid mixture for thermal energy storage with phase change material. Int J Energy Res 2006;30:741–9.

[12] Sarı A, Alkan C, Karaipekli A. Preparation, characterization and thermal properties of PMMA/n-heptadecane microcapsules as novel solid–liquid microPCM for thermal energy storage. Appl Energy 2010;87:1529–34. doi:10.1016/j.apenergy.2009.10.011.

[13] Borreguero a. M, Valverde JL, Rodríguez JF, Barber a. H, Cubillo JJ, Carmona M. Synthesis and characterization of microcapsules containing Rubitherm®RT27 obtained by spray drying. Chem Eng J 2011;166:384–90. doi:10.1016/j.cej.2010.10.055.

[14] Hawlader MNA, Uddin MS, Khin MM. Microencapsulated PCM thermal-energy storage system. Appl Energy 2003;74:195–202. doi:10.1016/S0306-2619(02)00146-0.

[15] Fei B, Lu H, Qi K, Shi H, Liu T, Li X, et al. Multi-functional microcapsules produced by aerosol reaction. J Aerosol Sci 2008;39:1089–98. doi:10.1016/j.jaerosci.2008.07.007.

[16] Davidson MW, Abramowitz M. Optical microscopy n.d.:1–40.

[17] Sánchez P, Sánchez-Fernandez MV, Romero A, Rodríguez JF, Sánchez-Silva L. Development of thermo-regulating textiles using paraffin wax microcapsules. Thermochim Acta 2010;498:16–21.

[18] Bayés-García L, Ventolà L, Cordobilla R, Benages R, Calvet T, Cuevas-Diarte M a. Phase Change Materials (PCM) microcapsules with different shell compositions: Preparation, characterization and thermal stability. Sol Energy Mater Sol Cells 2010;94:1235–40.

[19] Giro-Paloma J, Martínez M, Fernández AI, Cabeza LF. Microencapsulation of phase change materials. CRC Press, n.d.

[20] Pan L, Tao Q, Zhang S, Wang S, Zhang J, Wang S, et al. Preparation, characterization and thermal properties of micro-encapsulated phase change materials. Sol Energ Mater Sol Cells 2012;98:66–70. doi:10.1016/j.solmat.2011.09.020.

[21] www.horiba.com/us/particle n.d.

[22] De Boer GBJ, de Weerd C, Thoenes D, Goossens HWJ. Laser Diffraction Spectrometry: Fraunhofer Diffraction Versus Mie Scattering. Part Part Syst Charact 1987;4:14–9.

[23] Yu F, Chen Z-H, Zeng X-R. Preparation, characterization, and thermal properties of microPCMs containing n-dodecanol by using different types of styrene-maleic anhydride as emulsifier. Colloid Polym Sci 2009;287:549–60. doi:10.1007/s00396-009-2001-8.

[24] http://www.horiba.com/scientific/products/particle-characterization/education/general-information/data-interpretation/number-vs-volume-distributions/ n.d.

[25] Alkan C. Enthalpy of melting and solidification of sulfonated paraffins as phase change materials for thermal energy storage. Thermochim Acta 2006;451:126–30. doi:10.1016/j.tca.2006.09.010.

[26] Zhang T, Wang Y, Shi H, Yang W. Fabrication and performances of new kind microencapsulated phase change material based on stearic acid core and polycarbonate shell. Energy Convers Manag 2012;64:1–7. doi:10.1016/j.enconman.2012.04.011.

[27] Guang-Long Z, Xiao-Zheng L, Tan Z-C, Sun Li-Zian, Tao Z. Microencapsulation of n-hexadecane as a Phase Change Material in Polyurea. Acta Phys Chim Sin 2004;20:90–3.

[28] Gulmine J., Janissek P., Heise H., Akcelrud L. Polyethylene characterization by FTIR. Polym Test 2002;21:557–63. doi:10.1016/S0142-9418(01)00124-6.

[29] Zheng Y, Zhao W, Sabol JC, Tuzla K, Neti S, Oztekin A, et al. Encapsulated phase change materials for energy storage – Characterization by calorimetry. Sol Energy 2013;87:117–26.

[30] Sarı A, Alkan C, Karaipekli A, Uzun O. Microencapsulated n-octacosane as phase change material for thermal energy storage. Sol Energy 2009;83:1757–63.

[31] http://www.mt.com/ n.d.

[32] Fortuniak W, Slomkowski S, Chojnowski J, Kurjata J, Tracz A, Mizerska U. Synthesis of a paraffin phase change material microencapsulated in a siloxane polymer. Colloid Polym Sci 2013;291:725–33. doi:10.1007/s00396-012-2782-z.

[33] http://www.tainstruments.com/ n.d.

[34] Barreneche C, Solé A, Miró L, Martorell I, Fernández AI, Cabeza LF. New methodology developed for the differential scanning calorimetry analysis of polymeric matrixes incorporating phase change materials. Meas Sci Technol 2012;23.

[35] Alkan C, Sarı A, Karaipekli A. Preparation, thermal properties and thermal reliability of microencapsulated n-eicosane as novel phase change material for thermal energy storage. Energy Convers Manag 2011;52:687–92. doi:10.1016/j.enconman.2010.07.047.

[36] Sarı A, Biçer A, Karaipekli A, Alkan C, Karadag A. Synthesis, thermal energy storage properties and thermal reliability of some fatty acid esters with glycerol as novel solid–liquid phase change materials. Sol Energy Mater Sol Cells 2010;94:1711–5. doi:10.1016/j.solmat.2010.05.033.

[37] Silakhori M, Naghavi M, Metselaar H, Mahlia T, Fauzi H, Mehrali M. Accelerated Thermal Cycling Test of Microencapsulated Paraffin Wax/Polyaniline Made by Simple Preparation Method for Solar Thermal Energy Storage. Materials (Basel) 2013;6:1608–20.

[38] Sharma SD, Buddhi D, Sawhney RL. Accelerated thermal cycle test of latent heat-storage materials. Sol Energy 1999;66:483–90. doi:10.1016/S0038-092X(99)00045-6.

[39] Delgado M, Lázaro A, Mazo J, Marín JM, Zalba B. Experimental analysis of a microencapsulated PCM slurry as thermal storage system and as heat transfer fluid in laminar flow. Appl Therm Eng 2012;36:370–7.

[40] Zhang H, Sun S, Wang X, Wu D. Fabrication of microencapsulated phase change materials based on n-octadecane core and silica shell through interfacial polycondensation. Colloids Surfaces A Physicochem Eng Asp 2011;389:104–17. doi:10.1016/j.colsurfa.2011.08.043.

[41] TA instruments. Seminario de caracterización de materiales mediante técnicas de análisis térmico (DSC, MDSC, TGA, SDT) n.d.

[42] Menard KP. Dynamic Mechanical Analysis: A Practical Introduction, Second Edition. 2009.

[43] Jee A-Y, Lee M. Comparative analysis on the nanoindentation of polymers using atomic force microscopy. Polym Test 2010;29:95–9. doi:10.1016/j.polymertesting.2009.09.009.

[44] Díez-Pascual AM, Gómez-Fatou MA, Ania F, Flores A. Nanoindentation in polymer nanocomposites. Prog Mater Sci 2015;67:1–94.

[45] Schuh CA. Nanoindentation studies of materials. Mater Today 2006;9:32–40. doi:10.1016/S1369-7021(06)71495-X.

[46] Lee S, Wang S, Pharr GM. Evaluation of interphase properties in a cellulose fiber-reinforced polypropylene composite by nanoindentation and finite element analysis 2007;38:1517–24.

[47] Fang T-H, Chang W-J. Nanoindentation characteristics on polycarbonate polymer film. Microelectronics J 2004;35:595–9. doi:10.1016/j.mejo.2004.02.004.

[48] Hu Y, Shen L, Yang H, Wang M, Liu T, Liang T, et al. Nanoindentation studies on Nylon 11/clay nanocomposites. Polym Test 2006;25:492–7. doi:10.1016/j.polymertesting.2006.02.005.

[49] Su J-F, Wang X-Y, Dong H. Micromechanical properties of melamine–formaldehyde microcapsules by nanoindentation: Effect of size and shell thickness. Mater Lett 2012;89:1–4.

[50] Lee J, Zhang M, Bhattacharyya D, Yuan YC, Jayaraman K, Mai YW. Micromechanical behavior of self-healing epoxy and hardener-loaded microcapsules by nanoindentation. Mater Lett 2012;76:62–5. doi:10.1016/j.matlet.2012.02.052.

[51] Giro-Paloma J, Roa JJ, Díez-Pascual AM, Rayón E, Flores A, Martínez M, et al. Depth-sensing indentation applied to polymers: A comparison between standard methods of analysis in relation to the nature of the materials. Eur Polym J 2013;49:4047–53.

[52] Giro-Paloma J, Rayón E, Roa JJ, Martínez M, Fernández AI. Effect of the filler on the nanomechanical properties of polypropylene in contact with paraffinic phase change material. Eur Polym J 2015;63:29–36. doi:10.1016/j.eurpolymj.2014.11.029.

[53] Neubauer MP, Poehlmann M, Fery A. Microcapsule mechanics: from stability to function. Adv Colloid Interface Sci 2014;207:65–80. doi:10.1016/j.cis.2013.11.016.

[54] Giro-Paloma J, Oncins G, Barreneche C, Martínez M, Fernández AI, Cabeza LF. Physico-chemical and mechanical properties of microencapsulated phase change material. Appl Energy 2013;109:441–8. doi:10.1016/j.apenergy.2012.11.007.

[55] Giro-Paloma J, Barreneche C, Delgado M, Martínez M, Fernández AI, Cabeza LF. Physicochemical and thermal study of a MPCM of PMMA shell and paraffin wax as a core. Energy Procedia, vol. 48, 2014, p. 347–54.

[56] Griepentrog M, Krämer G, Cappella B. Comparison of nanoindentation and AFM methods for the determination of mechanical properties of polymers. Polym Test 2013;32:455–60.

[57] Ghorbanzadeh Ahangari M, Fereidoon A, Jahanshahi M, Sharifi N. Effect of nanoparticles on the micromechanical and surface properties of poly(urea–formaldehyde) composite microcapsules. Compos Part B Eng 2014;56:450–5. doi:10.1016/j.compositesb.2013.08.071.

[58] Giro-Paloma J, Oncins G, Barreneche C, Martínez M, Fernández AI, Cabeza LF. Physico-chemical and mechanical properties of microencapsulated phase change material. Appl Energy 2013;109:441–8. doi:10.1016/j.apenergy.2012.11.007.

[59] Giro-Paloma J, Konuklu Y, Fernández AI. Preparation and exhaustive characterization of paraffin or palmitic acid microcapsules as novel phase change material. Sol Energy 2015;112:300–9.

[60] Ribes A, Carrera G, Gallego E, Roca X, Berenguer MAJ, Guardino X. Development and validation of a method for air-quality and nuisance odors monitoring of volatile organic compounds using multi-sorbent adsorption and gas chromatography/mass spectrometry thermal desorption system. J Chromatogr A 2007;1140:44–55. doi:10.1016/j.chroma.2006.11.062.

[61] Comprehensive analysis of aroma compounds released from incense sticks using TD-GC/MS. Markes Int TDTS 10 n.d.

Chapter 4 . Characterization of MPCM

4.1 Characterization of Micronal® DS 5001

4.2 Characterization of laboratory MPCM. Comparison of MPCM with same shell and different core material

4.3 Comparison of MPCM with same core material and different shell

4.4 Comparison of commercial and laboratory MPCM including environmental characterization

As it was mentioned in Chapter 3, there are numerous techniques to characterize MPCM's properties. Hence, it is important to distinguish between the MPCM usages: in passive or active solar systems.

- A **passive solar system** does not involve mechanical devices neither conventional energy sources beyond that needed to regulate dampers and other controls. Examples of basic passive solar structures are greenhouses, sunrooms and solariums. In terms of design, the success of the passive solar system will depend on the orientation and the thermal mass of the structure's exterior walls, which means their ability to store and redistribute heat.
- **Active solar energy systems** use the same basic principles as passive systems except that they use a heat transfer fluid (for example water) to absorb heat. Active solar systems use external sources of energy to pumps and other types of equipment to collect, store and convert solar energy.

4.1 Characterization of Micronal® DS 5001

The most common MPCM used in passive systems is Micronal® DS 5001. This sample has been widely studied by several authors [1–10]. Most of them have characterized its thermal and chemical behavior, but none had evaluated its mechanical properties. As this sample has to be used by mixing it with other matrix materials in passive systems, the study of the mechanical behavior is a key point to determine the stiffness and the strength of the shell of Micronal® DS 5001. For this reason, it was considered very relevant to study this sample deeply. The mechanical response was evaluated by Atomic Force Microscopy (AFM) with indentation mode. To simulate real conditions in service, assays were done at different temperatures: at 25 ºC, with the PCM in solid state, and at 45 ºC and 80 ºC, with melted PCM. The obtained results were published in the article titled "**Physico-chemical and mechanical properties of microencapsulated phase change material**". It was published in **Applied Energy** journal in 2013 (volume 109, pages 441 - 448), as Figure 4.1 shows [11].

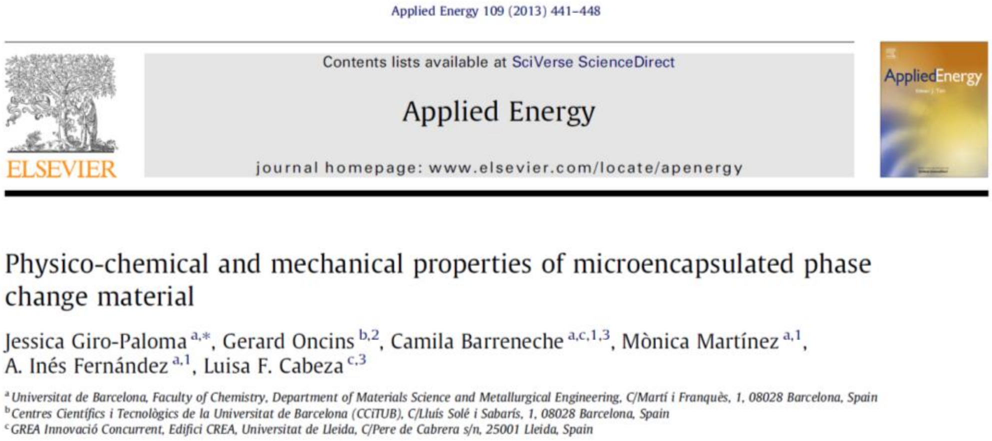

Applied Energy 109 (2013) 441–448

Contents lists available at SciVerse ScienceDirect

Applied Energy

journal homepage: www.elsevier.com/locate/apenergy

Physico-chemical and mechanical properties of microencapsulated phase change material

Jessica Giro-Paloma [a,*], Gerard Oncins [b,2], Camila Barreneche [a,c,1,3], Mònica Martínez [a,1], A. Inés Fernández [a,1], Luisa F. Cabeza [c,3]

[a] Universitat de Barcelona, Faculty of Chemistry, Department of Materials Science and Metallurgical Engineering, C/Martí i Franquès, 1, 08028 Barcelona, Spain
[b] Centres Científics i Tecnològics de la Universitat de Barcelona (CCiTUB), C/Lluís Solé i Sabarís, 1, 08028 Barcelona, Spain
[c] GREA Innovació Concurrent, Edifici CREA, Universitat de Lleida, C/Pere de Cabrera s/n, 25001 Lleida, Spain

Figure 4.1. Published paper in 2013 in Applied Energy journal titled “Physico-chemical and mechanical properties of microencapsulated phase change material”.

Physicochemical, thermal, mechanical and studies were needed to better complete the characterization of Micronal® DS 5001 sample, by using density, BET specific surface, Particle Size Distribution (PSD), Fourier-Transformed Infrared spectroscopy (FT-IR), X-Ray Fluorescence (XRF), Thermogravimetrical analysis (TGA), and Differential Scanning Calorimetry (DSC). Micronal® DS 5001 is composed by spherical agglomerates of 150 μm, which are formed by microspheres of 6 μm in size. Moreover, it was extracted the chemical composition of the sample, being 67 % composed by paraffin wax PCM, 23.5 % acrylate polymer, and 9% of a SiO$_2$ based compound. Taking into account the thermal properties, Micronal® DS 5001 showed a phase change temperature range between 26.09 ºC and 27.81 ºC, a melting enthalpy between 114.98 kJ·kg^{-1} and 142.55 kJ·kg^{-1}, and a solidification enthalpy between 117.85 kJ·kg^{-1} and 137.85 kJ·kg^{-1}. The mechanical property studied for this sample at different temperatures was the effective Young Modulus (E_{eff}), which it changes depending on the size of the particle and the temperature. For microspheres of 150 μm, the average value for E_{eff} at 25 ºC was 4.9 GPa and at 45 ºC was 7.2 GPa. Furthermore, for the 6 μm microparticles, the average value for E_{eff} at 25 ºC was 24.5 MPa, at 45 ºC was 24.9 MPa, and at 80 ºC was 7.4 MPa. As it can be observed for the 6 μm microparticles, there were no differences in the elastic response at 25 and 45 ºC, although it increases considerably at 80 ºC, because this temperature is close to the polymer shell glass transition temperature.

Applied Energy 109 (2013) 441–448

Contents lists available at SciVerse ScienceDirect

Applied Energy

journal homepage: www.elsevier.com/locate/apenergy

Physico-chemical and mechanical properties of microencapsulated phase change material

Jessica Giro-Paloma [a,*], Gerard Oncins [b,2], Camila Barreneche [a,c,1,3], Mònica Martínez [a,1], A. Inés Fernández [a,1], Luisa F. Cabeza [c,3]

[a] *Universitat de Barcelona, Faculty of Chemistry, Department of Materials Science and Metallurgical Engineering, C/Martí i Franquès, 1, 08028 Barcelona, Spain*
[b] *Centres Científics i Tecnològics de la Universitat de Barcelona (CCiTUB), C/Lluís Solé i Sabarís, 1, 08028 Barcelona, Spain*
[c] *GREA Innovació Concurrent, Edifici CREA, Universitat de Lleida, C/Pere de Cabrera s/n, 25001 Lleida, Spain*

HIGHLIGHTS

- Microencapsulated phase change material MPCM (Micronal* DS 5001) was evaluated in this study.
- Due to the reported microcapsules breakage, physical and mechanical properties were analysed.
- Mechanical response was evaluated by AFM with indentation mode under different temperatures.
- The main result is that stiffness of MPCM depends on the temperature assay and particle size.

ARTICLE INFO

Article history:
Received 31 July 2012
Received in revised form 30 October 2012
Accepted 3 November 2012
Available online 12 December 2012

Keywords:
Thermal energy storage
Microencapsulated phase change material
Atomic force microscopy
Stiffness

ABSTRACT

Microencapsulated phase change materials (MPCM) are well known in advanced technologies for the utilization in active and passive systems, which have the capacity to absorb and slowly release the latent heat involved in a phase change process. Microcapsules consist of little containers, which are made of polymer on the outside, and paraffin wax as PCM in the inside. The use of microencapsulated PCM has many advantages as microcapsules can handle phase change materials as core allowing the preparation of slurries. However there are some concerns about cycling of MPCM slurries because of the breakage of microcapsules during charging/discharging and the subsequent loss of effectiveness. This phenomenon motivates the study of the mechanical response when a force is applied to the microcapsule. The maximum force that Micronal® DS 5001 can afford before breaking was determined by Atomic Force Microscopy (AFM). To simulate real conditions in service, assays were done at different temperatures: with the PCM in solid state at 25 °C, and with the PCM melted at 45 °C and 80 °C. To better understand the behavior of these materials, Micronal® DS 5001 microcapsules were characterized using different physic-chemical techniques. Microcapsules Fourier Transform Infrared Spectroscopy (FT-IR) results showed the main vibrations corresponding to acrylic groups of the outside polymer. Thermal stability was studied by Thermogravimetrical Analysis (TGA), and X-ray Fluorescence (XRF) was used to characterize the resulting inorganic residue. The thermal properties were determined using Differential Scanning Calorimetry (DSC) curves. Particles morphology was studied with Scanning Electron Microscopy (SEM) and Mie method was used to evaluate the particle size distribution. Samples had a bimodal distribution of size and were formed by two different particles sizes: agglomerates of 150 μm diameter formed by small particles of 6 μm. Atomic Force Microscopy in nanoindentation mode was used to evaluate the elastic response of the particles at different temperatures. Different values of effective modulus E_{eff} were calculated for agglomerates and small particles. It was observed that stiffness depended on the temperature assay and particle size, as agglomerates showed higher stiffness than small particles, which showed an important decrease in elastic properties at 80 °C.

---

* Corresponding author. Tel.: +34 934021298; fax: +34 934035438.
E-mail addresses: jessicagiro@ub.edu (J. Giro-Paloma), goncins@ub.edu (G. Oncins), c.barreneche@ub.edu (C. Barreneche), monicamartinez@ub.edu (M. Martínez), ana_inesfernandez@ub.edu (A.I. Fernández), lcabeza@diei.udl.cat (L.F. Cabeza).
[1] Tel.: +34 934021298; fax: +34 934035438.
[2] Tel.: +34 934021352; fax: +34 934021398.
[3] Tel.: +34 973003576; fax: +34 973003575.

0306-2619/$ - see front matter Crown Copyright © 2012 Published by Elsevier Ltd. All rights reserved.
http://dx.doi.org/10.1016/j.apenergy.2012.11.007

1. Introduction

The phase change materials (PCMs) for thermal energy storage (TES) [1] must have both high latent heat and thermal conductivity as the main properties [2,3]. It has been found that with the help of PCMs the indoor temperature fluctuations can be reduced significantly whilst maintaining desirable thermal comfort [4,5]. Materials studied for this application are hydrated salt [6], paraffin waxes [7–9], fatty acids [10–13], fatty alcohols [14] and eutectics of organic and non-organic compounds [15,16]. Microencapsulated phase change materials [17] (MPCM) are used in composite formulations for thermal energy storage in passive systems or in active systems as aqueous slurries.

Microencapsulation is a process whereby small, spherical or rod-shaped particles are enclosed in a thin, high molecular weight polymeric film. Microcapsules are little containers made by a hydrophobic core material (phase change material, PCM) and a polymeric hard shell [18]. The advantages of MPCM are the protection against influences of the outside environment, the increase of the specific heat-transfer area, and improved tolerance to volume changes. Microencapsulation has been widely used to make copying paper, functional textiles, preservation or targeted delivery of chemical, food, etc.

In this study Micronal® DS 5001 from BASF® with a melting temperature between 26 and 27 °C was used. The application temperature range of the selected product was tailored particularly to its employment in buildings (10–30 °C). Micronal® has been incorporated in mortars, concrete or plasterboard as passive systems [19–21], and it is also used in active systems as slurries [22–29]. A better understanding of its performance and limitations in these systems needs more knowledge of the material properties, mainly thermal as well as chemical or mechanical properties. In its usage as slurries, the mechanical behavior of the microcapsules becomes a key issue during charging/discharging, as the mechanical integrity of the shell is essential for its performance during thermal cycling and pumping. When Micronal® is used as aqueous slurry in active storage systems, changes are observed after several thermal cycles that are attributed to a partial degradation of the microcapsules by breakage [30]. Therefore, this study has two main objectives: the first one is the characterization of chemical and physical properties of Micronal® DS 5001 like surface area, particle size distribution, and chemical composition. The second objective is the characterization of the mechanical performance of microcapsules at different temperatures using Atomic Force Microscope (AFM). This characterization should help us to better understand the behavior of Micronal® in the above cited applications.

2. Materials and methods

The physico-chemical characterization of Micronal® DS 5001 consisted in the determination of density, Specific BET surface area, and particle size distribution. Infrared spectroscopy (FT-IR) and X-Ray Fluorescence spectroscopy (XRF) were performed with Thermogravimetrical Analysis (TGA) to complete the chemical characterization. Thermal properties were evaluated with differential scanning calorimeter, and scanning electron microscopy was used to study the morphology of the sample.

2.1. Physicochemical characterization

2.1.1. Density and BET specific surface

Density was measured with a Micrometrics® Pycnometer AccuPyc 1330 at 24 °C and the specific surface BET was measured by Micrometrics® (TriStar 3000).

2.1.2. Particle size distribution

The sample was analyzed using a Beckman Coulter® LS™ 13 320 with Universal Liquid Module. The results were analyzed using the mathematical models Fraunhofer and Mie, as the use of one or the other depends on the particle size and the opacity of the material. The Fraunhofer model is used for opaque particles bigger than 30 μm, whereas the Mie model fits better for homogenous and spherical particles, opaque or transparent and with diameters below 30 μm [31].

2.1.3. Fourier transform infrared spectroscopy (FT-IR)

FT-IR spectroscopy is a powerful technique to identify functional groups in organic polymers or compounds. It was done through FT-IR Bomem ABB FTLA using a working range from 350 to 4000 cm^{-1}.

2.1.4. X-Ray Fluorescence (XRF)

X-ray fluorescence semi-quantitative analysis was performed on the calcined residue of Micronal® sample. A spectrophotometer Panalytical Philips PW 2400 sequential X-ray equipped with the software UniQuant® V5.0 was used.

2.1.5. Thermogravimetrical Analysis (TGA)

Thermal stability of the microcapsules was evaluated with a Simultaneous SDTQ600 TA Instruments under air atmosphere. The scanning rate was 0.5 K/min in the temperature range between 25 and 30 °C followed by an isothermal step during 300 min. Then, temperature was increased at 1 K/min from 30 to 100 °C, followed by an isothermal step during 300 min. The last heating ramp was at 5 K/min from 100 to 600 °C.

2.2. Thermal properties with Differential Scanning Calorimetry (DSC)

The most common methods used in DSC analysis of PCM are dynamic method and step method. The dynamic method consists on heating or cooling the sample at a constant rate while the heat flux of the sample is measured [32,33]. Generally, when the dynamic method is applied, the phase transition is not an isothermal process because the thermal equilibrium is not achieved. A possible option to solve this problem is collecting the data using the step method, where the heating rate is changed by temperature intervals (steps).

The thermal properties such as melting/solidification temperature and melting/solidification enthalpy of the microcapsules containing PCM were evaluated by the Research Group Grea at the University of Lleida, using both methods by DSC with a *DSC 822-e* from Mettler Toledo. An aluminum crucible of 40 μl under N_2 atmosphere flow of 80 mL/min was used. The heating rate used was 0.5 °C/min in both methodologies. This technique shows the melting temperature (T_m) and solidification temperature (T_s) of the sample and the enthalpy value for each process (melting and solidification, H_m and H_s respectively) which is equivalent to the area under the curve.

2.3. Scanning Electron Microscopy (SEM)

The morphology of the sample was characterized using an environmental scanning electron microscope (ESEM, Quanta 200 FEI, XTE 325/D8395). The sample was stuck on the sample holder using a double-sided tape and then the particle size and the morphology of the sample was observed. The working conditions were low vacuum and high voltage (15 kV), and the image obtained by secondary electrons.

2.4. Stiffness characterization by atomic force microscopy

To determine the mechanical properties of the sample of Micronal® DS 5001, AFM was performed at Scientific and Technological Centers of the Universitat de Barcelona (CCiTUB). AFM probes radius (R) was measured using the SPIP reconstruction software. R value was measured before and after every mechanical test in order to ensure that the tip shape did not change due to plastic deformation, which would invalidate stiffness value measurements through effective Young Modulus (E_{eff}).

AFM topographic images were acquired in intermittent contact mode using a MFP-3D system (Asylum Research). For this sort of measurements, Micronal® particles were glued on a metallic disk with epoxy. Care was taken to avoid an excess of glue around the particles that may result in a noticeable change in their mechanical properties. By means of the optical system attached to the AFM, only clean and spherical particles were chosen to be studied.

Topographic measurements as well as mechanical tests on Micronal® DS 5001 particles were performed with a diamond tip mounted on a stainless steel cantilever with a nominal k value of 265 nN/nm (Veeco). Nevertheless, k values of probes were individually measured by means of the thermal noise routine implemented in the software [34].

Mechanical measurements were performed with the Force Spectroscopy mode, using the AFM probe as a nanoindenter. As the goal of this experimental study is to assess the E_{eff} value, vertical forces applied by the AFM probe (F) were tuned so as to always remain in the elastic deformation region.

Two different sample sets were tested; one of them consisted on Micronal® particle aggregates exceeding 100 μm in diameter (agglomerates) and the other consisted on particles with diameters below 10 μm (small particles). The necessary F value to break the agglomerates and the small spheres was studied, so plastic deformation was topographically detected to take place at F values around 5 μN for the agglomerates and at 3 μN for the small particles; therefore measurements presented in this work were acquired at F values of 3 μN and 1.5 μN for the two different sets of particles, respectively. The elastic–plastic transition tested by AFM is depicted in Fig. 1 in a small particle without applying load (no contact), and after applying load (deformation of the sample).

Fig. 1 shows the vertical force *vs.* sample penetration curve obtained by processing the measurement of the cantilever deflection as it moves to the sample when a F value of 7 μN was applied (continuous line corresponds to tip sample approach process and dotted line corresponds to the tip retraction from the sample). It was the maximum F exerted, so plastic deformation was induced on the particle. The first region (flat, Fig. 1a) corresponds to the lack of contact between tip and sample. When contact is reached, the cantilever applies an increasing F on the sample, deforming it elastically.

The deformation process is depicted from Fig. 1a–c. So, Fig. 1a shows no contact between tip and the small particles. Then at a certain sample penetration value, F suddenly decreases as it can be seen in Fig. 1b, confirming the plastic penetration of the sample. As F and sample penetration continue increasing (Fig. 1c), the sample is further deformed. The retraction of the AFM probe is depicted by the dotted line. In this specific experiment, the F value needed to plastically deform the sample is approximately 4 μN.

Individual indentation experiments were performed in different spots of the upper flat-top part of Micronal® particles in order to avoid tip slippage due to sample curvature. F is calculated as in Eq. (1), where k is the AFM probe, and Δ_z is cantilever deflection in the z axis:

$$F = k \cdot \Delta_z \tag{1}$$

The cantilever deflection is expressed in Eq. (2), where ΔV is the increment in photodetector vertical signal as the tip contacts the sample and S is the sensitivity, which is the slope of the contact region of a force curve performed on a rigid sample:

$$\Delta_z = \Delta V/S \tag{2}$$

The sample penetration (δ) due to the exerted F value is evaluated as Eq. (3), where z represents the piezo-scanner displacement in the axis perpendicular to the sample plane:

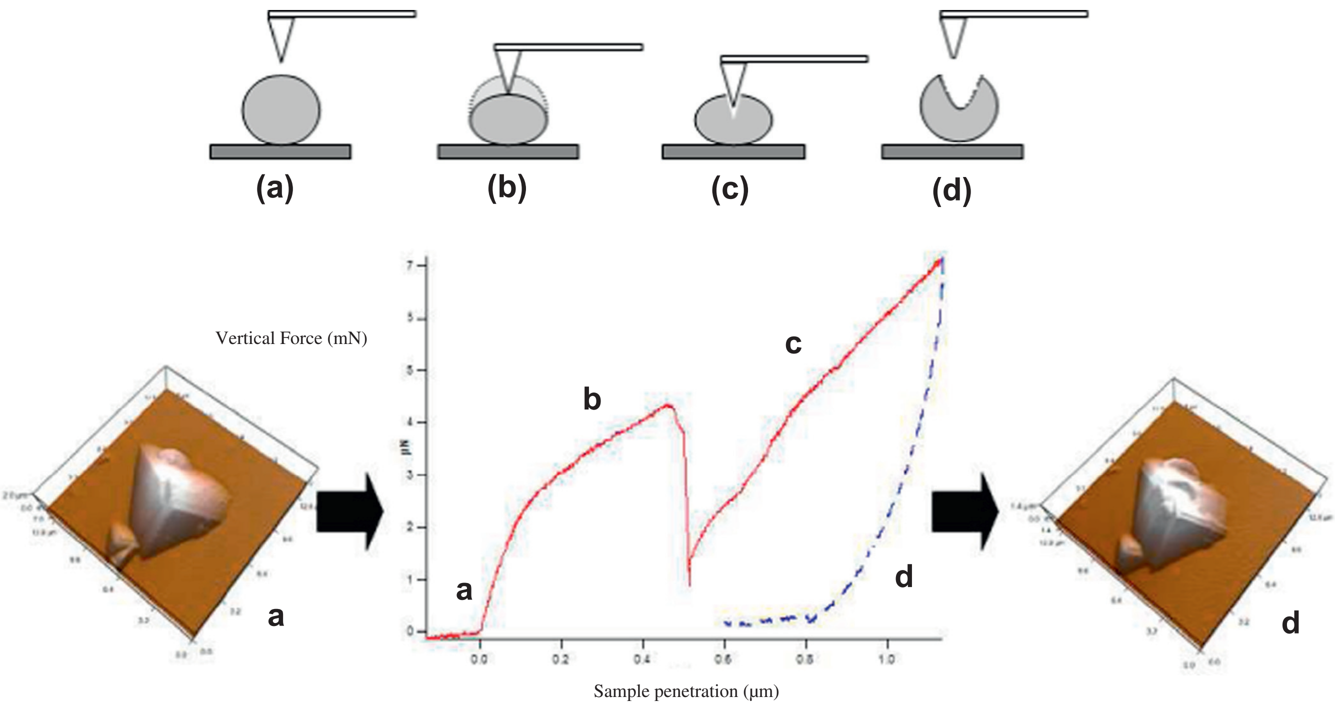

Fig. 1. Mechanical testing of the elastic-plastic region by AFM of a small particle, (a) no contact; (b) plastic penetration; (c) deformation of the sample; and (d) the retraction of the AFM probe.

$$\delta = z - \Delta_z \tag{3}$$

F vs. z curves obtained at a certain F value were analyzed using the Hertz model in the elastic region by means of Eq. (4), and effective Modulus (E_{eff}) value can be obtained using Eq. (5):

$$F = (3/4 \cdot E_{eff} \cdot R^{1/2}) \cdot \delta^{3/2} \tag{4}$$

$$1/E_{eff} = [(1-\nu^2)/E] + [(1-\nu_i^2)/E_i] \tag{5}$$

where ν is the Poisson ratio with a value of 0.33. Subindex i corresponds to the mechanical properties of the SiO_2 *AFM* probe ($E_i = 76$ GPa [35]) and $\nu_i = 0.17$ [36].

It is important to notice that a triangular dent in the top of the particle can be seen when it is plastically deformed by the AFM probe. The general shape of the particles also appears to be triangular; this corresponds to the shape of the AFM tip, which is pyramidal, and not to the real shape of the particle. Individual indentation experiments were performed in different spots of the upper flat-top part of Micronal® particles in order to avoid tip slippage due to sample curvature.

3. Results and discussion

3.1. Physicochemical characterization

3.1.1. Density and specific BET surface

The result of average density is 0.995 ± 0.003 g/cm^3. This value reflects the average density of two different materials: the density of the polymeric shell (1.0–1.2 g/cm^3) and the density of the paraffin wax core (0.76–0.88 g/cm^3).

The result of the BET surface area was 2.61 ± 0.04 m^2/g; this value is adequate to be used as filler in the polymer matrix, as values below 5 m^2/g are recommended to guarantee the effectiveness of a mixing process [37].

3.1.2. Particle size distribution

The calculations covered a range from 0.04 to 2000 μm. Before the assay, the sample was treated in an ultrasonic bath during 60 s in water with sodium pyrophosphate as dispersing agent, to promote deagglomeration of particles. Results calculated applying Fraunhofer model are shown in Fig. 2.

Fig. 2 shows a wide distribution with a mean value around 9 μm and agglomerates of 30 μm and 100 μm. For this reason, the dispersing agent and the experimental conditions were changed. The sample was mixed with water and a non-ionic surfactant, 0.01% of Tween 80 (Polysorbate 80), as a dispersing agent. In this case, the particle size distribution was calculated using the Mie method. Then, it was treated in an ultrasound bath during 30 s to favor deagglomeration. Particle size distribution calculated by the Mie method can be observed in Fig. 3.

Next experiment, tried to simulate real working conditions in a slurry, microcapsules were dispersed in water and how the particle size distribution changes with time and continuous stirring was evaluated. It is important to notice that stirring takes place during the measurement and for this reason, the sample will disaggregate as time goes by. Three replicates of the same slurry were measured being the time between replicates 30 s. As Fig. 4 shows, the average particle size moved through smaller sizes from 114 μm for the first replicate to 70 μm for the third one. These results demonstrate that aggregates break and the amount of smaller particles increase while bigger ones decrease.

3.1.3. Fourier Transform Infrared spectroscopy (FT-IR)

Fig. 5 shows the analysis by FT-IR spectrum. Peaks from 2954 cm^{-1} to 2850 cm^{-1} correspond to the aliphatic C–H stretching vibration. Vibration at 1728 cm^{-1} is attributed to the carbonyl group of acrylate, while the absorption peak at 1463 cm^{-1} is associated with the C–H bending vibration, and the absorption peak at 1111 cm^{-1} can be assigned to the C–O stretching of the ester group of acrylate.

3.1.4. X-Ray Fluorescence (XRF)

A Micronal® sample was calcined at 500 °C during 8 h and the composition of the residue was characterized by X-ray fluorescence. Results shown in Table 1 are stated as oxides, and reveal that the major component of this solid is silicon, probably as silicon oxide (93%), and some minor and trace elements as Na_2O, SO_2, and K_2O and CaO.

Silicon may be included in the polymer formulation as SiO_2 as the use of inorganic fillers in polymer formulations is widely described to improve their rigidity; otherwise silicon based compounds like silanes are also added in some polymer formulations, and may lead after a calcining step to SiO_2. With the analytical techniques used it was not possible to identify the silicon compound that origin a SiO_2 residue.

3.1.5. Thermogravimetrical Analysis (TGA)

As observed in the TGA of Micronal® microcapsules depicted in Fig. 6, thermal degradation takes place in two stages. The first one corresponds to the decomposition of the *PCM* paraffin wax between 53 and 202 °C and the associated loss is 67.17% of the sample. The second mass loss is attributed to the acrylate, and comprises the 23.45% of the Micronal® mass with an onset temperature around 280 °C. The total loss of ignition at 600 °C is 90.62% corresponding to the organic components paraffin and acrylate polymer.

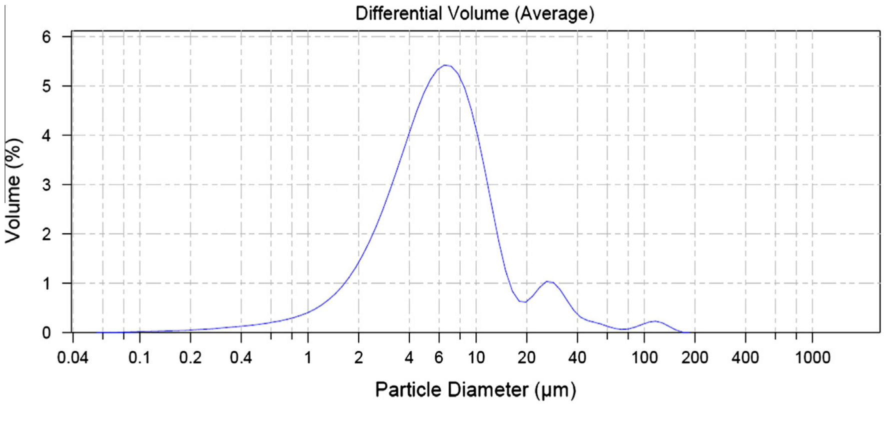

Fig. 2. Particle size distribution of Micronal® DS 5001 calculated using the Fraunhofer model.

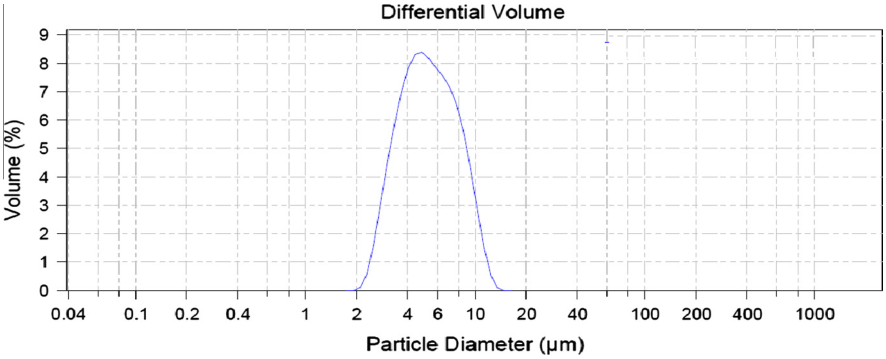

Fig. 3. Particle size distribution of Micronal® DS 5001 using the Mie model.

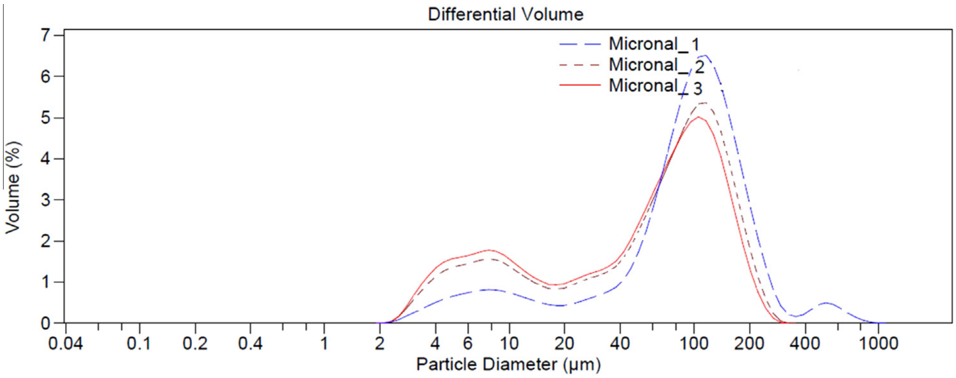

Fig. 4. Comparison of particle size distribution between three replicates with the Mie model.

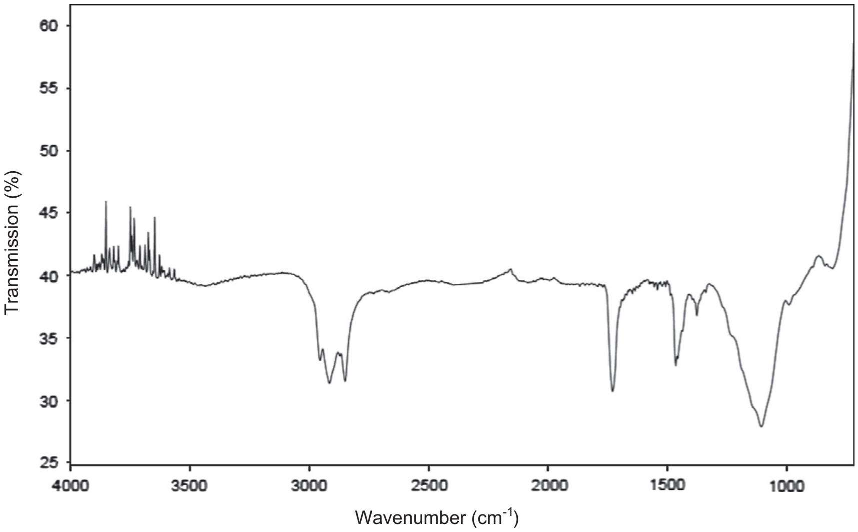

Fig. 5. Fourier transform FT-IR spectra of Micronal® DS 5001.

Table 1
XRF analysis of calcined Micronal® DS 5001, results stated as oxides.

	SiO_2	Na_2O	SO_3	K_2O	MgO	CaO
wt.%	93.0	1.6	0.8	0.3	0.1	0.1

Therefore, the chemical composition of the analyzed Micronal® sample is approximately 67.% paraffin wax PCM, 23% acrylate polymer and 9% of inorganic filler formed mainly by a Si based compound.

3.2. Thermal properties with Differential Scanning Calorimetry (DSC)

Fig. 7a shows the results obtained applying the dynamic method in DSC, where the melting enthalpy is 114.98 kJ/kg, the melting temperature is 27.81 °C, the solidification enthalpy is 117.85 kJ/kg and the solidification temperature is 26.98 °C. The results applying the step method are shown in Fig. 7b. The melting enthalpy obtained is 142.55 kJ/kg, the melting temperature is 27.87 °C, the solidification enthalpy is 137.85 kJ/kg and the solidification temperature is 26.09 °C.

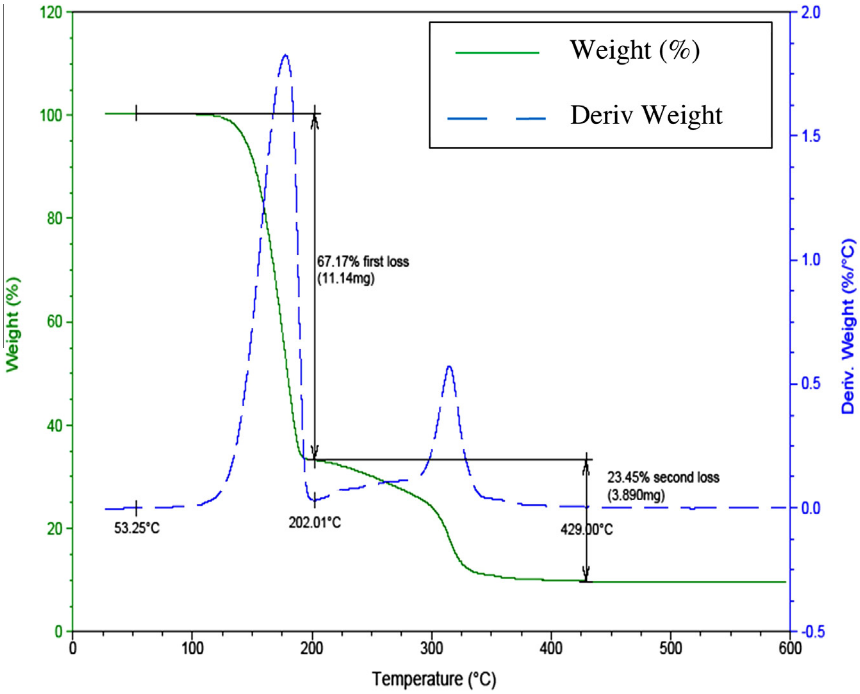

Fig. 6. Thermogravimetrical analysis of Micronal® DS 5001.

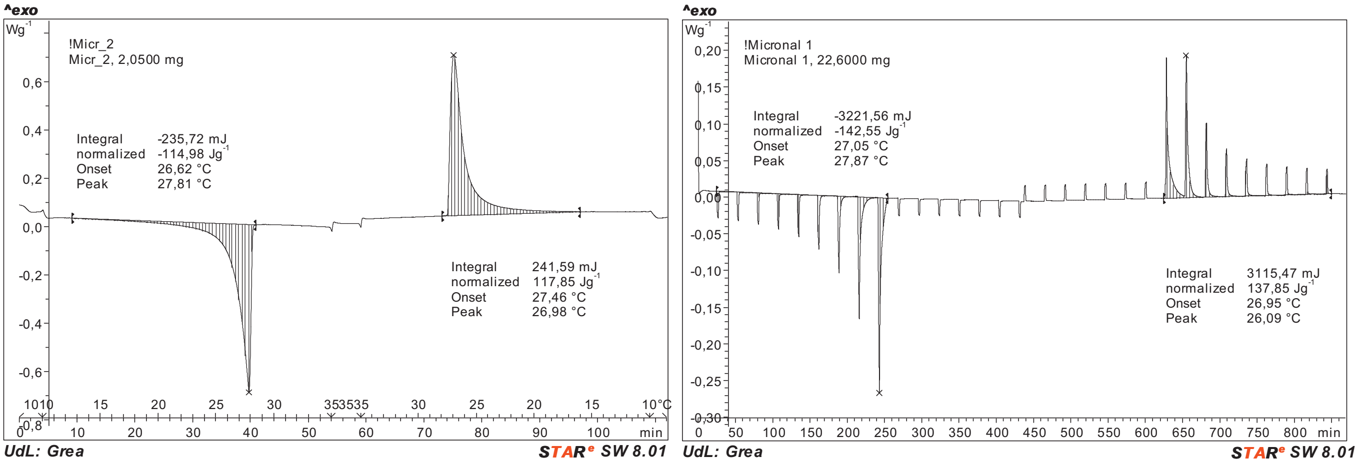

Fig. 7. DSC curves (heat flow vs. time and temperature of the sample) of Micronal® DS 5001 applying, (a) dynamic method (left); and (b) step method (right).

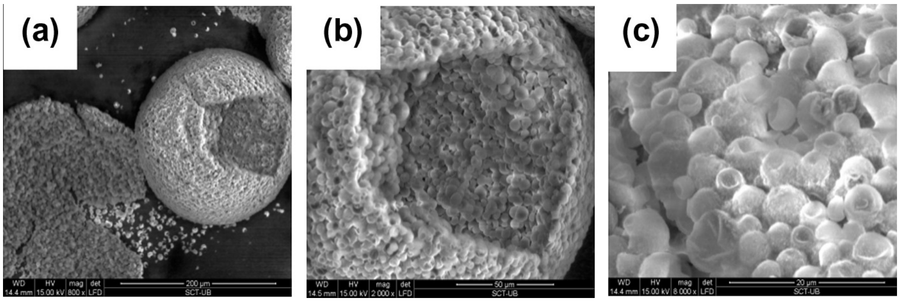

Fig. 8. Micrographies by secondary electron (*SE*) of the sample of Micronal® DS 5001 (a), (b) sample of 150 µm and (c) detail of a sphere of 6 µm.

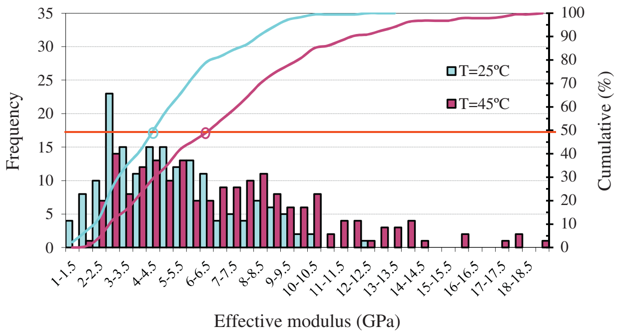

Fig. 9. E_{eff} value of agglomerate particles calculated from AFM nanoindentation experiments at 25 °C and 45 °C.

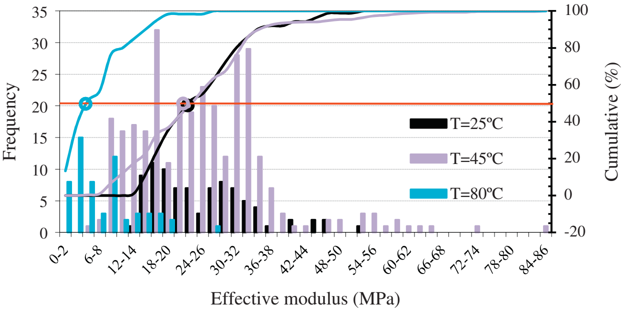

Fig. 10. E_{eff} value of small particles calculated from AFM nanoindentation experiments on Micronal® DS 5001 at 25 °C, 45 °C and 80 °C.

Temperatures of melting and solidification processes are similar comparing the results obtained with both methodologies. Applying both modes, the thermal equilibrium is achieved.

3.3. Scanning Electron Microscopy (SEM)

Fig. 8 shows the morphology and the size of the Micronal® particles. The Micronal® sample consists on microspheres of approximately 150 μm in diameter (Fig. 8a and b), which in turn are made of multiple spheres with diameters approximately 6 μm each (Fig. 8c).

3.4. Stiffness characterization by Atomic Force Microscope (AFM)

Intermittent contact mode topographic images were acquired on the top of the selected particles of 6 μm of Micronal® at 25 °C, 45 °C and 80 °C in order to determine the changes of the sample morphology. It is noticed that particles topography does not change significantly along the phase transition of the core material, indicating that the particles do not break as temperature increases until reaching 45 °C without any leakage, which would change surface topography.

To determine mechanical properties, 200 nanoindentation experiments were performed by AFM on different spots of the aggregate particles for each tested temperature. It is important to note that every nanoindentation by AFM was performed in a different spot on the top part of the particle in order to ensure that previous mechanical tests did not change the local mechanical response of the sample. Results are shown in Fig. 9 where the frequency of each result of calculated E_{eff} values is represented.

Results dispersion is due to the extremely local nature of AFM nanoindentation experiments, which are affected by local sample topography, surface defects and tilting and spurious contamination, and this is reflected in elevate standard deviation (s.d.). The E_{eff} mean value at room temperature is 4.9 GPa (s.d. 2.4 GPa) and E_{eff} mean value at 45 °C is 7.2 GPa (s.d. 4.2 GPa). Nevertheless, there is a remarkable increase of E_{eff} at 45 °C, that is, when the particles core is in liquid phase.

Fig. 10 shows the results obtained on single particles of Micronal® DS 5001. At room temperature the mean value of E_{eff} is 24.5 MPa (s.d. 9.1 MPa) and at 45 °C, the mean value is 24.9 MPa (s.d. 11.6 MPa). In this case, the results show no significant differences in the elastic response at 25 °C and 45 °C. As temperature increases up to 80 °C, E_{eff} mean value decreases drastically to 7.4 MPa (s.d. 5.6 MPa). This E_{eff} reduction is attributed to the temperature that is close to the glass transition temperature of acrylate shell (around 100 °C).

4. Conclusions

Microencapsulated Micronal® DS 5001 consists on paraffinic PCM core and an acrylate outer shell. The solid is made of spherical agglomerates of 150 μm, which are composed of microspheres of 6 μm in size (small particles). The chemical composition of the sample is approximately 67% paraffin wax PCM, 23.5% acrylate polymer, and 9% of a Si based compound. The material shows a phase change temperature range between 26.09 °C and 27.81 °C. The latent heat shows a melting enthalpy between 114.98 kJ/kg and 142.55 kJ/kg and a solidification enthalpy between 117.85 and 137.85 kJ/kg.

Different values were obtained for E_{eff} depending on the size of the particle and the temperature. For agglomerates the average value for E_{eff} at 25 °C was 4.9 GPa, and at 45 °C was 7.2 GPa. Besides, for the small particles the average value for E_{eff} at 25 °C was 24.5 MPa, at 45 °C was 24.9 MPa, and at 80 °C was 7.4 MPa. In case of small particles, there are no differences in the elastic response at 25 and 45 °C, but increases significantly at 80 °C because of this temperature is close to the polymer shell glass transition temperature.

Acknowledgements

The work is partially funded by the Spanish government (ENE2011-28269-C03-02 and ENE2011-22722) and the European Union (COST Action TU0802). The authors would like to thank the Catalan Government for the quality accreditation given to their research group GREA (2009 SGR 534) and research group DIOPMA (2009 SGR 645).

References

[1] Joulin A, Younsi Z, Zalewski L, Lassue Z, Rousse DR, Cavrot JP. Experimental and numerical investigation of a phase change material: thermal-energy storage and release. Appl Energy 2011;88(7):2454–62.
[2] Castellón C, Martorell I, Cabeza LF, Fernández AI, Manich AM. Compatibility of plastic with phase change materials (PCM). Int J Energy Res 2010;35:765–71.
[3] Bayés-García L, Ventolà L, Cordobilla R. Phase change materials (PCM) microcapsules with different shell compositions: preparation, characterization and thermal stability. Sol Energy Mater Sol Cells 2010;94:12535–40.
[4] Zhou D, Zhao CY, Tian Y. Review on thermal energy storage with phase change materials (PCMs) in building applications. Appl Energy 2012;92:593–605.
[5] Zhou G, Yang Y, Xu H. Performance of shape-stabilized phase change material wallboard with periodical outside heat flux waves. Appl Energy 2011;88(6):2113–21.
[6] Oró E, de Gracia A, Castell A, Farid MM, Cabeza LF. Review on phase change materials (PCMs) for cold thermal energy storage applications. Appl Energy 2012;99:513–33.
[7] Cai Y, Wei Q, Huang F, Gao W. Preparation and properties studies of halogen-free flame retardant form-stable phase change materials based on paraffin/high density polyethylene composites. Appl Energy 2008;85(8):765–75.
[8] Kravvaritis ED, Antonopoulos KA, Tzivanidis C. Experimental determination of the effective thermal capacity function and other thermal properties for various phase change materials using the thermal delay method. Appl Energy 2011;88(12):4459–69.
[9] Rao Z, Wang S, Peng F. Self diffusion of the nano-encapsulated phase change materials: a molecular dynamics study. Appl Energy 2012.

[10] Li M, Wu Z, Kao H. Study on preparation, structure and thermal energy storage property of capric-palmitic acid/attapulgite composite phase change materials. Appl Energy 2011;88(9):3125–32.
[11] Wang L, Meng D. Fatty acid eutectic/polymethyl methacrylate composite as form-stable phase change material for thermal energy storage. Appl Energy 2010;87(8):2660–5.
[12] Li M, Kao H, Wu Z, Tan J. Study on preparation and thermal property of binary fatty acid and the binary fatty acids/diatomite composite phase change materials. Appl Energy 2011;88(5):1606–12.
[13] Cai Y, Ke H, Dong J, Wei Q, Lin J, Zhao Y, et al. Effects of nano-SiO2 on morphology, thermal energy storage, thermal stability, and combustion properties of electrospun lauric acid/PET ultrafine composite fibers as form-stable phase change materials. Appl Energy 2011;88(6): 2106–12.
[14] Chen ZH, Yu F, Zeng XR, Zhang ZG. Preparation, characterization and thermal properties of nanocapsules containing phase change material *n*-dodecanol by miniemulsion polymerization with polymerizable emulsifier. Appl Energy 2012;91(1):7–12.
[15] Tyagi VV, Kaushik SC, Tyagi SK, Akiyama T. Development of phase change materials based microencapsulated technology for buildings: a review. Renew Sust Energy Rev 2011;15:1373–91.
[16] Farid MM, Khudhair AM, Razack SAK, Al-Hallaj S. A review on phase change energy storage: materials and applications. Energy Convers Manage 2004;45:1597–615.
[17] Chen B, Wang X, Zeng R, Zhang Y, Wang X, Niu J, et al. An experimental study of convective heat transfer with microencapsulated phase change material suspension: laminar flow in a circular tube under constant heat flux. Exp Therm Fluid Sci 2008;32:1638–46.
[18] Sari A, Alkan C, Karaipekli A, Uzun O. Microencapsulated *n*-octacosane as a phase change material for thermal energy storage. Sol Energy 2009;83:1757–63.
[19] Khudhair AM, Farid MM. A review on energy conservation in building applications thermal storage by latent heat using phase change materials. Energy Convers Manage 2004;45:263–75.
[20] Cabeza LF, Castel A, Barreneche C, de Gracia A, Fernández AI. Materials used as PCM in thermal energy storage in buildings: a review. Renew Sust Energy Rev 2011;15:1675–95.
[21] Su JF, Wang LX, Ren Li. Preparation and characterization of double-MF shell microPCMs used in building materials. J Appl Polym Sci 2005;97(5): 1755–62.
[22] Heinz A, Streicher W. Application of phase change materials and PCM-slurries for thermal energy storage. In: 10th International conference on thermal energy storage, Stockton; 2006.
[23] Zhang GH, Zhao CY. Thermal and rheological properties of microencapsulated phase change materials. Renew Energy 2011;36:2959–66.
[24] Yang R, Xu H, Zhang Y. Preparation, physical property and thermal physical property of phase change microcapsule slurry and phase change emulsion. Sol Energy Mater Sol Cells 2003;80:405–16.
[25] Hu X, Zhang Y. Novel insight and numerical analysis of convective heat transfer enhacement with microencapsulated phase change material slurries: laminar flow in a circular tube with constant heat flux. Int J Heat Mass Trans 2002;45:3163–72.
[26] Delgado M, Lázaro A, Mazo J, Marín JM, Zalba B. Experimental analysis of a microencapsulated PCM slurry as thermal system and as heat transfer fluid in laminar flow. Appl Therm Eng 2012;36(1):370–7.
[27] Lu W, Tassou SA. Experimental study of the thermal characteristics of phase change slurries for active cooling. Appl Energy 2012;91(1):366–74.
[28] Delgado M, Lázaro A, Mazo J, Zalba B. Review on phase change material emulsions and microencapsulated phase change material slurries: materials heat transfer studies and applications. Renew Sust Energy Rev 2012;16(1):253–73.
[29] Zhang Y, Wang S, Rao Z, Xie J. Experiment on storage characteristic of microencapsulated phase change material slurry. Sol Energy Mater Sol C 2011;95(10):2726–33.
[30] Diaconu BM, Varga S, Oliveira AC. Experimental assessment of heat storage properties and heat transfer characteristics of a phase change material slurry for air conditioning applications. Appl Energy 2010;87(2):620–8.
[31] de Boer GBJ, de Weerd C, Thoenes D, Goossens HWJ. Laser diffraction spectrometry: Fraunhofer diffraction versus Mie scattering. Part Syst Charact 1987;4:14–9. http://dx.doi.org/10.1002/ppsc.19870040104.
[32] Marin JM, Zalba B, Cabeza LF, Mehling H. Determination of enthalpy-temperature curves of PCM with the *t*-history method – improvement to temperature dependent properties. Meas Sci Technol 2003;14:184–9.
[33] Mehling H, Cabeza LF. Heat and cold storage with PCM. Springer-Verlag; 2008. ISBN-13: 9783540685562.
[34] Florin EL, Rief M, Lehmann H, Ludwig M, Dornmair C, Moy VT, et al. Sensing specific molecular-interactions with the atomic-force microscope. Biosens Bioelectron 1995;10:895–901.
[35] Namazu T, Isono Y. Quasi-satic bending test of nano-scale SiO_2 wire at intermediate temperatures using AFM-based technique. Sensor Actuator A 2003;194:78–85.
[36] Oliver WC, Pharr GM. An improved technique for determining hardness and elastic modulus using load and displacement sensing indentation experiments. J Mater Res 1992;7(6):1564–83.
[37] Rothon RN. Mineral fillers in thermoplastics: filler manufacture and characterisation. Adv Polym Sci 1999;139:67–107.

4.2 Laboratory MPCM characterization. Comparison of MPCM with same shell and different core material

Although there are a lot of studies considering commercial samples such as Micronal® DS 5001, there are also MPCM produced in research laboratories with significant good results, because not only the commercial ones have good properties, also the laboratory made ones. For this reason, it was thought that the characterization of laboratory MPCM could be an interesting issue for evaluating their possible usage at industrial scale. This work has been done in collaboration with Dr. Konuklu (Nigde University, Turkey), who is an expert in encapsulating and characterizing PCM [12–15].

The first study related to the laboratory made samples presented in this PhD Thesis compares two MPCM obtained via emulsion co-polymerization with same polymeric shell (Poly(styrene-co-ethylacrylate), PScEA) and different core materials (paraffin 42 - 44 and palmitic acid). These two types of microcapsules were developed for building applications. In this case, it was important to compare the mechanical response of the MPCM depending on the core material, paraffin wax *vs.* palmitic acid. The obtained results were published in **Solar Energy** journal in 2015 (volume 112, pages 300 - 309), as Figure 4.2 shows [16]. This article is titled "**Preparation and exhaustive characterization of paraffin or palmitic acid microcapsules as novel phase change material**".

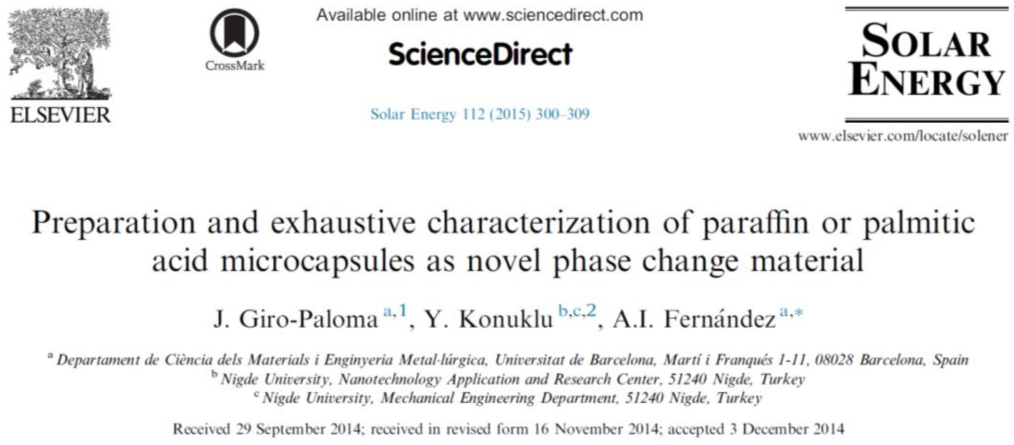

Available online at www.sciencedirect.com

ScienceDirect

Solar Energy 112 (2015) 300–309

SOLAR ENERGY

www.elsevier.com/locate/solener

Preparation and exhaustive characterization of paraffin or palmitic acid microcapsules as novel phase change material

J. Giro-Paloma [a,1], Y. Konuklu [b,c,2], A.I. Fernández [a,*]

[a] Departament de Ciència dels Materials i Enginyeria Metal·lúrgica, Universitat de Barcelona, Martí i Franqués 1-11, 08028 Barcelona, Spain
[b] Nigde University, Nanotechnology Application and Research Center, 51240 Nigde, Turkey
[c] Nigde University, Mechanical Engineering Department, 51240 Nigde, Turkey

Received 29 September 2014; received in revised form 16 November 2014; accepted 3 December 2014

Figure 4.2. Published paper in Solar Energy journal in 2015 titled "Preparation and exhaustive characterization of paraffin or palmitic acid microcapsules as novel phase change material".

The most important conclusions of this study for microspheres with paraffin in the core (capsules A, 166 nm) and with palmitic acid in the core (capsules B, 265 nm) are related to their good potential for energy storage and the success in the encapsulating process, denoting slightly higher thermal stability for sample B in the same working conditions. Besides, AFM results confirm that there are no differences in capsules A for Young’s modulus values and force applied to break the microcapsule at 25 ºC and 50 ºC, but capsules B does not have the same mechanical behavior at 25 ºC and 70 ºC, because the force is ten times lower at 70 ºC comparing the results with those at 25 ºC, although the Young’s modulus has a similar value. For capsule B, it was decided to increase the temperature until 70 ºC due to the phase change temperature of the PCM.

Available online at www.sciencedirect.com

ScienceDirect

Solar Energy 112 (2015) 300–309

SOLAR ENERGY

www.elsevier.com/locate/solener

Preparation and exhaustive characterization of paraffin or palmitic acid microcapsules as novel phase change material

J. Giro-Paloma [a,1], Y. Konuklu [b,c,2], A.I. Fernández [a,*]

[a] *Departament de Ciència dels Materials i Enginyeria Metal·lúrgica, Universitat de Barcelona, Martí i Franqués 1-11, 08028 Barcelona, Spain*
[b] *Nigde University, Nanotechnology Application and Research Center, 51240 Nigde, Turkey*
[c] *Nigde University, Mechanical Engineering Department, 51240 Nigde, Turkey*

Received 29 September 2014; received in revised form 16 November 2014; accepted 3 December 2014

Communicated by: Associate Editor Halime Paksoy

Abstract

In this study, two different types of Phase Change Materials (PCM) suitable for Thermal Energy Storage (TES) applications were used as a core material in a microencapsulation process. The wall material for these microencapsulated PCM (MPCM) was Poly(styrene-co-ethylacrylate) (PScEA). Microcapsules were prepared using an emulsion co-polymerization technique. The prepared MPCM were characterized as follows: morphology, shape and size were analyzed by Scanning Electron Microscopy (SEM) and Particle Size Distribution (PSD). Besides, Fourier Transformed Infrared spectroscopy (FT-IR) was used to perform the chemical characterization of the shell microcapsules. Moreover, thermophysical properties were analyzed by Differential Scanning Calorimetry (DSC) for the two PCM in usage (paraffin 42–44 and palmitic acid) meanwhile the thermal stability was evaluated by Thermogravimetrical Analysis (TGA). Mechanical characterization of the prepared microcapsules was performed by using the Atomic Force Microscopy (AFM) as indentor. Experiments were performed at two different temperatures 25 °C and 70 °C, and two parameters were evaluated: the Young's modulus on a punctual area and the vertical force required to plastically deform the MPCM. At the light of the results, it can be considered that these synthesized MPCM were successfully prepared being able to be used in a TES system.

Keywords: Phase Change Material; Microencapsulated phase change material; Atomic Force Microscopy; Differential Scanning Calorimetry; Thermogravimetrical Analysis; Fourier Transformed Infrared spectroscopy

1. Introduction

Phase Change Materials (PCM) are well known for Thermal Energy Storage (TES) applications and are reported as a promising energy technology for improving the energy efficiency (Gil et al., 2010), hence different kind of PCM have been studied for different applications. To avoid the leakage of the PCM and control the variation in the storage material volume as the phase change takes place, the development of microencapsulated phase change materials (MPCM) has become an area of interest (Tyagi et al., 2011; Konuklu et al., 2014; Jamekhorshid et al., 2014; Zhang et al., 2004; Zhao and Zhang, 2011). MPCM are little containers made of polymeric shell and contain PCM inside (Alkan et al., 2009). There are three prerequisites for the microencapsulation process: the construction of the shell involving the PCM, ensuring that no leakage and no impurities are incorporated in the core/shell MPCM

---

* Corresponding author. Tel.: +34 934021298; fax: +34 934035438.
E-mail addresses: jessicagiro@ub.edu (J. Giro-Paloma), ykonuklu@nigde.edu.tr (Y. Konuklu), ana_inesfernandez@ub.edu (A.I. Fernández).
[1] Tel.: +34 934021298; fax: +34 934035438.
[2] Tel.: +90 3882254492; fax: +90 3882250112.

http://dx.doi.org/10.1016/j.solener.2014.12.008
0038-092X/

system. The second requirement is that the coating material thickness has to achieve the efficiency of the MPCM. By this way, MPCM third specification is being resistant to thermal and mechanical stresses. Besides, there are different methodologies to microencapsulate PCM (Boh and Šumiga, 2008; Jyothi et al., 2010; Sánchez et al., 2008). Based on the mechanisms of microcapsules formation, methodologies are classified in chemical methods, physico-chemical methods, and physical and mechanical methods.

There are several possibilities or combinations of shell and core materials as a MPCM. Typical used shells are Poly(methyl methacrylate) (PMMA) (Alkan and Sarı, 2008; Wang et al., 2011) and melamine formaldehyde (MF) (Özonur et al., 2006), and the more usual PCM are paraffin (Sánchez-Silva et al., 2010) and particularly *n*-octadecane (Salunkhe and Shembekar, 2012; Zhang et al., 2012). Thus, there are a lot of recent studies with the preparation of MPCM made of PMMA and paraffin wax (Wang et al., 2012; Castellón et al., 2010; Ma et al., 2010), PMMA and *n*-octadecane (Giro-Paloma et al., 2013, 2014), MF and paraffin wax (Su et al., 2012; Šumiga et al., 2011), and finally MF and *n*-octadecane (Zhang and Wang, 2009). Although these two polymers are the most popular ones due their characteristics, polystyrene (PS) is also a popular container used as a shell in MPCM manufacturing. It can be mixed with different type of PCM, depending on the application and in the comfort temperature. Borreguero et al. (2011) produced by suspension polymerization technique microcapsules containing RT-27 and PS as a shell material. Although the MPCM was obtained, they concluded that for this kind of PCM is much better a shell of PE–EVA (polyethylene–ethyl vinyl acetate) because its thermal stability is better. Moreover, Sánchez et al. (2010) synthesized by suspension like polymerization MPCM for textiles made PS as a shell and paraffin wax as a core. Other authors used the same polymeric shell and changed the PCM obtaining MCPM to be used for Phase Change Slurries (PCS) and phase change emulsions, as Yang et al. (2003), where they prepared and characterized microcapsules containing *n*-tetradecane for improving the heat transfer ability and energy transport ability. Besides, Fang et al. (2008) studied nanoencapsulated PCM with PS *n*-octadecane, as a shell and as PCM, respectively. Their conclusion was that these capsules were successfully prepared by the ultrasonic assistant miniemulsion in-situ polymerization. Also, Sánchez-Silva et al. (2010) studied the MPCM of styrene mixed with another polymer in paraffin. The preparation of the microcapsules was done by suspension – like polymerization, and the main conclusion for the styrene–methyl methacrylate with paraffin was that it is impossible to microencapsulate the paraffin wax when the MMA/St is equal to 2.0. Also, styrene can be copolymerized with other substances creating the ABS (Acrylonitrile–Styrene–Butadiene), AB (Acrylonitrile–styrene copolymer), and the SBS (Styrene–butadiene–styrene). Examples of these are the ones of Yang et al. (2009) and Kenisarin and Kenisarina (2012), respectively. The first one prepared MPCM of ABS and AS with *n*-tetradecane in the core, remarking that their potential and flexibility as a shell material. The SBS MPCM study includes microparticles with paraffin wax as a core material and others with lauric acid.

In our literature survey, none reported preparation of paraffin and palmitic acid microcapsules with Poly(styrene-co-ethylacrylate) (PScEA) shells. In this paper is reported the microencapsulation and full characterization of paraffin and palmitic acid in PScEA shells by the emulsion co-polymerization method to obtain micro-nanocapsules for low temperatures solar thermal applications by Scanning Electron Microscopy (SEM), Particle Size Distribution (PSD), Fourier Transformed Infrared spectroscopy (FT-IR), Differential Scanning Calorimeter (DSC), Thermogravimetrical Analysis (TGA), Atomic Force Microscopy (AFM).

2. Materials and methods

2.1. Materials

Paraffin 42–44 and palmitic acid were used as core PCM. Styrene (>99%; Sigma Aldrich Company, USA) and ethyl acrylate, $C_5H_8O_2$ (>99%; Merck, Germany) were used as a shell material; ethylene glycol dimethacrylate (EGDMA), $C_{10}H_{14}O_4$ (Merck, Germany) was used as a crosslinking agent and it was distilled before use. The initiator of ammonium peroxodisulfate (Merck, Germany) and other analytical reagents tert-butylhydroperoxide (70%; Merck, Germany), Triton X-100 (Merck, Germany), iron (II) sulfate 7-hydrate ($FeSO_4{\cdot}7H_2O$) (Panreac, Spain), and sodium thiosulfate ($Na_2S_2O_3$) (Merck, Germany) were used without further purification.

2.2. Preparation of microcapsules

A typical emulsion polymerization process technique was used in the preparation of MPCM with PScEA shell. The emulsion co-polymerization method consists on mixing the polymer in an oiled system, adding an emulsifier. An emulsification is needed to create a water/oil emulsion and to generate a crosslinked system. Then, it will be needed the wash of the emulsion, to eliminate the oil, creating isolated microcapsules. Firstly, 120 ml of deionized water, 1.60 g of Triton X100, 28 g of core material were stirred for 30 min at 40 °C. Then, 14 g of styrene, 14 g of ethyl acrylate, 8 g of EGDMA, 1 ml of $FeSO_4{\cdot}7H_2O$ solution and 0.25 g of ammonium peroxodisulfate was stirred in a beaker, then added to emulsion, and stirring was continued at 1000 rpm. Then, 0.25 g of $Na_2O_3S_2$, 1 ml of tert-butylhydroperoxide was added to the emulsion and heated to 95 °C. The solution was stirred for 5 h and after this it was cooled down to room temperature and washed with water five times. Finally, the microcapsules were rinsed with deionized water, filtered and dried approximately 72 h at room conditions.

2.3. Characterization of microcapsules

2.3.1. Scanning Electron Microscopy (SEM)

The morphology of the samples was characterized using an environmental Scanning Electron Microscopy (Zeiss Evo 50, Zeiss, UK). The samples were fixed on the sample holder using a double-sided tape and then the particle size and the morphology of the samples were observed. The conditions were low vacuum and high voltage (15 kV), obtaining the image by secondary electrons.

2.3.2. Particle Size Distribution

The average particle size and size distribution of the micro-nanoPCMs were determined using a Nano Zetasizer (Malvern Instruments Ltd., UK). Measurements were carried out at 25 °C. To avoid multiple scattering effects, firstly, MPCM was mixed with water (1:100) and stirred 30 min in ultrasonic bath. The mean particles diameters were calculated from the average of three measurements.

2.3.3. Fourier-Transformed Infrared spectroscopy (FT-IR)

FT-IR spectroscopy is a potent technique to identify functional groups in organic polymers or compounds. The chemical characterization of the MPCM shells was performed by a Fourier Transformed Infrared (FT-IR) spectroscopy. It was used through FT-IR Spectrum Two™ from Perkin Elmer using a working range from 400 to 4000 cm^{-1}.

2.3.4. Differential Scanning Calorimeter (DSC)

The thermal properties melting/solidification temperature and melting/solidification enthalpy of the two types of microcapsules containing PCM were evaluated with a DSC (Perkin Elmer Diamond) with a heating–cooling rate of 5 °C min^{-1} in the range of 10–80 °C. During DSC analysis, about 5 mg of sample was used. This technique shows the melting temperature (T_m) and solidification temperature (T_s) of the sample and the enthalpy value for each process (melting and solidification, H_m and H_s respectively) which is equivalent to the area under the curve. The determination of the phase change material content in the MPCMs followed from the formula:

$$PCM(\%) = \Delta H_{microPCM} / \Delta H_{corePCM} \cdot 100 \tag{1}$$

2.4. Thermogravimetrical Analysis (TGA)

The thermal stability of the microcapsules was evaluated with a Simultaneous SDTQ600 TA Instruments under N_2 and air atmosphere. The scanning rate was 10 °C min^{-1} in the temperature range between 25 and 600 °C for 5.4420 mg of sample for both samples.

2.5. Atomic Force Microscopy (AFM)

Samples were suspended in ethanol, and 50 μl of suspension was poured on freshly cleaved mica and gently dried with a nitrogen stream. Then, sample was imaged in air. The experiments were performed in air using a Peak Force Quantitative NanoMechanics mode (QNM) with a system Multimode 8, Nanoscope V electronics. The AFM probe was a diamond MDNISP one, with a nominal spring constant: 388 nN nm^{-1}. The sensitivity was 68.2 nm V^{-1} with a set point between 400 and 550 nN. Moreover, the working conditions for the peak force amplitude were 150 nm, and the DMT Modulus limit 1 TPa. Both samples A and B were more soluble in ethanol than water. In order to break the aggregates, the samples were sonicated until the solution was homogeneous. Capsules A was tested at 25 °C and 50 °C, and Capsules B at 25 °C and 70 °C to evaluate the different behavior of the MPCM when the PCM is solid (around 25 °C) and liquid (up to 43 °C for A and up to 63 °C for B). It was measured the maximum force that is needed to apply at the top of a capsule to break it, as well as a Young's modulus map and Young's modulus histogram for some capsules at different temperatures.

Individual indentation tests were made in diverse particles of the upper flat-top part of the capsules in order to avoid tip slippage due to sample curvature. For all the force *vs.* Z graph representations, the blue line corresponds to tip sample approach process and the red one corresponds to the tip retraction from the sample. The first region corresponds to the no contact between the tip and the sample. Then, when the tip touches the surface of the sample, the cantilever applies an increasing force on the sample, deforming it elastically. Finally, the retraction of the AFM probe is represented by the red line. It is essential to notice that a three-sided dent in the upper site of the particle can be observed when it is plastically deformed by the AFM probe. Also, it has to be remarkable that usually the general profile of the particles seem to be triangular due to the pyramidal form of the AFM tip, and not due to the real profile of the particle. To calculate the force F, the following equation is used:

$$F = k \cdot \Delta_z \tag{2}$$

where k is the AFM probe, and Δ_z is cantilever deflection in the z axis. Besides, the cantilever deflection is expressed in Eq. (3) as:

$$\Delta_z = \Delta V / S \tag{3}$$

where ΔV is the increment in photodetector vertical signal as the tip contacts the sample. The S value is the sensitivity, which is the slope of the contact region of a force curve performed on a rigid sample. It is also needed to take into account the sample penetration (δ) because of the applied force value:

$$\delta = z - \Delta_z \tag{4}$$

where z represents the piezo-scanner displacement in the axis perpendicular to the sample plane. The F vs. z graphs achieved at a certain force value, and it was evaluated by the Hertz model in the elastic region with Eq. (5):

$$F = (3/4 \cdot E_{eff} \cdot R^{1/2}) \cdot \delta^{3/2} \quad (5)$$

Besides, the Young Modulus is considered following Eq. (6):

$$1/E_{eff} = [(1 - v^2)/E] + [(1 = v_i^2)/E_i] \quad (6)$$

and Young Modulus (E_{eff}) value can be obtained using Eq. (6), taking into consideration that v is the Poisson ratio with 0.33 as a value. Furthermore, the subindex i corresponds to the mechanical properties of the AFM probe, SiO_2. The values for the E_i and v_i are 76 GPa (Namazu and Isono, 2003) and 0.17 respectively (Oliver and Pharr, 1992).

3. Results and discussion

3.1. Scanning Electron Microscopy (SEM)

Fig. 1 shows SEM micrographs of the PScEA shell microcapsules obtained using emulsion co-polymerization technique. As it can be seen, microparticles almost have a spherical structure and the microcapsule stability after the coating process was confirmed.

3.2. Particle Size and Distribution Analysis (PSD)

Particle sizes distributions of sample A and sample B are shown in Fig. 2. Mean particle diameters for sample A and sample B were 165 and 265 nm, respectively. Smaller and uniform microcapsules were obtained with PScEA + paraffin.

3.3. Fourier-Transformed Infrared Spectroscopy

The FT-IR spectra of core material, shell material and MPCM are shown in Figs. 3 and 4. Each of the characteristic peaks belonging to the core material preserves itself after microencapsulation. These results in Transmittance (%) vs. Wavenumber (cm^{-1}) confirm that the encapsulation of paraffin and palmitic acid could be prepared within PScEA.

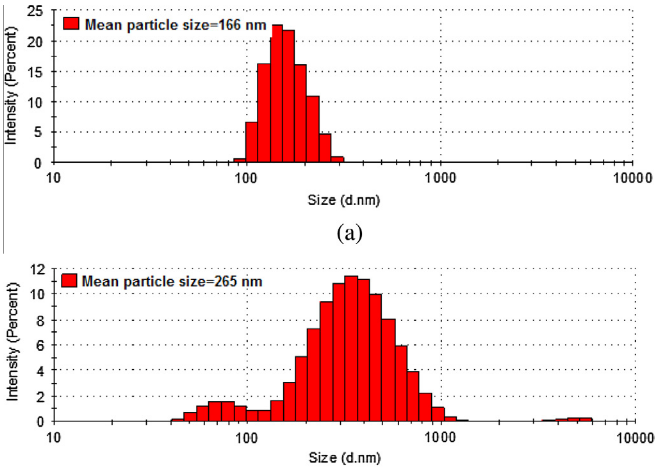

(a)

(b)

Fig. 2. PSD analysis of (a) capsule A: PScEA + paraffin and (b) capsule B: PScEA + palmitic acid.

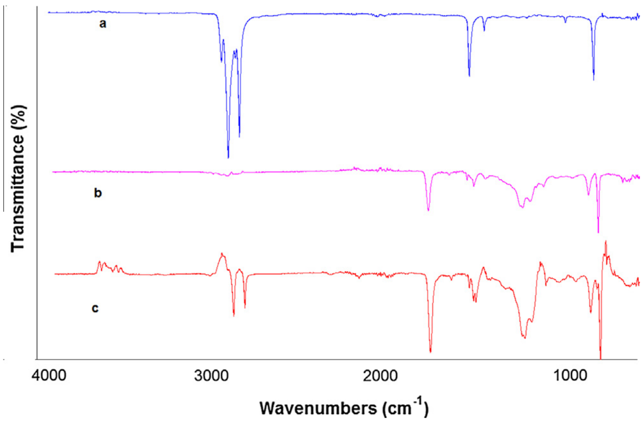

Fig. 3. FT-IR spectra of (a) paraffin, (b) PScEA, and (c) capsule A.

In general, FT-IR spectroscopy is used to describe the microcapsules shell structure. In this work, FT-IR shell spectra of the two samples under study were given in Fig. 5 to verify the presence of PScEA in both MPCM.

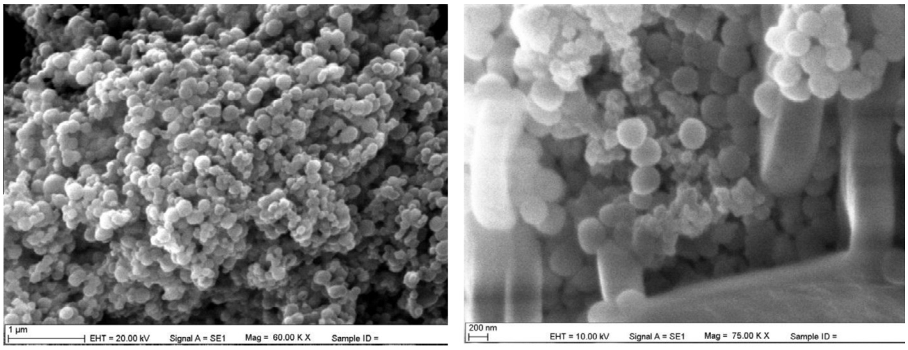

(a)

(b)

Fig. 1. SEM micrographies by secondary electrons of (a) sample A: PScEA + paraffin and (b) sample B: PScEA + palmitic acid.

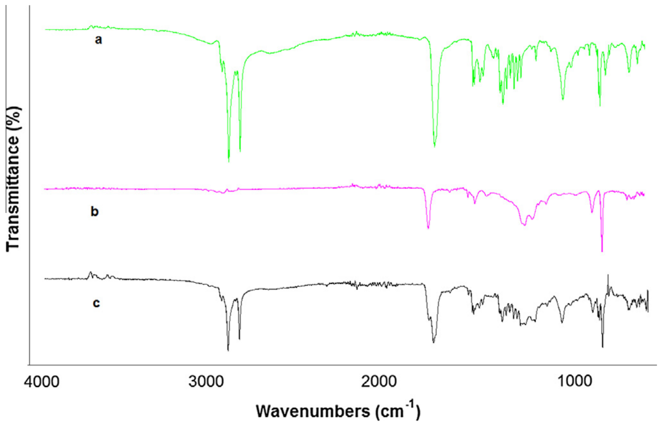

Fig. 4. FT-IR spectra of (a) palmitic acid, (b) PScEA, and (c) capsule B.

3.4. Differential Scanning Calorimeter (DSC)

Fig. 6 provides the curves of the DSC samples containing 32.1 wt.% paraffin and 47.8 wt.% palmitic acid at 5 °C min^{-1} scanning rate. Moreover, in Table 1 is shown the DSC numerical results for capsule A PScEA with Paraffin 42–44 in the core, and capsule B PScEA with palmitic acid as the PCM. It is indicated the onset melting temperature (T_{om}) of the DSC curve, the melting peak temperature (T_{pm}), the endset melting temperature (T_{em}), the melting enthalpy (H_m), onset the crystallizing temperature (T_{oc}), the crystallizing peak temperature (T_{pc}), the endset crystallizing temperature (T_{ec}), and finally the crystallization enthalpy (H_c). Fig. 6a and Table 1 indicate that the peak temperatures of melting and freezing were determined to be 44.23 °C and 36.84 °C for non-encapsulated A and 42.39 °C and 37.41 °C for capsule A. Furthermore, Fig. 6b and Table 1 indicate that the peak temperatures of melting and freezing were determined to be 64.57 °C and 57.00 °C for non-encapsulated B and 62.66 °C and 56.22 °C for capsule B. It is clear that, there is no significant temperature change observed after microencapsulation process. It was determined that, the microcapsules obtained in this study, capsule A and capsule B, are very suitable for Thermal Energy Storage applications. Moreover, the enthalpy values are 49 J g^{-1} for capsule A and 97 J g^{-1} for capsule B, which are very good values according to the reported data for the studied temperature ranges, thus being a good alternative for solar thermal applications.

3.5. Thermogravimetrical Analysis (TGA)

Thermal stabilities of the MPCM samples were evaluated by the TGA analysis. The two type of capsules showed two-step decomposition profiles (Fig. 7). The first-step weight loss of the microcapsules is due to the degradation of the core materials (paraffin wax and palmitic acid) and the second-step decomposition results from the degradation of the PScEA copolymer shell. Over 470 °C the microcapsules decomposed completely. For capsule A the first weight loss corresponds to the decomposition of the PCM paraffin wax around 200 °C and the associated loss is around a 40% of the sample. The second mass loss involves approximately the 60% of the sample mass with an onset temperature around 275 °C, being completely decomposed at 430 °C. Moreover, it can be observed the thermal degradation for the capsule B, where the first weight loss is due to the palmitic acid decomposition, representing almost the 50% by weight, and the second one fits with the shell, being completely decomposed at 450 °C. From these results, capsule B with higher melting point is more stable than capsule A.

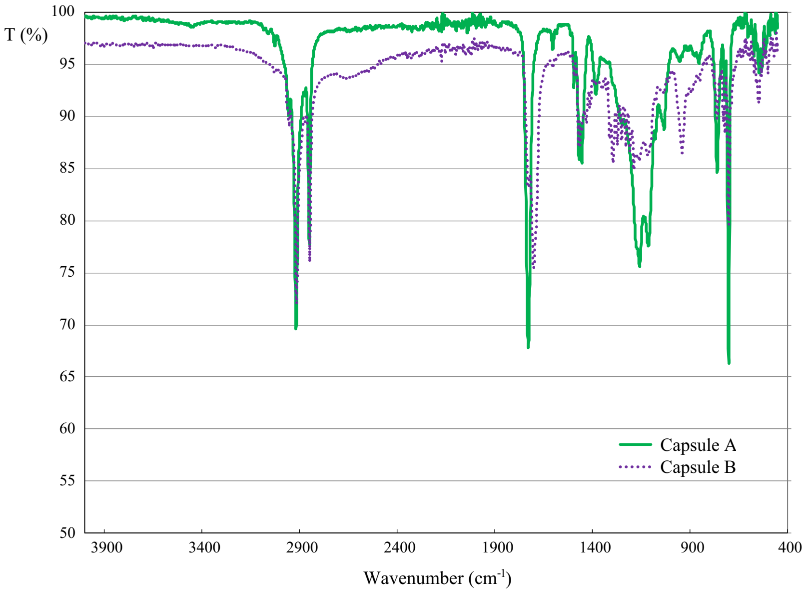

Fig. 5. FT-IR spectra of shell capsule A and capsule B.

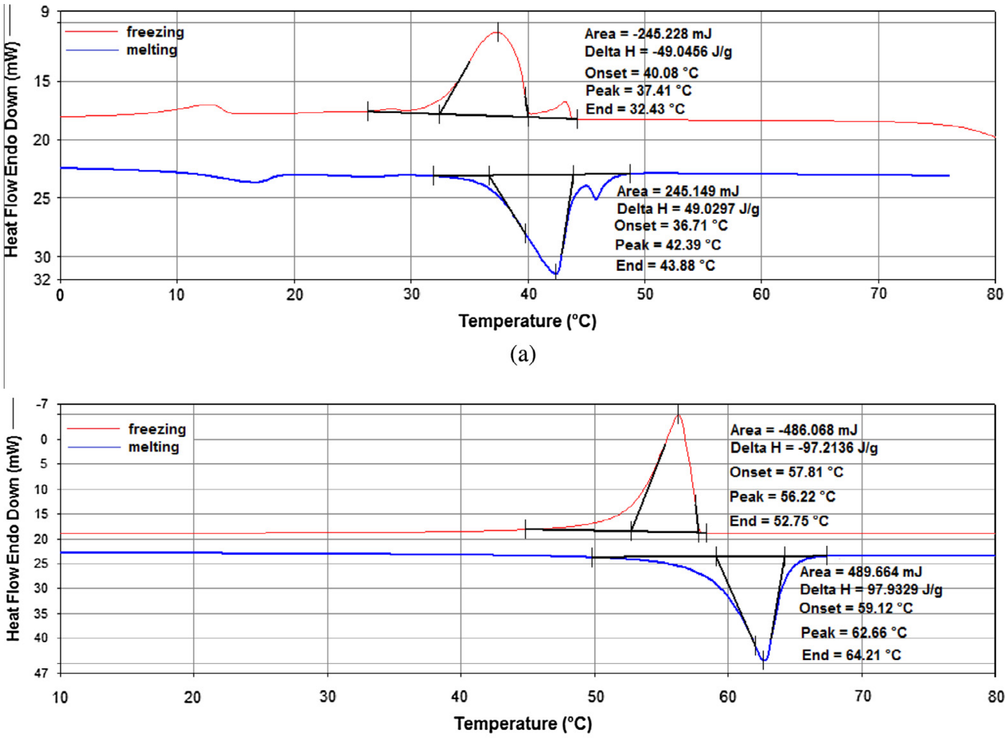

(a)

(b)

Fig. 6. DSC curves applying dynamic mode of (a) capsule A and (b) capsule B.

Table 1
DSC results for non-encapsulated A, capsule A, non-encapsulated B, and capsule B.

Sample	T_{om} (°C)	T_{pm} (°C)	T_{em} (°C)	H_m (J g^{-1})	T_{oc} (°C)	T_{pc} (°C)	T_{ec} (°C)	H_c (J g^{-1})	PCM content (%)
Non-encapsulated A	37.80	44.23	46.26	152.63	41.15	36.84	31.45	−157.25	100
Capsule A	36.71	42.39	43.88	49.03	40.08	37.41	32.43	−49.05	32.12
Non-encapsulated B	60.86	64.57	67.15	204.89	59.22	57.00	53.75	−215.94	100
Capsule B	59.12	62.66	64.21	97.93	57.81	56.22	52.75	−97.21	47.79

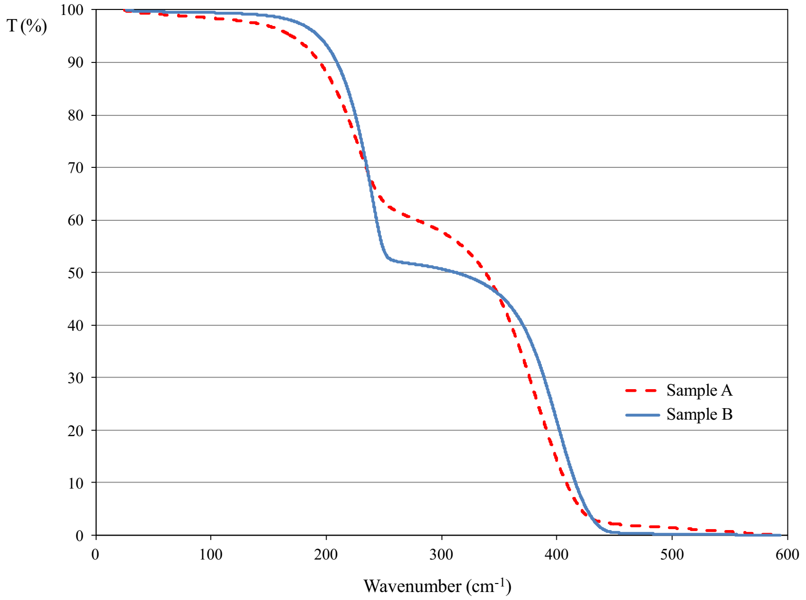

Fig. 7. Thermogravimetrical Analysis of MPCM sample A and sample B.

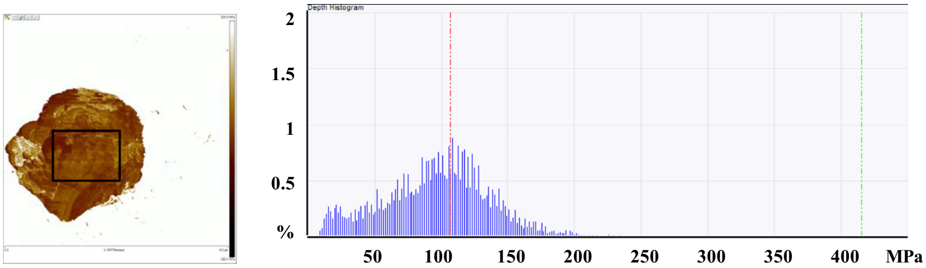

Fig. 8. Young’s modulus map and Young’s modulus histogram for capsule A at 25 °C.

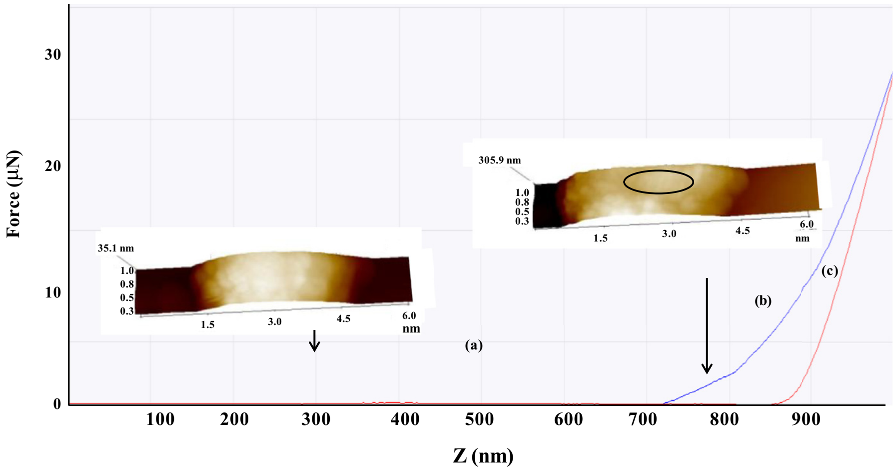

Fig. 9. Mechanical testing of the elastic–plastic region by AFM for sample A at 25 °C: (a) no contact, (b) deformation of the sample, and (c) the retraction of the AFM probe.

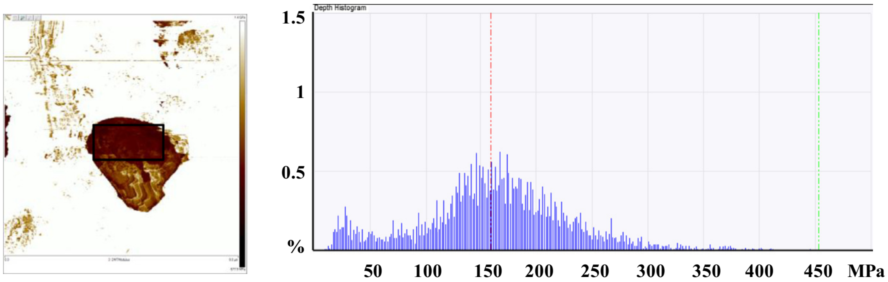

Fig. 10. Young’s modulus map and Young’s modulus histogram for capsule A at 50 °C.

3.6. Atomic Force Microscopy (AFM)

Considering one isolated capsule, and selecting a specific delimited area, it can be studied a Young’s modulus map and the histogram of the sample A at 25 °C, as Fig. 8 shows. The mean Young’s modulus value for this specific region is 106 MPa.

In Fig. 9 is shown the vertical force (µN) *vs*. sample penetration (nm) curve obtained by processing the measurement of the cantilever deflection at 25 °C. In view of all the equations and considerations explained previously, the average breakthrough force after three repetitions for sample A at 25 °C is 3.9 µN. It can be noticed in (b) point that there is a slight change in the slope curve, due to the breakage of the microcapsule shell.

It is needed to increase the temperature up to 50 °C to observe the mechanical differences. Around this value is reached the phase change temperature, so the PCM will be in liquid state.

It is seen in Fig. 10 that the average Young’s modulus histogram for the specific area delimited in the left image is 160 MPa. For this reason, it can be concluded that for sample A the Young’s modulus value looks independent from temperature, because the values obtained at room temperature and at 50 °C are extremely small.

Besides, in Fig. 11 is shown that the sample A at 50 °C has a maximum force before breaking at 5.4 µN, which is almost the same than at room temperature.

For sample A it can be concluded that the differences in temperature are not very significant, because the results at

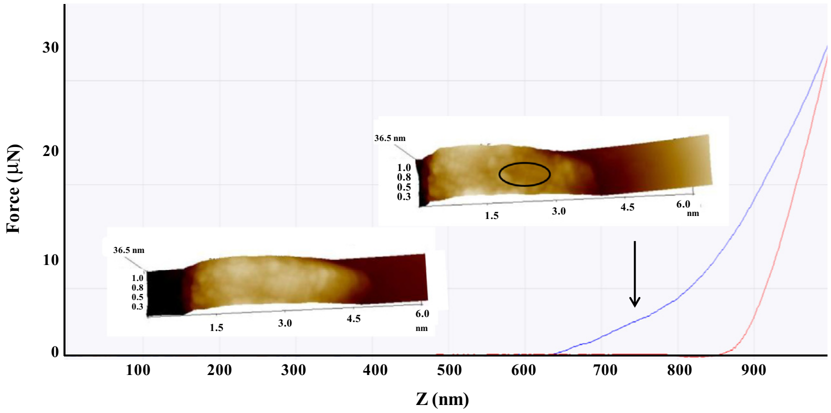

Fig. 11. Loading–unloading curve for sample A at 50 °C.

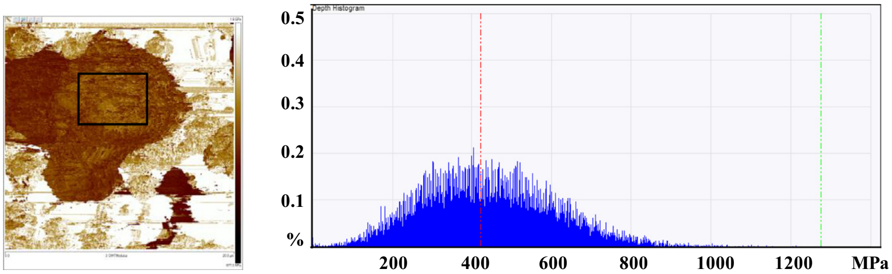

Fig. 12. Young’s modulus map and Young’s modulus histogram for capsule B at 25 °C.

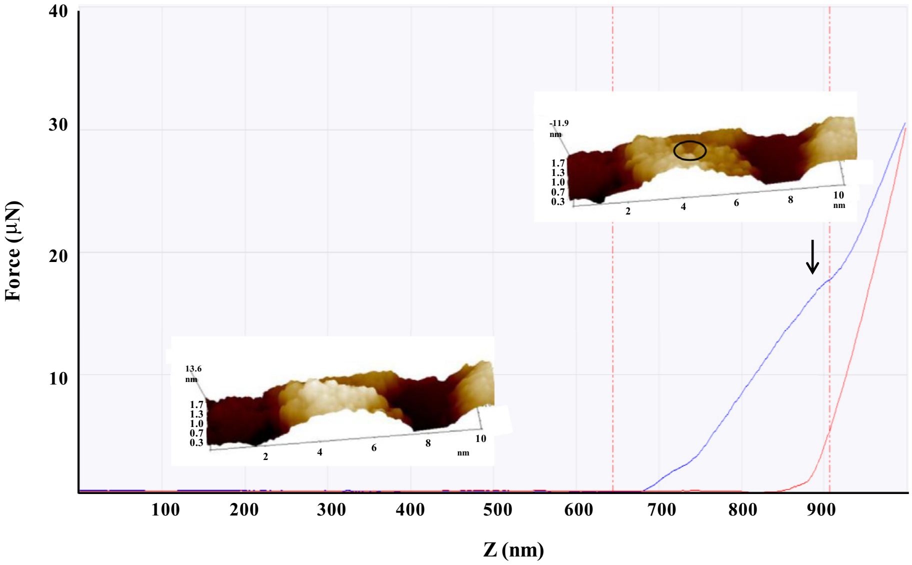

Fig. 13. Loading–unloading curve for capsule B at 25 °C. Average of three indentations.

both temperatures (25 °C and 50 °C) are quite similar for the Young’s modulus value and also for the maximum force that can be applied on the top of the microcapsules before breaking them. For this reason, it can be concluded that this sample A is suitable for using it at both temperatures without suffering any mechanical deformation. Otherwise, when sample B is studied, we can observe some more evidence differences.

Then, in Fig. 12 is evaluated the Young’s modulus in the specific area delimited with the black frame at 25 °C for sample B. The result gives a mean value of 422 MPa.

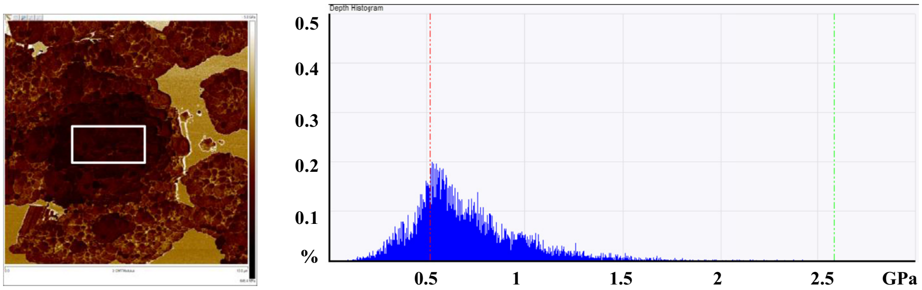

Fig. 14. Young's modulus map and Young's modulus histogram at 70 °C.

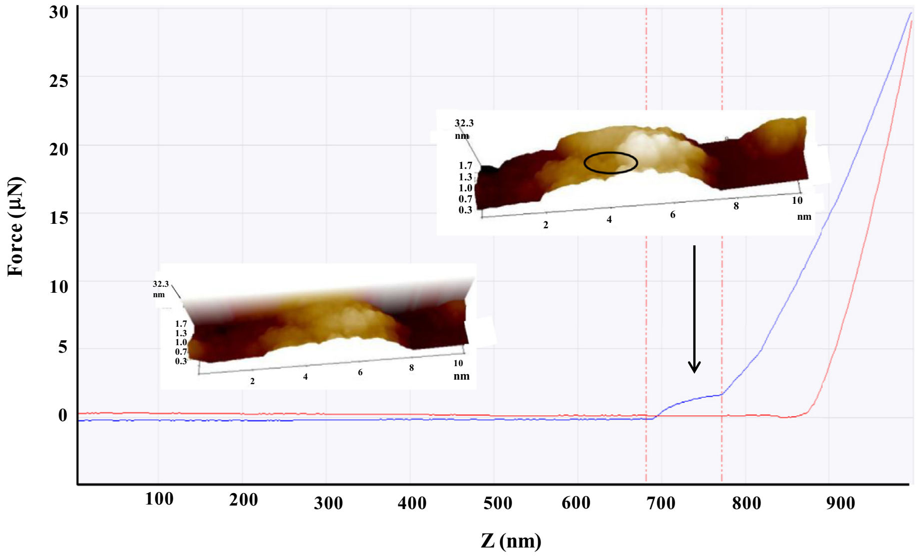

Fig. 15. Loading–unloading curve for capsule B at 70 °C. Average of three indentations.

The typical graph of loading–unloading is shown in Fig. 13 and denotes that for capsule B at room temperature there is a breakthrough force of 17.3 µN.

For capsule B case, it was decided to increase the temperature until 70 °C due to the phase change temperature of the PCM.

These microcapsules gives a result of 517 MPa at 70 °C when it is evaluated its Young's modulus, as Fig. 14 shows. Young's modulus values for room temperature and 70 °C are low, for this reason, the difference between them is not representative; hence, it can be assumed that *E* values do not change in front of the temperature.

Besides, in Fig. 15 it is shown the result for the maximum allowed force on the top of the capsule B at 70 °C. This value is around the 1.8 µN, ten times lower compared with 25 °C due to the experimental temperature. This result is really important because this sample can be damaged in an easiest way than the capsule A at higher temperatures.

4. Conclusions

In this research, paraffin and palmitic acid were microencapsulated with a Poly(styrene-co-ethylacrylate) PScEA shell via an emulsion co-polymerization technique. SEM results confirm that paraffin (capsule A) and palmitic acid (capsule B) encapsulated successfully in this study, and the diameters for capsule A and capsule B were analyzed by PSD being 166 nm and 265 nm, respectively. Besides, the encapsulated paraffin and palmitic acid can be considered to have good potential for energy storage. Also, TGA results denoted a slightly higher thermal stability for sample B in the same working conditions. The FT-IR results proved that paraffin and palmitic acid encapsulated successfully with a PScEA shell in this study. AFM results confirm that there are no differences in capsule A for Young's modulus and force applied to break the microcapsule at different temperatures (25 °C and 50 °C) because the results are similar. Capsule B does not have the same mechanical behavior at 25 °C and 70 °C, the force is ten times lower at 70 °C comparing the results with those at 25 °C although the Young's modulus has a similar value.

Acknowledgments

The work is partially funded by the Spanish government (ENE2011-28269-C03-02). The authors would like to thank the Catalan Government for the quality accreditation given to their research group DIOPMA (2014 SGR

1543). The research leading to these results has received funding from the European Union's Seventh Framework Programme (FP7/2007-2013) under grant agreement n° PIRSES-GA-2013-610692 (INNOSTORAGE). Also, preparation of microcapsules funded by The Scientific & Technical Research Council of Turkey (TUBITAK) (The Project Code: TUBITAK 111M614).

References

Alkan, C., Sarı, A., 2008. Fatty acid/poly(methyl methacrylate) (PMMA) blends as form-stable phase change materials for latent heat thermal energy storage. Sol. Energy 82, 118–124.

Alkan, C., Sarı, A., Karaipekli, A., Uzun, O., 2009. Preparation, characterization, and thermal properties of microencapsulated phase change material for thermal energy storage. Sol. Energy Mater. Sol. Cells 93, 143–147.

Boh, B., Šumiga, B., 2008. Microencapsulation technology and its applications in building construction materials. RMZ – Mater. Geoenviron. 55 (3), 329–344.

Borreguero, A.M., Valverde, J.L., Rodríguez, J.F., Barber, A.H., Cubillo, J.J., Carmona, M., 2011. Synthesis and characterization of microcapsules containing Rubitherm® RT27 obtained by spray drying. Chem. Eng. J. 166, 384–390.

Castellón, C., Medrano, M., Roca, J., Cabeza, L.F., Navarro, M.E., Fernández, A.I., Lázaro, A., Zalba, B., 2010. Effect of microencapsulated phase change material in sandwich panels. Renew. Energy 35, 2370–2374.

Fang, Y., Kuang, S., Gao, X., Zhang, Z., 2008. Preparation and characterization of novel nanoencapsulated phase change materials. Energy Convers. Manage. 49, 3704–3707.

Gil, A., Medrano, M., Martorell, I., Lázaro, A., Dolado, P., Zalba, B., Cabeza, L.F., 2010. State of the art on high temperature thermal energy storage for power generation. Part 1 – concepts, materials and modellization. Renew. Sust. Energy Rev. 14, 31–55.

Giro-Paloma, J., Oncins, G., Barreneche, C., Martínez, M., Fernández, A.I., Cabeza, L.F., 2013. Physico-chemical and mechanical properties of microencapsulated phase change material. Appl. Energy 109, 441–448.

Giro-Paloma, J., Barreneche, C., Delgado, M., Martínez, M., Fernández, A.I., Cabeza, L.F., 2014. Physicochemical and thermal study of a MPCM of PMMA shell and paraffin wax as a core. Energy Proc. 48, 347–354.

Jamekhorshid, A., Sadrameli, S.M., Farid, M., 2014. A review of microencapsulation methods of phase change materials (PCMs) as a thermal energy storage (TES) medium. Renew. Sust. Energy Rev. 31, 531–542.

Jyothi, N., Prasanna, M., Prabha, S., Ramaiah, P.S., Srawan, G., Sakarkar, S., 2010. Microencapsulation techniques, factors influencing encapsulation efficiency. J. Microencapsulation, 3187–3197.

Kenisarin, M.M., Kenisarina, K.M., 2012. Form-stable phase change materials for thermal energy storage. Renew. Sust. Energy Rev. 16, 1999–2040.

Konuklu, Y., Unal, M., Paksoy, H.Ö., 2014. Microencapsulation of caprylic acid with different wall materials as phase change material for thermal energy storage. Sol. Energy Mater. Sol. Cells 120B, 536–542.

Ma, S., Song, G., Li, W., Fan, P., Tang, G., 2010. UV irradiation-initiated MMA polymerization to prepare microcapsules containing phase change paraffin. Sol. Energy Mater. Sol. Cells 94, 1643–1647.

Namazu, T., Isono, Y., 2003. Quasi-static bending test of nano-scale SiO_2 wire at intermediate temperatures using AFM-based technique. Sens. Actuators A-Phys. 194, 78–85.

Oliver, W.C., Pharr, G.M., 1992. An improved technique for determining hardness and elastic modulus using load and displacement sensing indentation experiments. J. Mater. Res. 7 (6), 1564–1583.

Özonur, Y., Mazman, M., Paksoy, H.Ö., Evliya, H., 2006. Microencapsulation of coco fatty acid mixture for thermal energy storage with phase change material. Int. J. Energy Res. 30 (10), 741–749.

Salunkhe, P.B., Shembekar, P.S., 2012. A review on effect of phase change material encapsulation on the thermal performance of a system. Renew. Sust. Energy Rev. 16, 5603–5616.

Sánchez, L., Sánchez, P., Carmona, M., de Lucas, A., Rodríguez, J.F., 2008. Influence of operation conditions on the microencapsulation of PCMs by means of suspension-like polymerization. Colloids Polym. Sci. 286, 1019–1027.

Sánchez, P., Sánchez-Fernández, M.V., Romero, A., Rodríguez, J.F., Sánchez-Silva, L., 2010. Development of thermo-regulating textiles using paraffin wax microcapsules. Thermochim. Acta 498, 16–21.

Sánchez-Silva, L., Rodríguez, J.F., Romero, A., Borreguero, A.M., Carmona, M., Sánchez, P., 2010. Microencapsulation of PCMs with a styrene-methyl methacrylate copolymer shell by suspension-like polymerization. Chem. Eng. J. 157, 216–222.

Su, J.F., Wang, X.Y., Dong, H., 2012. Influence of temperature on the deformation behaviours of melamine-formaldehyde microcapsules containing phase change material. Mater. Lett. 84, 158–161.

Šumiga, B., Knez, E., Vrtacnik, M., Ferk-Savec, V., Staresinic, M., Boh, B., 2011. Production of melamine-formaldehyde PCM microcapsules with ammonia scavenger used for residual formaldehyde reduction. Acta Chim. Slov. 58, 14–25.

Tyagi, V.V., Kaushik, S.C., Tyagi, S.K., Akiyama, T., 2011. Development of phase change materials based microencapsulated technology for buildings: a review. Renew. Sust. Energy Rev. 15 (2), 1373–1391.

Wang, Y., Dong Xia, T., Xia Feng, H., Zhang, H., 2011. Stearic acid/polymethylmethacrylate composite as form-stable phase change materials for latent heat thermal energy storage. Renew. Energy 36, 1814–1820.

Wang, Y., Shi, H., Xia, T.D., Zhang, T., Feng, H.X., 2012. Fabrication and performances of microencapsulated paraffin composites with polymethylmethacrylate shell based on ultraviolet irradiation-initiated. Mater. Chem. Phys. 135, 181–187.

Yang, R., Xu, H., Zhang, Y., 2003. Preparation, physical property and thermal physical property of phase change microcapsule slurry and phase change emulsion. Sol. Energy Mater. Sol. Cells 80, 405–416.

Yang, R., Zhang, Y., Wang, X., Zhang, Y., Zhang, Q., 2009. Preparation of n-tetradecane-containing microcapsules with different shell materials by phase separation method. Sol. Energy Mater. Sol. Cells 93, 1817–1822.

Zhang, H., Wang, X., 2009. Fabrication and performances of microencapsulated phase change materials based on n-octadecane core and resorcinol-modified melamine-formaldehyde shell. Colloids Surf. A 332, 129–138.

Zhang, X.X., Tao, X.M., Yick, K.L., Wang, X.C., 2004. Structure and thermal stability of microencapsulated phase-change materials. Colloids Polym. Sci. 282 (4), 330–336.

Zhang, G.H., Bon, S.A.F., Zhao, C.Y., 2012. Synthesis, characterization and thermal properties of novel nanoencapsulated phase change materials for thermal energy storage. Sol. Energy 86, 1149–1154.

Zhao, C.Y., Zhang, G.H., 2011. Review on microencapsulated phase change materials (MEPCMs): fabrication, characterization and applications. Renew. Sust. Energy Rev. 15 (8), 3813–3832.

4.3 Comparison of MPCM with same core material and different shell

As it is compared the mechanical behavior of MPCM when the core material is different, the second study related to the laboratory made samples presented in this PhD Thesis compares two MPCM with the same core material but different polymeric shell. These results were performed in collaboration with Dr. Alkan and Dr. Sarı (Gaziosmanpasa Universitesi, Turkey), specialists in encapsulating PCM field [17–21], among others. Two different samples at laboratory scale were prepared to evaluate their stiffness and decide the best shell due to their mechanical properties. The procedure to manufacture the MPCM was in situ polymerization technology. The MPCM comparison was between Methyl methacrylate (MMA) and polystyrene (PS) shells and tetracosane as core PCM in both samples, with a encapsulation mass ratio of 1:3 (shell:core). The goal of the experiments was testing the mechanical properties (Young's modulus (*E*) and deformation) of two laboratory made MPCM with nominal diameters around 1 - 2 μm.

It was performed a mechanical test by AFM technique by using a Peak Force Quantitative NanoMechanics mode (QNM) instrument. The system used was a Multimode 8, Nanoscope V electronics. Besides, it was used a diamond AFM probe MDNISP, with a nominal spring constant of 388 $nN\cdot nm^{-1}$. The sensitivity was 68.2 $nm\cdot V^{-1}$, and the set point between 400 and 550 nN. The peak force amplitude was 150 nm. Sample preparation consists on dissolving them in ethanol, and 50 μl of solution were poured on freshly cleaved mica and gently dried with a nitrogen stream. The vertical force required to plastically deform the microcapsules was tested per triplicate for the MMA:tetracosane (1:3) and PS:tetracosane (1:3) samples. Furthermore, topographic images before and after each indentation were taken. These images before and after performing the tests were acquired for each sample at 23 ºC and 60 ºC to compare the properties of both behaviors when the PCM is in solid state (below its phase change) and liquid state (above to its phase change).

It was evaluated the Young's modulus (*E*) at 23 ºC and 60 ºC for three different samples at each temperature. It was tested on the top of the microcapsules. In Figure 4.3 the histogram results for the sample composed by MMA and tetracosane for both temperatures are shown, where it is a graphical representation of data distribution, as a probability distribution estimation of a quantitative variable. It is noticeable the difference obtained when increasing the temperature. At 23 ºC the Young's modulus value of the MMA microcapsules is 2.7 GPa, while at 60 ºC this value dramatically decreases to 0.1 GPa.

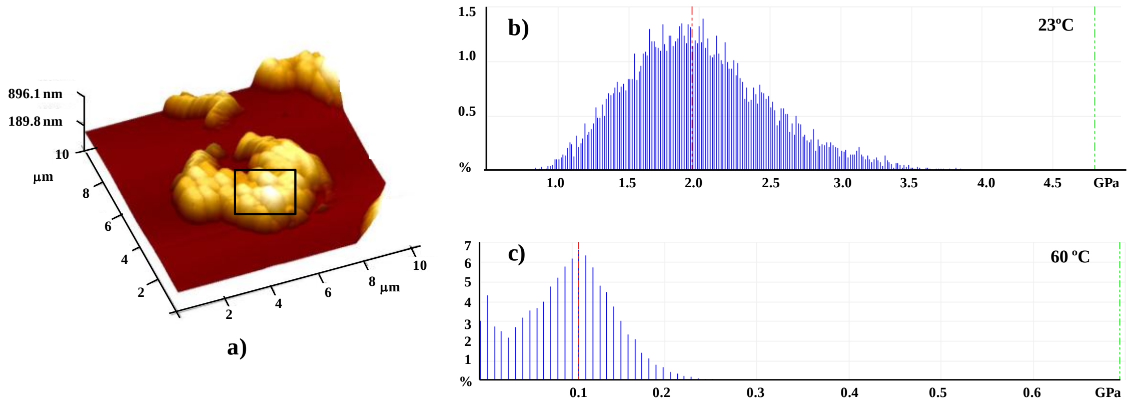

Figure 4.3. Results for MMA:tetracosane (1:3), a) 3D image tested, b) Young's modulus results at 23 ºC, c) Young's modulus results at 60 ºC.

The histogram results for PS and tetracosane (1:3) are in Figure 4.4. In this case, *E* at 23 ºC is 1.5 GPa, and *E* at 60 ºC is 1.1 GPa. It means a 27 % of Young's Modulus reduction between both temperatures. Evaluating these results, only taking into account the Young's modulus values, it will be better to use polystyrene (PS) as shell in a MPCM system due to the *E* value do not decrease abruptly when the temperature raises.

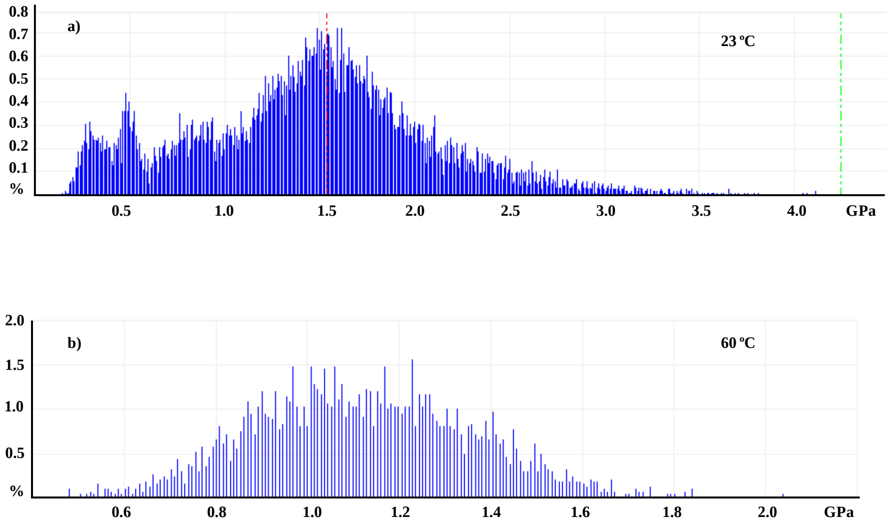

Figure 4.4. Results for PS:tetracosane (1:3), a)Young's modulus results at 23 ºC, b) Young's modulus results at 60 ºC.

Besides, it is performed tests to evaluate the maximum force that can be applied on the top of the microcapsule to break it. In the case of the MPCM formed by MMA as shell and tetracosane as a PCM, this force at 23 ºC is 31.2 µN, as in Figure 4.5 is shown. In the typical loading curve, the applied force is proportional to the deflection error, and Z (nm) is the penetration of the tip inside the sample. In these kinds of graphs, it is marked four subsections:

(a) No contact between sample and tip. In the graphs, an image of the sample is added in this point a) and an arrow, before applying forces. It is the first part of the blue continuous line.

(b) Plastic deformation or plastic penetration of the sample. There is a change in the slope, where it can be defined as the maximum force that can be applied on the sample. It is marked between two vertical discontinuous lines, and an arrow.

(c) Deformation of the sample.

(d) Retraction of the AFM probe until no contact between the tip and the sample. It is marked as a red discontinuous line. Most of the times, the end of line d) and the beginning of line a) are overlapped.

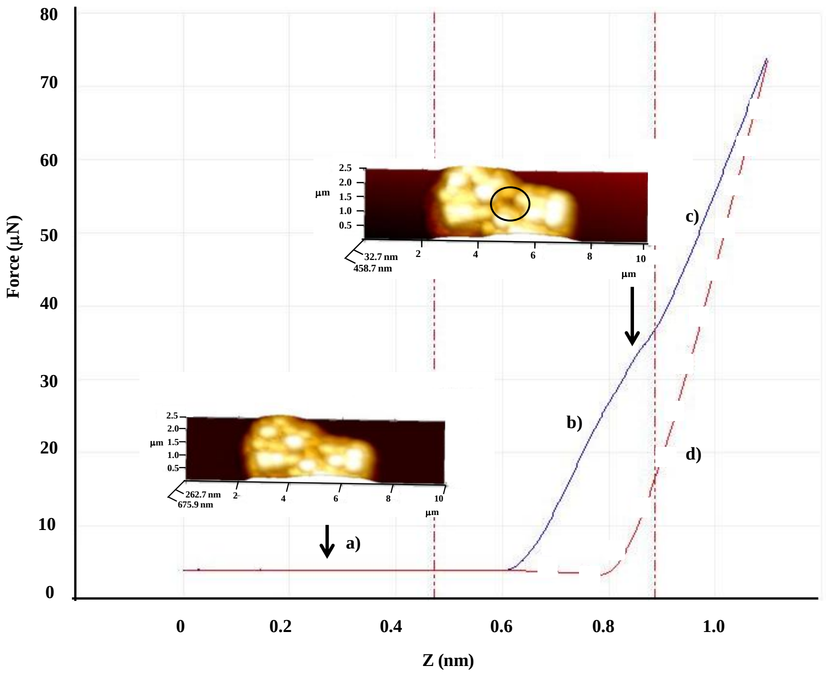

Figure 4.5. Mechanical testing of the elastic-plastic region by AFM of the MPCM composed by MMA:tetracosane (1:3) microcapsule at 23 ºC.

The same test is performed at 60 ºC, and the result is 11.4 µN, a 63.5 % less than at room temperature. This graph is shown in Figure 4.6.

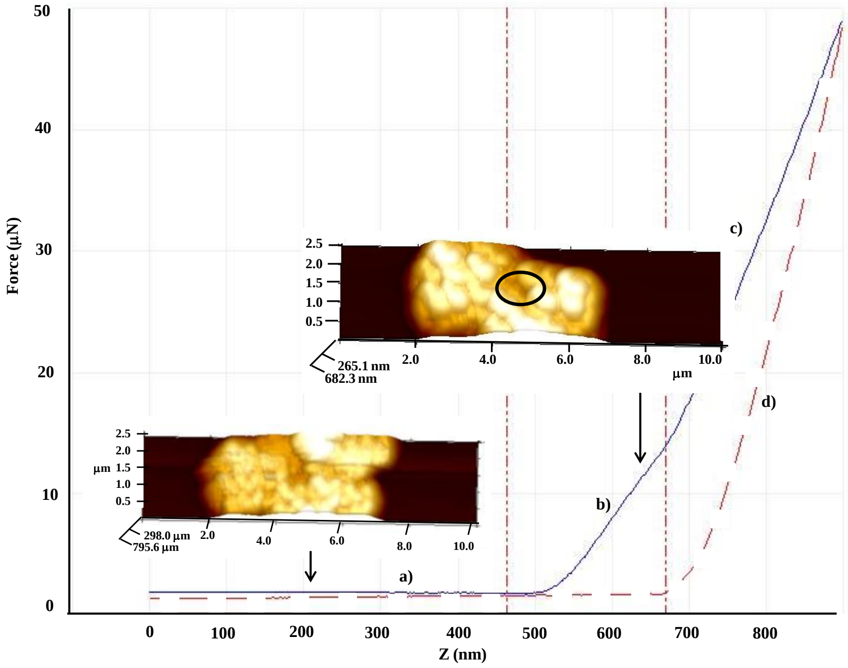

Figure 4.6. Mechanical testing of the elastic-plastic region by AFM of the MPCM composed by MMA:tetracosane (1:3) microcapsule at 60 ºC, (a) no contact, blue continuous line; (b) plastic penetration; (c) deformation of the sample; and (d) retraction of the AFM probe, red discontinuous line.

The same kind of tests was done for the sample composed by PS and tetracosane at 23ºC and 60 ºC. The results can be observed in Figure 4.7 and Figure 4.8. At 23 ºC the maximum force applied on the top of the microcapsule before breaking it was 13.2 µN.

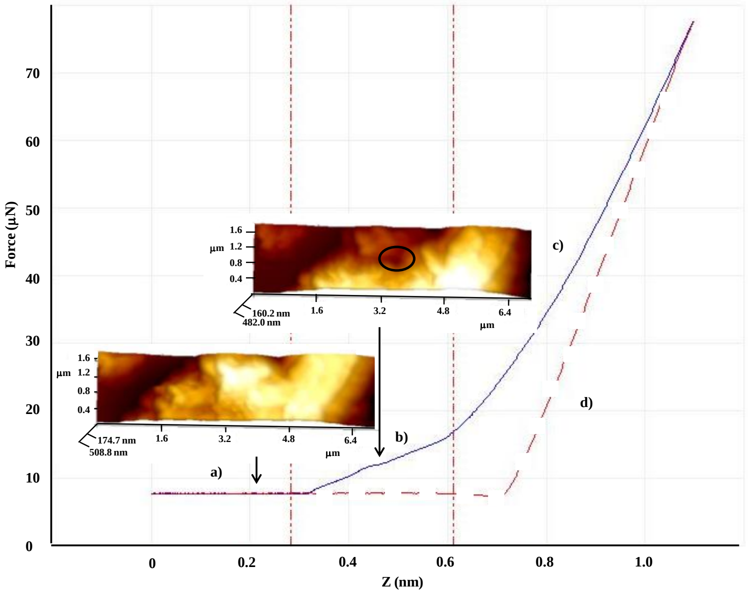

Figure 4.7. Mechanical testing of the elastic-plastic region by AFM of the MPCM composed by PS:tetracosane (1:3) microcapsule at 23 ºC, (a) no contact, continuous line; (b) plastic penetration; (c) deformation of the sample; and (d) retraction of the AFM probe, discontinuous line.

Meanwhile, at 60 ºC, this force was 5.3 µN as can be observed in Figure 4.8. In the light of the results, the force value diminished 60 % from room temperature to 60 ºC.

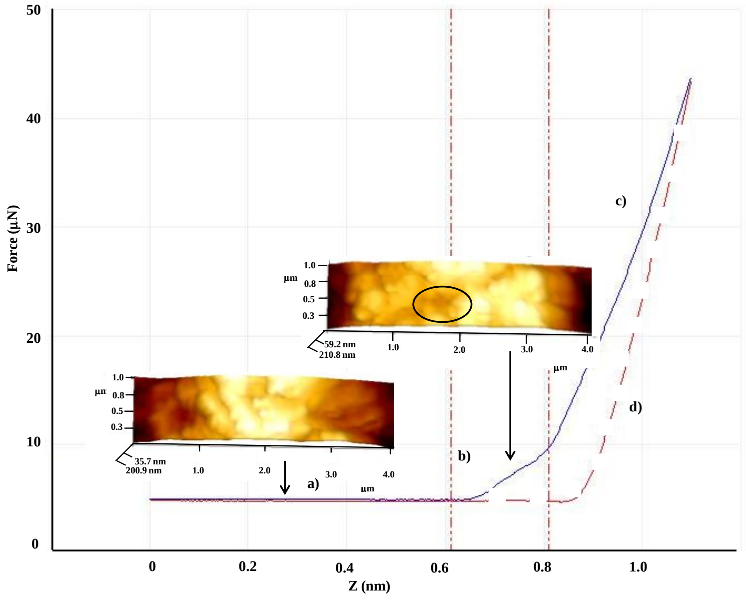

Figure 4.8. Mechanical testing of the elastic-plastic region by AFM of the MPCM composed by PS:tetracosane (1:3) microcapsule at 60 ºC, (a) no contact, continuous line; (b) plastic

penetration; (c) deformation of the sample; and (d) retraction of the AFM probe, discontinuous line.

As a conclusion of this first part of the study, polystyrene will be better as MPCM shell because the Young’s modulus value decreases 27 % (in front of the 96 % of MMA) when increasing the temperature from 23 ºC to 60 ºC. Besides, the needed force to break the MPCM decreases 60 % for the PS from 23 ºC to 60 ºC, while for MMA is 64 %, it means, that in this other case, PS seems to be better shell for MPCM with encapsulation ratio 1:3.

Beyond the studies comparing different cores and same shell, and different shell and same core, it was also evaluated the mechanical response of two samples depending on the encapsulation ratio. In this case, it was compared mechanically two samples of polystyrene (PS) as a shell and tetracosane as a core PCM, but one sample with an encapsulation mass ratio of 1:3 (results showed above) and the new one 1:1. It was chosen PS as shell because of the main conclusions of the first part of the study. It was performed the same methodology and the same equipments as it was explained in the previously measurements. The objective of this study was to perform the mechanical properties of two laboratory made MPCM with nominal diameters around 1 - 2 μm with different encapsulation mass ratios. In this case, it was also studied the Young's modulus (*E*) and the deformation of the MPCM.

Histogram *E* results for PS and tetracosane for mass ratio 1:1 are showed in Figure 4.9. At 23 ºC it was obtained a value of 0.9 GPa (Figure 4.9a), and at 60 ºC the value decrease until 0.1 GPa (Figure 4.9b). A reduction of *E* value around 87 % is reached increasing the temperature to 60 ºC. Comparing this value reduction with the 1:3 MPCM mass ratio, it is much better to use 1:3 because it decreases only 27 %.

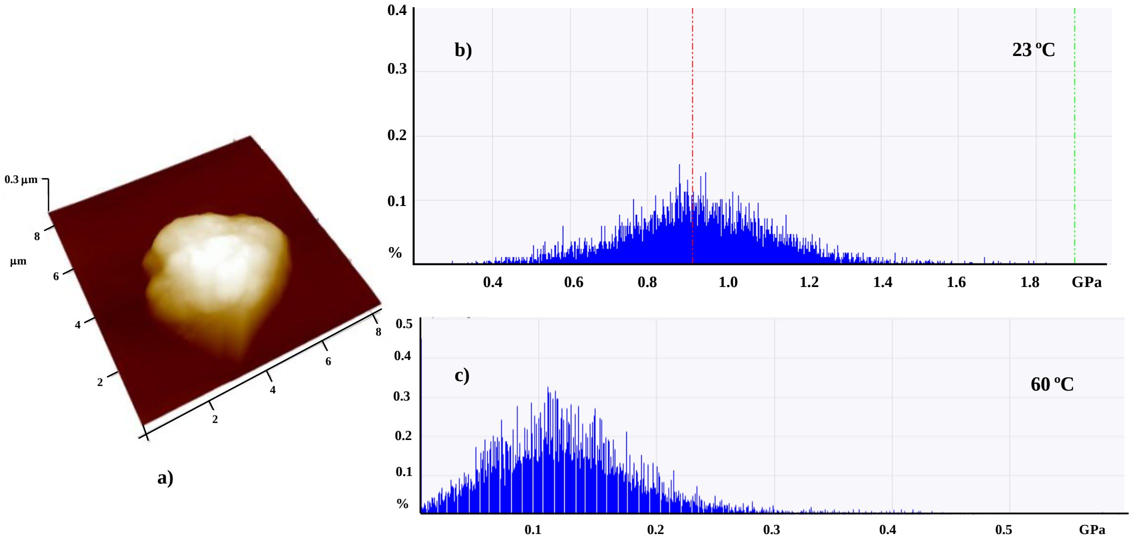

Figure 4.9. Results for PS and tetracosane for 1:1 encapsulation mass ratio, a) 3D image tested, b) Young's modulus results at 23 ºC, c) Young's modulus results at 60 ºC.

To evaluate the maximum force before achieving the plastic deformation it was performed the same type of tests as previously. In PS:tetracosane MPCM with 1:1 encapsulation mass ratio, it is needed 15.6 µN to break the shell at 23 ºC, as Figure 4.10 shows.

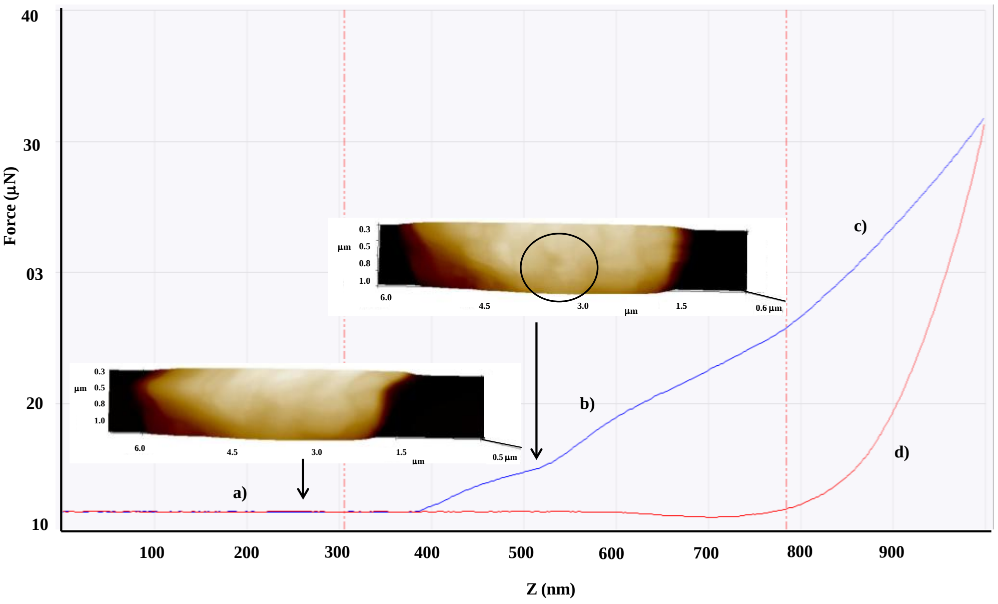

Figure 4.10. Mechanical testing of the elastic-plastic region by AFM of the MPCM composed by PS:tetracosane (1:1) microcapsule at 23 ºC, (a) no contact, blue continuous line; (b) plastic penetration; (c) deformation of the sample; and (d) retraction of the AFM probe, red continuous line.

At 60ºC (Figure 4.11), the needed force to break the shell thickness is 7.3 µN, 53.2 % less compared with room temperature.

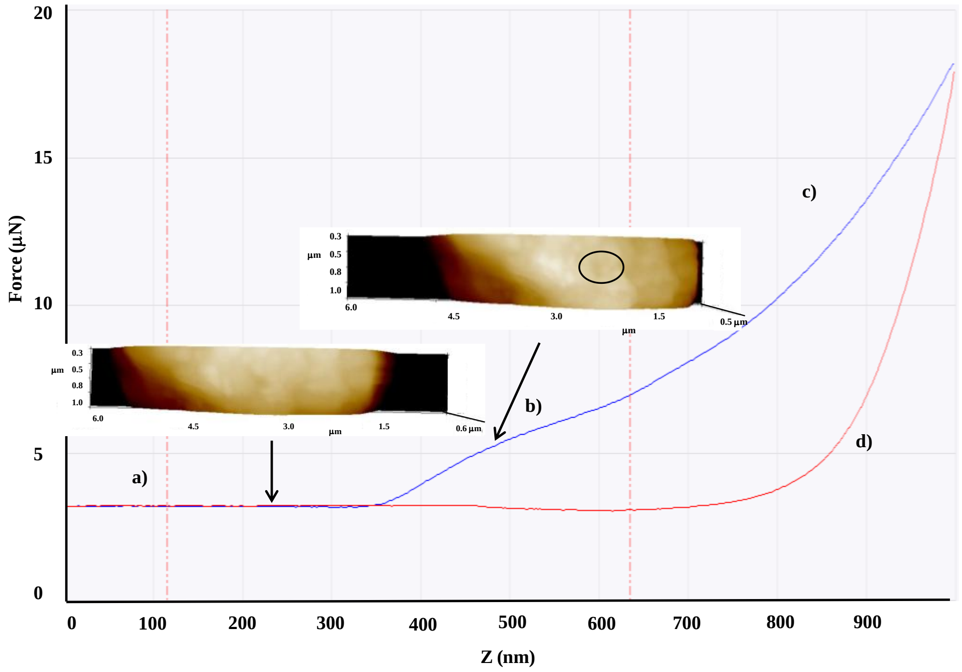

Figure 4.11. Mechanical testing of the elastic-plastic region by AFM of the MPCM composed by PS:tetracosane (1:1) microcapsule at 60 ºC, (a) no contact, blue continuous line; (b) plastic penetration; (c) deformation of the sample; and (d) retraction of the AFM probe, red continuous line.

In conclusion, for 1:1 encapsulation mass ratio, it is needed more force to penetrate the shell thickness than 1:3 encapsulation mass ratio for the same shell/PCM; hence, it will be more difficult to break the sample in a system for 1:1 encapsulation mass ratio. Therefore, the shell/core system will lasts more time inside the circuit. Then, to sum up, in terms of mechanical properties, the best combination core/sell/encapsulation mass ratio of the studies considering laboratory microcapsules is PS/tetrasosane/1:1.

4.4 Comparison of commercial and laboratory MPCM including environmental characterization

Besides all these previous studies, the environmental characterization of microcapsules is also a very important issue to consider in this kind of systems. The exposure to chemical compounds could cause health problems (nausea; dry skin; eye, nose or throat irritations; headache; irritated eyes; dizziness; difficulty in concentrating; psychological stress) in indoor environments (buildings, for example). These problems are known as sick building syndrome (SBS) [22–25].

VOC's (Volatile Organic Compounds) are defined as any organic compound having an initial boiling point less or equal than 250 ºC at a standard pressure of 101.3 kPa. VOC's are one of the most important groups from the atmosphere to trace contaminants by its photochemical, toxic and radioactive effects. For this reason there are some studies, guides [26,27] and database [28,29] related with this effect.

Formaldehyde [30–32] and benzene [33] are some of the most studied pollutants since they are classified in Group 1 of human carcinogens by the IARC 2004 (International Agency for Research on Cancer). They are toxic and have an associated possible health hazard. Other chemical components to take into account for their health effects are acetaldehyde, toluene, and xylenes [34].

There are studies over the past decade on measuring the air quality (indoor environment) in building materials through VOC's because they play a major role in construction [35–46]. Therefore, VOC's emissions from building materials can be studied experimentally and theoretically (using mathematical models) to predict the quality of indoor air. There are some others studies about the outdoor environment [47,48]. Also, it is studied that multi-layer materials have much longer VOC's emission time and a slower VOC's decay rate compared with single-layer materials [49]. Moreover, it has to take into account that the adsorption/desorption phenomena of relatively high vapor pressure compounds are negligible in building [50]. Besides, the percentage of approximately 40 % of the indoor air quality levels originated from building materials [51] are VOC's associated with the perception of bad odors. In renovated buildings or new constructive systems (considering *new* buildings that are less than 10 years old) the levels of indoor air pollutants are higher than the VOC's levels in aged buildings [52].

Implementing MPCM in gypsum board, concrete, plaster or other wallboard material, thermal storage can be a part of construction technology for light weight buildings, and the MPCM could be used for high density thermal energy storage [53,54], so the final product would achieve energy savings in buildings. The fact of using gypsum, cement and heavyweight sheet with PCM could produce some VOC's in the indoor air in a cubicle [55,56]. Consequently, it is important to preserve the air quality of a room. Hence, it is used MPCM to reduce the toxic effects that could be expelled in a system [57].

During my three months stage in Auckland (New Zealand), it was evaluated the physicochemical, thermal, mechanical, and environmental characterization of two different samples with the same core and shell, but comparing a laboratory MPCM with a commercial sample. The aim of this study was to highlight the environmental characterization is a property that must be studied and evaluated in active or passive systems containing MPCM samples. This study titled "**Characterization of Microencapsulated Phase Change Materials for use in Building Applications**" will be submitted in the near future.

Characterization of Microencapsulated Phase Change Materials for use in Building Applications

J. Giro-Paloma[1]; R. Al-Shannaq[2]; A. I. Fernández[1]; M. M. Farid[2,*]

[1] Universitat de Barcelona. Faculty of Chemistry. Department of Materials Science and Metallurgical Engineering. C/ Martí i Franquès, 1. 08028 Barcelona (Spain) Tel: +34-934021298, Fax: +34-934035438, e-mail: jessicagiro@ub.edu; ana_inesfernandez@ub.edu

[2] Department of Chemical & Materials Engineering, University of Auckland, Private Bag 92019, 20 Symonds st 1010 Auckland (New Zealand) Tel.: +64-9-373-7599; Fax: +64-9-373-7463, e-mail: rals187@aucklanduni.ac.nz; m.farid@auckland.ac.nz

* Corresponding author: m.farid@auckland.ac.nz

Abstract

A method for preparing and characterizing microencapsulated phase change materials (MPCM) was developed. A comparison with a commercial MPCM is also presented. Both MPCM contained paraffin wax as PCM with acrylic shell. The T_m of the PCM was around 21 °C, suitable for building applications. The M-2 (our laboratory made sample) and Micronal® DS 5008 X (BASF) samples were characterized using SEM, DSC, nano-indentation technique, and Gas Chromatography/Mass spectrometry (GC-MS). Both samples presented a 6 μm average size and a spherical shape. Thermal energy storage (TES) capacities were 111.73 and 99.3 J g^{-1} for M-2 and Micronal® DS 5008 X, respectively. Mechanical characterization of the samples was performed by nano-indentation technique in order to determine the Elastic modulus (E), load at maximum displacement (P_m), and displacement at maximum load (h_m), concluding that M-2 presented slightly better mechanical properties. Finally, an important parameter for considering use in buildings is the release of volatile organic compounds (VOC's). This characteristic was studied at 65 ºC by CG-MS. Both samples showed VOC's emission after 10 minutes of heating, however peaks intensity of VOC's generated from M-2 microcapsules showed a lower concentration than Micronal® DS 5008 X.

Keywords: Microencapsulated Phase Change Material; Volatile Organic Compounds; nano-indentation; Differential Scanning Calorimetry.

1. Introduction

Thermal Energy Storage (TES) using Phase Change Materials (PCM) has shown a significant increased attention because of its important role on energy conservation in buildings [1–4]. PCM can be used for TES in buildings [5] either in passive [6] or active systems [7–9], aiming to improve the thermal managements of these buildings. In most of the applications, PCM were used either in macroencapsulated [10,11] or microencapsulated [12–14] forms, for heating [15], air-conditioning [16], ventilation [17], refrigeration [18], and heat exchangers [19] for building applications [3,20–22].

Microencapsulation process is defined as a technique in which small particles or droplet are enclosed by a coating, or surrounded in a homogeneous or heterogeneous matrix, to provide microcapsules (1 - 100 μm). For this reason, the Microencapsulated Phase Change Materials (MPCM) are composed of PCM as a core and a polymer as a shell used to preserve the spherical shape of the microcapsule and avoid PCM leakage during phase change [12,23]. The use of MPCM in buildings [24–28] can decrease daily inner temperature fluctuation during summer and winter [29]. The suitability of the shell used in encapsulating specific core PCM is a key issue in order to ensure proper thermal performance of the MPCM [13,30,31], especially in preventing PCM leakage when it melts. Besides, MPCM can be easily incorporated in gypsum board [32,33], plaster [34], and concrete [35,36] used in buildings.

The complete characterization of materials used in indoor environments like MPCM is a very important. The exposure to chemical compounds could cause health problems (nausea; dry skin; eye, nose or throat irritations; headache; irritated eyes; dizziness; difficulty in concentrating; psychological stress) in indoor environments [37–40] (buildings, for example [41–49]) or outdoor environments [50]. These problems are known as sick building syndrome (SBS) [20–23,21]. Volatile Organic Compounds (VOC's) are defined as any organic compound having an initial boiling point less than or equal to 250 ºC at a standard pressure of 101.3 kPa [54]. VOC's are one of the most important groups of trace contaminants in the atmosphere known for its photochemical, toxic and radioactive effects. For this reason there are some studies, guides [55,56] and database [57,58] related to this effect. Formaldehyde [41,48,59] and benzene [60] are some of the most studied pollutants since they are classified in Group 1 of human carcinogens by the IARC 2004 (International Agency for Research on Cancer). Other chemicals known for their health hazard are acetaldehyde, toluene, and xylenes [61]. By this way, VOC's evaluation of the outdoor and indoor air quality has been evaluated [28–31] in materials for buildings like gypsum base PCM composites [62] but it has not been reported for building materials containing MPCM. For this reason, the characterization of VOC's of MPCM is an important contribution to the state of the art of the environmental properties of MPCM.

The aim of this study is to develop, prepare, and characterize microcapsules containing organic PCM in order to assess their suitability for use in buildings and other applications. It is important to establish a characterization methodology, which will include both volatile emission measurements and nano-indentation technique to measure the shell mechanical strength of the microcapsules. Two types of microcapsules were compared: a commercial MPCM, Micronal® DS 5008 X manufactured by BASF®, and laboratory microcapsules, M-2. They should have a high phase change enthalpy, uniform spherical shape, acceptable thermal stability, good mechanical properties and low release of hazardous gases in the form of volatile organic compounds.

2. Materials and methods

2.1 Materials

The chemical preparation of microcapsules required the following reagents:

- Shell: Methyl methacrylate (MMA) (99 %, contains ≤ 30 ppm monomethyl ether hydroquinone (MEHQ) as inhibitor, Sigma Aldrich, NZ) and pentaerythritol tetraacrylate (PETRA) (contains 350 ppm (MEHQ), Sigma Aldrich, NZ) were used as a monomer and cross-linking agent respectively in order to obtain proper shells for MPCM.
- Free radical thermal initiator: Luperox® A75, Benzoyl peroxide (BPO) (75 %, contains 25 % water, Sigma Aldrich, NZ) was used as free radical thermal initiator.
- Surfactants: Polyvinyl alcohol (PVA) (M_w 85,000-124,000, Sigma Aldrich, NZ) and sodium dodecyl sulfate (SDS) (BioXtra, 99 %, Sigma Aldrich, NZ) were used as a non-ionic and ionic surfactant, respectively.
- PCM: a commercial paraffinic PCM, Rubitherm® RT 21 (T_m= 21 ºC, ΔH_m= 135 $J \cdot g^{-1}$, RUBITHERM® Technologies GmbH, Germany) was used.

A commercial MPCM, Micronal® DS 5008 X from BASF®, was also selected for characterization and was compared with the microcapsules produced in this work. This sample is also composed by an acrylate shell and organic PCM in the core [13].

2.2 Synthesis of PCMs Microcapsules

2.2.1 Emulsification

A standard procedure was used as reported elsewhere [63]. Wherein; an aqueous solution of surface-active agent (called aqueous phase) and a mixture of MMA, PETRA, BPO and PCM (called organic phase) were prepared separately. The organic phase was added to the aqueous phase and emulsified mechanically using a high shear mixer (Silverson L5M-A laboratory Mixer). A stirring rate of 3000 rpm for 5 minutes was chosen to achieve the required emulsification.

2.2.2 Polymerization

The produced emulsion was transferred to a 2-L four-neck glass reactor (LR-2.ST laboratory reactor-IKA-Werke Gmbh@Co.KG) consisting of EUROSTAR 200 control P4, Anchor stirrer LR 2000.1, HBR 4 digital heating bath. The agitation speed was set at approximately 300 rpm; and the temperature of the water bath was maintained at 70 ºC for 2 hours, and then adjusted to 85 ºC for another 4 hours. The water bath was then switch off and allowed to cool down naturally to room temperature. After cooling, the suspension of PCM microcapsules was transferred to a clean glass beaker and washed three times with distilled water to remove the unreacted monomers and the non encapsulated PCM. The separated microcapsules were spread on a tray and placed in an oven at 50 ºC for 48 hours for drying. The dried microcapsules were then collected for testing.

3. Characterization of Microcapsules

3.1. Scanning Electron Microscopy (SEM)

To study the shape and size of microcapsules SEM was used (a FEI Quanta 200 FEG - Field Emission Gun with an EDS Detector SiLi (Lithium drifted) with a Super Ultra-Thin window). The sputter coater used was a Quorum Q150RS, and it is designed to give an appropriate thin, slight metal coating proper for SEM observation, using Pt as a target. The coating thickness and uniformity of the sample depends on different factors: distance between sample and target, topography of the sample, and affinity of the material with the metal coating.

3.2. Differential Scanning Calorimetry (DSC)

Phase change properties of the fabricated PCM microcapsules and the pure PCM (such as melting and solidification temperatures and their phase change enthalpies) were determined using a SHIMADZU DSC-60 differential scanning calorimeter. The measurements were performed by varying the temperature between -15 ºC and 40 ºC with heating and cooling rate of 3 $ºC\cdot min^{-1}$. Each sample was analysed for three times and the average was taken. Consequently, the percentage PCM encapsulated can be determined using DSC results and the following Equation 1 [64].

$$\%\ \mathrm{PCM\ in\ microcapsules\ by\ mass} = {}^{\Delta \mathrm{H}_{\mathrm{microcapsules}}}\!\big/\!{}_{\Delta \mathrm{H}_{\mathrm{Pure\ PCM}}} \times 100\% \qquad \text{Equation 1}$$

where $\Delta \mathrm{H}_{\mathrm{microcapsules}}$ ($J\cdot g^{-1}$) is the latent heat of the microcapsule containing PCM and $\Delta \mathrm{H}_{\mathrm{Pure\ PCM}}$ ($J\cdot g^{-1}$) is the latent heat of pure PCM (before encapsulation). In equation 1, it is assumed that the latent heat of the microcapsule without PCM is zero, which is true if the shell does not go phase change.

3.3. Nano-indentation technique

To characterize the mechanical properties of M-2 and commercial Micronal® DS 5008 X samples, nano-indentation technique was used. Nano-indentation is identified as an appropriate technique to test the strength of individual microcapsules [65]. MTS Nano Indenter XP was the instrument used. Aluminium stubs of 20 mm height and 30 mm diameter were needed to stick the samples at the top to characterize them using a red glue to stick the samples as shown in Figure 1. The instrument parameters were set the same for the two studied samples for a more accurate comparison.

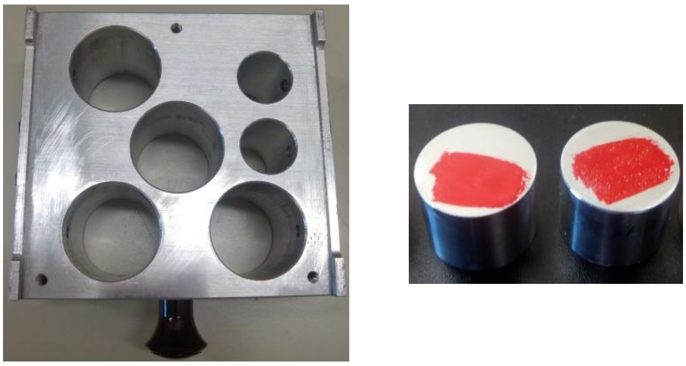

Figure 1. Holder and aluminum stubs with the sample over the red glue.

There are some required inputs to set before starting the experiments: strain rate target of 0.05 s^{-1}, allowable drift rate of 0.05 nm s^{-1}, a Poissons' ratio of 0.18 for the tip indenter [66,67] a peak hold time of 10 s, a surface speed of 10 nm s^{-1}, 25 % of surface approach sensitivity, 90 % to unload, an approach distance to store of 1000 nm, a surface approach distance of 1000 nm, and finally, a depth limit of 5000 nm [68].

To determine the Elastic modulus (E) of the studied samples, a Berkovich tip TB-13288 was used. The use of nano-indentation for the characterization of mechanical properties of materials has been extensively studied by several authors. Oliver and Pharr developed extensively the methodology for characterizing ceramic materials [67,69]. They described the typical load *vs*. displacement curve, where increasing the load (P) increases the displacement (h) until reaching a maximum load (P_{max}) and a maximum displacement (h_{max}). Following that, the indenter is removed out of the material (unloading section), the load will be zero, and the final displacement (h_f) will be measured. After that, the E value for each sample can be calculated. Hochstetter *et al*. [70] presented results for glassy polymers and Giro-Paloma *et al*. [71] compared both methodologies using continuous stiffness measurement (CSM) by applying a small oscillation to the quasi-static component of loading using different thermoplastics suitable as containers for PCM. They concluded that Loubet's method produce lower values of H and E because it uses a dynamic approach for stiffness measurements and the contact depth is larger due to the contribution of the apparent tip effect. In the light of these findings, it was concluded that Loubet's method should be used only with polymeric materials having a low viscous character ($T_g > T_{measurement}$). Besides, in depth sensing indentation (DSI), which is the mode used in this paper, load is applied as a function of penetration depth during loading and unloading cycle, as described by Fischer-Cripps [72]:

- Hardness (*H*) is defined as the maximum indentation load divided by the cross-sectional area of the indenter specified at the maximum indentation depth ($A(h_m)$).

- Load (P_m) at maximum displacement (mN): It is the load recorded at the maximum load, which occurs when sample fails.

- Elastic modulus (*E*) is evaluated from the nano-indentation test using the maximum indentation load (P_m) and the depth sensing indentation. Following that the hardness (*H*), the elastic work (W_e), and the total work (*W*) can be calculated by integrating the areas under the indentation unloading, following Equation 2 and 3:

$$\boldsymbol{H} = {}^{\boldsymbol{P_m}}\!/_{\boldsymbol{A}(\boldsymbol{h_m})} \qquad \text{Equation 2}$$

$$\boldsymbol{E} = {}^{\boldsymbol{H}}\!/_{\boldsymbol{\psi}(\frac{\boldsymbol{W_e}}{\boldsymbol{W}})} \qquad \text{Equation 3}$$

- Displacement (h_m) at maximum load (nm) is a measure of the extent the tip penetrates into the material.

3.4. Emission of Volatile Organic Compounds (VOC’s)

A GC-17A Gas chromatograph Shimadzu coupled to GCMS-QP5000 Gas chromatograph/Mass Spectrometer Shimadzu was used to characterize the VOC’s emissions from each sample. A calibration was performed for each pure compound: $C_{14}H_{30}$, $C_{15}H_{32}$, $C_{16}H_{34}$, $C_{17}H_{36}$, $C_{18}H_{38}$, $C_{20}H_{42}$, $C_{22}H_{46}$, and $C_{24}H_{50}$, at different temperatures: 25 ºC, 35 ºC, 45 ºC, 55 ºC, and 65 ºC. A total of 40 experiments for calibration were executed. When the calibration was completed, the same procedure was performed for the two studied samples; M-2 and Micronal® DS 5008 X.

Each sample was independently located inside a crystal vial HS of 50 ml capacity. The vials were submerged during 30 minutes in a water bath until reaching the required temperature. Later on, a fibber solid-phase microextraction (SPME) holder with lot number P268618D 57330-U, provided by Supelco, was punctured on the top of the silicone cap. Following that, 10 min desorption was applied. The temperature inside the device was 60 ºC during 2 min. After that, a ramp of 15 ºC min^{-1} was programmed.

A HP-5MS (1553434H) was the column used. Its thickness, length and diameter were 0.5 µm, 30 m, and 0.32 cm, respectively. Besides, the injection and interface temperature were 200 and 280 ºC, respectively inside the Gas Chromatographer. There were more parameters to take into account, such as inlet pressure: 1 kPa, flow: 1.1 ml min^{-1}, lineal velocity: 38.7 cm s^{-1}, split ratio between peaks of 20, and finally total flow for the He gas of 23.1 ml min^{-1}. On the other hand, the Mass Spectrometer m/z values are from 35 to 350. Moreover, the solvent cut time was 0.5 min.

4. Results and discussion

4.1. Characterization of MPCM shape, size, and morphology

SEM images for the two studied samples are shown in Figure 2. M-2 microcapsules morphology appears to be compact and with smooth surface as shown in Figure 2a. Besides, their size is around 6 μm and have a spherical shape. On the other hand, commercial Micronal® DS 5008 X looks made of a big sphere (around 150 μm) composed of hundreds of other small microcapsules (the ones which contain the PCM) with 6 μm in size, approximately as shown in Figure 2b. As Figure 2 shows, the 6 μm microcapsules of Micronal® DS 5008 X samples are deformed, which is probably due to the process of agglomerating of these microcapsules to form larger particle of 150 μm, which probably has been made for ease of handling.

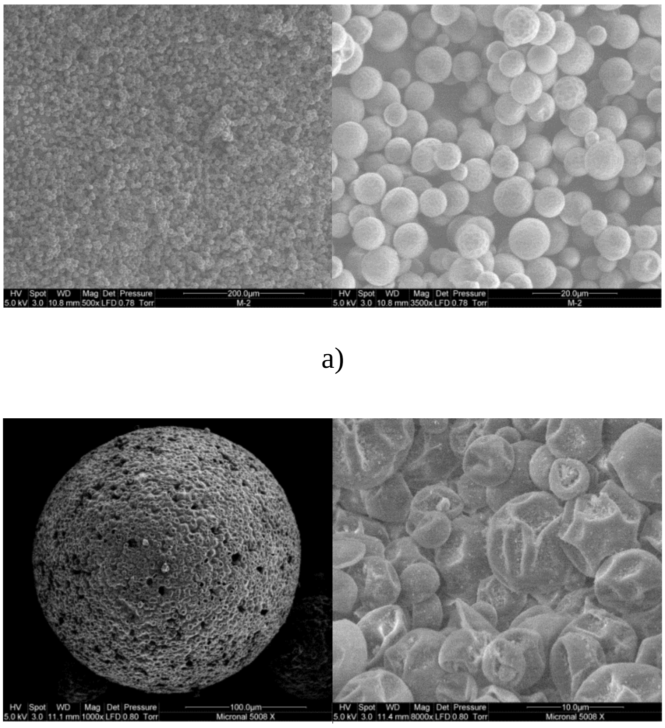

a)

b)

Figure 2. SEM images for the studied samples a) M-2 (magnification x 500 left and x 3500 right), b) Micronal® DS 5008 X (magnification: x 1000 left and x 8000 right).

4.2. Thermophysical properties of MPCM

Thermal properties of M-2 and Micronal® DS 5008 X in terms of phase change enthalpies and phase change temperatures were investigated using DSC as shown in Figure 3. The DSC results show that the thermal energy storage capacity of the M-2 is 113.8 J·g^{-1} which corresponds to 85 wt % of RT-21 encapsulation. The melting temperature of the RT-21 in M-2 microcapsules is similar to that of the bulk RT-21. In contrast, the solidification temperature of the PCM microcapsules was about 14 ºC lower than that of the bulk RT-21 (super-cooling phenomena) as previously reported [73] (see Table 1). The supercooling of PCM in microcapsules has also been reported by Qiu *et al*. [74]. The increase of the degree of super-cooling of RT-21 microcapsules could be attributed either to the decrease in the amount of RT-21 nuclei inside each microcapsule compared to the bulk RT-21 [75] or due to formation of vacuum pockets space inside the microcapsules [76]. To reduce the supercooling of PCM microcapsules, additives were mixed with the PCM prior encapsulation to act as a nucleating agent. These nucleating agents are usually materials with a similar crystal structure as the solid PCM which allow nucleation at their surface but have a higher melting temperature. Figure 4 shows the DSC curve for the microcapsules containing nucleating agent. Commercial RT-58 (paraffin) with peak melting temperatures of 58 ºC was used as nucleating agent. The degree of supercooling has been reduced dramatically as reported in Table 1 and shown in Figure 4.

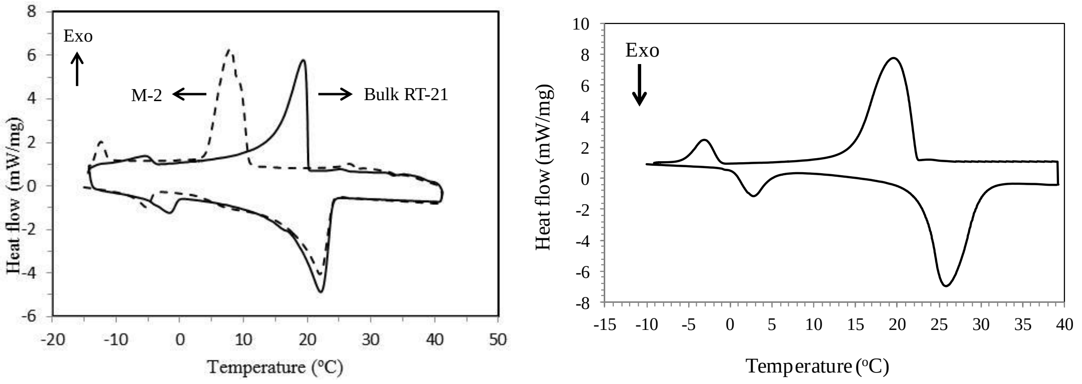

a) b)

Figure 3. DSC results for a) M-2 and b) Micronal® DS 5008 X.

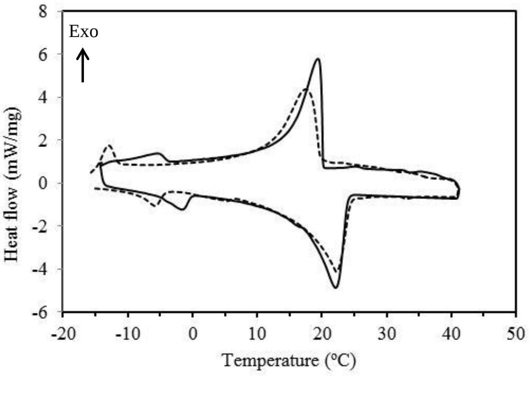

Figure 4. DSC curves of the bulk RT-21 (black solid line) and M-2 microcapsules containing nucleating agent, RT-58 (blue solid line).

Table 1. Thermophysical properties of fabricated M-2 and commercial Micronal® DS 5008 X.

		M-2	**RT-21**	**Micronal® DS 5008 X**	**M-2 containing RT-58**
Heating	**T_{onset} (ºC)**	16.7	16.5	22.1	16.1
	T_{peak} (ºC)	22.0	22.1	20.3	22.3
	T_{endset} (ºC)	24.0	23.9	26.3	24.3
	ΔH (J g^{-1})	113.9	132.0	99.9	110.4
Cooling	**T_{onset} (ºC)**	10.9	20.2	22.5	19.8
	T_{peak} (ºC)	7.9	19.4	24.2	17.5
	T_{endset} (ºC)	4.2	14.5	17.5	11.4
	ΔH (J g^{-1})	111.9	132.5	103.5	108.3

4.3. Mechanical properties of MPCM

Results of nano-indentation technique by DSI for the two samples were summarized in Table 2. Ten tests were performed for each sample, but some results were discarded because of the dispersion attributed to indentations in the edge of the microcapsules. For this reason, six results were finally selected. From these measurements the mean value and standard deviation of the Elastic modulus (*E*) were calculated for each sample. These results show that M-2 microcapsules are stiffer than Micronal® DS 5008 X ones.

Table 2. Elastic modulus results of M-2 and Micronal® DS 5008 X.

	E						Mean	Std. Dev.
M-2	1.89	1.04	1.16	1.68	1.38	1.9	1.51	0.37
Micronal® DS 5008 X	0.15	0.19	0.17	0.24	0.22	0.28	0.21	0.05

Figure 5 is a representation of the *P-h* curves for the M-2 and Micronal® respectively. The measured typical drift behaviour can be observed on the plateau at the end of the unloaded curve. It can be concluded that the mechanical response for M-2 is better than Micronal® DS 5008 X as M-2 microcapsules are more rigid and show higher strength. This fact can be attributed to various factors such as the differences in the encapsulation ratio between samples, shell thickness, type of polymers, as well as degree of polymerization of the shells.

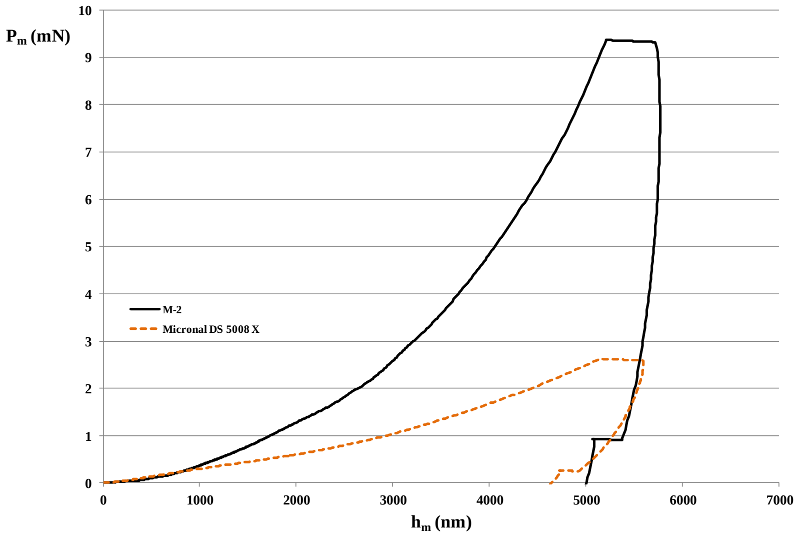

Figure 5. h_m *vs.* P_m, comparison of the samples under study.

4.4. Characterization of Volatile Organic Compounds (VOC's)

The results of VOC's emission from the two studied samples are shown in Table 3. Each peak in the GC spectra was given at a certain retention time (t_r, in minutes), which was related to a specific compound, according to the calibration conducted in this work.

Table 3. VOC's emission results for M-2 and Micronal® DS 5008 X samples.

	M-2		**Micronal® DS 5008 X**	
	t_r (min)	Compound	t_r (min)	Compound
25 °C	No signal		No signal	
35 °C	No signal		No signal	
45 °C	No signal		11.88	$C_{17}H_{36}$
			12.66	$C_{18}H_{38}$
55 °C	No signal		11.88	$C_{17}H_{36}$
			12.65	$C_{18}H_{38}$
65 °C	9.25	$C_{14}H_{30}$	-	-
	10.18	$C_{15}H_{32}$	-	-
	11.06	$C_{16}H_{34}$	-	-
	11.91	$C_{17}H_{36}$	11.85	$C_{17}H_{36}$
	12.68	$C_{18}H_{38}$	12.63	$C_{18}H_{38}$

It may be observed from the results that some emissions from Micronal® DS 5008 X sample after 10 minutes exposure at 45 and 55 °C were detected while nothing was detected from M-2 microcapsules. After 10 minutes exposure at 65 °C, both samples release volatile compounds, but with much lower level for M-2 microcapsules in comparison with Micronal® DS 5008 X. This is confirmed by the high intensity peak for Micronal® DS 5008 X comparing both figures in Figure 6. The multiple peaks for M-2 show the presence of tetradecane, pentacosane, hexadecane, heptadecane and octadecane in the original PCM, which is RT-21, while only two peaks were observed for the PCM used in Micronal® DS 5008 X, indicating that the latter is of higher purity.

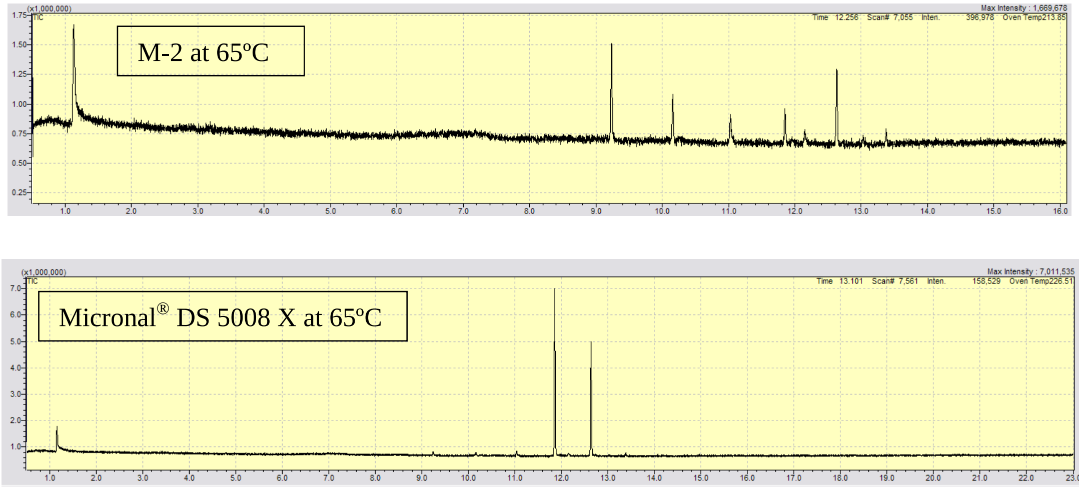

Figure 6.- Revealed peaks for the GC/MS analysis for a) M-2 and b) Micronal® DS 5008 X samples at 65 ºC.

5. Conclusions

A comparison for the characteristic of two MPCM samples was conducted; one sample was Micronal® DS5008 X while the other was made in our laboratory (M-2). The shell material for both samples is similar in terms of chemical composition. Following SEM observation, it can be concluded that the two samples have similar shape and diameter of about 6 μm, but they have different morphology since Micronal® DS 5008 X capsules were produced as aggregates of many microcapsules. Regarding the thermophysical properties for both samples, their thermal energy storage (TES) capacity were 111.7 and 99.3 J g^{-1} for M-2 and Micronal® DS 5008 X, respectively. The mechanical testing was performed by measuring Elastic modulus (E), load at displacement (P_m), and displacement at maximum load (h_m) using nano-indentation technique. Different results were obtained for both samples, showing that M-2 sample has better mechanical resistance and stiffness. Finally, a comparative evaluation of the VOC’s release at 25 ºC, 35 ºC, 45 ºC, 55 ºC, and 65 ºC was performed in order to study the volatiles emission from these microcapsules. M-2 microcapsules show better stability with less emission of VOC’s than Micronal® DS 5008 X.

Acknowledgments

Authors acknowledge the support received from the European Union's Seventh Framework Programme (FP7/2007-2013) under grant agreement nº PIRSES-GA-2013-610692

(INNOSTORAGE). Also, we would like to acknowledge the support we have received form Qatar Foundation in supporting the project No: NPRP 5-093-2-034.

References

[1] Zhou D, Zhao CY, Tian Y. Review on thermal energy storage with phase change materials (PCMs) in building applications. Appl Energy 2012;92:593–605. doi:10.1016/j.apenergy.2011.08.025.

[2] Sharma A, Tyagi VV, Chen CR, Buddhi D. Review on thermal energy storage with phase change materials and applications. Renew Sustain Energy Rev 2009;13:318–45. doi:10.1016/j.rser.2007.10.005.

[3] Kuznik F, David D, Johannes K, Roux J-J. A review on phase change materials integrated in building walls. Renew Sustain Energy Rev 2011;15:379–91. doi:10.1016/j.rser.2010.08.019.

[4] Farid MM, Khudhair AM, Razack SAK, Al-Hallaj S. A review on phase change energy storage: materials and applications. Energy Convers Manag 2004;45:1597–615. doi:10.1016/j.enconman.2003.09.015.

[5] Cabeza LF, Castell a., Barreneche C, de Gracia a., Fernández a. I. Materials used as PCM in thermal energy storage in buildings: A review. Renew Sustain Energy Rev 2011;15:1675–95. doi:10.1016/j.rser.2010.11.018.

[6] Soares N, Costa JJ, Gaspar a. R, Santos P. Review of passive PCM latent heat thermal energy storage systems towards buildings' energy efficiency. Energy Build 2013;59:82–103. doi:10.1016/j.enbuild.2012.12.042.

[7] Griffiths PW, Eames PC. Performance of chilled ceiling panels using phase change material slurries as the heat transport medium. Appl Therm Eng 2007;27:1756–60. doi:10.1016/j.applthermaleng.2006.07.009.

[8] Huang L, Petermann M, Doetsch C. Evaluation of paraffin/water emulsion as a phase change slurry for cooling applications. Energy 2009;34:1145–55. doi:10.1016/j.energy.2009.03.016.

[9] Youssef Z, Delahaye A, Huang L, Trinquet F, Fournaison L, Pollerberg C, et al. State of the art on phase change material slurries. Energy Convers Manag 2013;65:120–32. doi:10.1016/j.enconman.2012.07.004.

[10] Pendyala S. Macroencapsulation of Phase Change Materials for Thermal Energy Storage 2012.

[11] Calvet N, Py X, Olivès R, Bédécarrats J-P, Dumas J-P, Jay F. Enhanced performances of macro-encapsulated phase change materials (PCMs) by intensification of the internal effective thermal conductivity. Energy 2013;55:956–64. doi:10.1016/j.energy.2013.03.078.

[12] Zhao CY, Zhang GH. Review on microencapsulated phase change materials (MEPCMs): Fabrication, characterization and applications. Renew Sustain Energy Rev 2011;15:3813–32. doi:10.1016/j.rser.2011.07.019.

[13] Giro-Paloma J, Oncins G, Barreneche C, Martínez M, Fernández AI, Cabeza LF. Physico-chemical and mechanical properties of microencapsulated phase change material. Appl Energy 2013;109:441–8. doi:10.1016/j.apenergy.2012.11.007.

[14] Al Shannaq R, Farid MM. Advances in Thermal Energy Storage Systems (10 – Microencapsulation of phase change materials (PCMs) for thermal energy storage systems). Elsevier; 2015. doi:10.1533/9781782420965.2.247.

[15] Alvarado JL, Marsh C, Sohn C, Phetteplace G, Newell T. Thermal performance of microencapsulated phase change material slurry in turbulent flow under constant heat flux. Int J Heat Mass Transf 2007;50:1938–52. doi:10.1016/j.ijheatmasstransfer.2006.09.026.

[16] Diaconu BM, Varga S, Oliveira AC. Experimental study of natural convection heat transfer in a microencapsulated phase change material slurry. Energy 2010;35:2688–93. doi:10.1016/j.energy.2009.06.028.

[17] Zhang P, Ma ZW, Wang RZ. An overview of phase change material slurries: MPCS and CHS. Renew Sustain Energy Rev 2010;14:598–614. doi:10.1016/j.rser.2009.08.015.

[18] Zhang P, Ma ZW. An overview of fundamental studies and applications of phase change material slurries to secondary loop refrigeration and air conditioning systems. Renew Sustain Energy Rev 2012;16:5021–58. doi:10.1016/j.rser.2012.03.059.

[19] Medrano M, Yilmaz MO, Nogués M, Martorell I, Roca J, Cabeza LF. Experimental evaluation of commercial heat exchangers for use as PCM thermal storage systems. Appl Energy 2009;86:2047–55.

[20] Su J-F, Wang L-X, Ren L. Preparation and characterization of double-MF shell microPCMs used in building materials. J Appl Polym Sci 2005;97:1755–62. doi:10.1002/app.21205.

[21] Khudhair AM, Farid MM. A review on energy conservation in building applications with thermal storage by latent heat using phase change materials. Energy Convers Manag 2004;45:263–75. doi:10.1016/S0196-8904(03)00131-6.

[22] Alawadhi EM. Thermal analysis of a building brick containing phase change material. Energy Build 2008;40:351–7. doi:10.1016/j.enbuild.2007.03.001.

[23] Sarı A, Alkan C, Karaipekli A, Uzun O. Microencapsulated n-octacosane as phase change material for thermal energy storage. Sol Energy 2009;83:1757–63. doi:10.1016/j.solener.2009.05.008.

[24] Kuznik F, David D, Johannes K, Roux J-J. A review on phase change materials integrated in building walls. Renew Sustain Energy Rev 2011;15:379–91. doi:10.1016/j.rser.2010.08.019.

[25] Cabeza LF, Castellón C, Nogués M, Medrano M, Leppers R, Zubillaga O. Use of microencapsulated PCM in concrete walls for energy savings. Energy Build 2007;39:113–9. doi:10.1016/j.enbuild.2006.03.030.

[26] Castellón C, Medrano M, Roca J, Cabeza LF, Navarro ME, Fernández AI, et al. Effect of microencapsulated phase change material in sandwich panels. Renew Energy 2010;35:2370–4. doi:10.1016/j.renene.2010.03.030.

[27] Toppi T, Mazzarella L. Gypsum based composite materials with micro-encapsulated PCM: Experimental correlations for thermal properties estimation on the basis of the composition. Energy Build 2013;57:227–36. doi:10.1016/j.enbuild.2012.11.009.

[28] Entrop AG, Brouwers HJH, Reinders AHME. Experimental research on the use of micro-encapsulated Phase Change Materials to store solar energy in concrete floors and to save energy in Dutch houses. Sol Energy 2011;85:1007–20. doi:10.1016/j.solener.2011.02.017.

[29] Tyagi VV, Kaushik SC, Tyagi SK, Akiyama T. Development of phase change materials based microencapsulated technology for buildings: A review. Renew Sustain Energy Rev 2011;15:1373–91. doi:10.1016/j.rser.2010.10.006.

[30] Zalba B, Marín JM, Cabeza LF, Mehling H. Review on thermal energy storage with phase change: Materials, heat transfer analysis and applications. Appl Therm Eng 2003;23:251–83.

[31] Alkan C, Sari A. Fatty acid/poly(methyl methacrylate) (PMMA) blends as form-stable phase change materials for latent heat thermal energy storage. Sol Energy 2008;82:118–24. doi:10.1016/j.solener.2007.07.001.

[32] Zhang H, Xu Q, Zhao Z, Zhang J, Sun Y, Sun L, et al. Preparation and thermal performance of gypsum boards incorporated with microencapsulated phase change materials for thermal regulation. Sol Energy Mater Sol Cells 2012;102:93–102. doi:10.1016/j.solmat.2012.03.020.

[33] Borreguero AM, Garrido I, Valverde JL, Rodríguez JF, Carmona M. Development of smart gypsum composites by incorporating thermoregulating microcapsules. Energy Build 2014;76:631–9. doi:10.1016/j.enbuild.2014.03.005.

[34] Karkri M, Lachheb M, Albouchi F, Nasrallah S Ben, Krupa I. Thermal properties of smart microencapsulated paraffin/plaster composites for the thermal regulation of buildings. Energy Build 2015;88:183–92. doi:10.1016/j.enbuild.2014.11.068.

[35] Eddhahak-Ouni A, Drissi S, Colin J, Neji J, Care S. Experimental and multi-scale analysis of the thermal properties of Portland cement concretes embedded with microencapsulated Phase Change Materials (PCMs). Appl Therm Eng 2014;64:32–9. doi:http://dx.doi.org/10.1016/j.applthermaleng.2013.11.050.

[36] Cabeza LF, Castellón C, Nogués M, Medrano M, Leppers R, Zubillaga O. Use of microencapsulated PCM in concrete walls for energy savings. Energy Build 2007;39:113–9.

[37] Schlink U, Rehwagen M, Damm M, Richter M, Borte M, Herbarth O. Seasonal cycle of indoor-VOCs: comparison of apartments and cities. Atmos Environ 2004;38:1181–90. doi:10.1016/j.atmosenv.2003.11.003.

[38] Ayoko GA. Volatile Organic Compounds in Indoor Environments. 2004.

[39] Gallego E, Roca X, Perales JF, Guardino X. Determining indoor air quality and identifying the origin of odour episodes in indoor environments. J Environ Sci 2009;21:333–9. doi:10.1016/S1001-0742(08)62273-1.

[40] Missia DA, Demetriou E, Michael N, Tolis EI, Bartzis JG. Indoor exposure from building materials: A field study. Atmos Environ 2010;44:4388–95. doi:10.1016/j.atmosenv.2010.07.049.

[41] Shin SH, Jo WK. Volatile organic compound concentrations, emission rates, and source apportionment in newly-built apartments at pre-occupancy stage. Chemosphere 2012;89:569–78. doi:10.1016/j.chemosphere.2012.05.054.

[42] Huang H, Haghighat F. Building materials VOC emissions—a systematic parametric study. Build Environ 2003;38:995–1005. doi:10.1016/S0360-1323(03)00062-3.

[43] Zhang Y, Xu Y. Characteristics and correlations of VOC emissions from building materials. Int J Heat Mass Transf 2003;46:4877–83. doi:10.1016/S0017-9310(03)00352-1.

[44] Kim S, Choi Y-K, Park K-W, Kim JT. Test methods and reduction of organic pollutant compound emissions from wood-based building and furniture materials. Bioresour Technol 2010;101:6562–8. doi:10.1016/j.biortech.2010.03.059.

[45] Lee C-S, Haghighat F, Ghaly W. Conjugate Mass Transfer Modeling for VOC Source and Sink Behavior of Porous Building Materials: When to Apply It? J Build Phys 2006;30:91–111. doi:10.1177/1744259106067683.

[46] Haghighat F, Huang H. Integrated IAQ model for prediction of VOC emissions from building material. Build Environ 2003;38:1007–17. doi:10.1016/S0360-1323(03)00064-7.

[47] Lee C-S, Haghighat F, Ghaly WS. A study on VOC source and sink behavior in porous building materials - analytical model development and assessment. Indoor Air 2005;15:183–96. doi:10.1111/j.1600-0668.2005.00335.x.

[48] Kim S, Kim H-J, Moon S-J. Evaluation of VOC Emissions from Building Finishing Materials Using a Small Chamber and VOC Analyser. Indoor Built Environ 2006;15:511–23. doi:10.1177/1420326X06072040.

[49] Magee RJ, Bodalal A, Biesenthal TA, Lusztyk E, Brouzes M, Shaw CY. Prediction of VOC concentration profiles in a newly constructed house using samll chamber data and an IAQ simulation program. 9th Int. Conf. IAQ Clim., 2002, p. 298–303.

[50] Jia C, Batterman SA, Relyea GE. Variability of indoor and outdoor VOC measurements: an analysis using variance components. Environ Pollut 2012;169:152–9. doi:10.1016/j.envpol.2011.09.024.

[51] Norbäck D, Torgén M, Edling C. Volatile organic compounds , respirable dust , and personal factors related to prevalence and incidence of sick building syndrome in primary schools. Br J Ind Med 1990;47:733–41.

[52] Redlich CA, Sparer J, Cullen MR. Sick-building syndrome. Lancet 1997;349:1013–6. doi:10.1016/S0140-6736(96)07220-0.

[53] Apte MG, Daisey JM. VOCs and " Sick Building Syndrome ": Application of a New Statistical Approach for SBS Research to U . S . EPA BASE Study Data. Indoor Air 99, 1999, p. 2–7.

[54] Thomas E. Rufford, John Zhu DH-J. Green Carbon Materials: Advances and Applications. 2014.

[55] ASTM Standard D5116-97. Standard guide for small-scale environmental chamber determinations of organic emissions from indoor material/products, 1997.

[56] ASTM Standard D6007-96. Standard test Method for determining Formaldehyde Concentrations in Air from Wood Products Using a Small Scale Chamber, 1996.

[57] Won D, Magee RJ, Lusztyk E, Nong G, Zhu JP, Zhang JS, et al. A comprehensive VOC emission database for coomonly-used building materials. 7th Int. Conf. Heal. Build., 2003, p. 1–6.

[58] Ouazia B, Reardon J, Sander D. Making the Case of Reducing Ventilation Requirements Through Selection of Low-Emission Materials. NRC•CNRC n.d.

[59] Xiong J, Zhang Y, Huang S. Characterization of VOC and Formaldehyde Emission from Building Materials in Static Environmental Chamber: Model Development and Application. Indoor Built Environ 2011;20:217–25. doi:10.1177/1420326X10387480.

[60] Knöppel H, Schauenburg H. Screening of household products for the emission of volatile organic compounds. Environ Int 1989;15:413–8. doi:10.1016/0160-4120(89)90056-1.

[61] Lin C-C, Yu K-P, Zhao P, Whei-May Lee G. Evaluation of impact factors on VOC emissions and concentrations from wooden flooring based on chamber tests. Build Environ 2009;44:525–33. doi:10.1016/j.buildenv.2008.04.015.

[62] Safari V, Barreneche C, Castell A, Basatni A, Navarro L, Cabeza L, et al. Volatile organic emission from PCM building materials. Innostock 2012 - 12th Int. Conf. Energy Storage, 2012.

[63] Sánchez L, Sánchez P, de Lucas A, Carmona M, Rodríguez JF. Microencapsulation of PCMs with a polystyrene shell. Colloid Polym Sci 2007;285:1377–85. doi:10.1007/s00396-007-1696-7.

[64] Sánchez-Silva L, Rodríguez JF, Romero A, Borreguero AM, Carmona M, Sánchez P. Microencapsulation of PCMs with a styrene-methyl methacrylate copolymer shell by suspension-like polymerisation. Chem Eng J 2010;157:216–22. doi:10.1016/j.cej.2009.12.013.

[65] Rahman A, Dickinson ME, Farid MM. Microencapsulation of a PCM through membrane emulsification and nanocompression-based determination of microcapsule strength. Mater Renew Sustain Energy 2012;1:4. doi:10.1007/s40243-012-0004-8.

[66] Troyon M, Huang L. Correction factor for contact area in nanoindentation measurements. J Mater Res 2011;20:610–7. doi:10.1557/JMR.2005.0099.

[67] Oliver WC, Pharr GM. Measurement of hardness and elastic modulus by instrumented indentation: Advances in understanding and refinements to methodology. J Mater Res 2004;19:3–20. doi:10.1557/jmr.2004.19.1.3.

[68] Rahman A. Microencapsulation of Phase Change Materials with Membrane Emulsification , and Development of a Nanocompression Technique to Test Microcapsule Strength 2010.

[69] Oliver WC, Pharr GM. An improved technique for determining hardness and elastic modulus using load and displacement sensing indentation experiments. J Mater Res 1992;7(6):1564–80.

[70] Hochstetter G, Jimenez a., Loubet JL. Strain-rate effects on hardness of glassy polymers in the nanoscale range. Comparison between quasi-static and continuous stiffness measurements. J Macromol Sci Part B 2006;38:681–92. doi:10.1080/00222349908248131.

[71] Giro-Paloma J, Roa JJ, Díez-Pascual AM, Rayón E, Flores A, Martínez M, et al. Depth-sensing indentation applied to polymers: A comparison between standard methods of analysis in relation to the nature of the materials. Eur Polym J 2013;49:4047–53.

[72] Fischer-Cripps AC. Introduction to Contact Mechanics. 2nd ed. New York, USA: Springer; 2007.

[73] Al-Shannaq R, Farid M, Al-Muhtaseb S, Kurdi J. Emulsion stability and cross-linking of PMMA microcapsules containing phase change materials. Sol Energy Mater Sol Cells 2015;132:311–8. doi:10.1016/j.solmat.2014.08.036.

[74] Qiu X, Li W, Song G, Chu X, Tang G. Fabrication and characterization of microencapsulated n-octadecane with different crosslinked methylmethacrylate-based polymer shells. Sol Energy Mater Sol Cells 2012;98:283–93. doi:10.1016/j.solmat.2011.11.018.

[75] Zhang X, Fan Y, Tao X, Yick K. Crystallization and prevention of supercooling of microencapsulated n-alkanes. J Colloid Interface Sci 2005;281:299–306. doi:10.1016/j.jcis.2004.08.046.

[76] Chaiyasat P, Ogino Y, Suzuki T, Okubo M. Influence of water domain formed in hexadecane core inside cross-linked capsule particle on thermal properties for heat storage application. Colloid Polym Sci 2008;286:753–9. doi:10.1007/s00396-007-1831-5.

Chapter 4 References

[1] Ibarra LH. Máster de edificación proyecto final de máster 2012.

[2] Borreguero AM, Garrido I, Valverde JL, Rodríguez JF, Carmona M. Thermal characterization of gypsum composites by using differential scanning calorimetry. Introduction thermal energy storage materials. E2KW 2013, 2013.

[3] Eddhahak-Ouni A, Drissi S, Colin J, Neji J, Care S. Experimental and multi-scale analysis of the thermal properties of Portland cement concretes embedded with microencapsulated Phase Change Materials (PCMs). Applied Thermal Engineering 2014;64:32–9. doi:http://dx.doi.org/10.1016/j.applthermaleng.2013.11.050.

[4] Sari-Bey S, Fois M, Krupa I, Ibos L, Benyoucef B, Candau Y. Thermal characterization of polymer matrix composites containing microencapsulated paraffin in solid or liquid state. Energy Conversion and Management 2014;78:796–804.

[5] Franquet E, Gibout S, Tittelein P, Zalewski L, Dumas J-P. Experimental and theoretical analysis of a cement mortar containing microencapsulated PCM. Applied Thermal Engineering 2014;73:30–8. doi:http://dx.doi.org/10.1016/j.applthermaleng.2014.06.053.

[6] Delgado M, Lázaro A, Mazo J, Zalba B. Review on phase change material emulsions and microencapsulated phase change material slurries: Materials, heat transfer studies and applications. Renewable and Sustainable Energy Reviews 2012;16:253–73.

[7] Joulin A, Zalewski L, Lassue S, Naji H. Experimental investigation of thermal characteristics of a mortar with or without a micro-encapsulated phase change material. Applied Thermal Engineering 2014;66:171–80. doi:http://dx.doi.org/10.1016/j.applthermaleng.2014.01.027.

[8] Serrano S, Barreneche C, Rincón L, Boer D, Cabeza LF. Optimization of three new compositions of stabilized rammed earth incorporating PCM: Thermal properties characterization and LCA. Construction and Building Materials 2013;47:872–8. doi:10.1016/j.conbuildmat.2013.05.018.

[9] Serrano S, Barreneche C, Rincón L, Boer D, Cabeza LF. Stabilized rammed earth incorporating PCM: Optimization and improvement of thermal properties and Life Cycle Assessment. Energy Procedia 2012;30:461–70. doi:10.1016/j.egypro.2012.11.055.

[10] Menoufi K, Castell A, Navarro L, Pérez G, Boer D, Cabeza LF. Evaluation of the environmental impact of experimental cubicles using Life Cycle Assessment: A highlight on the manufacturing phase. Applied Energy 2012;92:534–44.

[11] Giro-Paloma J, Oncins G, Barreneche C, Martínez M, Fernández AI, Cabeza LF. Physico-chemical and mechanical properties of microencapsulated phase change material. Applied Energy 2013;109:441–8.

[12] Konuklu Y, Unal M, Paksoy HO. Microencapsulation of caprylic acid with different wall materials as phase change material for thermal energy storage. Solar Energy Materials and Solar Cells 2014;120:536–42. doi:10.1016/j.solmat.2013.09.035.

[13] Konuklu Y, Paksoy HO, Unal M, Konuklu S. Microencapsulation of a fatty acid with Poly(melamine–urea–formaldehyde). Energy Conversion and Management 2014;80:382–90. doi:10.1016/j.enconman.2014.01.042.

[14] Konuklu Y, Paksoy HO, Unal M. Nanoencapsulation of n-alkanes with poly(styrene-co-ethylacrylate) shells for thermal energy storage. Applied Energy 2015;150:335–40. doi:10.1016/j.apenergy.2014.11.066.

[15] Konuklu Y. Microencapsulation of phase change material with poly(ethylacrylate) shell for thermal energy storage. International Journal of Energy Research 2014;38:2019–29. doi:10.1002/er.3216.

[16] Giro-Paloma J, Konuklu Y, Fernández AI. Preparation and exhaustive characterization of paraffin or palmitic acid microcapsules as novel phase change material. Solar Energy 2015;112:300–9. doi:10.1016/j.solener.2014.12.008.

[17] Sari A, Alkan C, Biçer A, Altuntaş A, Bilgin C. Micro/nanoencapsulated n-nonadecane with poly(methyl methacrylate) shell for thermal energy storage. Energy Conversion and Management 2014;86:614–21. doi:10.1016/j.enconman.2014.05.092.

[18] Sari A, Alkan C, Kahraman Döğüşcü D, Biçer A. Micro/nano-encapsulated n-heptadecane with polystyrene shell for latent heat thermal energy storage. Solar Energy Materials and Solar Cells 2014;126:42–50. doi:10.1016/j.solmat.2014.03.023.

[19] Sari A, Alkan C, Bilgin C. Micro/nano encapsulation of some paraffin eutectic mixtures with poly(methyl methacrylate) shell: Preparation, characterization and latent heat thermal energy storage properties. Applied Energy 2014;136:217–27. doi:10.1016/j.apenergy.2014.09.047.

[20] Sari A, Alkan C, Özcan AN. Synthesis and characterization of micro/nano capsules of PMMA/capric-stearic acid eutectic mixture for low temperature-thermal energy storage in buildings. Energy and Buildings 2015;90:106–13. doi:10.1016/j.enbuild.2015.01.013.

[21] Sari A, Alkan C, Altintaş A. Preparation, characterization and latent heat thermal energy storage properties of micro-nanoencapsulated fatty acids by polystyrene shell. Applied Thermal Engineering 2014;73:1158–66. doi:10.1016/j.applthermaleng.2014.09.005.

[22] Gallego E, Roca X, Perales JF, Guardino X. Determining indoor air quality and identifying the origin of odour episodes in indoor environments. Journal of Environmental Sciences 2009;21:333–9. doi:10.1016/S1001-0742(08)62273-1.

[23] Norbäck D, Torgén M, Edling C. Volatile organic compounds , respirable dust , and personal factors related to prevalence and incidence of sick building syndrome in primary schools. British Journal of Industrial Medicine 1990;47:733–41.

[24] Redlich CA, Sparer J, Cullen MR. Sick-building syndrome. Lancet 1997;349:1013–6. doi:10.1016/S0140-6736(96)07220-0.

[25] Apte MG, Daisey JM. VOCs and “ Sick Building Syndrome ”: Application of a New Statistical Approach for SBS Research to U . S . EPA BASE Study Data. Indoor Air 99, 1999, p. 2–7.

[26] ASTM Standard D5116-97. Standard guide for small-scale environmental chamber determinations of organic emissions from indoor material/products, 1997.

[27] ASTM Standard D6007-96. Standard test Method for determining Formaldehyde Concentrations in Air from Wood Products Using a Small Scale Chamber, 1996.

[28] Won D, Magee RJ, Lusztyk E, Nong G, Zhu JP, Zhang JS, et al. A comprehensive VOC emission database for coomonly-used building materials. 7th international conference of healthy buildings, 2003, p. 1–6.

[29] Ouazia B, Reardon J, Sander D. Making the Case of Reducing Ventilation Requirements Through Selection of Low-Emission Materials. NRC•CNRC n.d.

[30] Kim S, Kim H-J, Moon S-J. Evaluation of VOC Emissions from Building Finishing Materials Using a Small Chamber and VOC Analyser. Indoor and Built Environment 2006;15:511–23. doi:10.1177/1420326X06072040.

[31] Shin SH, Jo WK. Volatile organic compound concentrations, emission rates, and source apportionment in newly-built apartments at pre-occupancy stage. Chemosphere 2012;89:569–78. doi:10.1016/j.chemosphere.2012.05.054.

[32] Xiong J, Zhang Y, Huang S. Characterization of VOC and Formaldehyde Emission from Building Materials in Static Environmental Chamber: Model Development and Application. Indoor and Built Environment 2011;20:217–25. doi:10.1177/1420326X10387480.

[33] Knöppel H, Schauenburg H. Screening of household products for the emission of volatile organic compounds. Environment International 1989;15:413–8. doi:10.1016/0160-4120(89)90056-1.

[34] Lin C-C, Yu K-P, Zhao P, Whei-May Lee G. Evaluation of impact factors on VOC emissions and concentrations from wooden flooring based on chamber tests. Building and Environment 2009;44:525–33. doi:10.1016/j.buildenv.2008.04.015.

[35] Huang H, Haghighat F. Building materials VOC emissions—a systematic parametric study. Building and Environment 2003;38:995–1005. doi:10.1016/S0360-1323(03)00062-3.

[36] Kim S, Choi Y-K, Park K-W, Kim JT. Test methods and reduction of organic pollutant compound emissions from wood-based building and furniture materials. Bioresource Technology 2010;101:6562–8. doi:10.1016/j.biortech.2010.03.059.

[37] Jia C, Batterman S, Godwin C. VOCs in industrial, urban and suburban neighborhoods, Part 1: Indoor and outdoor concentrations, variation, and risk drivers. Atmospheric Environment 2008;42:2083–100. doi:10.1016/j.atmosenv.2007.11.055.

[38] Jia C, Batterman S, Godwin C, Charles S, Chin J-Y. Sources and migration of volatile organic compounds in mixed-use buildings. Indoor Air 2010;20:357–69. doi:10.1111/j.1600-0668.2010.00643.x.

[39] Schlink U, Rehwagen M, Damm M, Richter M, Borte M, Herbarth O. Seasonal cycle of indoor-VOCs: comparison of apartments and cities. Atmospheric Environment 2004;38:1181–90. doi:10.1016/j.atmosenv.2003.11.003.

[40] Zhang Y, Xu Y. Characteristics and correlations of VOC emissions from building materials. International Journal of Heat and Mass Transfer 2003;46:4877–83. doi:10.1016/S0017-9310(03)00352-1.

[41] Lee C-S, Haghighat F, Ghaly WS. A study on VOC source and sink behavior in porous building materials - analytical model development and assessment. Indoor Air 2005;15:183–96. doi:10.1111/j.1600-0668.2005.00335.x.

[42] Lee C-S, Haghighat F, Ghaly W. Conjugate Mass Transfer Modeling for VOC Source and Sink Behavior of Porous Building Materials: When to Apply It? Journal of Building Physics 2006;30:91–111. doi:10.1177/1744259106067683.

[43] Ayoko GA. Volatile Organic Compounds in Indoor Environments. 2004.

[44] Magee RJ, Bodalal A, Biesenthal TA, Lusztyk E, Brouzes M, Shaw CY. Prediction of VOC concentration profiles in a newly constructed house using samll chamber data and an IAQ simulation program. 9th International Conference on IAQ and Climate, 2002, p. 298–303.

[45] Berrios IT, Zhang J, Guo B, Smith J, Zhang Z. Volatile organic compounds (VOCS) emissions from sources in a partitioned office environment and their impact on IAQ. 10th International conference on indoor air quality and climate (indoor air), 2005.

[46] Molhave L, Clausen G, Berglund B, Ceaurriz JDE, Kettrup A, Lindvall T. Total Volatile Organic Compounds (TVOC) in Indoor Air Quality Investigations ". Indoor Air 1997;7:225–40.

[47] Filella I, Peñuelas J. Daily, weekly, and seasonal time courses of VOC concentrations in a semi-urban area near Barcelona. Atmospheric Environment 2006;40:7752–69. doi:10.1016/j.atmosenv.2006.08.002.

[48] Jia C, Batterman SA, Relyea GE. Variability of indoor and outdoor VOC measurements: an analysis using variance components. Environmental Pollution (Barking, Essex : 1987) 2012;169:152–9. doi:10.1016/j.envpol.2011.09.024.

[49] Haghighat F, Huang H. Integrated IAQ model for prediction of VOC emissions from building material. Building and Environment 2003;38:1007–17. doi:10.1016/S0360-1323(03)00064-7.

[50] Huang H, Haghighat F, Blondeau P. Volatile organic compound (VOC) adsorption on material: influence of gas phase concentration, relative humidity and VOC type. Indoor Air 2006;16:236–47. doi:10.1111/j.1600-0668.2005.00421.x.

[51] Missia DA, Demetriou E, Michael N, Tolis EI, Bartzis JG. Indoor exposure from building materials: A field study. Atmospheric Environment 2010;44:4388–95. doi:10.1016/j.atmosenv.2010.07.049.

[52] Jalaludin J, Nordiyana MS., Suhaimi NF. Exposure to indoor air pollutants (formaldehyde, VOCs, ultrafine particles) and respiratory health symptoms among office workers in old and new buildings in Universiti Putra Malaysia. International Journal of Applied and Natural Sciences 2014;3:69–80.

[53] Cabeza LF, Castellón C, Nogués M, Medrano M, Leppers R, Zubillaga O. Use of microencapsulated PCM in concrete walls for energy savings. Energy and Buildings 2007;39:113–9. doi:10.1016/j.enbuild.2006.03.030.

[54] Lee SH, Yoon SJ, Kim YG, Choi YC, Kim JH, Lee JG. Development of building materials by using micro-encapsulated phase change material. Korean Journal of Chemical Engineering 2007;24:332–5. doi:10.1007/s11814-007-5054-8.

[55] Zhou G, Zhang Y, Wang X, Lin K, Xiao W. An assessment of mixed type PCM-gypsum and shape-stabilized PCM plates in a building for passive solar heating. Solar Energy 2007;81:1351–60. doi:10.1016/j.solener.2007.01.014.

[56] Safari V, Barreneche C, Castell A, Basatni A, Navarro L, Cabeza L, et al. Volatile organic emission from PCM building materials. Innostock 2012 - The 12th International Conference on Energy Storage, 2012.

[57] Hunger M, Entrop AG, Mandilaras I, Brouwers HJH, Founti M. The behavior of self-compacting concrete containing micro-encapsulated Phase Change Materials. Cement and Concrete Composites 2009;31:731–43. doi:10.1016/j.cemconcomp.2009.08.002.

Chapter 5 . Phase Change Slurries

5.1 Phase Change Slurries

5.2 Thermal reliability of PCS

5.3 Comparison of commercial PCS with a laboratory prepared sample

5.1 Phase Change Slurries

When MPCM is fabricated as a powder [1], it can be mixed with a carrier fluid such as water [2,3] or with other substances as glycol [4,5] or glycerol [6,7], creating a Phase Change Slurry (PCS), which are used in active systems. PCS not only acts as an energy storage device but also as a heat transport system, as Salunkhe *et al* [24] reported in their review.

Phase Change Slurries (PCS) [8,9] is one important application into the MPCM systems. These materials are widely used in several fields, like in pumping active systems [10], refrigeration [7,11], in air conditioning [12,13], in heat exchangers [14], heating [15,16], ventilation and air-conditioning (HVAC) [11,17,18], solar energy [2,9], and cold storage [10,19,20] applications, and the structure, the physical, and chemical properties of the PCS will define the final application. The purpose in these kinds of systems is to improve thermal performance of heat exchangers. Because the microcapsules into the PCS solution need to sustain the high shear caused by pumping the suspension without being broken [9,14,15,18,19,21–23], some of the aspects are related with the mechanical properties of the MPCM. The mechanical characterization allows information about the mechanical behavior of the samples when they are in service [24,25]. Therefore, the manner of pumping the slurries in an active system is an important issue to take into account [10,20]. Zeng *et al.* [26] studied numerically the influences of microparticles and phase change in fluid-pure water, PCS and MPCM. Besides, Huang *et al.* [27] and Günter *et al.* [28] studied the subcooling in PCM emulsion, remarking that in PCS applications, the changed nucleation and solidification behavior of different paraffin–water emulsions has shown that paraffins in emulsified form as finely dispersed droplets behave significantly different than in the bulk.

5.2 Thermal reliability of PCS

The study of the MPCM performance for their use in active systems is a key point before the system design. Due to the possible physicochemical changes of PCS after several thermal cycles attributed to a partial degradation of the microcapsules by breakage, physicochemical, thermophysical and mechanical properties of Micronal® DS 5007 X were reported in the paper titled “**Physicochemical and thermal study of a MPCM of PMMA shell**

and paraffin wax as a core”, published in 2014 in **Energy Procedia** journal in volume 48 between pages 347 - 354 [25] (Figure 5.1). Besides, this study was presented in an oral presentation in the congress **SHC 2013, International Conference on Solar Heating and Cooling for Buildings and Industry**, in 2013, in Freiburg (Germany).

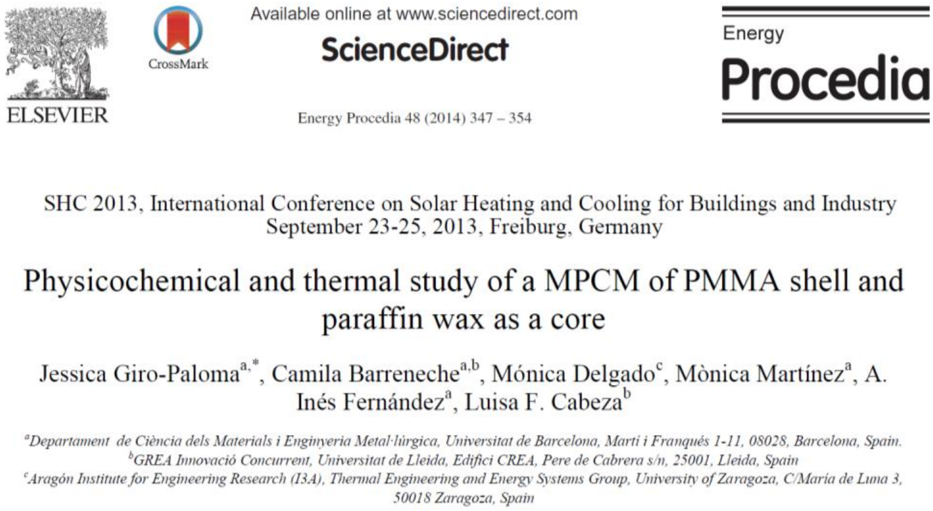

ELSEVIER

CrossMark

Available online at www.sciencedirect.com

ScienceDirect

Energy Procedia 48 (2014) 347 – 354

Energy Procedia

SHC 2013, International Conference on Solar Heating and Cooling for Buildings and Industry
September 23-25, 2013, Freiburg, Germany

Physicochemical and thermal study of a MPCM of PMMA shell and paraffin wax as a core

Jessica Giro-Paloma[a,*], Camila Barreneche[a,b], Mónica Delgado[c], Mònica Martínez[a], A. Inés Fernández[a], Luisa F. Cabeza[b]

[a]Departament de Ciència dels Materials i Enginyeria Metal·lúrgica, Universitat de Barcelona, Martí i Franqués 1-11, 08028, Barcelona, Spain.
[b]GREA Innovació Concurrent, Universitat de Lleida, Edifici CREA, Pere de Cabrera s/n, 25001, Lleida, Spain
[c]Aragón Institute for Engineering Research (I3A), Thermal Engineering and Energy Systems Group, University of Zaragoza, C/María de Luna 3, 50018 Zaragoza, Spain

Figure 5.1.Paper published in 2014 in Energy Procedia journal titled: “Physicochemical and thermal study of a MPCM of PMMA shell and paraffin wax as a core”.

The studied PCS, Micronal® DS 5007 X, consists on a water suspension and spherical Micronal® DS 5001 X microcapsules (BASF). The microcapsules of 5 μm consist on paraffin PCM core and an acrylic shell, with shell thickness of 0.5 μm. In Figure 5.2 is shown an image of the studied sample, Micronal® DS 5007. As it can be seen, after several days resting on, the slurry was separated into two phases and the sample was not stable enough.

Figure 5.2. Image of Micronal® DS 5007 X sample used for the study titled “Physicochemical and thermal study of a MPCM of PMMA shell and paraffin wax as a core”.

Characterization of the sample by thermogravimetrical analysis demonstrates that the sample decomposes in three steps. The first one due to the evaporation of the water content of the sample (65.6 %), then the PCM content, which is 22.46 % in weight, and the third step is related to the acrylic shell decomposition and it corresponds to a 6.66 % in weight. There was a residue content of 5.13 %. The thermal performance by DSC revealed that the melting temperature and the solidification temperature are 23.4 ºC and 22.3 ºC, respectively. Besides, the results of the melting enthalpy and solidification enthalpy, although they are not repeatable because of the difficulty of taking a homogeneous PCS aliquot, are 98.3 $kJ\cdot kg^{-1}$ and 75.8 $kJ\cdot kg^{-1}$, respectively. In addition, it was evaluated the required force to break the microcapsules and the effective Young’s Modulus (E_{eff}) at 23 ºC and 45 ºC to distinguish the mechanical MPCM behavior when the PCM is melted and solidified. The fracture load to break the MPCM at 23 ºC is 11 μN and 1.7 μN at 45 ºC, and the E_{eff} result for the sample at 23 ºC is 200 MPa and at 45 ºC is 50 MPa. Hence, the most important conclusion is related to the mechanical properties, which depend on the working temperature.

Available online at www.sciencedirect.com

ScienceDirect

Energy Procedia 48 (2014) 347 – 354

Energy Procedia

SHC 2013, International Conference on Solar Heating and Cooling for Buildings and Industry
September 23-25, 2013, Freiburg, Germany

Physicochemical and thermal study of a MPCM of PMMA shell and paraffin wax as a core

Jessica Giro-Paloma[a,*], Camila Barreneche[a,b], Mónica Delgado[c], Mònica Martínez[a], A. Inés Fernández[a], Luisa F. Cabeza[b]

[a]*Departament de Ciència dels Materials i Enginyeria Metal·lúrgica, Universitat de Barcelona, Martí i Franqués 1-11, 08028, Barcelona, Spain.*
[b]*GREA Innovació Concurrent, Universitat de Lleida, Edifici CREA, Pere de Cabrera s/n, 25001, Lleida, Spain*
[c]*Aragón Institute for Engineering Research (I3A), Thermal Engineering and Energy Systems Group, University of Zaragoza, C/María de Luna 3, 50018 Zaragoza, Spain*

Abstract

The present work studies a Phase Change Slurry (PCS) as a proposed Thermal Energy Storage (TES) medium. Microencapsulation is an advanced technology to implement PCMs (Phase Change Material) avoiding leakage from building materials. The morphology and physicochemical properties of this Microencapsulated Phase Change Material (MPCM) sample were analyzed using some analytical techniques like Scanning Electron Microscopy (SEM), Infrared Spectroscopy (FT-IR), Thermogravimetrical Analysis (TGA), Differential Scanning Calorimeter (DSC), and Atomic Force Microscopy (AFM). The results showed that Micronal® DS 5007 is a suitable candidate to be used as slurry in active systems due to their studied mechanical properties.

Selection and peer review by the scientific conference committee of SHC 2013 under responsibility of PSE AG

Keywords: Microencapsulated Phase Change Material; Phase Change Slurry; PSD; SEM; FTIR; TGA; DSC; AFM

---

1. Introduction

Phase Change Materials (PCM) are commonly contained in microcapsules in order to avoid the leakage, and conserve the efficiency of the thermophysical properties when they are implemented in slurry active systems [1]. These microcapsules comprise a polymeric shell where a PCM, usually a paraffinic one, is contained at the core. PCM have been developed in slurries form to improve the heat transfer rate of the carrier fluid, obtaining the Phase Change Slurries (PCS). There are several applications where PCS can be implemented such as heating [1],

Selection and peer review by the scientific conference committee of SHC 2013 under responsibility of PSE AG
doi:10.1016/j.egypro.2014.02.040

refrigeration [2], air-conditioning [3], heat exchangers [4], and ventilation [5]. It is well known that there are physicochemical changes on this type of PCS after several thermal cycles [6]. These changes are attributed to a partial degradation of the microcapsules by breakage [7]. For this purpose, physicochemical, thermophysical and mechanical properties of Micronal® DS 5007 are studied in this paper. Micronal® DS 5007 from BASF® consist on a suspension of water and microcapsules (5:2). Moreover, the structure and the physicochemical properties of the slurries will define the final application. Therefore, the main objective of this paper is to study the mechanical performance of this Microencapsulated Phase Change Material (MPCM) to be applied as PCS for their use in active systems.

2. Materials and methodology

Micronal® DS 5007 is a PCS which is normally used in active systems. To characterize this sample deeply, Fourier Transformed Infrared Spectroscopy (FT-IR) was used to characterize the polymeric shell of this PCS with a Spectrum Two™ from Perkin Elmer. Microcapsules' size and morphology were studied evaluating the Particle Size Distribution (PSD) using a Beckman Coulter® LSTM 13 320, and microcapsules were observed with Scanning Electron Microscopy (SEM) using a Jeol JSM-6510.

Thermal stability of the samples was evaluated with a Simultaneous SDTQ600 TA Instruments device under dried air atmosphere. The scanning rate of the Thermogravimetrical Analysis (TGA) used was 0.5 $K\cdot min^{-1}$ in the temperature range between 25 and 30 ºC. Then, temperature was increased under 1 $K\cdot min^{-1}$ heating rate from 30 to 100 ºC and 5 $K\cdot min^{-1}$ from 100 to 600 ºC. Hyphenated technique is used coupling a FT-IR detector in the TGA gas output to analyze the gradation products. In addition, Differential Scanning Calorimetry (DSC) was used to analyze the melting temperature and the melting enthalpy of PCM between 10 ºC and 40 ºC, applying 0.5 $K\cdot min^{-1}$ dynamic mode, following the study of Barreneche *et al.* [8] using a DS 822e by Mettler Toledo. Finally, Atomic Force Microscopy (AFM) was performed to determine the force that has to be applied to break the shell of the Micronal® DS5007 MPCM with a Peak Force Quantitative Nanomechanics mode (QNM), with a diamond probe from Bruker which has 388 $Nn\cdot nm^{-1}$ spring constant.

3. Results and discussion

3.1. Physicochemical and thermophysical characterization

3.1.1. Size and morphology of MPCM

The PSD in volume shows unimodal distribution of particle size ranging in the interval between 2 and 12 μm. The average diameter of the PCS was 4.880 μm as it can be observed in Fig. 1.

Furthermore, MPCM morphology was analyzed by Scanning Electron Microscopy (SEM), the sample under study was pretreated by drying the microcapsules at room temperature before its observation. The size morphological results of the Micronal® DS 5007 show that the capsules are roughly 5 μm diameter as it is observed in Figure 2a, which agree with the PSD results. Besides, the wall thickness was estimated for broken microcapsules (deformed by compaction) showing a thickness around 0.5 μm (Figure 2b).

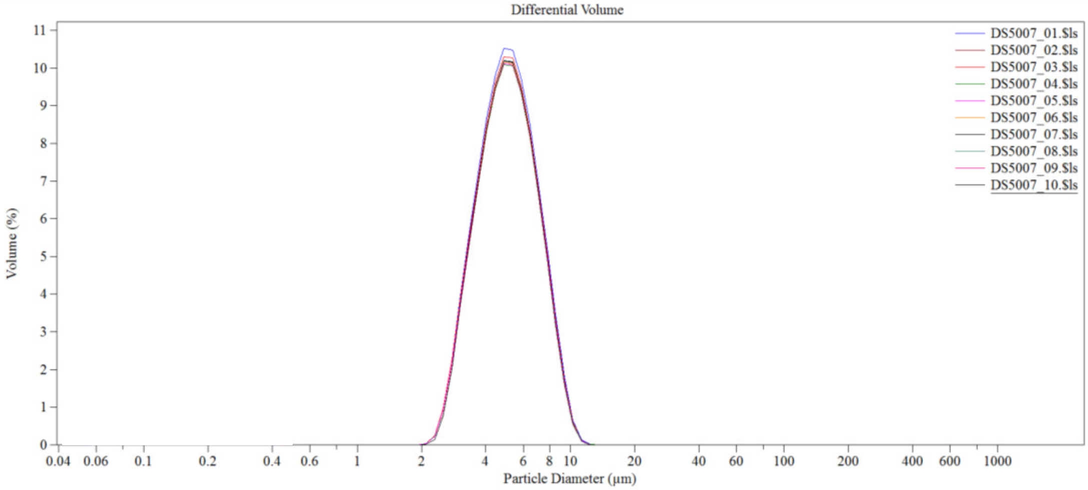

Fig. 1. Particle Size Distribution (PSD) of Micronal® DS 5007.

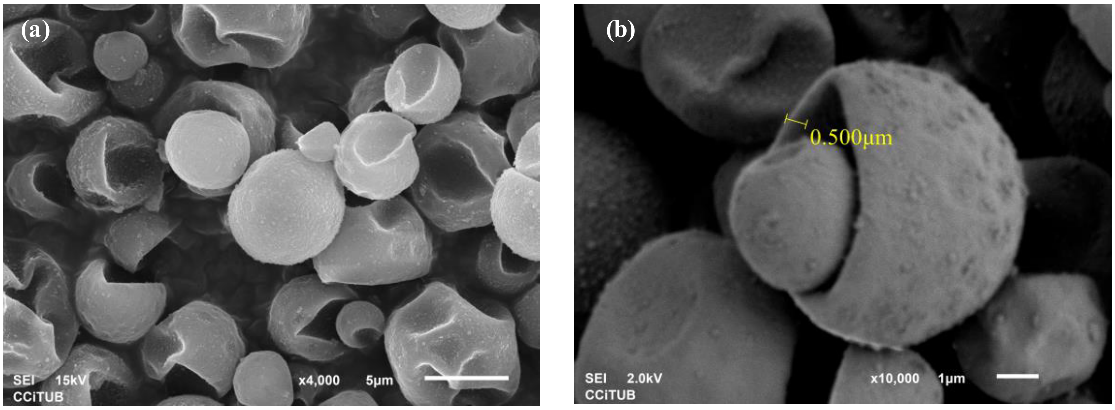

Fig. 2. Scanning Electron Microscopy (SEM) images of Micronal® DS 5007 (a) shape and size of the microcapsules; (b) wall shell thickness.

3.1.2. Chemical characterization

Chemical characterization of the shell was performed with Fourier-Transformed Infrared (FT-IR) by Attenuated Total Reflectance (ATR), which was used to characterize the most important peaks for the polymeric shell of the MPCM. Table 1 lists the characteristic peaks found. Thereby, these peaks correspond to an acrylic polymer like PMMA.

Table 1. FT-IR characteristic peaks obtained from MPCM shell.

FTIR Peak (cm^{-1})	3368.9	2920.9	2852.0	1729.5	1466.6	1123.5	720.5
Attributed to	aqueous suspension	aliphatic C-H stretching vibration	aliphatic C-H stretching vibration	ester carbonyl group stretching vibration	C-H bending vibration	C-O stretching vibration of the ester group	C-H bending

3.1.3. Thermal stability

The thermal degradation of Micronal® DS 5007 sample was evaluated and three processes from TGA results were observed, as it is shown in Figure 3. The first weight loss from 25 ºC to 93.9 ºC is due to the water content of the PCS, and it corresponds to 65.60 % wt. The second one from 93.9 ºC to 245.1 ºC confirms the presence of the paraffin wax contained inside the shell, and it represents the 65.73 % wt. of the dry sample. Finally, the third weight loss from 245.1 ºC to 408.6 ºC is due to the acrylic shell [9], and the thermal degradation contributes on 19.36 % wt. of the dry sample. The wall shell degradation step is the last one and it starts after the microcapsule degradation. The total residue of the dry sample is 14.91 % wt.

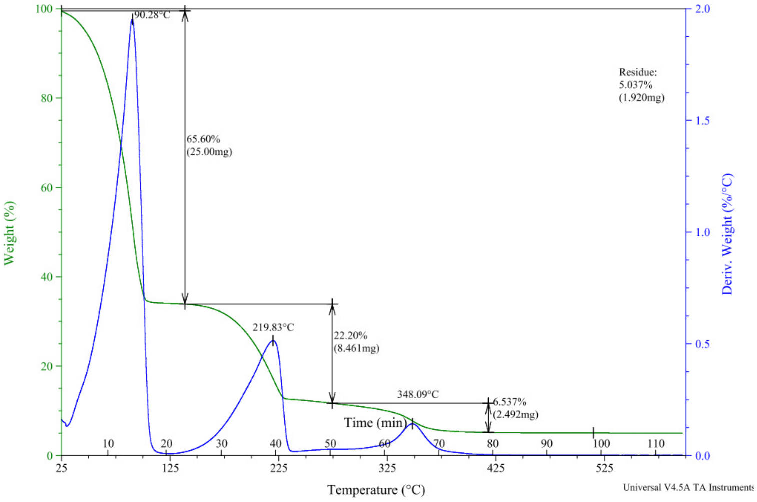

Fig. 3. Thermogravimetrical Analysis (TGA) of the PCS Micronal® DS 5007.

After coupling the TGA with the FT-IR, the gas was analyzed over time and 0 s, 1900 s, 3400 s, and 7600 s spectra are shown in Fig. 4. As it is observed in this figure, there are two different signals on the FT-IR spectra: at the beginning and at the end of the analysis (0 s and 7600 s) there were not characteristic peaks, and it can be observed that at 1900 s and 3400 s the corresponding peaks of functional groups resulting from the thermal degradation of an acrylic polymer.

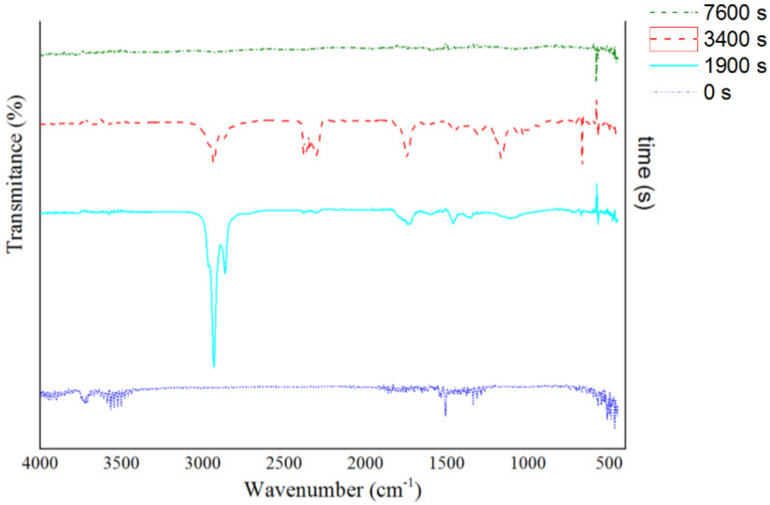

Fig. 4. FT-IR gas analysis from a calcinated Micronal® DS 5007 sample of TGA

3.1.4. Differential Scanning Calorimetry (DSC)

The results obtained from DSC analysis were 98.3 kJ·kg^{-1} and 75.8 kJ·kg^{-1} for the melting enthalpy and solidification enthalpy, respectively. Thereby, the sample studied with DSC contemplates all the system composed by water-dispersant/shell/PCM. The results were not repeatable due to the difficulty of taking a homogeneous PCS aliquot.

Moreover, the melting temperature obtained for this PCS is 23.4 ºC and the solidification temperature is 22.3 ºC (both between 14-24 ºC).

3.2. Stiffness characterization

Several experiments were carried out using Atomic Force Microscopy in nanoindentation mode [10] to evaluate the required force to break the microcapsules to use it in active systems. In addition, effective Young's Modulus (E_{eff}) at different temperatures (23 ºC and 45 ºC) was evaluated in order to distinguish the mechanical MPCM behavior when the PCM is melted and solidified.

The main results obtained are shown in Fig. 5 and 6, where it is shown that the fracture load for the microcapsules at 23 ºC was 11 μN, and 1.7 μN at 45 ºC. The deflection error is proportional to the applied force.

Furthermore, the shape of the MPCM changes when Micronal® DS 5007 is heated up, producing an expansion of the microcapsule, as it can be observed in Fig. 7.

Moreover, effective Young's modulus (E_{eff}) mapping is shown in Fig. 8 at 0.5 kHz per second. The flatter area studied was 10 x10 μm MPCM region at 23 ºC.

Besides, the deformation histogram is evaluated in Fig. 8 and a deformation from 10 to 20 nm with a great distribution of values is observed. The *y* axis represents the total pixels amounts for this area, and a 0.1 % of the total pixels belong to the results. Moreover, when a vertical force of 500 nN is applied on the top of the MPCM, the E_{eff} value was 200 MPa.

Furthermore, the same study was performed at 45 ºC, and it is shown in Fig. 9. In this case, the deformation histogram was given between 5 to 30 nm, and the result of the E_{eff} histogram applying 500 nN was 50 MPa, four times lower due to the softening of the polymer as well as liquid state of PCM.

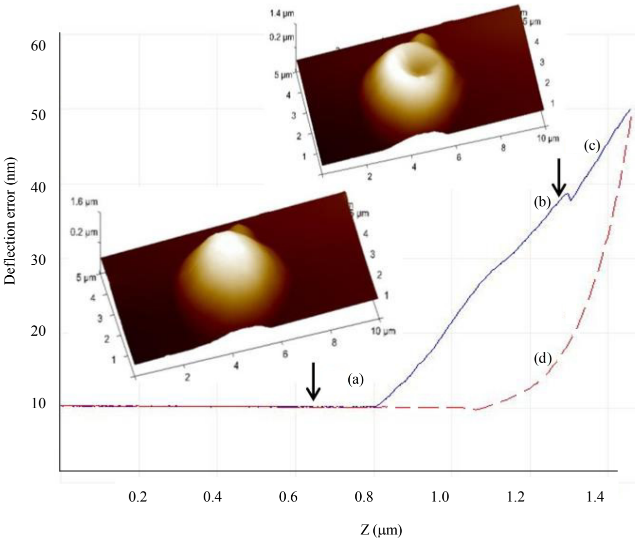

Fig. 5. Topographic Atomic Force Microscopy (AFM) images for Micronal® DS 5007 at 23 ºC, (a) unbroken microcapsule; (b) plastic penetration where the fracture load was 11 μN; (c) deformation of the sample; and (d) unbroken microcapsule. The solid line was the deflection error (nm), and the dotted line was the retraction of the AFM probe.

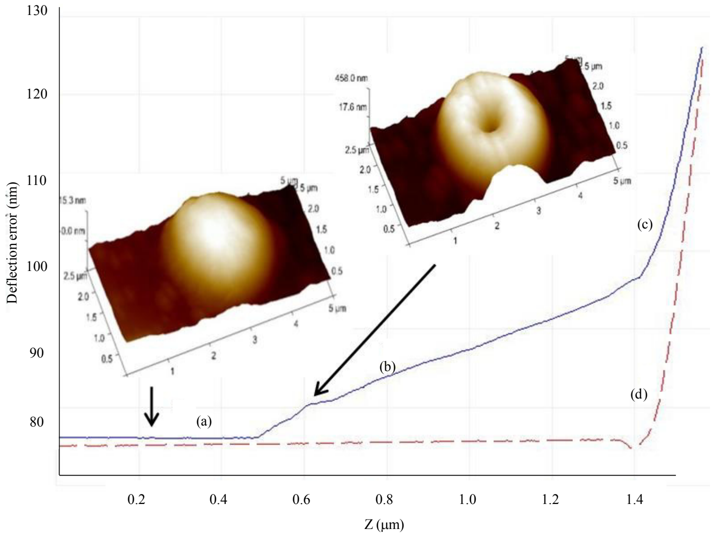

Fig. 6. Topographic Atomic Force Microscopy (AFM) images for Micronal® DS 5007 at 45 ºC, (a) unbroken microcapsule; (b) fracture load of 1.7 µN in the plastic penetration; (c) deformation of the sample; and (d) unbroken microcapsule. The solid line was the deflection error (nm), and the dotted line was the retraction of the AFM probe.

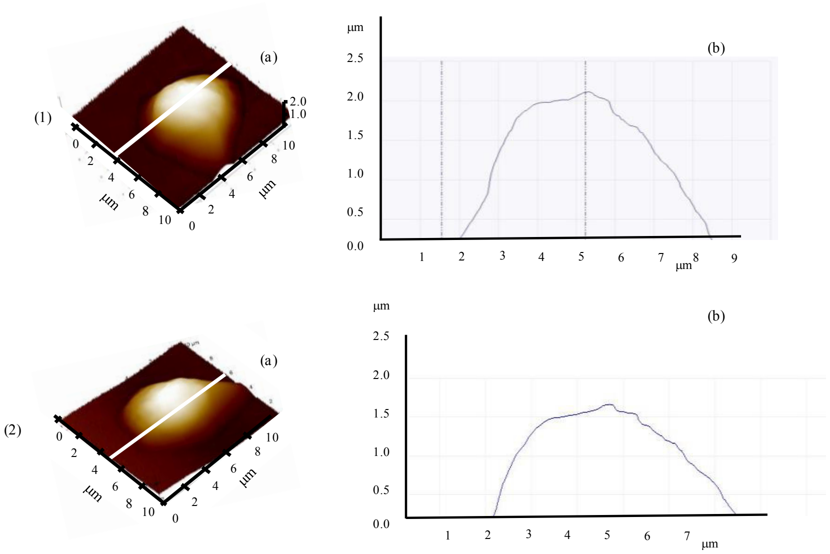

Fig. 7. Micronal® DS 5007's sample at (1) 23 ºC and, (2) 45 ºC; (a) 3D view, and (b) topographic image of 10x10 µm

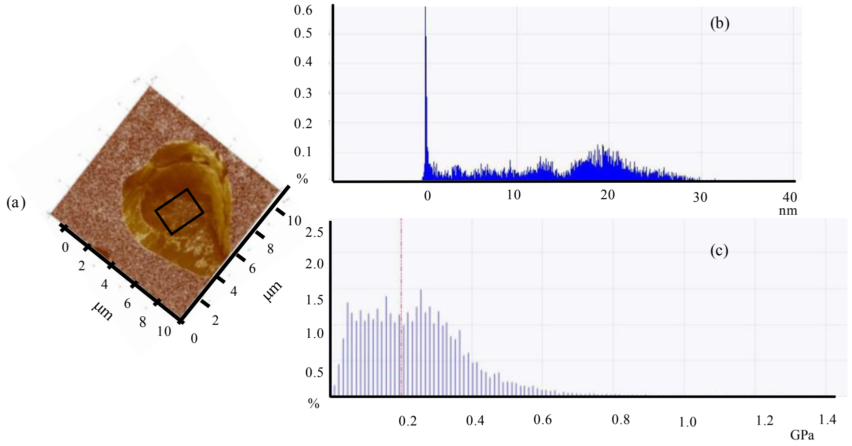

Fig. 8. Effective Young's modulus (E_{eff}) mapping of Micronal® DS 5007 at 23 ºC; (a) 3D view; (b) Deformation histogram; (c) E histogram.

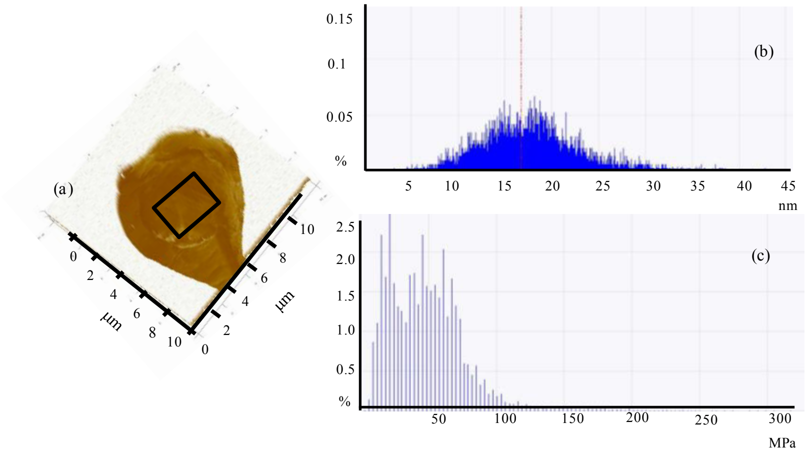

Fig. 9. Effective Young's modulus (E_{eff}) mapping for Micronal® DS 5007 at 45 ºC; (a) 3D view; (b) Deformation histogram; (c) E histogram

4. Conclusions

The PCS Micronal® DS 5007 consists on paraffin PCM core and PMMA as a shell as FT-IR results showed. The study of the size and morphology of the microcapsules reveal spherical particles of 5 µm diameter and 0.5 µm wall shell thickness. The thermal degradation was observed in three steps. Moreover, the required applied load in order to break the sample was not constant and it depends on the working temperature. Hence, the temperature is a key point to take into account considering these systems.

In summary, from the mechanical point of view, acrylate groups to be used as a shell of microcapsules are a suitable choice for TES active systems for the obtained results in this paper.

Acknowledgements

The work is partially funded by the Spanish government (ENE2011-28269-C03-02, ENE2011-22722, and ENE2011-28269-C03-01). The authors would like to thank the Catalan Government for the quality accreditation given to their research group GREA (2009 SGR 534) and research group DIOPMA (2009 SGR 645).

References

[1] Griffiths PW, Eames PC. Performance of chilled ceiling panels using phase change materials slurries as the heat transport medium. Appl Therm Eng 2007; 27:1756-1766.

[2] Youssef Z, Delahaye A, Huang L, Trinquet F, Fournaison L, Pollerberg C, Doetsch C. State of the art on phase change material slurries. Energ Convers Manage 2013; 65:120-132.

[3] Diaconu BM, Varga S, Olivera AC. Experimetal assessment of heat storage properties and heat transfer characteristics of a phase change material slurry for air conditioning applications. Appl Energ 2010; 87:620-628.

[4] Delgado M, Lázaro A, Mazo J, Zalba B. Review on phase change material emulsions and microencapsulated pahse change material slurries: Materials, heat transfer studies and applications. Renew Sust Energ Rev 2012; 16:253-273.

[5] Abduljalil A Al-Abidi, Sohif Bin Mat, K Sopian, MY Sulaiman, CH Lim, Abdulrahman Th. Review of thermal energy storage for air conditioning systems. Renew Sust Energ Rev 2012; 16:5802-5819.

[6] Alkan C, Sari A, Karaipekli A, Uzun O. Preparation, characterization, and thermal properties of microencapsulated phase change material for thermal energy storage. Sol Energ Mat Sol C 2009; 93:143-147.

[7] Diaconu BM, Varga S, Oliveira AC. Experimental assessment of heat storage properties and heat transfer characteristics of a phase change material slurry for air conditioning applications. Appl Energ 2010; 87(2):620-628.

[8] Barreneche C, Solé A, Miró L, Martorell I, Fernández AI, Cabeza LF. Thermochim Acta 2013;553:23-26.

[9] Costache MC, Wang D, Heidecker MJ, Manias E, Wilkie CA. The thermal degradation of poly(methyl methacrylate) nanocomposites with montmorillonite, layered double hydroxides and carbon nanotubes. Polym. Adv. Technol. 2006; 17: 272-280.

[10] Giro-Paloma J, Oncins G, Barreneche C, Martínez M, Fernández AI, Cabeza LF. Physico-chemical and mechanical properties of microencapsulated phase change material. Appl Energ 2013; 109:441-448.

5.3 Comparison of a commercial PCS with a laboratory prepared sample

It is very important to follow a protocol in measuring the PCS properties taking into account some parameters such as type of core, shell, encapsulation ratio, etc. Moreover, it is especially significant to emphasize the provenance of the sample: commercial or laboratory preparation because it is indispensable to compare the chemical, physical, thermal, and mechanical properties of microcapsules to better characterize the laboratory samples and commercialize them. In this case, it was studied the commercial sample Micronal® DS 5007 X from BASF and a laboratory made named PCS28. Both samples may act as PCS used in active systems. Micronal® DS 5007 X is a microencapsulated slurry sample composed by water and an acrylic shell and *n*-octadecane as MPCM, with a ratio water:MPCM of 2.4:1, and an average size of the microcapsules around 7.5 μm. On the other hand, PCS28 (Figure 5.3) is a laboratory prepared sample at University of Ljubljana (Slovenia) based on water and MPCM composed by melamine-formaldehyde (MF) as a shell and *n*-octadecane as PCM, with a proportion of water:MPCM of 2:1. The average size of this PCS is 6.6 μm.

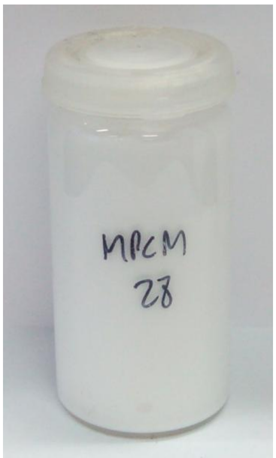

Figure 5.3. Image of PCS28. It is one of the samples used in the studies titled “Comparison of Phase Change Slurries. Physicochemical and thermal properties” and “Mechanical response evaluation of microcapsules from different slurries”. The other sample of the study was shown in Figure 5.2.

Two manuscripts were published in 2015. The first one was published in **Energy** journal in volume 87, between pages 223 - 227, as Figure 5.4 shows, with the title

“**Comparison of Phase Change Slurries. Physicochemical and thermal properties**”. The impact factor of this journal in 2013 was 4.159. The second paper was accepted in 2015 to **Renewable Energy** journal in volume 85, between pages 732 - 739, and its titled is “**Mechanical response evaluation of microcapsules from different slurries**”, as Figure 5.5 shows. This journal had an impact factor of 3.361 in 2013.

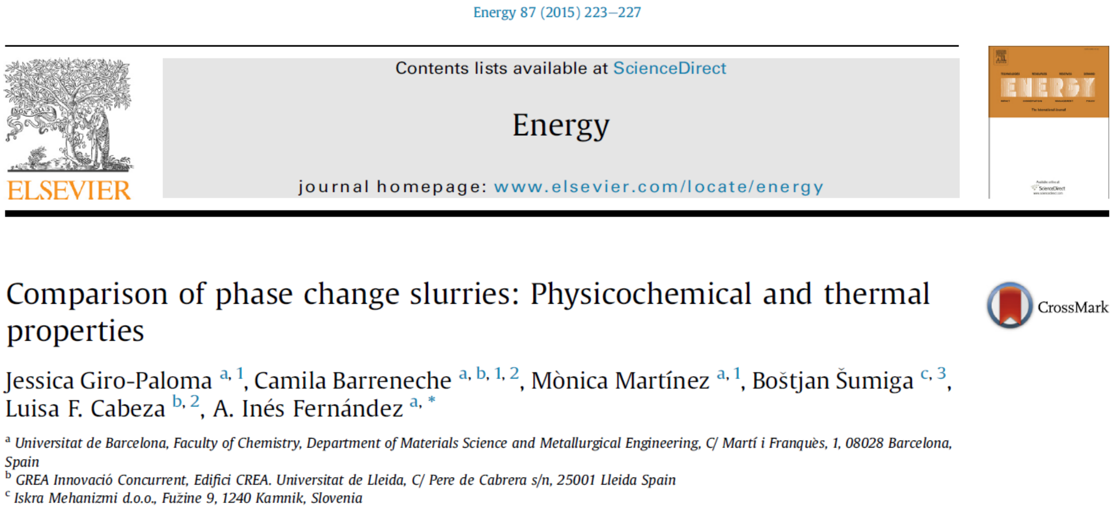

Energy 87 (2015) 223–227

Contents lists available at ScienceDirect

Energy

journal homepage: www.elsevier.com/locate/energy

Comparison of phase change slurries: Physicochemical and thermal properties

Jessica Giro-Paloma [a, 1], Camila Barreneche [a, b, 1, 2], Mònica Martínez [a, 1], Boštjan Šumiga [c, 3], Luisa F. Cabeza [b, 2], A. Inés Fernández [a, *]

[a] Universitat de Barcelona, Faculty of Chemistry, Department of Materials Science and Metallurgical Engineering, C/ Martí i Franquès, 1, 08028 Barcelona, Spain
[b] GREA Innovació Concurrent, Edifici CREA. Universitat de Lleida, C/ Pere de Cabrera s/n, 25001 Lleida Spain
[c] Iskra Mehanizmi d.o.o., Fužine 9, 1240 Kamnik, Slovenia

Figure 5.4. Paper published in Energy journal titled: “Comparison of Phase Change Slurries. Physicochemical and thermal properties”.

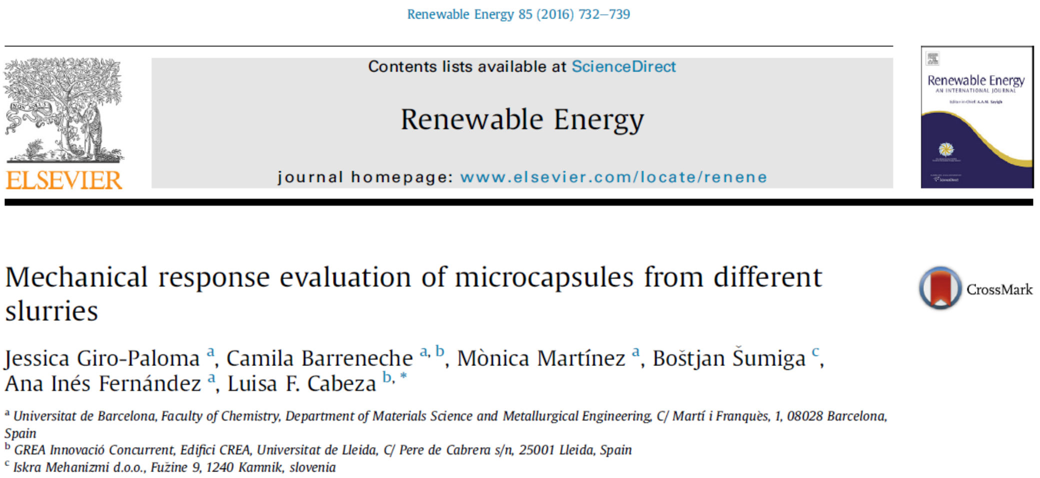

Renewable Energy 85 (2016) 732–739

Contents lists available at ScienceDirect

Renewable Energy

journal homepage: www.elsevier.com/locate/renene

Mechanical response evaluation of microcapsules from different slurries

Jessica Giro-Paloma [a], Camila Barreneche [a, b], Mònica Martínez [a], Boštjan Šumiga [c], Ana Inés Fernández [a], Luisa F. Cabeza [b, *]

[a] Universitat de Barcelona, Faculty of Chemistry, Department of Materials Science and Metallurgical Engineering, C/ Martí i Franquès, 1, 08028 Barcelona, Spain
[b] GREA Innovació Concurrent, Edifici CREA, Universitat de Lleida, C/ Pere de Cabrera s/n, 25001 Lleida, Spain
[c] Iskra Mehanizmi d.o.o., Fužine 9, 1240 Kamnik, slovenia

Figure 5.5. Published paper in Renewable energy journal titled: “Mechanical response evaluation of microcapsules from different slurries”.

5.3.1. Physico-chemical and thermal properties

The first one titled “**Comparison of Phase Change Slurries. Physicochemical and thermal properties**” is based on the thermal properties of both PCS, using Differential Scanning Calorimetry (DSC), Thermogravimetrical analysis (TGA), Fourier Transformed Infrared Spectroscopy (FT-IR) with ATR, and TGA coupled with FT-IR. In this paper, the most important conclusions about the two different PCS samples (Micronal® DS 5007 X and PCS28) which contain different materials for the shell (acrylic polymer and melamine-formaldehyde, respectively) and different core reported that the phase change of Micronal® DS 5007 X is between 21 ºC and 23 ºC with an enthalpy around 90 $kJ \cdot kg^{-1}$ a melting temperature between 22 ºC and 27 ºC with an enthalpy of 50 $kJ \cdot kg^{-1}$ for PCS28. Thermogravimetrical investigation (TGA) showed better thermal stability for PCS28 than Micronal® DS 5007 X. Overall, both PCS are totally capable of developing their role in thermal energy storage field, and they can be considered as PCS candidates for TES in active or passive building applications.

Energy 87 (2015) 223–227

Contents lists available at ScienceDirect

Energy

journal homepage: www.elsevier.com/locate/energy

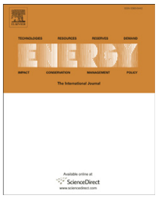

Comparison of phase change slurries: Physicochemical and thermal properties

Jessica Giro-Paloma [a, 1], Camila Barreneche [a, b, 1, 2], Mònica Martínez [a, 1], Boštjan Šumiga [c, 3], Luisa F. Cabeza [b, 2], A. Inés Fernández [a, *]

[a] *Universitat de Barcelona, Faculty of Chemistry, Department of Materials Science and Metallurgical Engineering, C/ Martí i Franquès, 1, 08028 Barcelona, Spain*
[b] *GREA Innovació Concurrent, Edifici CREA. Universitat de Lleida, C/ Pere de Cabrera s/n, 25001 Lleida Spain*
[c] *Iskra Mehanizmi d.o.o., Fužine 9, 1240 Kamnik, Slovenia*

ARTICLE INFO

Article history:
Received 20 November 2014
Received in revised form
10 April 2015
Accepted 26 April 2015
Available online 16 May 2015

Keywords:
Phase change materials
Microencapsulated phase change material
Phase change slurry
Thermophysical properties
FT-IR
DSC

ABSTRACT

Phase change slurries (PCS) consist on a carrier fluid binary system, where water is mostly used as continuous phase and micro-encapsulated phase change materials (MPCM) are used as dispersed phase. PCS are used in Thermal Energy Storage (TES) for building applications, combining the latent heat capacity of the MPCM with the sensible heat capacity of the carrier fluid, and at the same time giving the PCM pumpable properties. In this study, two PCS samples are compared and characterized, the commercial Micronal® DS 5007 X from BASF and a laboratory made PCS28. Thereby, in this paper thermal stability is studied by using thermogravimetrical analysis (TGA) and the main components of the MPCM have been studied using Fourier transformed infrared spectroscopy (FT-IR). Moreover, TGA coupled with FT-IR is used to study deeply the thermal decompositions of the PCS microcapsules and products derived thereof. Finally, differential scanning calorimetry (DSC) is performed to study the melting enthalpy and the melting temperature range of the phase change material (PCM). This paper concludes that both types of PCS have good potential from thermal energy storage purposes such as solar space heating applications.

1. Introduction

Phase Change Materials (PCM) absorb energy during the heating process and release the energy to the environment during the cooling process. One of the biggest drawbacks of the PCM incorporation for technical used is due to the liquid migration (leakage). Accordingly, microcapsules were thought to solve this problem. Microencapsulated Phase Change Materials (MPCM) are composed by a PCM as a core [1] and a polymer or an inorganic wall used as shell [2]. They are micro-containers with a hydrophobic core material and a hard shell which accept volume changes, maintaining the shape to conserve the form and avoid the PCM leakage when the phase change occurs. MPCM attribute thermoregulatory properties to materials [3] and they must be enclosed in thin and resistant polymer shells for changing solid to liquid phase change and back again within the shells.

Organic PCM have been proposed as one of the most significant thermal energy storage materials [4–6] because of their advantageous thermal and heat transfer characteristics [7]. Moreover, PMMA is also a widely used polymer as a shell [8–12]. Nevertheless, the PCM which is mainly used and studied is *n*-octadecane [13–16]. This PCM is commonly encapsulated with melamine-formaldehyde shell [7,17–19], although there are a lot of PCM possibilities as a core, and materials as a shell [20,21]. It is known that the physicochemical properties of all type of microcapsules after several thermal cycles change [22], and these changes are attributed to a partial degradation of the microcapsules by breakage [23].

Encapsulating PCM in a firm substance with small enough diameter to be suspended in a liquid (partially melting and

---

[*] Corresponding author. Tel.: +34 934021298; fax: +34 934035438.
E-mail addresses: jessicagiro@ub.edu (J. Giro-Paloma), c.barreneche@ub.edu (C. Barreneche), monicamartinez@ub.edu (M. Martínez), bostjan.sumiga@iskra-mehanizmi.si (B. Šumiga), lcabeza@diei.udl.cat (L.F. Cabeza), ana_inesfernandez@ub.edu (A.I. Fernández).
[1] Tel.: +34 934021298; fax: +34 934035438.
[2] Tel.: +34 973003576; fax: +34 973003575.
[3] Tel.: +386 18309850; fax: +386 18309867.

http://dx.doi.org/10.1016/j.energy.2015.04.071
0360-5442/© 2015 Elsevier Ltd. All rights reserved.

solidifying slurries) can be done with high energy densities and heat transfer rates [24]. Phase change slurries (PCS) consist on a carried fluid binary system (water is mostly used as a continuous phase) and MPCM (as a dispersed phase) [25], and may be used in active or passive systems [26–28], having several applications in different fields [29] such as heating [30], air-conditioning [31] and ventilation [32], refrigeration [33] and heat exchangers, most of them in buildings [34–38].

In this study, an evaluation between two PCS able to be used for thermal energy storage (TES) in buildings was performed. The main objective is the characterization and the comparison of two different PCS, a commercial one and a laboratory made one. The most important reason to compare two PCS samples with different types of microcapsules is based on deciding the best candidate to be used in a TES field for active systems in building applications. Besides, as novelty, two different PCS sources (commercial and laboratory made) were compared to ensure that the obtained thermal properties for both samples are similar and good enough to choose both as possible samples to apply in an active system. This paper includes thermophysical and chemical properties of the two studied slurries, while other properties will be covered in a second paper [39]. It was evaluated different techniques to compare them physicochemically and thermally. Thermogravimetrical analysis (TGA) and differential scanning calorimetry (DSC) were used to measure the thermophysical properties and the thermal stability of the PCS under study. Furthermore, to study the composition of the polymer used as the shell of the microcapsules it was performed a Fourier transform infrared (FT-IR). Besides, the characterization of the chemical functionality for the volatile emissions during the decomposition of the PCS microcapsules was studied with TGA coupled with FT-IR.

2. Materials and methods

2.1. Materials

Micronal® DS 5007 X from BASF company is a microencapsulated slurry sample which is used in active systems and composed of an acrylic shell and *n*-octadecane as PCM with an average size of the microcapsules is around 7.5 μm. The other sample is a laboratory suspension of microcapsules prepared at the University of Ljubljana (Slovenia) named PCS28 based on analysis and experimental optimization of in situ polymerisation technology composed of melamine-formaldehyde (MF) as a shell and *n*-octadecane as PCM, and with an average size of 6.6 μm. Working temperatures for both samples are around 24–28 °C, considered close to the indoor comfort temperature in buildings.

2.2. Methods

2.2.1. Fourier transform infrared spectroscopy (FT-IR)

Chemical characterization of PCS shell composition was carried out using FT-IR spectroscopy. A Spectrum Two™ from Perkin Elmer supported by Dynascan™ interferometer and OpticsGuard™ technology was used to perform the analyses. This equipment can measure substances at liquid and solid state, and it was optimized by a wavelength range between 4000 cm^{-1} and 350 cm^{-1} and its standard spectral resolution is 0.5 cm^{-1}.

2.2.2. Thermogravimetrical analysis (TGA)

The thermal stability of the samples under study was evaluated with a Simultaneous SDTQ600 from TA Instruments under nitrogen flow. The heating rate applied was 0.5 K min^{-1} between 25 and 30 °C. Then, the temperature was increased applying 1 K min^{-1} heating rate from 30 to 100 °C. The last heating ramp was using 5 K min^{-1} heating rate from 100 to 600 °C. Sample mass used was around 38 mg for both samples.

2.2.3. TGA coupled with FT-IR

The TGA coupled with IR was performed in order to characterize the chemical functionality of volatile emissions during the decomposition of the microcapsules. The temperature range used to perform the evaluation of the microcapsules degradation was between 25 °C and 250 °C applying 10 °C min^{-1} heating rate. All measurements were performed in alumina vessels (90 μL) under 50 mL min^{-1} flow rate of N_2.

2.2.4. Differential scanning calorimetry (DSC)

Differential scanning calorimetry (DSC) was used to assess the melting range, melting enthalpy, as well as thermal stability of compounds [40–42]. The analyses were carried out using a DS 822e by Mettler Toledo at 0.5 K min^{-1} heating/cooling rate between 10 and 45 °C under constant 80 mL min^{-1} flow of N_2. Furthermore, crucibles used were 40 μL closed aluminium.

3. Results and discussion

3.1. Fourier transformed infrared spectroscopy (FTIR)

3.1.1. Micronal® DS 5007 X

The spectrum of Micronal® DS 5007 X is shown in Fig. 1. In this figure, it is shown the spectra of wet and dried sample, just to evaluate the suspension, comparing both spectra. Hence, the sample was dried at 35 °C during 24 h in an oven to obtain the ratio microcapsules: water, being 1:2.4. The broad intense peak in Fig. 1 at 3368.9 cm^{-1} corresponds to the aqueous suspension of the microcapsules. Then, the sharp intense peaks at 2921.0 cm^{-1} and 2852.0 cm^{-1} are due to the presence of the aliphatic C–H stretching vibration. The two peaks related to the presence of ester carbonyl group stretching vibration are in 1729.5 cm^{-1} for the dried sample and 1646.0 cm^{-1} for the slurry one. This wavenumber difference may be attributed to two possible reasons. The first one ascribed to the hydrogen bounding with the presence of the carbonyl group enfeebles the molecule producing a peak at less frequency. The second probable cause of this displacement may be assigned to the presence of monomers in the slurry, and when the air dried process is achieved, these monomers are evaporated causing a displacement of the carbonyl peak at higher frequencies. Besides, the peak at 1466.6 cm^{-1} was associated to the C–H bending vibration. The broad peak ranging at 1123.5 cm^{-1} is explained owing to the C–O

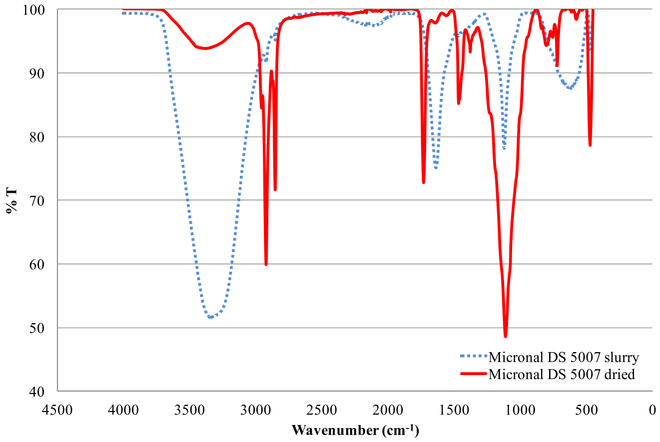

Fig. 1. FT-IR spectrum of Micronal® DS 5007 X in PCS form and dried form.

(ester bond) stretching vibration. Moreover, the peak at 720.5 cm^{-1} corresponds to the bending of C—H. This study confirms that the suspension contains an acrylic polymer as microspheres wall shell.

3.1.2. PCS28

The study of the PCS28 by FT-IR elucidates precisely the functional groups of the shell. Several transcendental peaks such as the intense peak at 3367.9 cm^{-1} which reflected the overlapping stretching frequencies of ν_{OH} and ν_{NH} absorption are shown in Fig. 2. Moreover, the peaks obtained at 2913.6 cm^{-1} and 2848.4 cm^{-1} provide information about the asymmetric and symmetric stretching vibration of the aliphatic methylene group C—H of the polymeric chains. Besides, the intense peaks at 1564.1 cm^{-1} and 1471.0 cm^{-1} are assigned to the C═N vibrations (triazine ring) and the weak ones at 1368.5 cm^{-1} represents the β_{CH} deformation of heterocyclic rings. Finally, the peak at 716.3 cm^{-1} was due to the bending C—H. Therefore, this spectrum is clearly recognizable a melamine-formaldehyde (MF) resins as wall material for the microcapsules.

Drying the sample at 35 °C during 24 h in an oven showed the ratio microcapsules: water, which is 1:2, less fluid than Micronal® DS 5007 X. The dried PCS28 sample spectrum is also presented in Fig. 2, and it shows that the carrier fluid is water. The rest of characteristics peaks are the same obtained for the sample PCS28 wet slurry.

3.2. Thermogravimetrical analysis (TGA)

3.2.1. Micronal® DS 5007 X

Micronal® DS 5007 X sample degrades in three steps as it is seen in Fig. 3. The first weight loss is 72% wt. due to water evaporation between 24 and 180 °C. The second decomposition is 18% wt. ending around 260 °C, and it is attributed to the paraffinic wax decomposition. The third weight loss is around 6% wt. and it corresponds to decomposition of the acrylic shell and it was complete at 385 °C. A 5% wt. solid residue is observed at 600 °C and it is identified as a Si based compound [43].

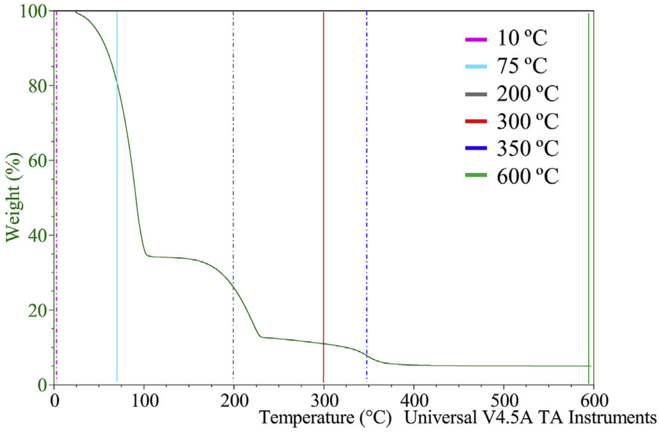

Fig. 3. Thermogravimetrical analysis of PCS Micronal® DS 5007 X.

3.2.2. PCS28

Fig. 4 shows the weight loss variation for this slurry over temperatures for PCS28. Also three steps of decomposition can be observed, from 25 to 125 °C, from 125 to 325 °C, and from 325 to 600 °C, respectively. At the beginning of the first decomposition, water evaporation and the self-condensation of methylol groups represent a 59% wt. The second weight loss is due to the PCM decomposition and partly degradation of MF shell and it is a 31% wt. of the total amount of the sample, and occurs in the temperature range between 180 °C and 330 °C. Finally, the weight loss beyond 330 °C is 8% wt. attributed to the condensation reaction between melamine, methylol group, some emulsifying agent (in this case styrene-maleic acid anhydride copolymer), the elimination of formaldehyde from the ether bridge forming methylene bridge, the breakdown of the methylene bridges, and the thermal degradation of the triazine ring, and it is assumed that MF resin progressively transform to HCN. The final residue is around 2% wt.

3.3. FT-IR coupled to TGA

3.3.1. Micronal® DS 5007 X

The decomposition of PCS samples was deeply analyzed by coupling the FT-IR with TGA. In a three dimensional graph the Transmittance (%) in front of the Wavenumber (cm^{-1}) and *vs.* time (s) is represented (Fig. 5). It is represented the most important spectra taking into account the degradation temperatures of the TGA results (Fig. 3). It means six different spectra at 25 °C (around 600 s), 75 °C (around 1000 s), 200 °C (around 1800 s), 300 °C (around 2400 s), 350 °C (around 2700 s), and 600 °C (around 4200 s). As it can be observed in Fig. 5, at the beginning of the experiment, no signals can be observed. Around 1800 s the degradation of the paraffin wax should be seen, although its spectrum is almost 100% Transmittance. Then, the ones at 2400 s is represented, which is the most important spectrum, due to it is

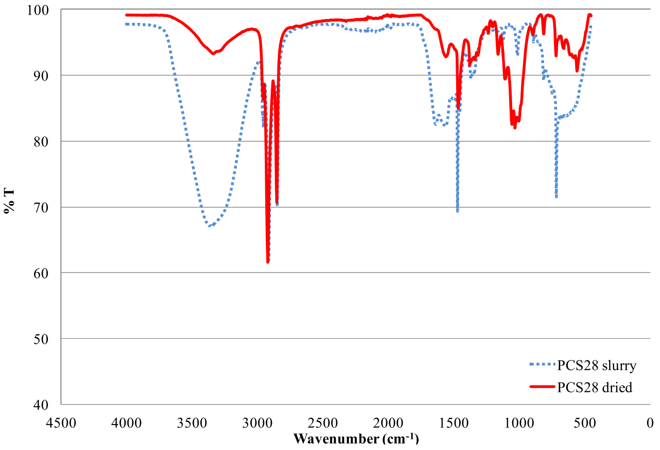

Fig. 2. FT-IR spectra of the PCS28.

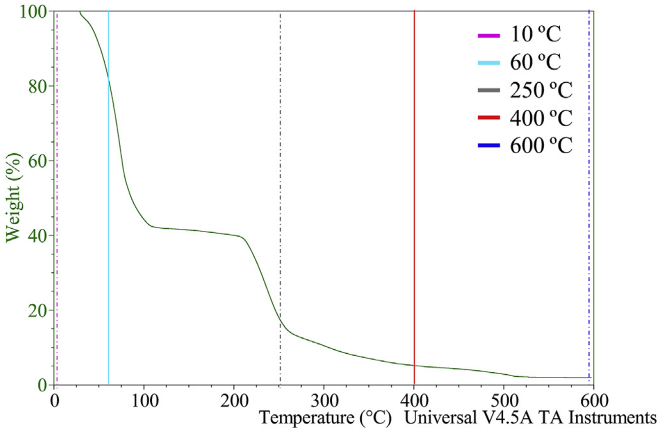

Fig. 4. Thermogravimetrical analysis of PCS28.

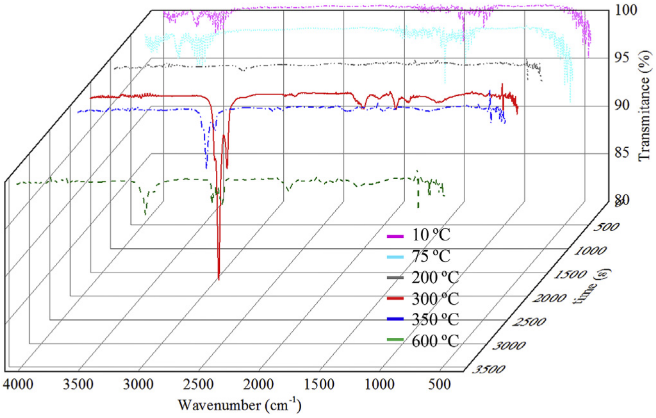

Fig. 5. FT-IR results after TG analysis of PCS Micronal® DS 5007 X.

related to the shell degradation. This degradation can be observed until the end of the experiment.

3.3.2. PCS28

FT-IR device coupled with TGA give the decomposition spectra of the PCS over time in a three dimensional figure (Transmittance in % *vs*. Wavenumber in cm^{-1} *vs*. time in s) (Fig. 6). Five different spectra related to TGA temperatures in Fig. 4 are represented: 25 °C (around 0 s), 60 °C (around 360 s), 250 °C (around 660 s), 400 °C (around 2400 s), and 600 °C (around 3600 s). The three first spectra have very high transmittance, therefore it is very difficult to attribute and characterize peaks, although as it is exposed in 3.2.2 section, these are related to the water and PCM decomposition. The spectrum related to the MF shell is the one at 2400 s, and its degradation is prolonged until the end on the experiment.

3.4. Differential scanning calorimetry (DSC)

DSC curves results of DSC samples characterization under study are summarized in Table 1 and presented in Fig. 7.

Results show that the latent heat observed is almost equal between melting and solidification processes for both samples. Besides, the phase change temperature remains roughly constant for Micronal® DS 5007 X, but accounts 7 °C in the case of PCS28 due to the solidification will present subcooling as was stated by Günther et al. [44].

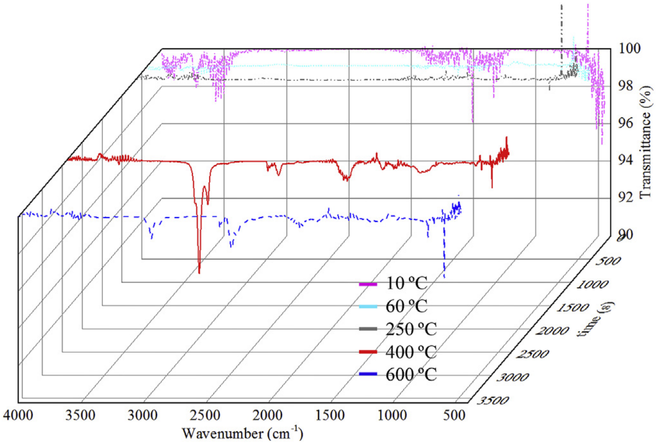

Fig. 6. FT-IR results after TG analysis of PCS28.

Table 1
Differential Scanning Calorimetry results for Micronal® DS 5007 X and PCS28.

	Micronal® DS 5007 X		PCS28	
	Melting	Solidification	Melting	Solidification
Enthalpy ($kJ \cdot kg^{-1}$)	87.48	89.73	50.36	50.78
T (°C)	23.54	21.07	27.68	20.34

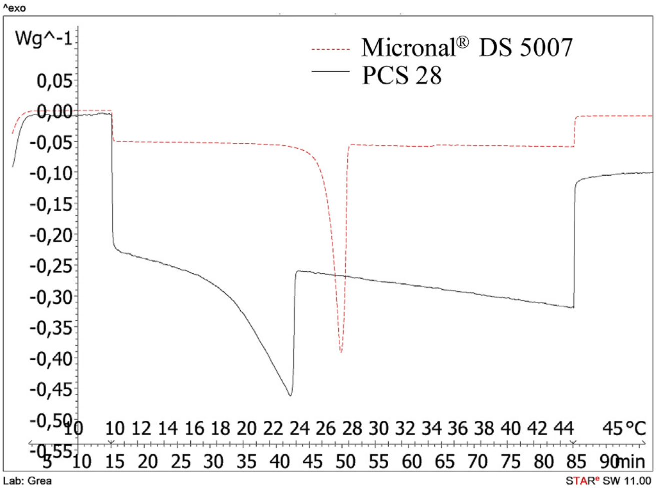

Fig. 7. Differential scanning calorimetry curves of the two samples using dynamic method.

The main property in this article to highlight that the two reported PCS are proper candidates to be used in TES building heating and cooling applications is DSC, as it provides highly enough values for melting and solidification latent heat to confirm their capability of developing their role in thermal energy storage field, concluding a good potential from TES functions for both PCS.

4. Conclusions

Two different PCS samples which contain different materials for the shell and the core were evaluated. FT-IR results reported that for Micronal® DS 5007 X the shell is an acrylate polymer. The FT-IR spectra corresponding to PCS28 sample concluded that the external polymeric shell is melamine-formaldehyde. Thermogravimetrical investigation (TGA) showed that Micronal® DS 5007 X slurry decomposed in three steps and in two steps for the dried sample. Moreover, PCS28 decomposed in three steps (the carrier fluid, the PCM and the wall shell) and shows better thermal stability than Micronal® DS 5007 X. In addition, the temperature and latent heat of melting and solidification of the PCS samples were determined using DSC analysis method. For the Micronal® DS 5007 X is shown a phase change between 21 °C and 23 °C and an enthalpy around 90 $kJ\ kg^{-1}$. Otherwise, PCS28 slurry has a melting temperature between 22 °C and 27 °C with an enthalpy of 50 $kJ\ kg^{-1}$. Overall, the studied PCS are totally capable of developing their role in the thermal energy storage field, and they can be considered as PCM candidates for TES in active building applications.

Acknowledgements

The work is partially funded by the Spanish government (ENE2011-28269-C03-02 and ENE2011-22722). The authors would like to thank the Catalan Government for the quality accreditation given to their research group GREA (2014 SGR 123) and research group DIOPMA (2014 SGR 1543). The research leading to these results has received funding from the European Union's Seventh Framework Programme (FP7/2007-2013) under grant agreement n° PIRSES-GA-2013-610692 (INNOSTORAGE).

References

[1] Farid MM, Khudhair AM, Razack SAK, Al-Hallaj S. A review on phase change energy storage: materials and applications. Energy Convers Manag 2004;45:1597–615. http://dx.doi.org/10.1016/j.enconman.2003.09.015.

[2] Delgado M, Lázaro A, Mazo J, Zalba B. Review on phase change material emulsions and microencapsulated phase change material slurries: materials, heat transfer studies and applications. Renew Sustain Energy Rev 2012;16:253–73.

[3] Salunkhe PB, Shembekar PS. A review on effect of phase change material encapsulation on the thermal performance of a system. Renew Sustain Energy Rev 2012;16:5603–16. http://dx.doi.org/10.1016/j.rser.2012.05.037.

[4] Pan L, Tao Q, Zhang S, Wang S, Zhang J, Wang S, et al. Preparation, characterization and thermal properties of micro-encapsulated phase change materials. Sol Energy Mater Sol Cells 2012;98:66–70. http://dx.doi.org/10.1016/j.solmat.2011.09.020.

[5] Fang G, Li H, Liu X. Preparation and properties of lauric acid/silicon dioxide composites as form-stable phase change materials for thermal energy storage. Mater Chem Phys 2010;122:533–6. http://dx.doi.org/10.1016/j.matchemphys.2010.03.042.

[6] Özonur Y, Mazman M, Paksoy HÖ, Evliya H. Microencapsulation of coco fatty acid mixture for thermal energy storage with phase change material. Int J Energy Res 2006;30:741–9. http://dx.doi.org/10.1002/er.1177.

[7] Zhang T, Wang Y, Shi H, Yang W. Fabrication and performances of new kind microencapsulated phase change material based on stearic acid core and polycarbonate shell. Energy Convers Manag 2012;64:1–7. http://dx.doi.org/10.1016/j.enconman.2012.04.011.

[8] Wang Y, Xia TD, Feng HX, Zhang H. Stearic acid/polymethylmethacrylate composite as form-stable phase change materials for latent heat thermal energy storage. Renew Energy 2011;36:1814–20. http://dx.doi.org/10.1016/j.renene.2010.12.022.

[9] Alkan C, Sarı A, Karaipekli A. Preparation, thermal properties and thermal reliability of microencapsulated n-eicosane as novel phase change material for thermal energy storage. Energy Convers Manag 2011;52:687–92. http://dx.doi.org/10.1016/j.enconman.2010.07.047.

[10] Sarı A, Alkan C, Karaipekli A. Preparation, characterization and thermal properties of PMMA/n-heptadecane microcapsules as novel solid–liquid microPCM for thermal energy storage. Appl Energy 2010;87:1529–34. http://dx.doi.org/10.1016/j.apenergy.2009.10.011.

[11] Sánchez-Silva L, Rodríguez JF, Romero A, Borreguero AM, Carmona M, Sánchez P. Microencapsulation of PCMs with a styrene-methyl methacrylate copolymer shell by suspension-like polymerisation. Chem Eng J 2010;157:216–22. http://dx.doi.org/10.1016/j.cej.2009.12.013.

[12] Wang L, Meng D. Fatty acid eutectic/polymethyl methacrylate composite as form-stable phase change material for thermal energy storage. Appl Energy 2010;87:2660–5. http://dx.doi.org/10.1016/j.apenergy.2010.01.010.

[13] Zhang GH, Bon SAF, Zhao CY. Synthesis, characterization and thermal properties of novel nanoencapsulated phase change materials for thermal energy storage. Sol Energy 2012;86:1149–54. http://dx.doi.org/10.1016/j.solener.2012.01.003.

[14] Qiu X, Li W, Song G, Chu X, Tang G. Microencapsulated n-octadecane with different methylmethacrylate-based copolymer shells as phase change materials for thermal energy storage. Energy 2012;46:188–99. http://dx.doi.org/10.1016/j.energy.2012.08.037.

[15] Li W, Song G, Tang G, Chu X, Ma S, Liu C. Morphology, structure and thermal stability of microencapsulated phase change material with copolymer shell. Energy 2011;36:785–91. http://dx.doi.org/10.1016/j.energy.2010.12.041.

[16] Tang X, Li W, Zhang X, Shi H. Fabrication and characterization of microencapsulated phase change material with low supercooling for thermal energy storage. Energy 2014;68:160–6. http://dx.doi.org/10.1016/j.energy.2014.03.002.

[17] Palanikkumaran M, Gupta KK, Agrawal AK, Jassal M. Effect of emulsion preparation method on microencapsulation of n -octadecane using melamine-formaldehyde pre-polymers. Indian J Fibre Text Res 2010;35:101–6.

[18] Sumiga B, Knez E, Vrtačnik M, Ferk-Savec V, Starešinič M, Boh B. Production of melamine-formaldehyde PCM microcapsules with ammonia scavenger used for residual formaldehyde reduction. Acta Chim Slov 2011;58:14–25.

[19] Zhang H, Wang X. Fabrication and performances of microencapsulated phase change materials based on n-octadecane core and resorcinol-modified melamine–formaldehyde shell. Colloids Surfaces A Physicochem Eng Asp 2009;332:129–38. http://dx.doi.org/10.1016/j.colsurfa.2008.09.013.

[20] Castellón C, Martorell I, Cabeza LF, Fernández AI, Manich AM. Compatibility of plastic with phase change materials (PCM). Int J Energy Res 2011;35:765–71.

[21] Bayés-García L, Ventolà L, Cordobilla R, Benages R, Calvet T, Cuevas-Diarte MA. Phase change materials (PCM) microcapsules with different shell compositions: preparation, characterization and thermal stability. Sol Energy Mater Sol Cells 2010;94:1235–40. http://dx.doi.org/10.1016/j.solmat.2010.03.014.

[22] Alkan C, Sarı A, Karaipekli A, Uzun O. Preparation, characterization, and thermal properties of microencapsulated phase change material for thermal energy storage. Sol Energy Mater Sol Cells 2009;93:143–7. http://dx.doi.org/10.1016/j.solmat.2008.09.009.

[23] Diaconu BM, Varga S, Oliveira AC. Experimental assessment of heat storage properties and heat transfer characteristics of a phase change material slurry for air conditioning applications. Appl Energy 2010;87:620–8. http://dx.doi.org/10.1016/j.apenergy.2009.05.002.

[24] Griffiths PW, Eames PC. Performance of chilled ceiling panels using phase change material slurries as the heat transport medium. Appl Therm Eng 2007;27:1756–60. http://dx.doi.org/10.1016/j.applthermaleng.2006.07.009.

[25] Huang L, Petermann M, Doetsch C. Evaluation of paraffin/water emulsion as a phase change slurry for cooling applications. Energy 2009;34:1145–55. http://dx.doi.org/10.1016/j.energy.2009.03.016.

[26] Youssef Z, Delahaye A, Huang L, Trinquet F, Fournaison L, Pollerberg C, et al. State of the art on phase change material slurries. Energy Convers Manag 2013;65:120–32. http://dx.doi.org/10.1016/j.enconman.2012.07.004.

[27] Lu W, Tassou SA. Experimental study of the thermal characteristics of phase change slurries for active cooling. Appl Energy 2012;91:366–74. http://dx.doi.org/10.1016/j.apenergy.2011.10.004.

[28] Delgado M, Lázaro A, Mazo J, Marín JM, Zalba B. Experimental analysis of a microencapsulated PCM slurry as thermal storage system and as heat transfer fluid in laminar flow. Appl Therm Eng 2012;36:370–7. http://dx.doi.org/10.1016/j.applthermaleng.2011.10.050.

[29] Zhao CY, Zhang GH. Review on microencapsulated phase change materials (MEPCMs): fabrication, characterization and applications. Renew Sustain Energy Rev 2011;15:3813–32. http://dx.doi.org/10.1016/j.rser.2011.07.019.

[30] Alvarado JL, Marsh C, Sohn C, Phetteplace G, Newell T. Thermal performance of microencapsulated phase change material slurry in turbulent flow under constant heat flux. Int J Heat Mass Transf 2007;50:1938–52. http://dx.doi.org/10.1016/j.ijheatmasstransfer.2006.09.026.

[31] Diaconu BM, Varga S, Oliveira AC. Experimental study of natural convection heat transfer in a microencapsulated phase change material slurry. Energy 2010;35:2688–93. http://dx.doi.org/10.1016/j.energy.2009.06.028.

[32] Zhang P, Ma ZW, Wang RZ. An overview of phase change material slurries: MPCS and CHS. Renew Sustain Energy Rev 2010;14:598–614. http://dx.doi.org/10.1016/j.rser.2009.08.015.

[33] Zhang P, Ma ZW. An overview of fundamental studies and applications of phase change material slurries to secondary loop refrigeration and air conditioning systems. Renew Sustain Energy Rev 2012;16:5021–58. http://dx.doi.org/10.1016/j.rser.2012.03.059.

[34] Zhou D, Zhao CY, Tian Y. Review on thermal energy storage with phase change materials (PCMs) in building applications. Appl Energy 2012;92:593–605. http://dx.doi.org/10.1016/j.apenergy.2011.08.025.

[35] Khudhair AM, Farid MM. A review on energy conservation in building applications with thermal storage by latent heat using phase change materials. Energy Convers Manag 2004;45:263–75. http://dx.doi.org/10.1016/S0196-8904(03)00131-6.

[36] Kuznik F, David D, Johannes K, Roux J-J. A review on phase change materials integrated in building walls. Renew Sustain Energy Rev 2011;15:379–91. http://dx.doi.org/10.1016/j.rser.2010.08.019.

[37] Su J-F, Wang L-X, Ren L. Preparation and characterization of double-MF shell microPCMs used in building materials. J Appl Polym Sci 2005;97:1755–62. http://dx.doi.org/10.1002/app.21205.

[38] Alawadhi EM. Thermal analysis of a building brick containing phase change material. Energy Build 2008;40:351–7. http://dx.doi.org/10.1016/j.enbuild.2007.03.001.

[39] Giro-Paloma J, Barreneche C, Martínez M, Sumiga B, Cabeza LF FA. Mechanical response evaluation of microcapsules from different slurries n.d.

[40] Zhang S, Tao Q, Wang Z, Zhang Z. Controlled heat release of new thermal storage materials: the case of polyethylene glycol intercalated into graphene oxide paper. J Mater Chem 2012;22:20166. http://dx.doi.org/10.1039/c2jm33316c.

[41] Zhang S, Wang S, Zhang J, Jiang Y, Ji Q, Zhang Z, et al. Increasing phase change latent heat of stearic acid via nanocapsule interface confinement. J Phys Chem C 2013;117:23412–7. http://dx.doi.org/10.1021/jp408478h.

[42] Pan L, Ji Q, Qin Y, Jiang Y, Zhang Z, Zhang S, et al. Diverting phase transition of high-melting-point stearic acid to room temperature by microencapsulation in boehmite. RSC Adv 2013;3:22326. http://dx.doi.org/10.1039/c3ra43936d.

[43] Giro-Paloma J, Oncins G, Barreneche C, Martínez M, Fernández AI, Cabeza LF. Physico-chemical and mechanical properties of microencapsulated phase change material. Appl Energy 2013;109:441–8. http://dx.doi.org/10.1016/j.apenergy.2012.11.007.

[44] Günther E, Schmid T, Mehling H, Hiebler S, Huang L. Subcooling in hexadecane emulsions. Int J Refrig 2010;33:1605–11. http://dx.doi.org/10.1016/j.ijrefrig.2010.07.022.

5.3.2. Mechanical properties

Mechanical tests of PCS Micronal® DS 5007 X and PCS 28 were performed to better characterize the samples. This study was published in 2015 as “**Mechanical response evaluation of microcapsules from different slurries”** in Renewable Energy journal. The mechanical behavior using AFM, the observation of the shape and size of the PCS by Particle Size Distribution and Scanning Electron Microscopy were evaluated. The most important conclusions for the study related with the mechanical properties of two different PCS (Micronal® DS 5007 X and PCS28) reveals that it is very important to take into account the temperature, because the mechanical properties decrease when the temperature increases, having an abruptly reduction when the temperature is close to the glass transition, overall for Micronal® DS 5007 X. In case of PCS28, its reduction is due to nature of prepared microcapsule wall using in situ polymerization. Also, it is important to consider the change in shape of the microcapsules when increasing the temperature. The higher the temperature, the lower the mechanical properties. From the mechanical point of view, an acrylate group (Micronal® 5007 X) to be used as a shell in microcapsules is a better choice than melamine-formaldehyde resin (PCS28), taking into account that both samples have the same thickness shell as SEM results reveal. However, these measurements were performed using static samples. As a future study, these samples should be tested in a real system, pumping it and evaluating their mechanical properties after several cycles.

Renewable Energy 85 (2016) 732–739

Contents lists available at ScienceDirect

Renewable Energy

journal homepage: www.elsevier.com/locate/renene

Mechanical response evaluation of microcapsules from different slurries

Jessica Giro-Paloma [a], Camila Barreneche [a, b], Mònica Martínez [a], Boštjan Šumiga [c], Ana Inés Fernández [a], Luisa F. Cabeza [b, *]

[a] Universitat de Barcelona, Faculty of Chemistry, Department of Materials Science and Metallurgical Engineering, C/ Martí i Franquès, 1, 08028 Barcelona, Spain
[b] GREA Innovació Concurrent, Edifici CREA, Universitat de Lleida, C/ Pere de Cabrera s/n, 25001 Lleida, Spain
[c] Iskra Mehanizmi d.o.o., Fužine 9, 1240 Kamnik, slovenia

ARTICLE INFO

Article history:
Received 24 March 2015
Received in revised form
7 July 2015
Accepted 11 July 2015
Available online xxx

Keywords:
Phase change slurry (PCS)
Particle size distribution (PSD)
Scanning electron microscopy (SEM)
Atomic force microscope (AFM)
Mechanical characterization

ABSTRACT

Thermal energy storage (TES) is one method to accumulate thermal energy. In TES, latent heat storage using phase change materials (PCM) has attracted a lot of interest, recently. Phase change slurries (PCS) consist on a carrier fluid binary system composed of water as the continuous phase and micro-encapsulated PCM as the dispersed phase. In this paper, two PCS to be used for TES in buildings were studied: Micronal® DS 5007 X, from BASF company, and PCS28, a laboratory made sample. Both samples were characterized using particle size distribution and scanning electron microscopy, to observe the regular spherical microcapsules, the surface morphology, and the wall shell thickness of the microcapsules. Atomic force microscopy was used to analyze the force needed to break the PCS microcapsules, a critical parameter when the PCS are to be used in active pumpable systems, and also to evaluate the effective Young's modulus. Both samples were studied with the microcapsules broken and unbroken. The physicochemical and thermal properties were reported in a previous paper, and it can be concluded that both are proper candidates to be used in TES building heating and cooling applications, but the acrylic shell microcapsules present better breakage resistance to be used in active systems.

1. Introduction

Phase Change Materials (PCM) are well known in Thermal Energy Storage (TES) because of their capacity to absorb and slowly release the latent heat involved in the phase change process [1], as well as the ability to store a large amount of energy in relatively small volumes. TES with PCM achieves energy conservation in buildings with thermal comfort [2]. Energy storage is very important where the energy source is intermittent, as in solar energy field, and it can decrease the time between energy supply and energy demand. For this reason, energy storage is essential in energy conservation issues. There are some reported methods to include PCM in building walls [3] such as with impregnation. There is also in the literature some studies [4,5] exposing the introduction of PCM in constructive materials [6], such as gypsum [7,8], concrete [9], wood [10], etc. As there is leakage when mixing PCM with building materials, PCM has to be encapsulated for technical use and microcapsules were considered to address this issue [11]. Microencapsulated Phase Change Materials (MPCM) [12–14] are small vessels with a hydrophobic core material and a hard covering that accepts size alterations, maintains its shape and avoids corrosion problems. MPCM temperature remains unchanged during the heat absorption/release process and these can be applied in passive storage systems such as component in buildings envelopes [15], as well as, in sandwich panels [16]. MPCM can also be added to a fluid in order to be transported or pumped in an active storage system. They can be used in active storage systems such as pumping slurries [17–19], which are microcapsules suspensions or emulsions [20–22] using a dispersant agent in order to stabilize the distribution of the microcapsules in order to enhance its thermal behavior. These slurries are known as Phase Change Slurries (PCS).

Different core/shell combinations that have been studied take into account the external polymer and the PCM nature (inorganic or

---

[*] Corresponding author.
E-mail addresses: jessicagiro@ub.edu (J. Giro-Paloma), c.barreneche@ub.edu (C. Barreneche), monicamartinez@ub.edu (M. Martínez), bostjan.sumiga@iskra-mehanizmi.si (B. Šumiga), ana_inesfernandez@ub.edu (A.I. Fernández), lcabeza@diei.udl.cat (L.F. Cabeza).

http://dx.doi.org/10.1016/j.renene.2015.07.033

organic) [23,24]. In this particular case, the core samples are saturated hydrocarbon paraffin wax as the PCM. In this paper, two samples were characterized: Micronal® DS 5007 X provided by BASF® and a laboratory prepared suspension of microcapsules based on analysis and experimental optimization of in situ polymerisation technology for its preparation from scientific and patent literature [25]. This comparison aspect between both types of MPCM is very important as it is wanted to identify the best MPCM laboratory manufactured, or at least, the most similar commercial MPCM in a laboratory preparation. The two samples have melting temperatures around 24–28 °C that are considered close to the indoor comfort temperature in buildings [26]. The physicochemical and thermal properties were evaluated in a previous paper [27].

The main objective of this study is to compare the physical and mechanical behavior of two PCS samples able to be used in active systems in order to discern the most proper microcapsules for using them in a TES media for heating and cooling applications.

2. Materials and methods

2.1. Materials

Two types of PCS were studied in this paper. Micronal® DS 5007 X which has an acrylate polymer as a shell in a slurry medium, with a proportion of 2:5, (slurry + dispersant):water, and paraffin wax in the core. The other sample is PCS28 which is a laboratory made sample, and the shell was prepared with a melamine-formaldehyde (MF) resin. The paraffin wax inside the microcapsules PCS28 is *n*-octadecane. The phase change temperature of PCS28 is around 28 °C and the proportional relation is 1:2, (slurry + dispersant):water [27]. The main reason for choosing these two types of MPCM was to compare the different mechanical behavior related to the MPCM polymeric shell (acrylic or MF) and to decide which shell is better to microencapsulate the PCM.

2.2. Methodology

The size of the microcapsules was studied analyzing the Particle Size Distribution (PSD). Also, by using Scanning Electron Microscopy (SEM) the dimensions of the microcapsules can be measured. Finally, they were analyzed by Atomic Force Microscopy (AFM) [12,28,29], which is commonly used to examine the nano- or microscale properties of the surface and in close proximity surface regions. AFM is a powerful tool for evaluating polymeric materials on a sub-micrometer scale because it admits lesser forces and higher upper resolutions than nanoindenters [30]. In this study, it was identified the maximum force that can be applied on the top of microcapsules (dried PCS) to break them, analyzing the typical deflection-indentation curves. Besides, it was calculated the Effective Young's modulus (*E*) distribution in a specific region of each microsphere for the two studied samples. The tests were done at 23 °C and 45 °C for both samples, which is with the core material in solid and liquid phase.

2.2.1. Particle size measurements and scanning electron microscopy

The Particle Size Distribution (PSD) was analyzed using a Beckman Coulter® LSTM 13 320 with Universal Liquid Module. The results were analyzed applying the Mie mathematical model, because it fits well for homogenous, spherical, and transparent or opaque particles with diameter below 50 μm. Afterwards, each sample was circulated separately a total of 10 min in order to estimate sample volume changes, to evaluate possible MPCM degradation or MPCM accumulation.

Samples morphologies were observed by Scanning Electron Microscopy (SEM) using a Jeol JSM-6510 instrument under vacuum atmosphere, high voltage (15 kV), and images obtained by secondary electrons. Furthermore, the microcapsules were broken in purpose applying a compressive strength to study the wall shell thickness, which is directly related with the mechanical properties of the microcapsules.

2.2.2. Atomic force microscopy (AFM)

The AFM equipment used to evaluate the mechanical properties of microcapsules (two dried PCS samples) was Multimode 8 and Nanoscope V electronics from Bruker with a Peak Force Quantitative Nanomechanics mode (QNM). The diamond probe used was from Bruker, with a 388 nN nm^{-1} spring constant. Therefore, the peak force amplitude was 300 nm, the peak force frequency was 0.5 kHz, and finally, the maximum vertical force was 500 nN. One aliquot of each PCS was diluted in water in a small beaker. Then, 50 μl of this solution were poured on a freshly cleaved mica surface under a N_2 stream until complete dryness. The samples were observed and mechanically tested without further treatment.

The goal of the first assay is to quantify the highest vertical force that the samples were able to resist after creating a permanent elastic deformation executing a force. It was obtained microcapsules images at 23 °C, and after that, it was applied a force on the top of the microcapsule until breaking the shell to perform a force curve. Subsequently, the particle was imaged again. This process was repeated three times at 23 °C for each microcapsule (PCM in solid state); following that, PCS microcapsules temperature was raised to 45 °C (PCM in liquid state), and the whole process was repeated again three times for each sample. A total of 18 tests were performed. The second set of experiments consists on testing the stiffness and calculate the Effective Young's modulus (*E*) of the dried PCS microcapsules at the two different temperatures performing two repetitions at 23 °C and 45 °C (PCM in solid and liquid state, respectively). In all the cases, the temperature was measured with a micro-thermocouple type-K in contact with the sample holder.

3. Results and discussion

3.1. Particle size measurements

3.1.1. Particle size distribution (PSD)

PSD was evaluated following the Mie mathematic model, and Table 1 lists the main results obtained. The parameter d_{10} means that 10% of the volume of the particles had a diameter below the given value; for d_{50}, 50% of the particles had a diameter below the given value, and finally, 90% of particles had a size volume below d_{90}.

At the light of the results, PCS28 presents lower values than Micronal® DS 5007X. Thereby, the repeatability over the measurements is shown in Fig. 1 for Micronal® DS 5007 X. The profile curves obtained are almost identical, showing a quite narrow distribution, being assured the repeatability between the different experiments.

The evolution over time for PCS28 results is plotted in Fig. 2. This graph illustrates that at the beginning of the experiment there was

Table 1
Particle Size Distribution results from microcapsules under study.

	Micronal® DS 5007 X	PCS28
PSD d_{10} (μm)	2.79	0.14
PSD d_{50} (μm)	4.88	3.46
PSD d_{90} (μm)	7.48	6.62
PSD mean (μm)	4.88	3.14
Standard deviation (μm)	2.09	2.62

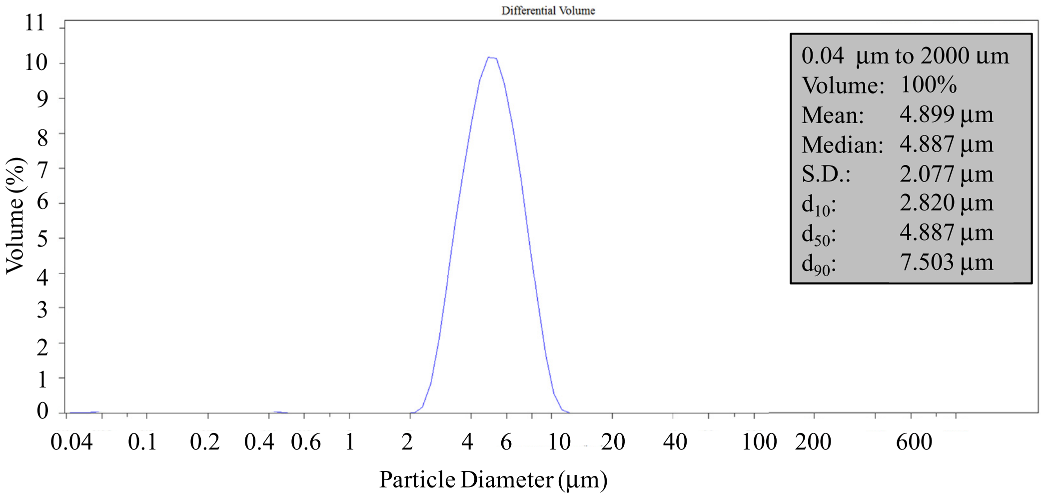

Fig. 1. Particle Size Distribution of PCS Micronal® 152 DS 5007 X.

a bimodal distribution showing two peaks, one corresponding to a fraction of particles with smaller size and the other one corresponding to bigger particles. After 10 min (1 min per each cycle) inside the circuit, the distribution shows one peak. Therefore, an agglomeration particle process was obtained over time for this sample.

3.1.2. *Scanning electron microscopy (SEM)*

SEM images of the two samples are shown in Fig. 3. It was done a drying process at room temperature to better observe the size of the PCS microcapsules, followed by a compression of the sample to crash the microcapsules. Particle sizes (left) and wall thicknesses (right) are detailed in this figure. For both samples, Micronal® DS 5007 X and PCS28, the particle size is variable. Note that the samples under study show approximately the same shell thickness, which is around 0.5 µm. Furthermore, the main results for microcapsules size and wall shell thickness are listed in Table 2.

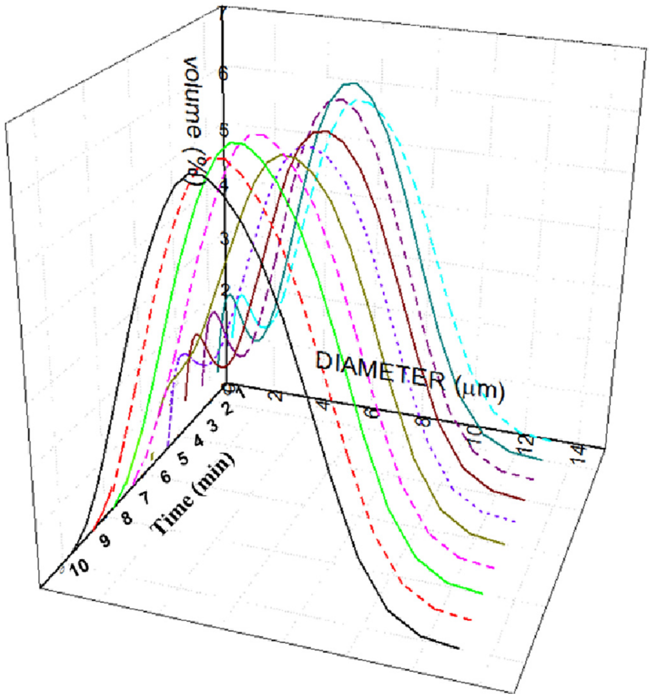

Fig. 2. Particle Size Distribution progress of the PCS28 slurry in front of time.

3.2. *Atomic Force Microscopy*

3.2.1. *Micronal®DS 5007 X*

The typical loading curve for Micronal® DS 5007 X at 23 °C is shown in Fig. 4. The deflection error *vs*. Z is represented, where the deflection error is proportional to the applied force, and Z is the penetration of the tip inside the sample. At the beginning of the experiment there is no force applied (a). Subsequently, in this case, applying 11 µN of load (transition (b) to (c)) the microcapsule breaks. The tip penetrated around 0.6 µm, allowing to observe the created hole in the position where the AFM probe has punctured. Finally, the unloading curve shows the retracting of the tip (d).

The same procedure of puncturing the sample was done at 45 °C, as Fig. 5 shows. In this case, the indentation breakthrough occurs at 1.8 µN, because the higher the temperature, the softer the polymer.

It is important to note that when a microcapsule is heated up, the topographic section may change. This effect can be observed in Fig. 6 where it can be seen the 3D view (Figs. 6, 1a and 2a) and the profile of the white line of a microsphere (Figs. 6, 1b and 2b) at different temperatures, 23 °C and 45 °C.

Furthermore, a mechanical map at 23 °C and 0.5 KHz per second in Giro-Paloma et al. study was evaluated [17] obtaining a great dispersion of values, being between 10 and 20 nm of deformation. Besides, applying a vertical force of 500 nN on the top of the microcapsule, *E* values show a great dispersion being the mean value about 200 MPa.

E mapping diagram for Micronal® DS 5007 X was measured also at 45 °C, and the region studied is shown in Fig. 7a. The total pixels amount of the area selected is represented the Y axis. In this case, from the deformation histogram, deformation varies around 20 nm (b), and the calculated results of the *E* histogram applying 500 nN were around 50 MPa (c), four times lower than the experiments at 23 °C due to the softening of the particle shell as well as the liquid state of PCM. The mechanical properties hastily reduced when the temperature increase and it is close to the glass transition, for Micronal® samples.

3.2.2. *PCS28*

The experimental procedure at 23 °C was also performed for PCS28. The mechanical testing loading AFM curve of deflection

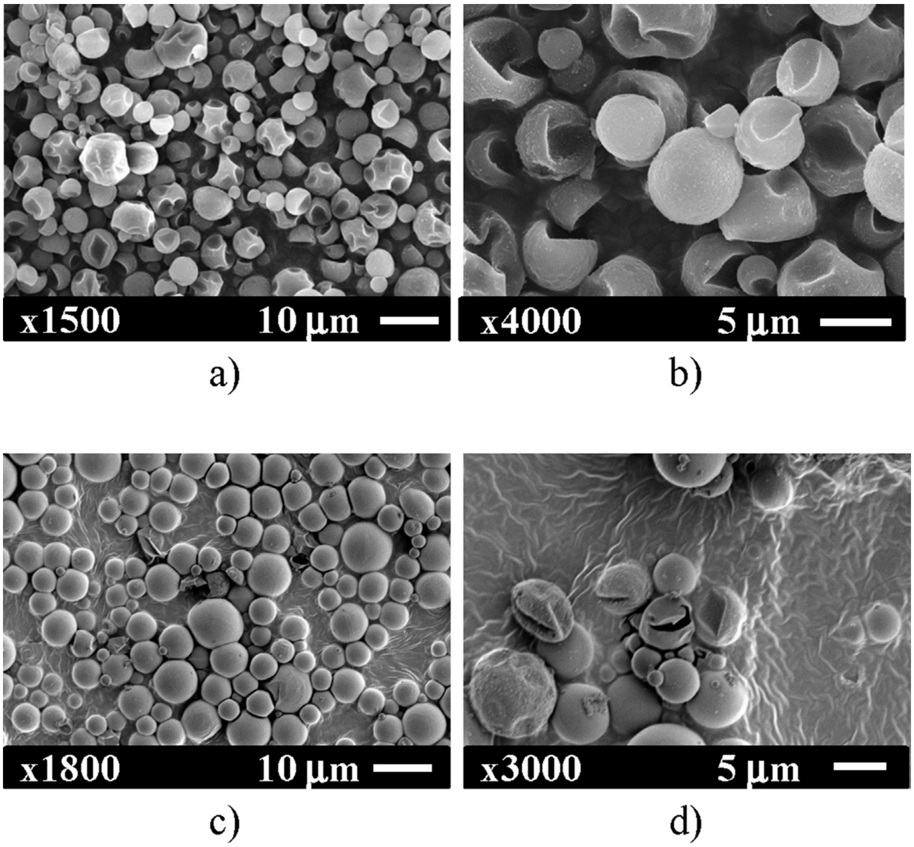

Fig. 3. SEM images. (a) PCS Micronal® DS 5007 X × 1,500, (b) PCS Micronal® DS 5007 X × 4000; and (c) PCS28 × 1,600, (d) PCS28 × 3000.

Table 2
SEM results from microcapsules under study.

	Micronal® DS 5007 X	PCS28
Size (µm)	4.0–8.0	2.1–10.2
Size wall thickness shell (µm)	0.5	0.5

error *vs.* Z is shown in Fig. 8. Then, applying 2.5 µN the sample breaks and a permanent indenter print is observed in the sample (Fig. 8b).

Afterwards, an identical process of penetrating the microsphere with a tip was done at 45 °C, as it is seen in Fig. 9. This microsphere breaks at lower force (0.9 µN) compared with the experiment performed at 23 °C. The particle was punctured, and the inner

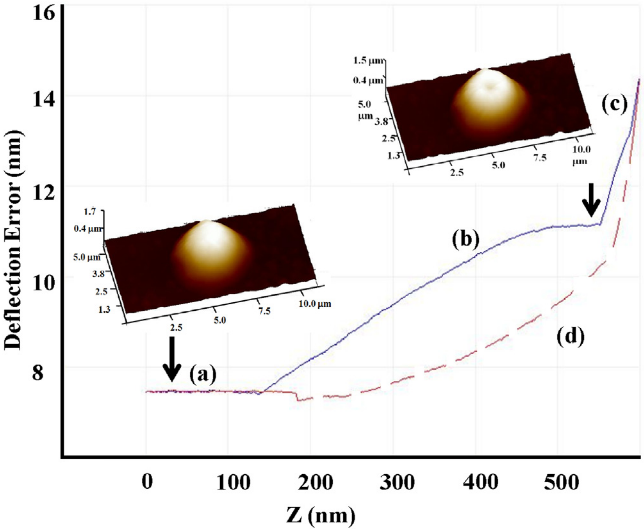

Fig. 4. Mechanical testing of the elastic-plastic region by AFM of a Micronal® DS 5007 X microcapsule at 23 °C, (a) no contact, continuous line; (b) plastic penetration; (c) deformation of the sample; and (d) retraction of the AFM probe, discontinuous line.

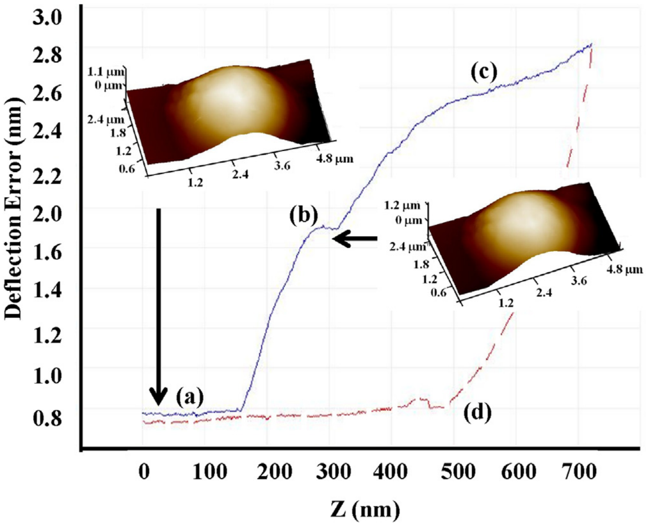

Fig. 5. Mechanical testing of the elastic-plastic region by AFM of Micronal® DS 5007 X microcapsule at 45 °C; (a) no contact, continuous line; (b) plastic penetration; (c) deformation of the sample; and (d) retraction of the AFM probe, discontinuous line.

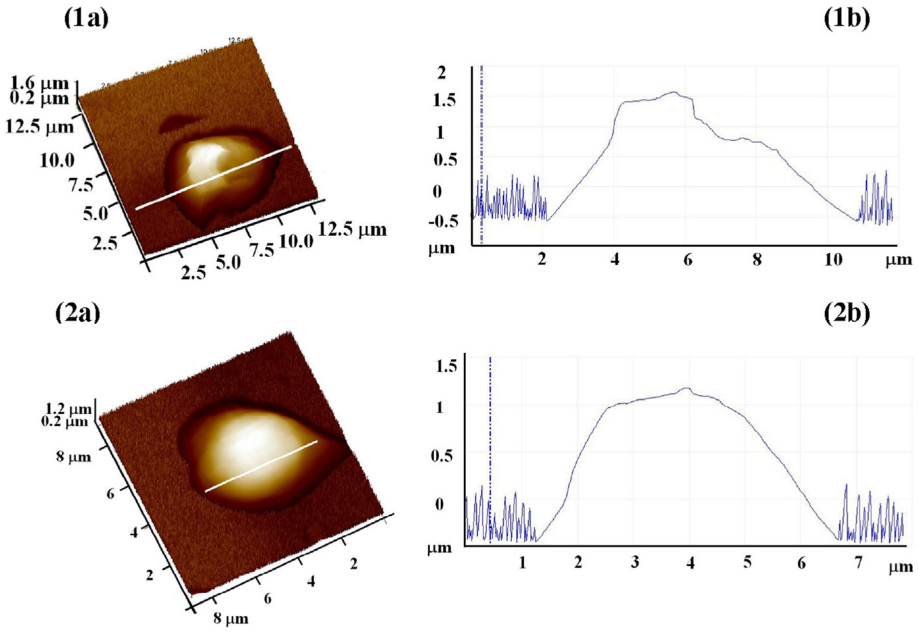

Fig. 6. Micronal® DS 5007 X sample (1a) 3D view at 23 °C; (2a) 3D view at 45 °C; (1b) topographic image at 23 °C; (2b) topographic image at 45 °C.

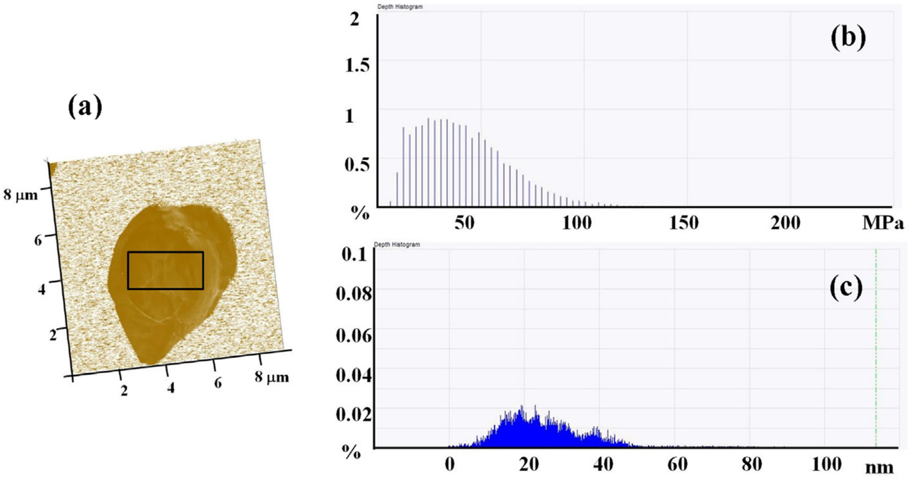

Fig. 7. Effective Young's modulus mapping of Micronal® DS 5007 X at 45 °C; (a) 3D view; (b) Deformation histogram (nm); (c) *E* histogram (GPa).

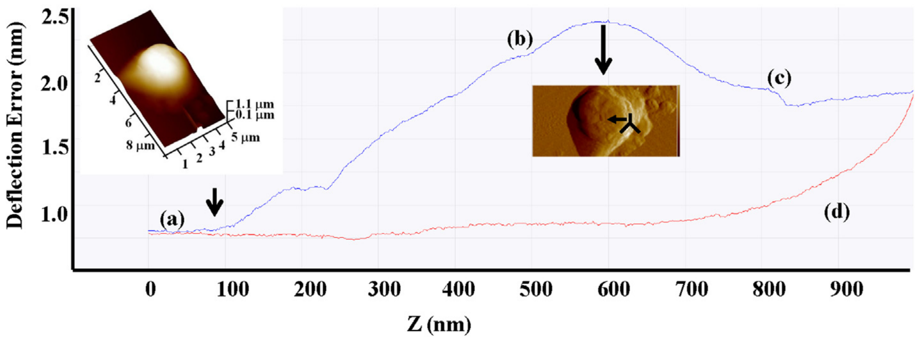

Fig. 8. Mechanical testing of the elastic-plastic region by AFM of a microcapsule of PCS28 at 23 °C; (a) no contact, continuous line; (b) plastic penetration; (c) deformation of the sample; and (d) retraction of the AFM probe (red line). (For interpretation of the references to colour in this figure legend, the reader is referred to the web version of this article.)

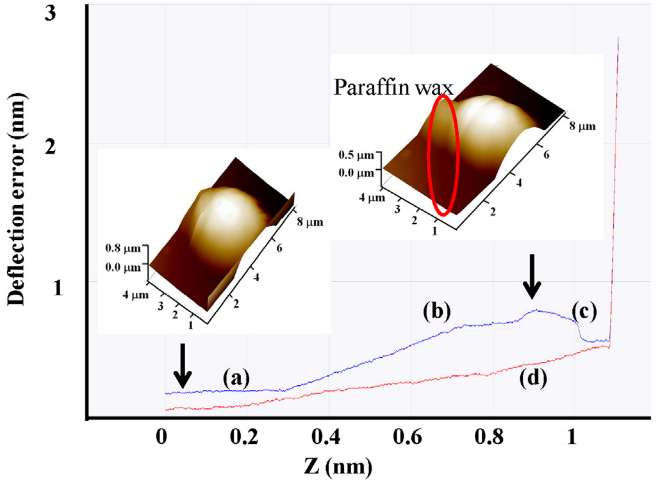

Fig. 9. Mechanical testing of the elastic-plastic region by AFM of a microcapsule of PCS28 at 45 °C; (a) no contact, continuous line; (b) plastic penetration; (c) deformation of the sample; and (d) retraction of the AFM probe (red line). (For interpretation of the references to colour in this figure legend, the reader is referred to the web version of this article.)

phase change wax material spread on the mica surface, as (b) confirms.

When heating a microcapsule of PCS28 from 23 to 45 °C, the topographic section of 10 × 10 µm corresponding to the white line in the image changes. This mentioned change is shown in Fig. 10.

The 3D view *E* map (a), the deformation histogram (b), and *E* histogram (c) of PCS28 at 23 °C are presented in Fig. 11. The obtained results were 70 nm for the mean deformation and 43 MPa applying a vertical force of 500 nN. These results show that PCS28 particles are clearly softer than the Micronal® DS 5007 X resulting in more deformable particles.

Additionally, *E* mapping at 45 °C for PCS28 is shown in Fig. 12. As it happens with Micronal® DS 5007 X, the obtained values at 45 °C are even lower compared to those achieved at 23 °C. The deformation values were between 70 and 300 nm, and the mean *E* result was 30 MPa using 500 nN of load.

The mechanical properties when increasing the temperature for PCS28 sample also decrease because of the MF polymeric shell, since is a thermoset resin has the tendency to have more fragile and pressure-sensitive walls compared with acrylic one, it is susceptible to break and degrade more easily. Therefore, results demonstrate that acrylic polymeric shell for MPCM for PCS is a better option compared to MF. Nevertheless, the measurements were not performed in pumping conditions.

Table 3 summarizes the obtained results by means AFM technique.

4. Conclusions

Two different samples of PCS containing microcapsules with different polymeric shell and paraffin wax as PCM were compared in this paper. Micronal® DS 5007 X presents a bigger particle size than PCS28 sample. Furthermore, PCS28 sample shows an agglomeration over time. Additionally, the samples under study have similar wall shell thickness, around 0.5 µm. From the mechanical viewpoint, AFM technique demonstrates that it is very important to take into consideration the assay temperature, because the mechanical properties decrease abruptly when the temperature increases. The mechanical properties are reduced abruptly when the temperature is close to the glass transition for Micronal® samples. In case of PCS28 its reduction is due to nature of prepared microcapsule wall using in situ polymerisation and melamine-formaldehyde as shell material, which tend to have more brittle and pressure-sensitive walls, and were prone to cracking. Also, it is essential to consider the change in shape of the microcapsules with an increment of temperature for the studied

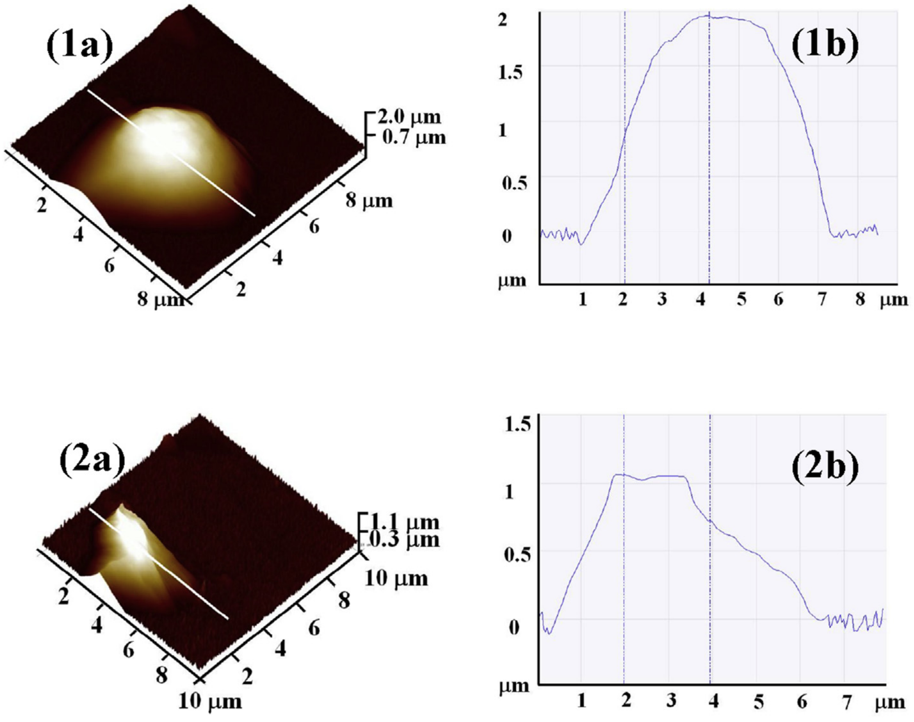

Fig. 10. PCS28 sample at (1) 23 °C and, (2) 45 °C; (a) 3D view, and (b) topographic image.

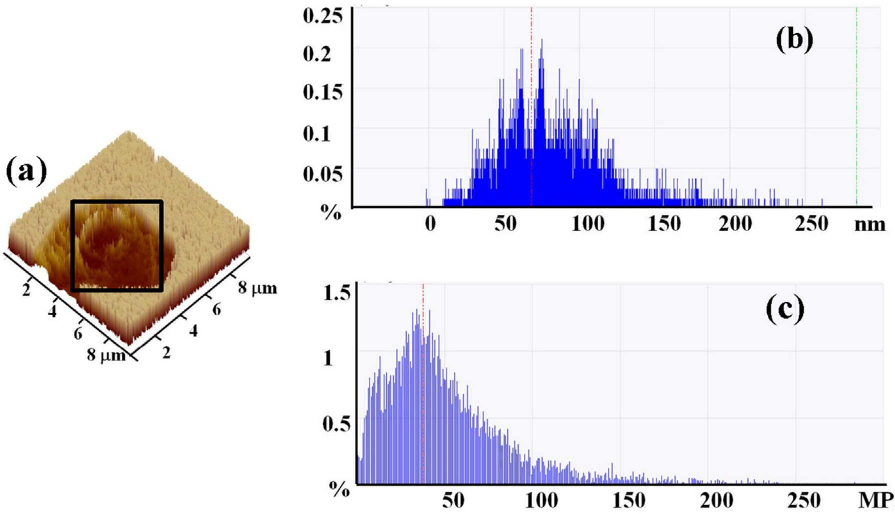

Fig. 11. Effective Young's modulus mapping of PCS28 at 23 °C; (a) 3D view; (b) Deformation histogram; (c) *E* histogram.

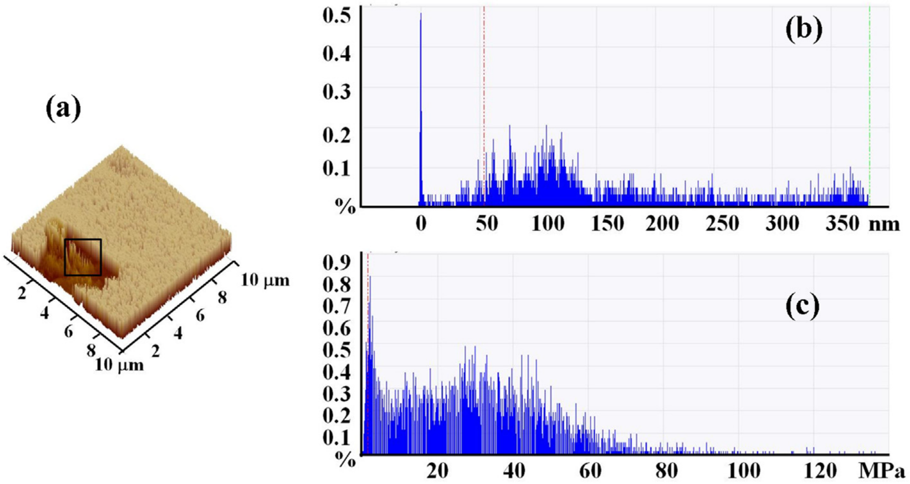

Fig. 12. Effective Young's modulus mapping of PCS28 at 45 °C; (a) 3D view; (b) Deformation histogram; (c) E histogram.

Table 3
Summary of the main results.

	Micronal® DS 5007 X		PCS 28	
	23 °C	45 °C	23 °C	45 °C
Needed force to break the MPCM (µN)	11.0	1.8	2.5	0.9
Deformation (nm)	10–20	20	70	70–300
Mean Effective Young's modulus (*E*) value applying 500 nN (MPa)	200	50	43	30

samples. The higher the temperature, the lower the mechanical properties and this fact also is influenced by the liquid state of the paraffin wax. The needed force to break Micronal® DS 5007 X microcapsules decrease one order of magnitude when changing the temperature from 23 °C to 45 °C. Comparing Micronal® DS 5007 X with PCS28, the properties obtained from the mechanical performance are higher. In summary, from the mechanical point of view, an acrylate group to be used as a shell of microcapsules is better than a melamine-formaldehyde resin taking into account that both samples have the same thickness shell as SEM results elucidate. But, using MF as an MPCM shell, walls can be improved getting more durable, and this is also influenced by the fabrication process: laboratory or industrial. Hence, results show that acrylic polymeric shell is a better choice in comparison to MF, where it is difficult to change its wall brittle nature to desire more elastic. However, these measurements were performed using static samples. More experiments must be performed under pumping conditions.

Acknowledgments

The work is partially funded by the Spanish government (ENE2011-28269-C03-02 and ENE2011-22722). The authors would like to thank the Catalan Government for the quality accreditation given to their research group GREA (2014 SGR 123) and research group DIOPMA (2014 SGR 1543). The research leading to these results has received funding from the European Union's Seventh Framework Programme (FP7/2007-2013) under grant agreement nº PIRSES-GA-2013-610692 (INNOSTORAGE).

References

[1] H. Mehling, L.F. Cabeza, Heat and Cold Storage with PCM, Springer-Verlag, 2008. ISBN-13: 9783540685562.

[2] D. Zhou, C.Y. Zhao, Y. Tian, Review on thermal energy storage with phase change materials (PCMs) in building applications, Appl. Energ 92 (2012) 593–605.

[3] F. Kuznik, D. David, K. Johannes, J.J. Roux, A review on phase change materials integrated in building walls, Renew. Sust. Energ Rev. 15 (2011) 379–391.

[4] A. Sharma, V.V. Tyagi, C.R. Chen, D. Buddhi, Review on thermal energy storage with phase change materials and applications, Renew. Sust. Energ Rev. 13 (2009) 318–345.

[5] F. Agyenim, N. Hewitt, P. Eames, M. Smyth, A review of materials, heat transfer and phase change problem formulation for latent heat thermal energy storage systems (LHTESS), Renew. Sust. Energ Rev. 14 (2010) 615–628.

[6] P. Schossig, H.M. Henning, S. Gschwander, T. Haussmann, Micro-encapsulated phase change materials integrated into construction materials, Sol. Energ Mat. Sol. C 89 (2005) 297–306.

[7] V.V. Tyagi, D. Buddhi, PCM thermal storage in buildings: a state of the art, Renew. Sust. Energ Rev. 11 (2007) 1146–1166.

[8] A.M. Borreguero, M. Carmona, M.L. Sánchez, J.L. Valverde, J.F. Rodríguez, Improvement of the thermal behavior of gypsum blocks by the incorporation of microcapsules containing PCMs obtained by suspension polymerization with an optimal core/coating mass ratio, Appl. Therm. Eng. 30 (2010) 1164–1169.

[9] T.C. Ling, C.S. Poon, Use of phase change materials for thermal energy storage in concrete: an overview, Constr. Build. Mater 46 (2013) 55–62.

[10] J. Vectstaudza, J. Locs, D. Bajāre, C. Barreneche, A.I. Fernández, Characterization of Wood/PCM composites for building applications, in: The 2nd International Energy Stoarge Conference. Sustainable Energy Storage in Buildings, 2013.

[11] L. Bayés-García, L. Ventolà, R. Cordobilla, Phase change materials (PCM) microcapsules with different shell compositions: preparation, characterization and thermal stability, Sol. Energ Mater Sol. C 94 (2010) 12535–12540.

[12] J. Giro-Paloma, G. Oncins, C. Barreneche, M. Martínez, A.I. Fernández, L.F. Cabeza, Physico-chemical and mechanical properties of microencapsulated phase change material, Appl. Energ 109 (2013) 441–448.

[13] C.Y. Zhao, G.H. Zhang, Review on microencapsulated phase change materials (MEPCMs): fabrication, characterization and applications, Renew. Sust. Energ Rev. 15 (2011) 3813–3832.

[14] P.B. Salunkhe, P.S. Shembekar, A review on effect of phase change material encapsulation on the thermal performance of a system, Renew. Sust. Energ Rev. 16 (2012) 5603–5616.

[15] V.V. Tyagi, S.C. Kaushik, S.K. Tyagi, T. Akiyama, Development of phase change materials based microencapsulated technology for buildings: a review, Renew. Sust. Energ Rev. 15 (2011) 1373–1391.

[16] C. Castellon, M. Medrano, J. Roca, L.F. Cabeza, M.E. Navarro, A.I. Fernandez, Effect of microencapsulated phase change material in sandwich panels, Renew. Energ 35 (10) (2010) 2370–2374.

[17] J. Giro-Paloma, C. Barreneche, M. Delgado, M. Martínez, A.I. Fernández, L.F. Cabeza, Physicochemical and thermal study of a MPCM of PMMA shell and paraffin wax as a core, Energy Procedia 48 (2014) 347–354.

[18] M. Delgado, A. Lázaro, J. Mazo, J.M. Marín, B. Zalba, Experimental analysis of a microencapsulated PCM slurry as thermal system and as heat transfer fluid in laminar flow, Appl. Therm. Eng. 36 (1) (2012) 370–377.

[19] W. Lu, S.A. Tassou, Experimental study of the thermal characteristics of phase change slurries for active cooling, Appl. Energ 91 (1) (2012) 366–374.

[20] S. Zhang, J. Niu, Experimental investigation of effects of super-cooling on microencapsulated phase-change material (MPCM) slurry thermal storage capacities, Sol. Energ. Mat. Sol. C 94 (6) (2010) 1038–1048.

[21] Z. Youssef, A. Delahaye, L. Huang, F. Trinquet, L. Fournaison, C. Pollerberg, C. Doetsch, State of the art on phase change material slurries, Energ Convers. Manage 65 (2013) 120–132.

[22] M. Delgado, A. Lázaro, J. Mazo, B. Zalba, Review on phase change material emulsions and microencapsulated phase change material slurries: materials heat transfer studies and applications, Renew. Sust. Energ Rev. 16 (1) (2012) 253–273.

[23] C. Castellón, I. Martorell, L.F. Cabeza, A.I. Fernández, A.M. Manich, Compatibility of plastic with phase change materials (PCM), Int. J. Energ Res. 35 (2010) 765–771.

[24] G.H. Zhang, C.Y. Zhao, Thermal and rheological properties of microencapsulated phase change materials, Renew. Energ 36 (2011) 2959–2966.

[25] Šumiga B. Ph.D Thesis, University of Ljubljana, 2013.

[26] J.F. Su, L.X. Wang, L. Ren, Preparation and characterization of double-MF shell microPCMs used in building materials, J. Appl. Polym. Sci. 97 (5) (2005) 1755–1762.

[27] J. Giro-Paloma, C. Barreneche, M. Martínez, B. Sumiga, L.F. Cabeza, A.I. Fernández, Comparison of phase change slurries: physicochemical and thermal properties, Energy 87 (2015) 223–227.

[28] M.R. VanLandingham, J.S. Villarrubia, G.F. Meyers, Nanoindentation of polymers: overview, Polym. Prepr. 41 (2) (2000) 1412.

[29] C.A. Clifford, M.P. Seah, Nanoindentation measurement of effective Young's modulus for compliant layers on stiffer substrates including the effect of Poisson's ratios, Nanotechnology 20 (2009) 1–8.

[30] J. Giro-Paloma, J.J. Roa, A.M. Díez-Pascual, E. Rayón, A. Flores, M. Martínez, J.M. Chimenos, A.I. Fernández, Depth-sensing indentation applied to polymers: a comparison between standard methods of analysis in relation to the nature of the materials, Eur. Polym. J. 49 (2013) 4047–4053.

Chapter 5 References

[1] Dry powder mixes comprising Phase change Materials. Patent US 5370814, n.d.

[2] Baronetto S, G S, F G, M P. Numerical Model of a Slurry PCM-Based Solar Thermal Collector. Proc. 8th Int. Symp. Heating, Vent. Air Cond. Lect. Notes Electr. Eng., 2014, p. 13–20.

[3] Huang L, Petermann M, Doetsch C. Evaluation of paraffin/water emulsion as a phase change slurry for cooling applications. Energy 2009;34:1145–55. doi:10.1016/j.energy.2009.03.016.

[4] Stamatiou E, Kawaji M. Thermal and flow behavior of ice slurries in a vertical rectangular channel. Part I: Local distribution measurements in adiabatic flow. Int J Heat Mass Transf 2005;48:3527–43. doi:10.1016/j.ijheatmasstransfer.2005.03.020.

[5] Knodel BD, France DM, Choi US, Wambsganss MW. Heat transfer and pressure drop in ice-water slurries. Appl Therm Eng 2000;20:671–85. doi:10.1016/S1359-4311(99)00046-0.

[6] Sarı A, Biçer A, Karaipekli A, Alkan C, Karadag A. Synthesis, thermal energy storage properties and thermal reliability of some fatty acid esters with glycerol as novel solid–liquid phase change materials. Sol Energy Mater Sol Cells 2010;94:1711–5. doi:10.1016/j.solmat.2010.05.033.

[7] Inaba H, Zhang Y, Horibe A, Haruki N. Numerical simulation of natural convection of latent heat phase-change-material microcapsulate slurry packed in a horizontal rectangular enclosure heated from below and cooled from above. Heat Mass Transf 2007;43:459–70. doi:10.1007/s00231-006-0121-y.

[8] Youssef Z, Delahaye A, Huang L, Trinquet F, Fournaison L, Pollerberg C, et al. State of the art on phase change material slurries. Energy Convers Manag 2013;65:120–32. doi:10.1016/j.enconman.2012.07.004.

[9] Huang MJ, Eames PC, McCormack S, Griffiths P, Hewitt NJ. Microencapsulated phase change slurries for thermal energy storage in a residential solar energy system. Renew Energy 2011;36:2932–9. doi:10.1016/j.renene.2011.04.004.

[10] Lu W, Tassou SA. Experimental study of the thermal characteristics of phase change slurries for active cooling. Appl Energy 2012;91:366–74. doi:10.1016/j.apenergy.2011.10.004.

[11] Zhang P, Ma ZW. An overview of fundamental studies and applications of phase change material slurries to secondary loop refrigeration and air conditioning systems. Renew Sustain Energy Rev 2012;16:5021–58. doi:10.1016/j.rser.2012.03.059.

[12] Al-Abidi A a., Bin Mat S, Sopian K, Sulaiman MY, Lim CH, Th A. Review of thermal energy storage for air conditioning systems. Renew Sustain Energy Rev 2012;16:5802–19. doi:10.1016/j.rser.2012.05.030.

[13] Domínguez M, García C. Aprovechamiento de los Materiales de Cambio de Fase (PCM) en la Climatización. Inf Tecnológic 2009;20:107–15.

[14] Delgado M, Lázaro A, Mazo J, Zalba B. Review on phase change material emulsions and microencapsulated phase change material slurries: Materials, heat transfer studies and applications. Renew Sustain Energy Rev 2012;16:253–73. doi:10.1016/j.rser.2011.07.152.

[15] Alvarado JL, Marsh C, Sohn C, Phetteplace G, Newell T. Thermal performance of microencapsulated phase change material slurry in turbulent flow under constant heat flux. Int J Heat Mass Transf 2007;50:1938–52. doi:10.1016/j.ijheatmasstransfer.2006.09.026.

[16] Griffiths PW, Eames PC. Performance of chilled ceiling panels using phase change material slurries as the heat transport medium. Appl Therm Eng 2007;27:1756–60. doi:10.1016/j.applthermaleng.2006.07.009.

[17] Huang L, Doetsch C, Pollerberg C. Low temperature paraffin phase change emulsions. Int J Refrig 2010;33:1583–9. doi:10.1016/j.ijrefrig.2010.05.016.

[18] Zhang P, Ma ZW, Wang RZ. An overview of phase change material slurries: MPCS and CHS. Renew Sustain Energy Rev 2010;14:598–614. doi:10.1016/j.rser.2009.08.015.

[19] Augood PC, Newborough M, Highgate DJ. Thermal behaviour of phase-change slurries incorporating hydrated hydrophilic polymeric particles. Exp Therm Fluid Sci 2001;25:457–68. doi:10.1016/S0894-1777(01)00099-1.

[20] Zhang S, Niu J. Experimental investigation of effects of supercooling on microencapsulated phase-change material (MPCM) slurry thermal storage capacities. Sol Energy Mater Sol Cells 2010;94:1038–48. doi:10.1016/j.solmat.2010.02.022.

[21] Yang R, Xu H, Zhang Y. Preparation, physical property and thermal physical property of phase change microcapsule slurry and phase change emulsion. Sol Energy Mater Sol Cells 2003;80:405–16. doi:10.1016/j.solmat.2003.08.005.

[22] Wang X, Niu J. Heat Transfer of Microencapsulated PCM Slurry Flow in a Circular Tube 2008;54. doi:10.1002/aic.

[23] Gschwander S, Schossig P, Henning H. Micro-encapsulated paraffin in phase-change slurries. Sol Energy Mater Sol Cells 2005;89:307–15. doi:10.1016/j.solmat.2004.12.008.

[24] Salunkhe PB, Shembekar PS. A review on effect of phase change material encapsulation on the thermal performance of a system. Renew Sustain Energy Rev 2012;16:5603–16. doi:10.1016/j.rser.2012.05.037.

[25] Giro-Paloma J, Barreneche C, Delgado M, Martínez M, Fernández AI, Cabeza LF. Physicochemical and thermal study of a MPCM of PMMA shell and paraffin wax as a core. Energy Procedia, vol. 48, 2014, p. 347–54.

[26] Zeng R, Wang X, Chen B, Zhang Y, Niu J, Wang X, et al. Heat transfer characteristics of microencapsulated phase change material slurry in laminar flow under constant heat flux. Appl Energy 2009;86:2661–70. doi:10.1016/j.apenergy.2009.04.025.

[27] Huang L, Günther E, Doetsch C, Mehling H. Subcooling in PCM emulsions—Part 1: Experimental. Thermochim Acta 2010;509:93–9. doi:10.1016/j.tca.2010.06.006.

[28] Günther E, Huang L, Mehling H, Dötsch C. Subcooling in PCM emulsions – Part 2: Interpretation in terms of nucleation theory. Thermochim Acta 2011;522:199–204. doi:10.1016/j.tca.2011.04.027.

Chapter 6. Characterization of Micronal® DS 5045 X

6.1 Thermal properties importance in Phase Change Slurries

6.2 Micronal® DS 5045 X

6.3 Characterization of Micronal® DS 5045 X

6.4 Optimum conditions by Thermogravimetrical analysis

6.1 Thermal properties importance in Phase Change Slurries

Due to importance of evaluating the durability of PCS under cycling tests, an evaluation of the thermal properties of the samples allows describing the thermal stability of the PCS slurry Thermal properties of Phase Change Slurries (PCS) are frequently performed by thermogravimetric analysis (TGA) and differential scanning calorimetry (DSC) techniques. Hence, different TGA curves recorded at different heating rates can offer precise information concerning the mechanism and the kinetics of the investigated thermal degradation process [1]. The TGA technique can analyze materials that exhibit loss or gain of mass due to thermal decomposition, oxidation or dehydration [2]. However, it is important to highlight that there are differences considering the thermal behavior of PCS by means of TGA when PCS is a slurry or a dried slurry [3]. For this reason, it is important to characterize and compare PCS samples in both states. It is essential to notice that, when the PCS is dried, it is considered as MPCM.

Given that thermogravimetrical analysis is widely used to characterize MPCM [4–9], the important issue using this technique is to define the best parameters and conditions for studying the decomposition of MPCM and PCS. A complete evaluation of the sample by TGA at different atmospheres allows describing the thermal stability of PCS sample. Some authors evaluated different MPCM shell compositions [10–12] by using TGA curves, where samples were firstly maintained at 100 ºC for 90 minutes before heated at 10 $ºC·min^{-1}$. Otherwise, this prior treatment could may cause the loss of the major part of the core material, affecting the measurement of the mass loss percentage [13].

6.2 Micronal® DS 5045 X

It is considered very interesting to evaluate a methodology to characterize the thermal behavior of PCS in general, Micronal® DS 5045 X in particular, by means of TGA. For this reason, it was seen the necessity to continue investigating the characterization of PCS slurries, overall in the thermal and cycling properties, because results can change drastically depending on the considered analysis parameters [14]. The studied sample was Micronal® DS 5045 X, a commercial PCS used in active systems, which consists on an aqueous suspension made of microcapsules of a highly cross linked methyl methacrylate (MMA) shell and *n*-octadecane as core PCM, with a phase change between 24 and 28 ºC. The PCS has a pH value of 6.61.

The Micronal® DS 5045 X was characterized as a suspension, and also it was dried at room temperature up to 24 hours in order to evaluate its properties and compare them with the original PCS. In Figure 6. 1 is shown the Micronal® DS 5045 X sample used. This sample was used in the study **Thermal Cycle Feasibility of Phase Change Slurry”** [3] presented as oral communication in the **Eurotherm Seminar #99, Advances in Thermal Energy Storage** [15]. In this Chapter will be presented the study exposed in the conference.

Figure 6. 1. a) Image of Micronal® DS 5045 X sample used for the study untitled “Thermal Cycle Feasibility of Phase Change Slurry”, b) Image of dried Micronal® DS 5045 X.

This study evaluated the durability of the shell and its thermal stability. For this reason, in order to perform the physico-chemical characterization, it was used a cycling system to evaluate the behavior of the PCS before and after pumping the sample between 21 and 28 ºC. The pH of the sample increases reaching the 7.23 when it was cycled 5000 times, and after 7000 cycles the PCS has a pH value of 7.36. In this way, the objective of this study was to evaluate the physico-chemical behavior of Micronal® DS 5045 X sample before and after cycling the sample 5000 and 7000 times.

In the left side of Figure 6. 2 is shown the PCS Micronal® DS 5045 X sample cycled 7000 times, and in the right side it is shown the dried PCS Micronal® DS 5045 X sample 7000 times cycled. The green color for both samples is due to the possible remains of copper after passing through in the pipeline. As it was noticed above, due to the high density of the original Micronal$^{®}$ DS 5045 X sample, a 20 % aliquot of the sample was pumped.

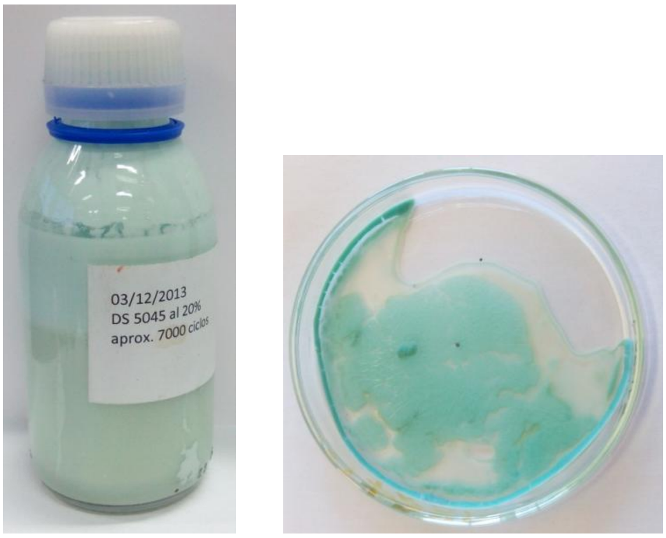

Figure 6. 2. a) Image of the 7000 cycles Micronal$^{®}$ DS 5045 X sample used for the study untitled "Thermal Cycle Feasibility of Phase Change Slurry", b) Image of dried Micronal$^{®}$ DS 5045 X.

The original sample and the 5000 cycled one were evaluated through Scanning Electron Microscopy (SEM) coupled to a cryogenic N_2 system. Moreover, the Fourier-Transformed Infrared Spectroscopy allows detecting the MPCM shell structural differences of the PCS. Taking into account the thermal parameters of the sample, the Thermogravimetrical Analysis (TGA) and Differential Scanning Calorimeter (DSC) were used for Micronal$^{®}$ DS 5045 X before and after cycling the sample. TGA allows determining the weight loss in front of the temperature, and DSC studies the melting temperature and enthalpy.

6.3 Characterization of Micronal$^{®}$ DS 5045 X

6.3.1 Cycles

The PCS Micronal$^{®}$ DS 5045 X was pumped and cycled by Dr. Delgado in the experimental installation located at Universidad de Zaragoza. The characterization of the sample was performed at Universitat de Barcelona.

The experimental installation is designed to study flow and heat transfer characteristics of PCM slurries. This setup cause the sample to solidification and melting cycles, and at the same time the sample is being pumped. The PCS was pumped from the thermostatic bath, where the PCM of the microcapsules in suspension were in solid phase. After flowing through the loop, and passing through the heat transfer section, the PCM of the PCS was melted. After the heat transfer section, the PCS returns to the thermostatic bath for cooling and solidifying the PCM microcapsules. More technical details of the installation can be found in the following reference [16].

Since Micronal® DS 5045 X changes its phase in a temperature range of 21 - 28 ºC, 21 ºC has been chosen as set temperature of the thermostatic bath. Due to the high density of the initial PCS sample, a 20 % aliquot was prepared. It was pumped at 21ºC through the flow loop, where the control valve has been adjusted to test with a mass flow of approximately 50 $kg \cdot h^{-1}$. The heat flux supplied on the heat transfer section was controlled by a phase angle regulator, so that the fluid temperature at the outlet of this section increased up to 28 ºC, and to guarantee that the PCM microcapsules in suspension have melted. This temperature has been measured by a 4-wire Pt100 datalogger. In this manner it is guaranteed that the microcapsules in suspension have melted. From the velocity of the PCS and from the volume of the installation (that is from the volume of the pumped PCS), the necessary time for a melting-solidification cycle can be calculated. Thus, the total number of cycles can be obtained. From the drainage valve, different samples of the PCS pumped and cycled have been extracted. Specifically, a sample at 5000 cycles and at 7000 cycles (both solidification and melting cycles between 21 and 28 ºC) have been extracted in order to evaluate its different thermal properties and compare with the initial sample without cycling and pumping. In total, the PCS slurry has been pumped under these conditions during one month approximately.

6.3.2 Scanning Electron Microscopy (SEM)

Scanning Electron Microscopy (SEM) was used to characterize the shape and the size of the Micronal® DS 5045 X. The sample preparation for SEM analysis differed from the conventional method, as cryogenic N_2 was used to solidify the PCS. A Cryo Unit GATAN accessory (Alto 1000 model) was used at the Scientific and Technological Centers (CCTiUB) at Universitat de Barcelona for preparing the samples at 0 and 5000 cycles. Due to the nature of the sample a conductive carbon coating was also required. Besides, the images were obtained by secondary electrons (SE) and at 10 KV through a JEOL JSM-6510.

SEM images show that the sample at 0 cycles (Figure 6. 3a) is formed by microcapsules that appear unbroken in the two magnifications used, x 2200 and x 5500, respectively. Some holes can be observed corresponding to the space provided by some MPCM that leave their position after the cryogenic preparation prior the observation. Nevertheless, when the PCS has been pumped 5000 times (see Figure 6. 3b) it is observed in magnification x 7500 that some microcapsules are broken. It is important to note also the capsules shape deformation. The durability of these microcapsules seems to be lower than 5000 charge/discharge cycles.

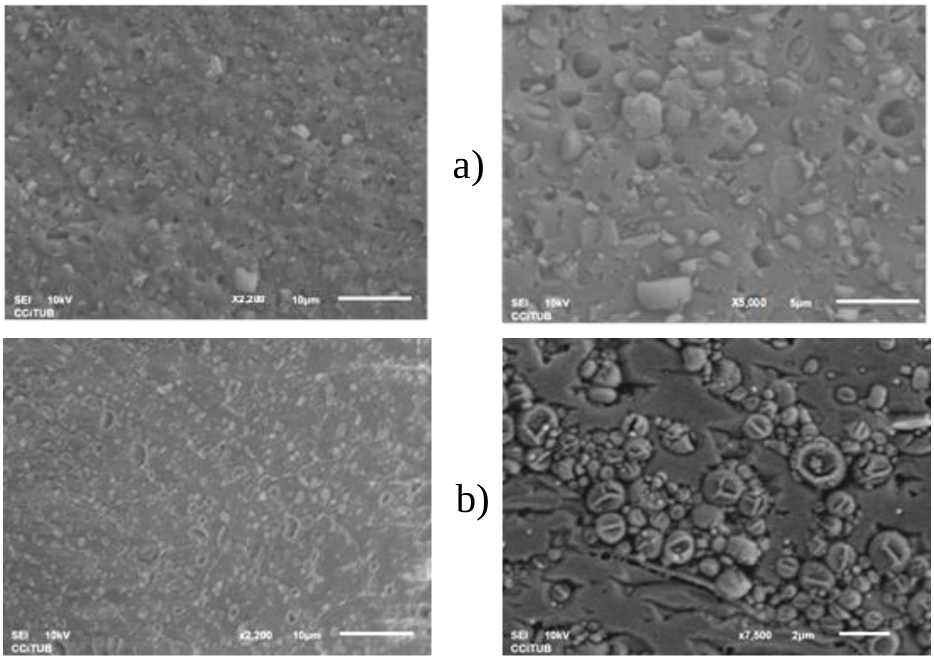

Figure 6. 3. SEM images by secondary electrons (SE) a) 0 cycles, b) 5000 cycles.

6.3.3 Fourier-Transformed Infrared (FT-IR)

The chemical characterization of the shell was performed by a Fourier-Transformed Infrared (FT-IR) with Attenuated Total Reflectance (ATR), which was used to characterize the principal peaks of the MPCM. The FT-IR spectra obtained for samples after 5000 and 7000 cycles showed no significant differences both as slurry and dried PCS, as Figure 6.4 shows.

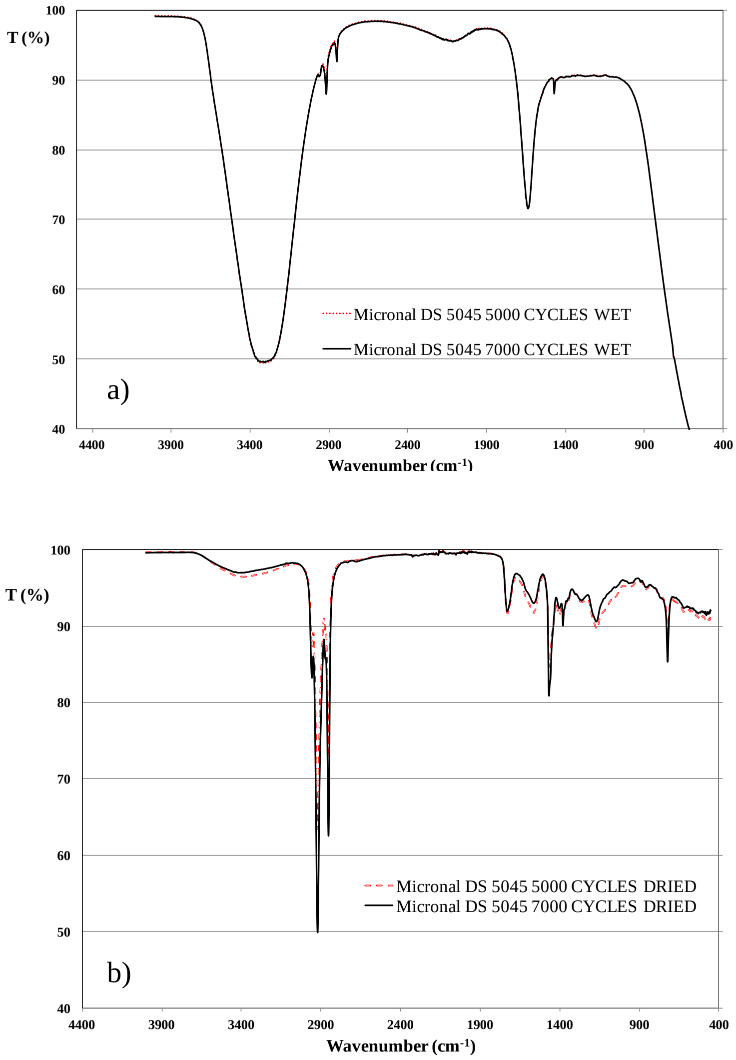

Figure 6. 4. FT-IR spectra for a) slurry Micronal® DS 5045 X after 5000 and 7000 cycles and b) dried PCS.

Furthermore, the spectrum of the 7000 cycles sample is compared with the non-cycled one. In Figure 6. 5a is shown the FT-IR spectra of the PCS at 0 and 7000 cycles. Once the PCS was air dried during 24 h, the important peaks are more defined than in the slurries spectra (Figure 6. 5b). It may be seen that Micronal® DS 5045 X and Micronal® DS 5045 X after 7000 cycles have practically the same spectra. The slightly differences in intensity between slurry and dried spectra are related to the concentration of the microcapsules. In Table 6. 1 is summarized the main peaks for the samples.

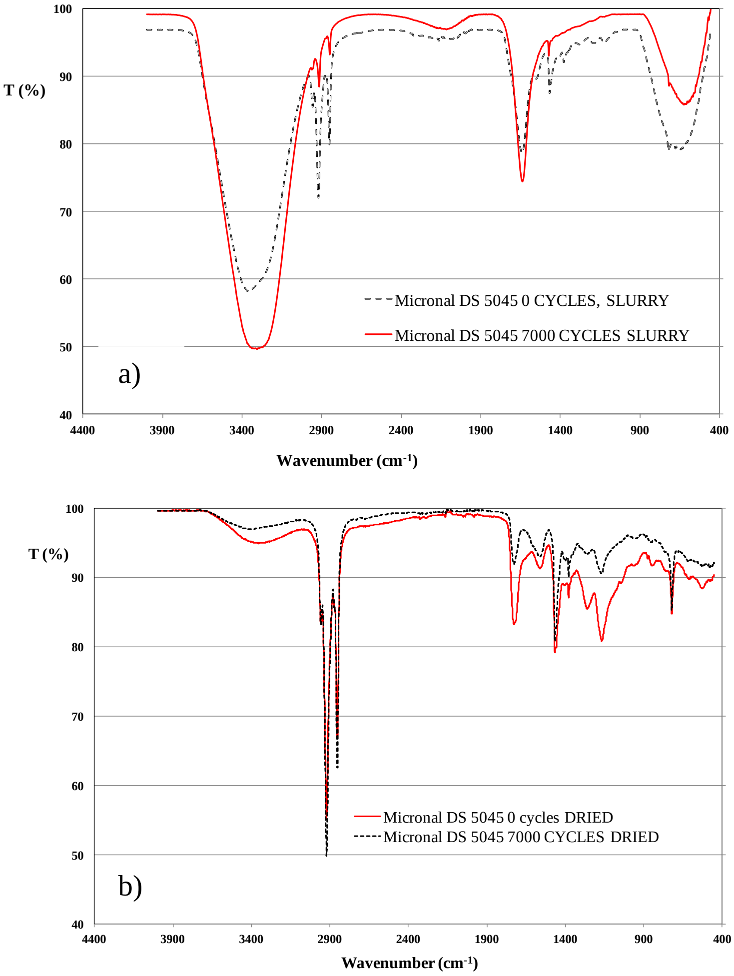

Figure 6. 5. FT-IR analysis for PCS Micronal ® DS 5045 X sample for 0 cycles and 7000 cycles, in a) PCS and b) dried PCS.

Table 6. 1. Characteristic peaks obtained from FT-IR of PCS Micronal® DS 5045 X.

0 cycles	Wavenumber (cm^{-1})	3368	2920.7	2851	1634.0	1466	1118	719
	Transmittance (%)	58.2	72.0	79.9	78.7	87.5	94.6	79.0
7000 cycles	Wavenumber (cm^{-1})	3307	2916.3	2849.7	1637.7	1471.7	1123	620.23
	Transmittance (%)	49.5	88.0	92.7	71.6	88.1	98.8	85.8
Attributed to		Aqueous suspension	aliphatic C-H stretching vibration	aliphatic C-H stretching vibration	ester carbonyl group stretching vibration	C-H bending vibration	C-O stretching vibration of the ester group	C-H bending

For liquid samples in ATR mode, the results are quantitative (take into consideration that the 5000 and 7000 cycles sample are a 20 % aliquot of the 0 cycled sample). Thereby, the peaks correspond to an acrylic polymer. Notice that the shell does not present chemical changes, because the principal peaks of 0 cycles and 7000 cycles match.

6.3.4 Differential Scanning Calorimetry (DSC)

The instrument used to characterize the melting temperature and the melting enthalpy of the dried PCS at 0, 5000 and 7000 cycles was a DS 822e by Mettler Toledo between 10 and 40 ºC, applying 0.5 ºC·min^{-1} dynamic heating rate, following the methodology proposed by Barreneche *et al*. [17].

DSC results for Micronal® DS 5045 X before and after 5000 and 7000 cycles, both as dried PCS, are presented in Figure 6. 6. DSC results for dried Micronal® DS 5045 X for 0, 5000, and 7000 cycles. The sample was air dried because it is important to proper determine the melting and solidification temperatures and enthalpies of the PCM without considering the water of the PCS. DSC curve obtained before cycling process shows a single peak at 28 ºC while the other two curves which were cycled 5000 and 7000 times shows a slight double peak. This fact discerns that the paraffin is becoming two different substances concerning two different melting points. The main DSC results are summarized in Table 6. 2, where melting and solidification temperatures and enthalpies are presented.

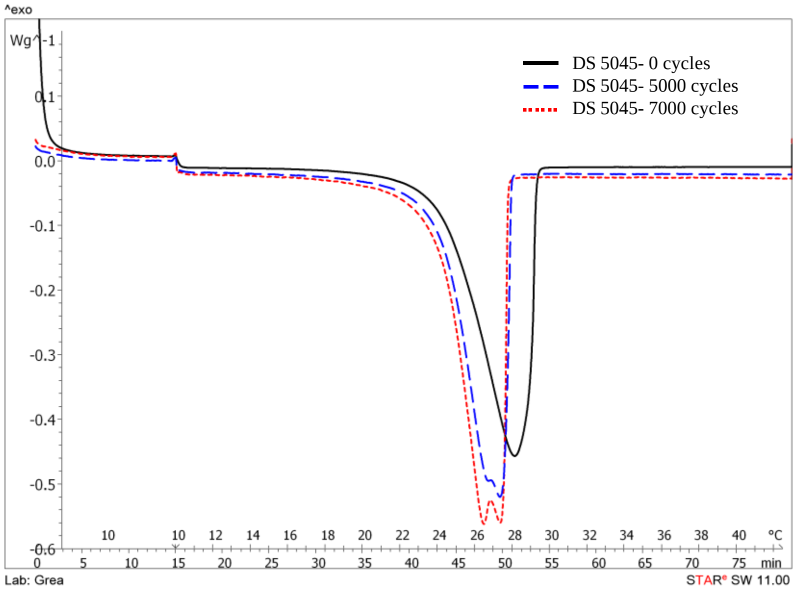

Figure 6. 6. DSC results for dried Micronal® DS 5045 X for 0, 5000, and 7000 cycles.

Taking into account these results and the DSC profile, the changes between samples may be attributed to a structural degradation in the carbon chain from the paraffin for the 5000 and 7000 cycled samples because a single clear peak is not obtained.

Table 6. 2. DSC results for heating and cooling processes. Calculated percent change.

Micronal® DS 5045 X	Melting temperature (ºC)	Melting enthalpy (kJ·kg^{-1})	Solidification temperature (ºC)	Solidification enthalpy (kJ·kg^{-1})
0 cycles	28	183	22	133
5000 cycles	26-27	168	23	122
7000 cycles	26-27	187	23	136

Considering the thermal behavior, there is a slightly change between 0 and 5000 cycles, and between 0 and 7000 cycles. The melting enthalpy difference between the samples is lower than 10 %. In the light of the results, the thermophysical properties almost do not change, and the thermal behavior of the final application will be practically equal.

6.3.5 Thermogravimetrical Analysis (TGA)

Sample thermal stability was evaluated with a Simultaneous SDTQ600 TA Instruments device under 50 ml·min^{-1} N_2 atmosphere. The experiments were performed from 25 ºC to 600 ºC at 10 ºC·min^{-1} for 0, 5000 and 7000 cycles air dried Micronal® DS 5045 X. In Figure 6. 7 is shown the thermogravimetrical decomposition of the sample with and without cycling it. The sample was air dried because it is important to see the detailed weight losses of the MPCM (PCM + shell) without taking into account the water evaporation of the sample if tested as PCS.

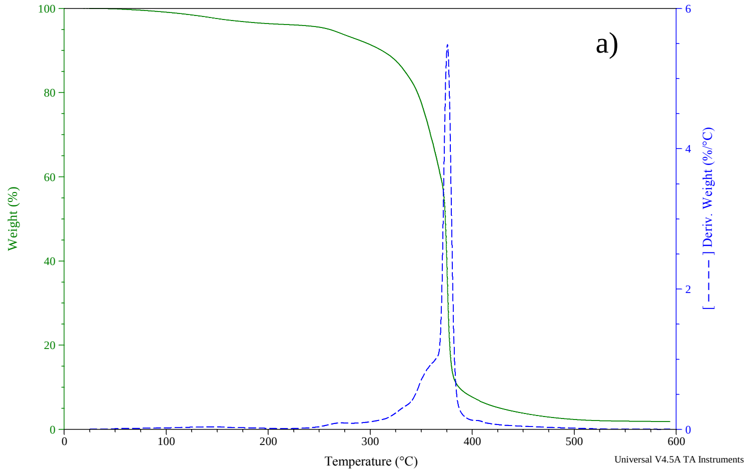

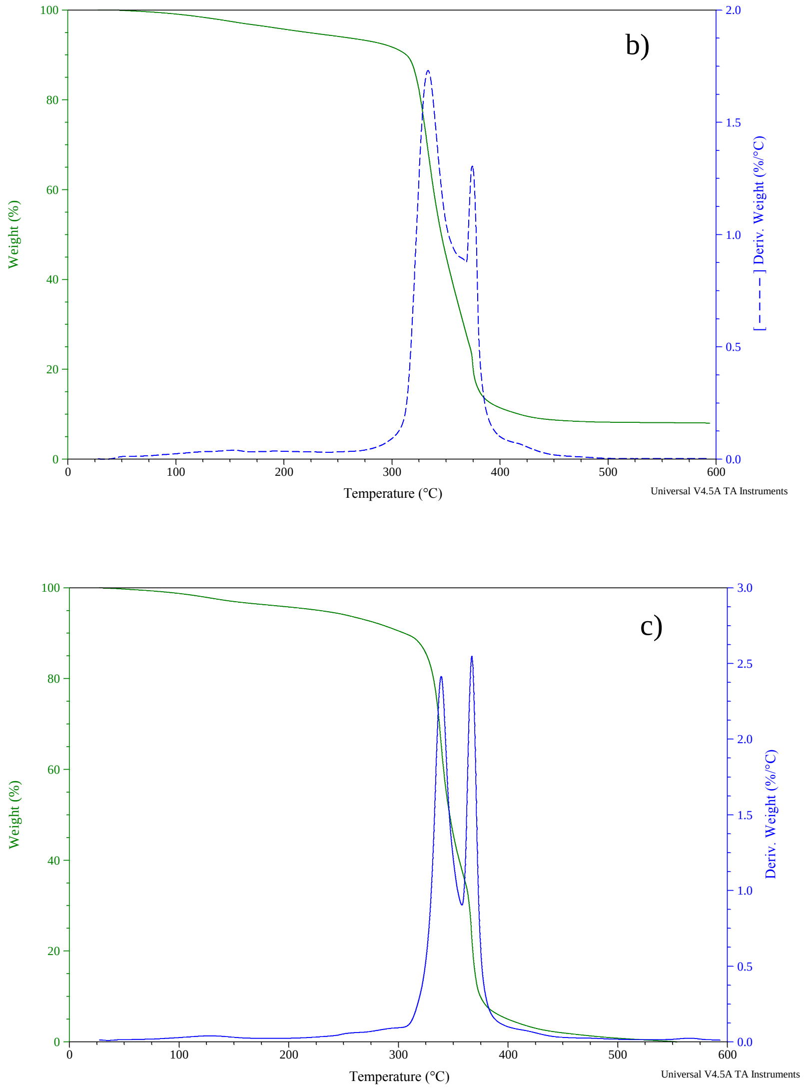

Figure 6. 7. TGA thermograms of dried Micronal® DS 5045 X for a) 0, b) 5000, and c) 7000 cycles.

Furthermore, Table 6. 3 summarize the weight loses of the experiments performed on the PCS samples and on the dried samples of Micronal® DS 5045 X. Moreover, the amount of sample in each assay is also showed, as well as the range degradation temperatures for both types of samples. It is explained the correspondence of each degradation, and the amount of residue after achieving 600 ºC. It is important to emphasize that the cycled sample was a 20 % aliquot of the original PCS, and for this reason, in the case of the wet PCS, it is impossible to distinguish between the PCM and the shell. Besides, the percentages of each component (water/PCM/shell) differ comparing the 0 cycles sample with the 5000 and 7000 cycles ones. However, these percentages are slightly equal for the samples 5000 and 7000 times cycled.

Table 6. 3. Thermogravimetrical results of Micronal® DS 5045 X in slurry and dried PCS.

	PCS					DRIED PCS				
cycles	sample (mg)	Range T (ºC)	Weight (%)	Due to	Residue (%)	sample (mg)	Range T (ºC)	Weight (%)	Due to	Residue (%)
0	16.834	26 – 145	56.64	water	1.25	23.388	25 – 144	2.17	water	1.94
		145 – 309	21.90	PCM			144 – 376	62.75	PCM	
		309 – 623	19.60	shell			376 – 536	33.24	shell	
5000	19.565	20 – 126	84.47	water	1.27	9.302	25 – 153	2.618	water	8.10
							153 – 333	28.47	PCM	
		126 – 551	13.64	MPCM			333 – 374	46.39	PCM	
							374 – 524	14.34	shell	
7000	24.263	27 – 133	84.87	water	0.97	11.257	25 – 129	2.249	water	0.00
							129 – 339	32.14	PCM	
		133 – 548	13.45	MPCM			339 – 367	42.67	PCM	
							367 - 531	22.58	shell	

It can be observed several differences between the PCS and the dried PCS samples, due to the water signal disappears, and the weight losses are better defined when the water was evaporated. Moreover, there are significant differences between the 0 cycles sample and the 5000 and 7000 cycled sample. The number of weight losses is diverse and the percentage is also diverse. For the cycled samples, both have similar degradations. It can be observed in Table 6. 3 that the initial temperature where the PCM starts its degradation for the dried sample for 5000 and 7000 cycles increases in some degrees. This fact it can be attributed to a possible degradation of the paraffin wax of the MPCM.

Hence, it can be concluded that there is almost no thermogravimetrical significant differences between 5000 and 7000 cycles. TGA is considered a powerful tool to study PCS thermal degradations and thus an exhaustive methodology has to be evaluated and applied for slurry samples to define a proper protocol to better compare different slurry samples.

6.3.6 Conclusions

At 7000 cycles the shape of the PCS Micronal® DS 5045 X starts a change, observing a breakage in the surface of the shell of some microcapsules, allowing the PCM leakage from the MPCM, as in SEM images can be observed. Although its spread, the thermal properties do not change abruptly, as the study by TGA and DSC techniques. So, it can be concluded that even though at 7000 cycles the physical properties of the sample changed, this sample still works in an active system, but it could be interesting to study this sample cycling it until 10000 cycles to evaluate the life cycle assessment of this PCS.

6.4 Optimum conditions by Thermogravimetrical analysis

After deeply analyzing Micronal® DS 5045 X sample as PCS and dried PCS, it was decided to explore the optimum conditions for study the thermal behavior of PCS by TGA, varying the parameter conditions for obtaining T_{peak} and heat flow due to different results obtained above depending on the sample conditions (wet/dried). The main purposes of this study are to determine the best conditions to analyze PCS samples and to proper interpret PCS samples. The factors that were taken into account were focused on the state of the sample (PCS and dried PCS), the atmosphere of study (air and N_2) and the heating rate (0.5, 1, 5, and 10 $ºC·min^{-1}$).

The samples under study were the ones showed above in Table 6. 4: Micronal® DS 5045 X (it will be named M) and dried Micronal® DS 5045 X (it will be named MD). The TGA was performed by means of a SDT Q600 from TA Instruments under N_2 and air atmosphere. The scanning rates were 0.5, 1, 5 and 10 $K·min^{-1}$ for both atmospheres in a temperature range between 20 ºC and 600 ºC. The procedure of the sample preparation prior TG analysis was the same for both samples, and the sample amount was kept in a mass range of 10.000 ± 0.5 mg. The differences observed in the TGA studies were evaluated by assessing the weight loss (%).

Table 6. 4. Summary of the experiments performed by TGA.

		10 $ºC·min^{-1}$		5 $ºC·min^{-1}$		1 $ºC·min^{-1}$		0.5 $ºC·min^{-1}$	
		N_2	Air	N_2	Air	N_2	Air	N_2	Air
Micronal® DS 5045 X	M	v	v	v	v	v	v	v	v
Micronal® DS 5045 X dried	MD	v	v	v	v	v	v	v	v

As this study is still running, few results and conclusions will be presented in this Chapter. Currently, it has been investigating the optimum conditions for PCS that have been cycled to better characterize and evaluate the proper parameters of these samples.

6.4.1. Characterization of Micronal® DS 5045 X slurry (M)

When comparing M sample at 10 ºC·min^{-1} in air and N_2 atmospheres it is observed that the main difference between both experiments is located in the second weight loss (> 250 ºC) in which the N_2 atmosphere showed to enhanced stability (Figure 6. 8). This fact is attributed to the thermo-oxidative degradation of the polymeric shell that takes place in air atmosphere. The same behavior is observed at 5, 1, and 0.5 ºC·min^{-1}.

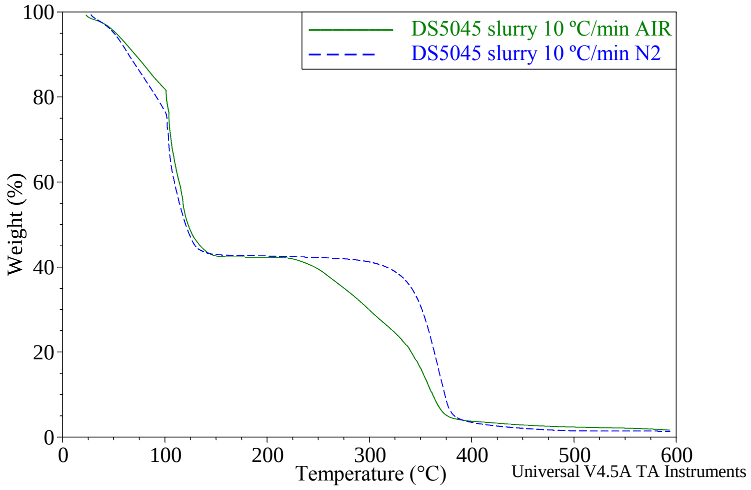

Figure 6. 8. Thermogram comparison for M sample (Micronal® DS 5045 X slurry) in air and N_2 atmospheres at 10 ºC·min^{-1}.

Concerning about M sample, in Figure 6. 9 is compared the N_2 and air conditions at different heating rates. In Figure 6. 9a can be observed that as higher heating rate, more stability of the sample, although the signal profile is very similar between the four samples. In Figure 6. 9b is compared the M sample in air atmosphere at different heating rates. As it is shown, as higher is the heating rate, the weight loss take place at higher temperatures, meaning more stability.

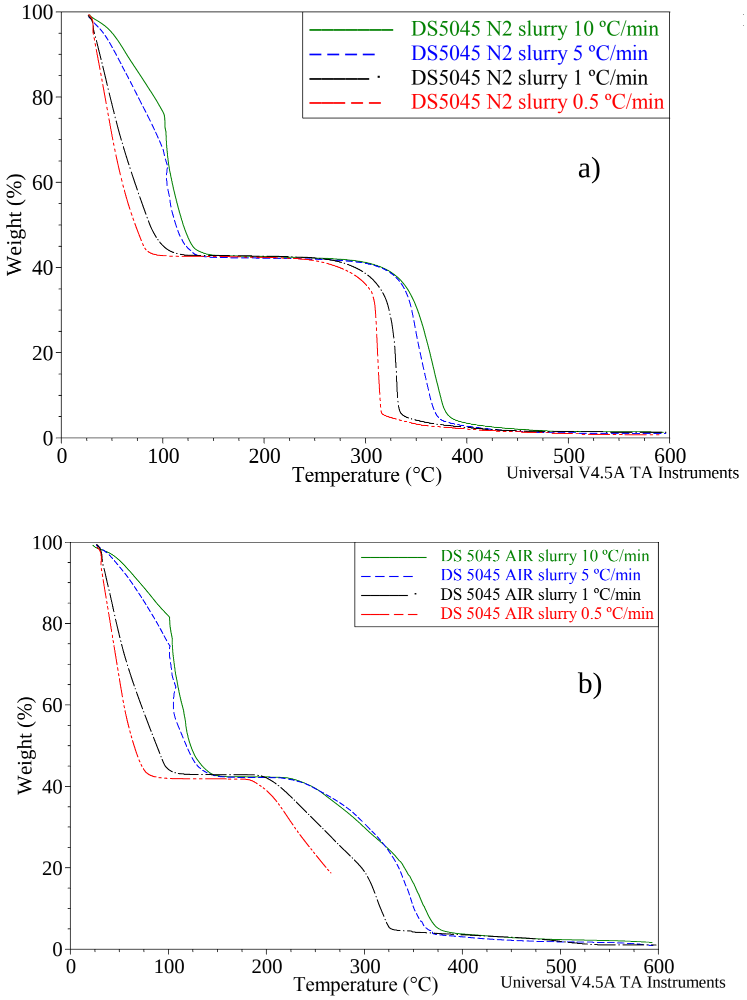

Figure 6. 9. Thermograms comparison at different heating rates (10 ºC·min^{-1}, 5 ºC·min^{-1}, 1 ºC·min^{-1}, and 0.5 ºC·min^{-1}) for the M (Micronal® DS 5045 X slurry) sample, a) in N_2 atmosphere, b) and air atmosphere.

6.4.2. Characterization of dried Micronal® DS 5045 X slurry (MD)

When M sample is dried at room conditions up to 24 h, it becomes MD (dried Micronal® DS 5045 X slurry). It has been performed the same experimental trials as M sample, with the same experimental conditions, as Figure 6. 10 shows. The main difference relays in air conditions; the curve has an interesting behavior. The reduction in temperature starting over 320 ºC in the TGA signal, having a maximum peak around 350 ºC, and ending at 370 ºC) matches with the exothermic peak in the DSC analysis (as it will be stated later).This occurs always in air atmosphere at different heating rates. It has been assumed that the heat generated by the exothermic reaction heats the pan, and therefore, overestimates the thermocouple temperature. The exothermic heat exhaustion, temperature decreases slightly, explaining the overestimation in reading and the observed mismatch. This is an ordinary behavior in PCS. Other authors, such as Zhang *et al*. [18,19], have found it in their PCS samples but they do not describe the phenomenon.

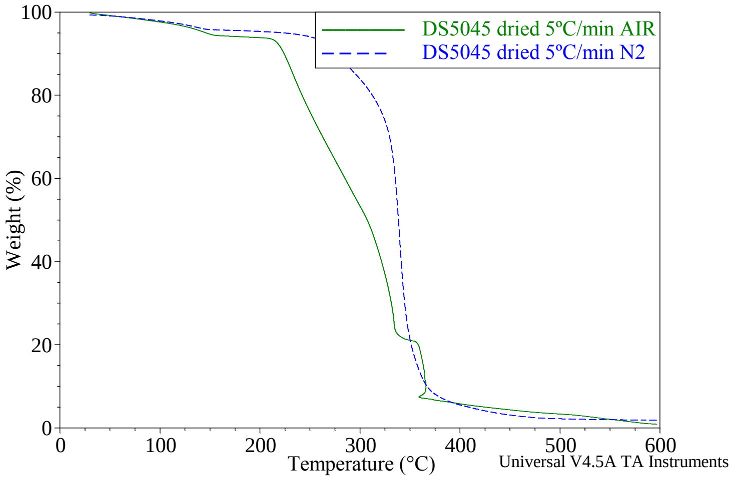

Figure 6. 10. Thermogram comparison for MD sample (dried Micronal® DS 5045 X slurry) in air and N_2 atmospheres at 5 ºC·min^{-1}.

Comparing the different heating rates for the dried sample (MD) at N_2 (Figure 6.11a) and air atmospheres (Figure 6.11b), it can be observed that the higher the heating rate, the higher is the stability of the sample in both atmospheres. Taking into account the shape of the weight loss curve, it is easier to interpret the ones performed in N_2 atmosphere than the air ones.

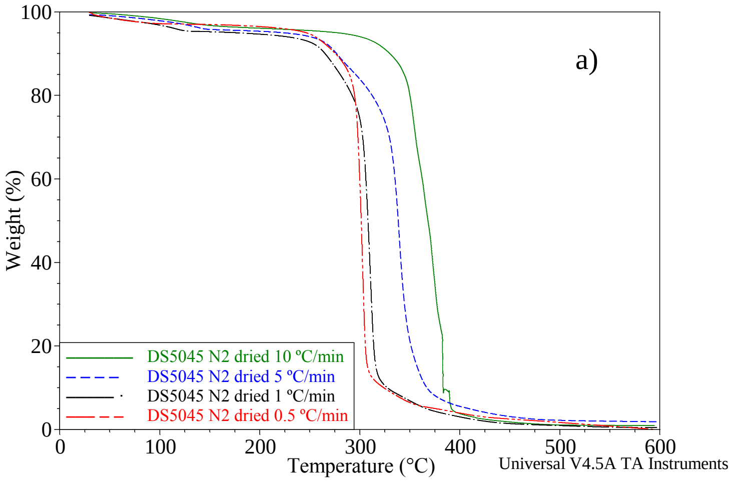

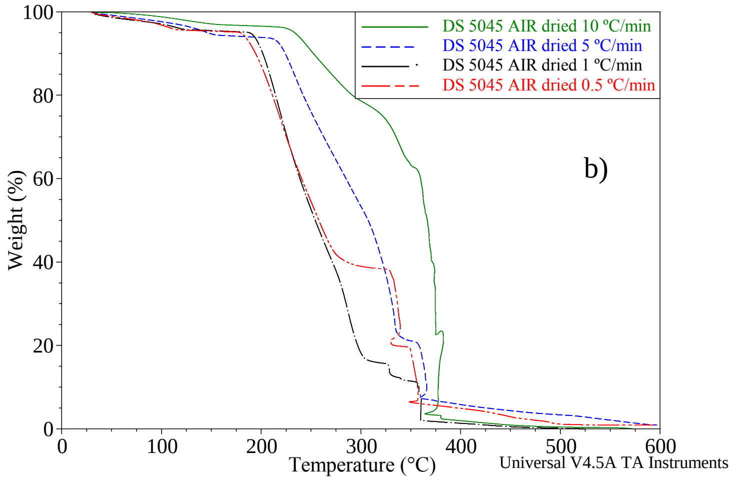

Figure 6. 11. Thermograms comparison at different heating rates (10 ºC·min^{-1}, 5 ºC·min^{-1}, 1 ºC·min^{-1}, and 0.5 ºC·min^{-1}) for the MD sample, a) in N_2 atmosphere, b) and air atmosphere.

In Figure 6. 12 is illustrated the comparison between M and MD samples in N_2 atmosphere. As it can be observed, the sample degrades different: one step for the dried MD sample and two steps for the M sample. The same behavior can be observed in these conditions when decreasing the heating rate.

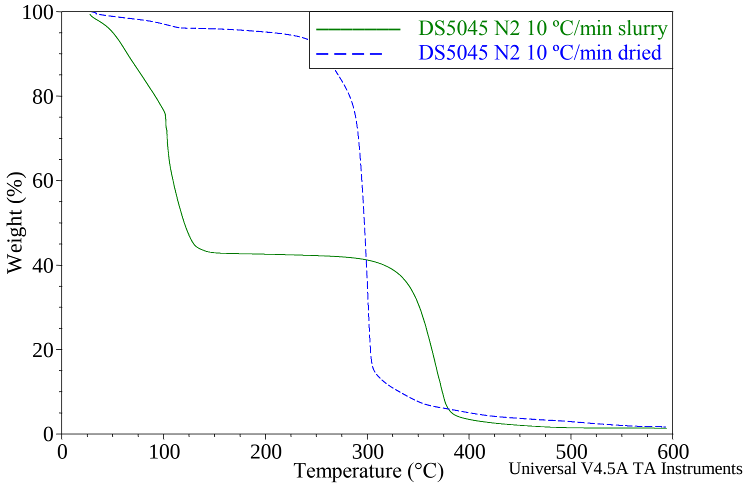

Figure 6. 12. Thermogram comparison in N_2 atmosphere at 10 ºC·min^{-1} for M and MD samples.

Nevertheless, when M and MD sample are compared in air conditions, a very different behavior can be elucidated, as Figure 6. 13 shows.

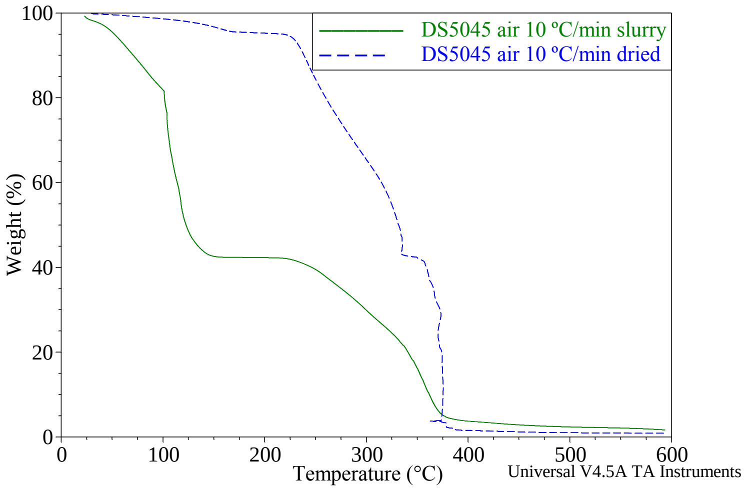

Figure 6. 13. Thermogram comparison in air atmosphere for M and MD samples at 10 ºC·min^{-1}.

The water component of the PCS sample interferes on the profile of the decomposition. Besides, the decomposition peaks of the MD sample can be more accurately defined due to the water component disappears, and the signal is focused only on the MPCM (shell + core), which two main decomposition peaks can observed. The first one is due to the paraffin wax, and the second step is attributed to the decomposition of the shell. Once again, the temperature decrease around 350 ºC can be observed (as it has been noticed above, this fact only happens in air atmosphere conditions). Another possible explanation for this behavior can be the increase of the gas content when increasing the temperature. Then, there is no mass change inside the pan, the density of the system decrease, and the contact between the pan and the sample may decrease, giving a decrease in temperature due to the response of the instrument. All these differences are under investigation.

As a main conclusion of this part of the study, it can be stated that to better characterize PCS samples by thermogravimetric analysis, the dried conditions allows to better distinguish between the different weigh losses steps. For this reason is important to decide the optimum conditions to compare PCS samples with the same parameters, as the results can change drastically.

6.4.3. Conclusions

TGA technique allows measuring several parameters in one experiment which aids saving time during characterization. On one hand, the best conditions for determining the T$_{peak}$ of this material as dried PCS are at a heating rate of 1 ºC·min^{-1} and in a N$_2$ atmosphere. In this sense, PCS are expected to be employed in cases with low heating rates. At the light of the results, experimental conditions exert a special influence over the results obtained. This study partially determined the best options for obtaining T_{peak} and heat flow more accurately. Other parameters such as the amount of sample, number of cycles, as well as the varying gas flow are currently under research.

Chapter 6 References

[1] Budrugeac P. The evaluation of the non-isothermal kinetic parameters of the thermal and thermo-oxidative degradation of polymers and polymeric materials: its use and abuse. Polymer Degradation and Stability 2000;71:185–7. doi:10.1016/S0141-3910(00)00148-8.

[2] Brown ME. Introduction to Thermal Analysis: Techniques and Applications. Springer Netherlands; 2001. doi:10.1007/0-306-48404-8.

[3] Giro-Paloma J, Delgado M, Barreneche C, Martínez M, Cabeza LF, Fernández AI. Thermal Cycle Feasibility of Phase Change Slurry. Eurotherm Seminar #99 Advances in Thermal Energy Storage, Lleida (Spain): 2014.

[4] Tyagi VV, Kaushik SC, Tyagi SK, Akiyama T. Development of phase change materials based microencapsulated technology for buildings: A review. Renewable and Sustainable Energy Reviews 2011;15:1373–91. doi:10.1016/j.rser.2010.10.006.

[5] Zhang P, Ma ZW, Wang RZ. An overview of phase change material slurries: MPCS and CHS. Renewable and Sustainable Energy Reviews 2010;14:598–614. doi:10.1016/j.rser.2009.08.015.

[6] Ma Y, Chu X, Tang G, Yao Y. Adjusting phase change temperature of microcapsules by regulating their core compositions. Materials Letters 2012;82:39–41. doi:10.1016/j.matlet.2012.05.033.

[7] Hawlader MNA, Uddin MS, Khin MM. Microencapsulated PCM thermal-energy storage system. Applied Energy 2003;74:195–202. doi:10.1016/S0306-2619(02)00146-0.

[8] Qiu X, Li W, Song G, Chu X, Tang G. Microencapsulated n-octadecane with different methylmethacrylate-based copolymer shells as phase change materials for thermal energy storage. Energy 2012;46:188–99. doi:10.1016/j.energy.2012.08.037.

[9] Ma Y, Chu X, Li W, Tang G. Preparation and characterization of poly(methyl methacrylate-co-divinylbenzene) microcapsules containing phase change temperature adjustable binary core materials. Solar Energy 2012;86:2056–66. doi:10.1016/j.solener.2012.04.008.

[10] Su J-F, Wang L-X, Ren L. Synthesis of polyurethane microPCMs containing n-octadecane by interfacial polycondensation: Influence of styrene-maleic anhydride as a surfactant. Colloids and Surfaces A: Physicochemical and Engineering Aspects 2007;299:268–75. doi:10.1016/j.colsurfa.2006.11.051.

[11] Wang X, Zhang X, Tao X, Yick K. Structure and thermal stability of microencapsulated phase-change materials. Colloid & Polymer Science 2004;282:330–6. doi:10.1007/s00396-003-0925-y.

[12] Li W, Zhang X-X, Wang X-C, Niu J-J. Preparation and characterization of microencapsulated phase change material with low remnant formaldehyde content. Materials Chemistry and Physics 2007;106:437–42. doi:10.1016/j.matchemphys.2007.06.030.

[13] Smith MC. Microencapsulated Phase Change Materials for Thermal Energy Storage. 2008.

[14] Zhang GH, Bon SAF, Zhao CY. Synthesis, characterization and thermal properties of novel nanoencapsulated phase change materials for thermal energy storage. Solar Energy 2012;86:1149–54. doi:10.1016/j.solener.2012.01.003.

[15] http://www.eurotherm-seminar99.eu/ (14/10/2014) n.d.

[16] Giro-Paloma J, Barreneche C, Delgado M, Martínez M, Fernández AI, Cabeza LF. Physicochemical and thermal study of a MPCM of PMMA shell and paraffin wax as a core. Energy Procedia, vol. 48, 2014, p. 347–54. doi:10.1016/j.egypro.2014.02.040.

[17] Barreneche C, Solé A, Miró L, Martorell I, Fernández a. I, Cabeza LF. Study on differential scanning calorimetry analysis with two operation modes and organic and inorganic phase change material (PCM). Thermochimica Acta 2013;553:23–6. doi:10.1016/j.tca.2012.11.027.

[18] Zhang GH, Zhao CY. Thermal property investigation of aqueous suspensions of microencapsulated phase change material and carbon nanotubes as a novel heat transfer fluid. Renewable Energy 2013;60:433–8. doi:10.1016/j.renene.2013.05.041.

[19] Zhang GH, Zhao C-Y. Thermal and rheological properties of microencapsulated phase change materials. Renewable Energy 2011;36:2959–66. doi:doi:10.1016/j.renene.2011.04.002.

[20] Giro-Paloma J, Oncins G, Barreneche C, Martínez M, Fernández AI, Cabeza LF. Physico-chemical and mechanical properties of microencapsulated phase change material. Applied Energy 2013;109:441–8. doi:10.1016/j.apenergy.2012.11.007.

[21] Brown ME. Introduction of Thermal Analysis. Techniques and Applications. 2001.

[22] Del Valle-Zermeño R, Chimenos JM, Formosa J, Fernández AI. Hydration of a low-grade magnesium oxide. Lab-scale study. Journal of Chemical Technology and Biotechnology 2012;87:1702–8.

Conclusions

The main conclusions of this PhD Thesis may be found throughout the chapters, as well as in conclusions subsection, inside each article. Therefore, this section is aimed to highlight the contribution of this PhD Thesis in the state of the art of the PCM and MPCM for thermal energy storage in buildings.

Conclusions Block I:

1) Nanoindentation is an adequate tool to evaluate nanomechanical properties for polymers, even though the polymeric viscoelastic character make necessary to deeply evaluate the experiment conditions.

2) Methodologies proposed by Loubet and Oliver & Pharr are limited in polymers because of the stiffness of these materials. Loubet method should be restricted to polymeric materials with low viscous character, i.e., with T_g well above the temperature of measurement. It tends to yield lower values of the mechanical properties, closer to the modulus data determined by means of DMA. On the other hand, Oliver & Pharr method has higher values when studying indentation hardness as well as elastic modulus. Both methodologies are suitable to measure both polymer strength and Young's modulus.

3) The usage of flame retardant filler in PP caused significant increases in Hardness, Young's modulus, and loss modulus compared to those samples without filler. Moreover, when the composite is in contact with PCM, the material properties severely decreased because the PCM acts as a plasticizer, and polymer softens. It was also observed that the material properties worsened as the temperature assay increased.

Conclusions Block II:

1) An exhaustive bibliographic search of PCM, methods to microencapsulate PCM, techniques to characterize MPCM, and applications have been done for organic PCM.

2) Atomic Force Microscopy is a useful technique to characterize shell stiffness and Young's modulus of MPCM. It is possible to compare and analyze:

   a. Commercial MPCM with MPCM fabricated in laboratories.
   b. MPCM with different polymeric shells.
   c. MPCM with different PCM cores.
   d. MPCM with different encapsulation ratios.

3) It has been performed the characterization of MPCM by AFM at different temperatures to simulate the PCM in solid or liquid state as in real service.

4) It has been achieved the observation of Phase Change Slurries by Scanning Electron Microscopy by using a cryogenic system.

5) Due to the thermal behavior of Phase Change Slurries can be measured as dry or wet basis resulting important differences in weight losses, it has been explored the optimum conditions for analyzing its thermal behavior by thermogravimetric analysis.

Future work

With this PhD we contribute to the knowledge of MPCM mechanical properties in a microscopic level. Nevertheless, a deeper study is needed to use these data in a macroscopic scale, where the performance in service conditions needs to be predicted. For instance, mechanical integrity is required when MPCM are used in composite materials in passive applications, and reliable slurry is needed when an active system is designed.

List of of acronyms and symbols

A

α parameter coefficient equal to 1.2 when a Berkovich tip indenter is employed

A_c Contact area

ABS acrylonitrile butadiene styrene

AFM Atomic Force Microscopy

B

b slope of the straight line in measurement of tip defect

β shape factor for a nanoindentor (24.56 for Berkovich tip)

C

C_p large specific heat capacity

CSM Continuous Stiffness Measurement

D

δ Sample penetration

δ density

DMA/DMTA Dynamic mechanical analysis/thermal analysis

DSC Differential Scanning Calorimetry

E

E Young's modulus

E_{loss} Loss modulus

E' Storage modulus, material's capacity to store energy. It is the component in phase with the applied displacement or load

E'' Loss modulus, represents the material's capacity to dissipate energy. It is the component 90° out of phase with the applied displacement or load

ε constant. 0.75 for Berkovich indenter

F

F Force

FT-IR Fourier Transformed Infrared Spectroscopy

H

H Hardness

h_o tip defect

h'_r plastic deformation depth

h_{max} maximum indentation depth

ΔH Enthalpy

HCS Harmonic Contact Stiffness

HDPE High Density Polyethylene

H_{IT} Indentation hardness

HVAC ventilation and air-conditioning

K

k large thermal conductivity

L

LDPE Low-density polyethylene

LHS Latent Heat Storage

LLALS Low Angle Laser Light Scattering

M

MF melamine-formaldehyde

$Mg(OH)_2$ Magnesium hydroxide

MMA Methyl methacrylate

MPCM Microencapsulated Phase Change Material

O

OM Optical Microscopy

P

P_{max} Maximum applied load during a nanoindentation test

P–h curve Loading-unloading curve (applied load-displacement into surface)

PA6 polyamide/Nylon 6

PC polycarbonate

PCM Phase Change Material

PCS Phase Change Slurry

PE Polyethylene

PET amorphous polyethylene terephthalate

PMMA Poly methyl methacrylate

PP Polypropylene

PS Polystyrene

PSD Particle Size Distribution

S

$S_{contact}$ contact stiffness calculated from an unloading curve

SEM Scanning Electron Microscopy

T

T temperature

T_g glass transition temperature

tan δ =E’’/E’ loss factor used as a measure of damping in a linear viscoelastic material

TEM Transmission Electron Microscopy

TES Thermal Energy Storage

TGA Thermogravimetric analysis

V

ν Poisson ratio

W

WAXS Wide Angle X-ray Scattering

X

XRD X-Ray Diffraction

XRF X-ray Fluorescence

Z

z piezo-scanner displacement in the axis perpendicular to the sample plane

Sumari

L'ús de fonts de calor renovables té com a resultat una disminució en el consum de recursos fòssils, encara que el seu ús sigui discontinu i habitualment no coincideixi amb la demanda. Un correcte disseny del sistema d'emmagatzematge d'energia tèrmica pot eliminar aquest problema reduint el consum de recursos no renovables i millorant l'eficiència energètica on es faci servir. En el cas específic dels edificis, l'emmagatzematge d'energia tèrmica mitjançant materials de canvi de fase (PCM) és un instrument útil per a arribar a un descens del consum d'energia, tal i com es posa de manifest en molts treballs publicats. Aquests sistemes poden incorporar-se tant en climatització passiva (a l'envoltant) com en activa (a les instal·lacions). Així doncs, una adequada selecció dels materials i una caracterització exhaustiva per al seu ús en emmagatzematge d'energia tèrmica és crític tant en un sistema de nova construcció com els ja construïts. La reducció en el impacte ambiental dels sistemes de climatització ha de ser viable tècnica i econòmicament.

La present Tesi es presenta com a compendi d'articles publicats en revistes científiques indexades en les àrees de Materials, Enginyeria, i Energia, on es fa especial èmfasi en la caracterització química, física, tèrmica, mecànica i ambiental tant dels PCM com dels MPCM (materials de canvi de fase microencapsulats) i PCS (polpes amb canvi de fase). Es va considerar interessant dur a terme una caracterització exhaustiva d'aquests materials, degut a que certs estudis científics revelen que quan els PCM són mesclats amb materials de construcció, aquests pateixen fuites. Una alternativa per conservar els PCM dins del material de construcció és encapsulant-los per exemple amb un polímer, constituint un sistema que s'anomena MPCM quan es tracta de microcàpsules. Aquesta Tesi es divideix en dos blocs:

- **Bloc I, Mostres macroscòpiques** (Capítol 2): usant mostres macroscòpiques, s'ha explorat la caracterització de termoplàstics mitjançant nanoindentació que, fins aquest moment, tenia pocs precedents. Com les propietats mecàniques són un criteri fonamental per a la selecció de materials i la tècnica de la nanoindentació permet avaluar-les, s'han estudiat la duresa i el mòdul elàstic de diferents materials polimèrics a través dels mètodes de Loubet i Oliver & Pharr, per discernir quin és el més adequat segons les característiques viscoelàstiques del propi polímer. Els valors obtinguts a través del mètode d'Oliver & Pharr són funció de l'anàlisi de la corba de descàrrega; per contra, aquests valors són funció de la profunditat de penetració de la indentació si s'analitzen mitjançant Loubet. A través d'aquesta tècnica també s'han estudiat els canvis mecànics que es produeixen quan un polímer que conté càrrega ignifugant en la seva formulació se submergeix continuadament en PCM. S'ha observat que l'ús de $Mg(OH)_2$ augmenta la rigidesa, la resistència mecànica, redueix l'efecte de degradació evitant una possible fallada mecànica prematura, i millora les propietats contra el foc. Aquest bloc conté dos articles científics.

- Bloc II, Mostres microscòpiques (Capítols 3, 4, 5, 6): Aquest bloc es basa en l'estudi de PCM microencapsulats (MPCM). S'ha dut a terme una revisió de publicacions per altres autors relacionats amb els PCM, MPCM, i polpes (PCS) (mateix embolcall i diferent PCM; diferent embolcall i mateix PCM; mateix embolcall i mateix PCM, però en diferents proporcions). Seguidament, s'han avaluat les propietats químiques, físiques, tèrmiques, mecàniques, i ambientals de diferents mostres de MPCM i PCS. S'ha conclòs que l'ús d'AFM és una eina útil per caracteritzar la rigidesa i el mòdul de Young dels MPCM. A causa de que la temperatura és un paràmetre clau per a sistemes que contenen PCM, els experiments realitzats amb AFM s'han dut a terme a diferents temperatures, amb l'objectiu de simular el PCM en estat sòlid i/o líquid. S'han observat mostres de PCS amb l'ús de SEM amb un sistema de crionització acoplat, i s'han estudiat les propietats mediambientals per cromatografia de gasos (VOC 's). A més, s'han ciclat PCS per veure la durabilitat de la paret polimèrica després de certs cicles de bombament i per comparar les propietats químiques i termofísiques abans i després de bombar la mostra. Finalment, a causa de que els resultats del comportament tèrmic del PCS segons si es troba líquid o sec van mostrar canvis significatius, s'han investigat les condicions òptimes mitjançant anàlisi termogravimètrica per als PCS. Aquest segon bloc conté sis articles científics publicats, un article finalitzat sense enviar a revista, i un estudi en investigació.

Finalment, es presenten les conclusions principals de la contribució d'aquesta tesi doctoral en l'estat de l'art dels PCM, MPCM, i PCS per a emmagatzematge d'energia en edificis.

Sumario

El uso de fuentes de calor renovables tiene como resultado una disminución en el consumo de recursos fósiles, aunque su uso es discontinuo y habitualmente no coincide con la demanda. Un correcto diseño del sistema de almacenamiento de energía térmica puede eliminar este problema reduciendo el consumo de recursos no renovables y mejorando la eficiencia energética donde se use. En el caso específico de los edificios, el almacenamiento de energía térmica mediante materiales de cambio de fase (PCM) es un instrumento útil para alcanzar un descenso del consumo de energía, tal y como se pone de manifiesto en muchos trabajos publicados. Estos sistemas pueden incorporarse tanto en climatización pasiva (en el envolvente) como en activa (en las instalaciones). Así pues, una adecuada selección de los materiales y una caracterización exhaustiva para su uso en almacenamiento de energía térmica es crítico tanto en un sistema de nueva construcción como los ya construidos. La reducción en el impacto ambiental de los sistemas de climatización tiene que ser viable técnica y económicamente.

La presente Tesis se presenta como compendio de artículos publicados en revistas científicas indexadas en las áreas de Materiales, Ingeniería, y Energía, donde se hace especial émfasis en la caracterización química, física, térmica, mecánica y ambiental tanto de PCM como de MPCM (materiales de cambio de fase microencapsulados) y PCS (pulpas con cambio de fase). Se consideró interesante llevar a cabo una caracterización exhaustiva de estos materiales, debido que ciertos estudios científicos revelan que, cuando los PCM son mezclados con materiales de construcción, éstos sufren fugas. Una alternativa para conservar los PCM dentro del material de construcción es encapsulándolos por ejemplo con un polímero, constituyendo un sistema que se denomina MPCM cuando se trata de microcápsulas. Esta Tesis se divide en dos bloques:

- **Bloque I, Muestras macroscópicas** (Capítulo 2): usando muestras macroscópicas, se ha explorado la caracterización de termoplásticos mediante nanoindentación que, hasta ése momento, tenía pocos precedentes. Como las propiedades mecánicas son un criterio fundamental para la selección de materiales y la técnica de la nanoindentación permite evaluarlas, se han estudiado la dureza y el módulo elástico de diferentes materiales poliméricos a través de los métodos de Loubet y Oliver & Pharr, para discernir cuál es el más adecuado según las características viscoelásticas del propio polímero. Los valores obtenidos a través del método de Oliver & Pharr son función del análisis de la curva de descarga; por el contrario, éstos valores son función de la profundidad de penetración de la indentación si se analizan mediante Loubet. A través de esta técnica también se han estudiado los cambios mecánicos que se producen cuando un polímero que contiene carga ignifugante en su formulación se sumerge continuadamente en PCM. Se ha observado que el uso de $Mg(OH)_2$ aumenta la rigidez, la resistencia mecánica, reduce el efecto de degradación evitando un possible fallo mecánico prematuro, y mejora las propiedades contra el fuego. Este bloque contiene dos artículos científicos.

- **Bloque II, Muestras microscópicas** (Capítulos 3, 4, 5, 6): Este bloque se basa en el estudio de PCM microencapsulados (MPCM). Se ha llevado a cabo una revisión de publicaciones por otros autores relacionados con los PCM, MPCM, y pulpas (PCS) (misma cáscara y diferente PCM; distinta cáscara y mismo PCM; misma cáscara y mismo PCM, pero en diferentes proporciones). Seguidamente, se han evaluado las propiedades químicas, físicas, térmicas, mecánicas, y ambientales de diferentes muestras de MPCM y PCS. Se ha concluído que el uso de AFM es una herramienta útil para caracterizar la rigidez y el módulo de Young de los MPCM. Debido a que la temperatura es un parámetro clave para sistemas que contienen PCM, los experimentos realizados con AFM se han llevado a cabo a diferentes temperaturas, con el objetivo de simular el PCM en estado sólido y/o líquido. Se han observado muestras de PCS mediante el uso de SEM acoplado a un sistema de crionizado, y se han estudiado las propiedades medioambientales por cromatografía de gases (VOC's). Además, se han ciclado PCS para ver la durabilidad de la pared polimérica después de ciertos ciclos de bombeo y para comparar las propiedades químicas y termofísicas antes y después de bombear la muestra. Finalmente, debido a que los resultados del comportamiento térmico del PCS según si se encuentra líquido o seco mostraron cambios significativos, se han investigado las condiciones óptimas mediante análisis termogravimétrico para los PCS. Este segundo bloque contiene seis artículos científicos publicados, un artículo finalizado sin enviar a revista, y un estudio en investigación.

Finalmente, se presentan las conclusiones principales de la contribución de esta Tesis Doctoral en el estado del arte de los PCM, MPCM, y PCS para almacenaje de energía en edificios.

Summary

The use of renewable heat decreases the consumption of fossil resources, although its usage is intermittent and usually does not match the demand. A proper thermal energy storage system design can eliminate this problem by reducing the consumption of non-renewable resources and improving energy efficiency where used. In the specific case of buildings, thermal energy storage using phase change materials (PCM) is a useful tool to achieve reduction in energy consumption, as reflected by many published studies. These can be incorporated into passive (in the envelope) or/and active (on site) systems. Thus, a proper selection of materials and extensive characterization for its usage in thermal energy storage is critical for new construction systems as well as for those already constructed. The reduction in the environmental impact of air conditioning systems has to be technically and economically viable.

This PhD Thesis is presented as a compendium of published articles in scientific journals indexed in the areas of Materials, Engineering, and Energy. The strong emphasis is made in the chemical, physical, thermal, mechanical and environmental characterization of PCM, MPCM (microencapsulated phase change materials), and PCS (phase change slurries). The main purpose is to perform an exhaustive characterization of this kind of materials because several scientific studies have highlighted that PCM mixed with construction materials can suffer leakage. An alternative for retaining PCM inside building materials is by means of encapsulation using a polymer, resulting in a system named MPCM. This PhD Thesis is divided in two blocks:

- **Block I, Macroscopic samples** (Chapter 2): the nanoindentation tecnique has been used to characterize thermoplastics that, so far, have had few precedents. Taking into account that mechanical properties of materials are an important criterion for their selection and that nanoindentation allows their evaluation, we have studied the hardness and elastic modulus of different polymeric materials through Loubet and Oliver & Pharr methodologies, to discern which is the most suitable concerning the viscoelastic properties. The obtained values by Oliver & Pharr method are based on the unloading curve analysis; in case of the evaluation by Loubet methodology, these values are a function of the penetration depth of the indentation. By using this technique, we have also studied the mechanical changes that occur when a polymer that contains a flame retardant is immersed in PCM. It has been observed that using $Mg(OH)_2$ increases stifness and mechanical strength while reducing the degradation effect and improving the properties against fire. This block contains two scientific published papers.

- **Block II, Microscopic samples** (Chapters 3, 4, 5, 6): This block is based on the microencapsulated PCM (MPCM) study. A review of publications related to PCM, MPCM and slurries (PCS) (same shell and different PCM; different shell and same PCM; same shell and same PCM, but different encapsulation ratios) was prepared. Then, the evaluation of the chemical, physical, thermal, mechanical, and environmental properties of different MPCM and PCS samples was performed. It has concluded that AFM is a useful tool to characterize the stifness and Young's modulus of MPCM. Because temperature is a key parameter in systems that contain PCM, AFM experiments were carried out at different temperatures, in order to simulate the PCM in solid and/or liquid state. PCS samples were observed using SEM device coupled to a cryogenic system. Besides, environmental properties of PCS have been studied by gas chromatography (VOC’s). In addition, PCS were cycled for the evaluation of the polymeric shell durability after pumping the sample several cycles. Also, the chemical and thermophysical properties before and after pumping the sample were compared. Finally, due to the thermal behavior results of PCS in some performed studies, and depending on the liquid or dried PCS sample, the optimum conditions by means thermogravimetric analysis were evaluated. The second block contains six scientific published articles, one article under review after its first revision, one article finished without being submitted to a journal, and one unfinished research.

Finally, the contribution in the state of the art of this PhD Thesis related with thermal energy storage in buildings using PCM, MPCM, and PCS is presented.